Exelon Nuclear

RS-05-112

August 24, 2005

U. S. Nuclear Regulatory Commission
ATTN: Document Control Desk
Washington, DC 20555-0001

Dresden Nuclear Power Station, Units 2 and 3
Renewed Facility Operating License Nos. DPR-19 and DPR-25
NRC Docket Nos. 50-237 and 50-249

Quad Cities Nuclear Power Station, Units 1 and 2
Renewed Facility Operating License Nos. DPR-29 and DPR-30
NRC Docket Nos. 50-254 and 50-265

Subject: Technical Documentation Related to Analysis and Design of Quad Cities Replacement Steam Dryers

Reference: Letter from K. R. Jury (Exelon Generation Company, LLC) to U. S. NRC, "Commitments and Plans Related to Extended Power Uprate Operation," dated July 26, 2005

In the reference, Exelon Generation Company, LLC (EGC) made several commitments regarding the extended power uprate (EPU) operation of Dresden Nuclear Power Station (DNPS), Units 2 and 3, and Quad Cities Nuclear Power Station (QCNPS), Units 1 and 2, including a commitment to submit detailed evaluations of the QCNPS Unit 1 replacement steam dryer. These evaluations are required to be submitted within 80 days of steam dryer data collection at the maximum reactor thermal power level achieved during the startup test. The maximum reactor thermal power level achieved during the startup test for QCNPS Unit 1 occurred on June 5, 2005; therefore, the 80-day report is due to be submitted to the NRC no later than August 24, 2005. The enclosures to this letter contain the information committed to be provided in the reference letter.

Enclosure 1 contains a summary of the engineering assessments related to the steam dryer design project. Enclosure 2 provides the detailed evaluations of data collected on QCNPS Unit 1 during startup and power ascension testing following steam dryer replacement. The attached reports include detailed evaluations of comparisons of the predicted QCNPS Unit 1 steam dryer loads, developed using the acoustic circuit model, with the actual QCNPS Unit 1 loads obtained from main steam line strain gauge data and the instrumented steam path.

EGC provided General Electric (GE) Report GENE-0000-0043-5391-01, "Quad Cities Unit 1 Replacement Steam Dryer Stress and Fatigue Analysis at EPU Power Level of 2957 MWt

Based on Measured EPU Conditions," (i.e., Attachments 10 and 11 of Enclosure 2) to the NRC via electronic mail on August 17, 2005. Subsequently, this report was revised to illustrate the change in damping coefficients applied during analysis of the skirt area of the QCNPS Unit 1 steam dryer. Figure 6-14, "Frequency Response QC1D – 10%: Skirt," was deleted, and Figure 6-18, "Frequency Response QC1B +10%: Skirt," was modified to include results of the revised damping coefficient. Attachments 10 and 11 of Enclosure 2 provide the revised report.

Attachment 10 of Enclosure 2 contains information considered proprietary to GE. Therefore, EGC requests that this information be withheld from public disclosure in accordance with 10 CFR 2.390, "Public inspections, exemptions, requests for withholding," paragraph (a)(4), and 10 CFR 9.17, "Agency records exempt from public disclosure," paragraph (a)(4). An Affidavit attesting to the proprietary nature of this document is included in the attachment, and a non-proprietary version of the report is provided in Enclosure 2, Attachment 11.

Should you have any questions concerning this letter, please contact Mr. Thomas G. Roddey at (630) 657-2811.

Respectfully,

Patrick R. Simpson

Patrick R. Simpson
Manager – Licensing

Enclosures:

1. Quad Cities Nuclear Power Station, Unit 1 – Summary of 80-Day Report to the NRC
2. Engineering Evaluation of the Quad Cities Unit 1 Replacement Steam Dryer
   Attachments:
   1. Exelon Report Number AM-2005-013, "Quad Cities Unit 1 New Steam Dryer Outage Startup Test Report," Revision 0, dated July 28, 2005
   2. Structural Integrity Associates Letter KKF-05-036, "Quad Cities Unit 1 Main Steam Line Strain Gage Reductions," dated July 6, 2005
   3. Exelon Report Number AM-2005-003, "Engineering Evaluation of Reduced Strain Gage Data Sets on the Quad Cities Unit 1 Test Condition 15A," dated June 29, 2005
   4. Exelon Report Number AM-2005-006, "Comparison of Acoustic Circuit Dryer Loads for Missing MS Line Strain Gages to Acoustic Circuit Dryer Loads with All MS Line Strain Gages," Revision 0, dated July 19, 2005
   5. Exelon Report Number AM-2005-008, "An Assessment of the Effects of Uncertainty in the Application of Acoustic Circuit Model Predictions to the Calculation of Stresses in the Replacement Quad Cities Units 1 and 2 Steam Dryers," Revision 0, dated August 19, 2005
   6. Exelon Report Number AM-2005-007, "AM-2005-007 Assessment of the Revised QC1 Minimum Error ACM Loads Using All Main Steam Line Strain Gages," Revision 0, dated August 2, 2005
   7. Structural Integrity Associates Letter KJO-05-004, "Vibration Comparison of Quad Cities Units 1 and 2 Power Ascension Accelerometer Spectra Data," dated July 14, 2005

8. C.D.I. Technical Note No. 05-34,"Test Condition TC15a Load Comparison for Quad Cities Unit 1," Revision 0, dated August 2005
9. GE Report GE-NE-0000-0041-9435, "Quad Cities 1 & 2 Steam Dryer Replacement – 4% Structural Damping for Steam Dryer Skirt FIV Analysis," dated June 16, 2005
10. Affidavit and GE Report GENE-0000-0043-5391-01-P, "Quad Cities Unit 1 Replacement Steam Dryer Stress and Fatigue Analysis at EPU Power Level of 2957 MWt Based on Measured EPU Conditions," Revision 1, GE Proprietary, dated August 16, 2005
11. GE Report GENE-0000-0043-5391-01, "Quad Cities Unit 1 Replacement Steam Dryer Stress and Fatigue Analysis at EPU Power Level of 2957 MWt Based on Measured EPU Conditions," Revision 1, Non-Proprietary, dated August 2005
12. Structural Integrity Associates Letter KKF-05-037, "Comparison of Quad Cities Unit 1 and Quad Cities Unit 2 Main Steam Line Strain Gage Data," Revision 1, dated July 18, 2005

ENCLOSURE 1

Quad Cities Nuclear Power Station, Unit 1 – Summary of 80-Day Report to the NRC

Quad Cities Nuclear Power Station, Unit 1 – Summary of 80-Day Report to the NRC

Executive Summary

After experiencing steam dryer degradation at Quad Cities Nuclear Power Station (QCNPS) during extended power uprate (EPU) operations, Exelon Generation Company, LLC (EGC) and General Electric (GE) embarked on a project to design new steam dryers for both QCNPS units.

Dryer Design Is More Robust and Less Susceptible to Flow-Induced Vibration

The new dryer design relied on operating experience, data previously collected on instrumented steam dryers, and the advanced boiling water reactor (BWR) steam dryer design. Every effort was made to eliminate stress concentration points by using full penetration welds wherever possible, use of pre-shaped components that moved welds from high-stress areas of the dryer, and implementing BWR Vessel Internals Project (BWRVIP)-84 material and fabrication guidelines to minimize IGSCC susceptibility. In addition, new dryer components were fabricated using thicker material sections, which significantly improved the dryer's load carrying capacity. This is especially evident in the front hood areas, which were increased to 1-inch thick plate material. The overall effect was a new dryer with significantly improved design margin for fatigue life. EGC previously submitted reports that described this design effort.

Comprehensive Analysis of Design

Design Loads

Because the dryer loads were not clearly defined, two design basis load cases were developed. The first was based on QCNPS Unit 2 in-plant data from two water reference legs, four venturi instrument lines, and one strain gauge, along with acoustic circuit (AC) analysis that included the new dryer shape. The second load case was derived from scale model tests (SMT) of the QCNPS Unit 1 steam path. After performing an evaluation of the ability of the AC analysis to transfer loads, the measured pressures from the SMT at EPU conditions were transformed into refined load cases for finite element analysis (FEA) of the new dryer. Both load cases consisted of approximately 15,000 node points that defined the differential pressure across the dryer surface for the FEA of the dryer. EGC previously submitted reports that described this design effort.

FEA

To assist in validating analytical methodologies, GE and XGEN Engineering (XGEN) developed two completely independent finite element models (FEMs) of the new dryer. Both load cases were run on the GE model. To ensure the analysis adequately accounted for potential variations between the FEM and the physical dryer natural frequencies, three time history analyses were executed for both load cases as follows:

- Minus 10% on the time step
- Nominal time step
- Plus 10% on the time

The XGEN model was analyzed using the QCNPS Unit 2 in-plant load case with a nominal time step as an independent verification of the GE model and analysis results.

Based on the most conservative of the seven finite element analysis evaluations, modifications were added to the new dryer design to lower the stress concentrations across

the entire structure to within the design criteria. EGC previously submitted reports that described this design effort.

Independent Review
EGC's Independent Review Team, consisting of MPR Associates and Structural Integrity Associates (SIA), reviewed the new dryer design activities, including load definition, dryer design, dryer fabrication, and stress analyses. Review comments were addressed with closure issued by formal documentation from EGC.

Extensive Startup Testing

Data collection efforts on QCNPS Unit 1 included installation of strain gauges and accelerometers on the main steam lines (MSLs) and steam path components. This information was used to evaluate AC analysis and MSL vibration. Prior to startup, detailed go/no-go criteria were developed for strain gauges and accelerometers. The startup test included 15 data collection power levels up to the maximum thermal power achievable at 2902 megawatts-thermal (MWt). The QCNPS Unit 1 Startup Test Report (i.e., Reference 1) provides the results of the evaluations performed on the data collected during the startup test program.

Evaluation of the QCNPS Unit 1 Startup Test

Five different analyses were conducted with the startup test data, including the following.

- Evaluation of AC analysis
- Evaluation of SMT
- Finite element analysis of the new dryer using an AC in-plant load case
- MSL vibration
- Moisture carryover (MCO)

AC Analysis
The AC analysis methodology was evaluated using data collected on QCNPS Unit 2. EGC first compared the AC analysis predictions to the in-plant dryer pressure measurements without providing the data to Continuum Dynamics, Inc. (CDI). After the first evaluation, CDI was provided with the in-plant dryer pressure transducer data to refine the AC load prediction methodology.

By comparing the predicted and measured pressure amplitudes and frequency content, these assessments provide confidence that realistic dryer pressure loads are defined for the QCNPS Unit 1 dryer finite element analysis. Loads are accurately predicted on the outer hoods where most of the historical dryer issues and highest loads occur. The AC analysis "modified prediction" in Reference 3 tended to under-predict at low-pressure locations, and over-predicted pressures acting on the skirt. Comparing the strain gauge data from the new dryer finite element analysis with actual in-plant dryer strain measurements gave additional assurance that the AC load definition provided reliable structural response.

SMT
The QCNPS Unit 1 in-plant pressure data was compared to QCNPS Unit 1 SMT results. The conclusion for the interim SMT report is that low to mid-range frequencies are over-predicted and higher frequencies above 135 hertz are under-predicted. Additional efforts are underway that include using more detailed as-built information of the Safety/Relief Valves (S/RVs) and Electromatic Relief Valves (ERVs), and scale model testing of the

QCNPS Unit 2 as-built steam path, so that a direct comparison can be made. Reference 4 contains the interim SMT report.

Finite Element Analysis
Part of the new dryer design strategy is to compare the finite element analysis actual in-plant loads with the new dryer design load cases. To accomplish this, all MSL and QCNPS Unit 2 new dryer instrumentation data was provided to CDI to develop a refined load case using the AC methodology after it was evaluated at the highest thermal power level achieved.

- Finite element analysis results indicate that dryer integrity is assured at 2957 MWt with acceptable margin. This analysis includes a conservative shift in the defined load frequency content of +/- 10 % to address uncertainties in the FEM dynamic characteristics. These analyses showed that the stresses on the outer hood areas where the historical dryer damage occurred, and where the dryer loads are the highest, are very low.
- Since the highest thermal power achieved during startup was still approximately 70 MWt below full EPU power, finite element analysis stresses were scaled upward by a factor of 1.10. This represents a stress increase that is based on a steam velocity to the fourth power increase. This analysis showed that the new dryer is structurally adequate for EPU power levels up to 2957 MWt.

Reference 5 contains the GE stress report that summarizes the dynamic, stress, and fatigue analyses that demonstrates that the replacement steam dryer is adequate for EPU operations.

MSL Vibration Evaluation

As part of the QCNPS Unit 1 startup, both strain gauge and accelerometer data was collected on the four MSLs. This information was evaluated during the startup test and determined to be acceptable for EPU operation. Reference 1 contains the QCNPS Unit 1 startup test results.

MCO

As part of the QCNPS Unit 1 MCO evaluation, data was collected at various power levels. This information was assessed during the startup test and determined to be acceptable for current EPU operation. Reference 1 contains the QCNPS Unit 1 startup test results.

Quad Cities Nuclear Power Station, Unit 1 – Summary of 80-Day Report to the NRC

References

1) Exelon Report Number AM-2005-013, "Quad Cities Unit 1 New Steam Dryer Outage Startup Test Report," Revision 0, dated July 28, 2005
2) Exelon Report Number AM-2005-002, "Acoustic Circuit Benchmark, Quad Cities Unit 2 Instrumented Steam Path, 790 and 930 MWe Power Levels," dated June 15, 2005
3) CDI Report Number 05-10, "Benchmark of Continuum Dynamics, Inc. Steam Dryer Load Methodology Against Quad Cities Unit 2 In-Plant Data," dated July 2005
4) GE Report GENE-0000-0042-7471-01, "Interim Comparison of Quad Cities Unit 1 Scale Model Test Data with Quad Cities Unit 2 Plant Data," dated July 2005
5) GE Report GENE-0000-0043-5391-01-P, "Quad Cities Unit 1 Replacement Steam Dryer Stress and Fatigue Analysis at EPU Power Level of 2957 MWt Based on Measured EPU Conditions, GE Proprietary, dated August 16, 2005

ENCLOSURE 2

Engineering Evaluation of the Quad Cities Unit 1 Replacement Steam Dryer

ENCLOSURE 2

Attachment 1

Exelon Report Number AM-2005-013, "Quad Cities Unit 1 New Steam Dryer Outage Startup Test Report," Revision 0, dated July 28, 2005

Report Number AM-2005-013, Rev. 0
July 28, 2005

Quad Cities Unit 1 New Steam Dryer Outage Startup Test Report

Prepared By: Brian R. Strub 7/28/05
Brian R. Strub

Reviewed By: 7/28/05
Keith R. Moser

Approved By: Robert Strahnick for 7/28/05
Roman A. Gesior

Table of Contents

		Page
1.	Executive Summary	4
2.	Startup Test Purpose	4
3.	Startup Plan Overview	5
4.	Startup Testing Results	6
5.	EPU Related Startup Testing Results	7

Attachment 1 – Unit 1 Startup Test Timeline 14

Figure 1 – U1 Startup After Q1M18 18
Figure 2 – S1/S3 MSL A 651' Elev (In Plane) 19
Figure 3 – S2/S4 MSL A 651' Elev (Out of Plane) 20
Figure 4 – S5/S5A MSL A 624' Elev (In Plane) 21
Figure 5 – S6/S6A MSL A 624' Elev (Out of Plane) 22
Figure 6 – S7/S9 MSL B 651' Elev (In Plane) 23
Figure 7 – S8/S10 MSL B 651' Elev (Out of Plane) 24
Figure 8 – S11/S11A MSL B 624' Elev (In Plane) 25
Figure 9 – S12/S12A MSL B 624' Elev (Out of Plane) 26
Figure 10 – S31/S33 MSL C 651' Elev (In Plane) 27
Figure 11 – S32/S34 MSL C 651' Elev (Out of Plane) 28
Figure 12 – S35/S35A MSL C 624' Elev (In Plane) 29
Figure 13 – S36/S36A MSL C 624' Elev (Out of Plane) 30
Figure 14 – S37/S39 MSL D 651' Elev (In Plane) 31
Figure 15 – S38/S40 MSL D 651' Elev (Out of Plane) 32
Figure 16 – S41/S41A MSL D 624' Elev (In Plane) 33
Figure 17 – S42/S42A MSL D 624' Elev (Out of Plane) 34
Figure 18 – MSL A 624' Elev PSD 35
Figure 19 – MSL C 651' Elev PSD 36

Table of Contents – (continued) **Page**

Figure 20 – Quad Cities Unit 1 Moisture Carryover..... 37
Figure 21 – Quad Cities Unit 1 Reactor Water Level..... 38
Figure 22 – Quad Cities Unit 1 Reactor Pressure / Turb Throttle Pressure.....39
Figure 23 – Quad Cities Unit 1 Main Steam Line Flows..... 40
Figure 24 – Quad Cities Unit 1 Reactor Pressure / Pressure Drop / Rx Power.....41
Figure 25 – Quad Cities Unit 1 Steam Flows Deviations From Average.....42
Figure 26 – Quad Cities Unit 1 Steam Flow/Feedwater Flow Mismatch.....43
Figure 27 – Quad Cities Unit 1 Feedwater Flow.....44
Figure 28 – Quad Cities Unit 1 – Total Steam Flow/ Feedwater Flow/ Rx Power Comparisons.....45
Figure 29 – Unit 1 Startup 06/19/2005 (2898 MWt) MSL A&D 651.....46
Figure 30 – Unit 1 Startup 06/19/2005 (2898 MWt) MSL A&D 651 PSD.....47
Figure 31 – Unit 1 Startup 06/19/2005 (2898 MWt) MSL A&D 624.....48
Figure 32 – Unit 1 Startup 06/19/2005 (2898 MWt) MSL A&D 624 PSD.....49
Figure 33 – Unit 1 Startup 06/19/2005 (2898 MWt) MSL A&D 613.....50
Figure 34 – Unit 1 Startup 06/19/2005 (2898 MWt) MSL A&D 613 PSD.....51
Figure 35 – Unit 1 Startup 06/19/2005 (2898 MWt) MSL B 651..... 52
Figure 36 – Unit 1 Startup 06/19/2005 (2898 MWt) MSL B 651 PSD.....53
Figure 37 – Unit 1 Startup 06/19/2005 (2898 MWt) MSL C 651.....54
Figure 38 – Unit 1 Startup 06/19/2005 (2898 MWt) MSL C 651 PSD.....55
Figure 39 – Unit 1 Startup 06/19/2005 (2898 MWt) MSL B 624.....56
Figure 40 – Unit 1 Startup 06/19/2005 (2898 MWt) MSL B 624 PSD.....57
Figure 41 – Unit 1 Startup 06/19/2005 (2898 MWt) MSL C 624..... 58
Figure 42 – Unit 1 Startup 06/19/2005 (2898 MWt) MSL C 624 PSD.....59
Figure 43 – Unit 1 Startup 06/19/2005 (2898 MWt) MSL B&C 613..... 60
Figure 44 – Unit 1 Startup 06/19/2005 (2898 MWt) MSL B&C 613 PSD..... 61

Quad Cities Unit 1 New Steam Dryer Outage Startup Test Report

1. Executive Summary

On May 28, 2005, through June 2, 2005, Quad Cities Unit 1 was shutdown for Maintenance Outage, Q1M18, to install its new steam dryer. The unit was started up and testing was in progress from June 2, 2005, until June 5, 2005. On June 5, the unit achieved 2900 MWt (98.1%) and 920 MWe. Main generator limitations at 920 MWe and mega-volt amps reactive (MVAR) (reactive power) limitations of the grid limited the power ramp. The unit maintained a power level above 900 MWe for 6 hours, while data was recorded and compared to conservative acceptance criteria. The power level on the unit was then decreased to 2410 MWt (81.5%) (750 MWe), to a value in which all main steam line strain gauges met their Level 2 criteria. The unit was held at this power level until June 8, 2005, when EC 355874, Revision 0, authorized operation at 2511 MWt (84.9%). The unit was held at 2511 MWt until July 26, 2005, when EC 356409, Revision 0, authorized operation at 2642 MWt (89.3%). Unit 1 is expected to remain at 2642 MWt until an alternate analysis can be completed in which it is demonstrated that the steam dryer loads are acceptable at full rated power of 2957 MWt.

Because the new Unit 1 steam dryer was not instrumented, a direct measurement of the dryer loading could not be made. Instead, strain gauges were installed on the main steam lines, in the drywell, in similar locations, as strain gauges that were installed on Unit 2. The strain gauges are used to determine the time variance of pressure inside the main steam line pipe. A process was benchmarked on Unit 2, in which the main steam line strain gauges were used as the input to an acoustic circuit model that predicts pressure loadings on the steam dryer. These pressure predictions were compared to actual measurements that were part of the Unit 2 instrumented dryer. Once the ability of main steam line strain gauges to accurately predict dryer pressures was validated, Unit 1 strain gauges were to be used to determine Unit 1 dryer pressure loadings. Unfortunately, 5 of the necessary 32 strain gauges failed during Unit 1 startup. These 32 strain gauges are needed to input to the acoustic circuit model. At each location where a pressure variance signal inside the main steam line is to be obtained, 4 strain gauges are arranged around the pipe. These are located at 2 locations on each of the 4 main steam lines for a total of 32 strain gauges providing input to the acoustic circuit model. When some strain gauges are inoperable, the data from the remaining strain gauge includes more than the pipe breathing modes due to acoustic pressure oscillations. This additional content due to pipe shell mode response produces a conservative pressure load definition when the acoustic circuit methodology is applied.

2. Startup Test Purpose

The purpose of the startup test procedure was to provide step-by-step instructions in carrying out the start-up test program to Extended Power Uprate (EPU) conditions, with the Replacement Reactor Vessel Steam Dryer (Steam Dryer) in place. The incremental power increase methodology was intended to ensure a careful, monitored approach to achieve each next targeted higher power level. First and foremost in the performance of the test was the safety of the reactor and nuclear plant. The startup test procedure was written with this specifically in mind, providing the necessary criteria, instruction, oversight, and precautions to successfully execute the Reactor Vessel Steam Dryer Replacement Power Ascension Test Program.

3. Startup Plan Overview

Reactor power was raised on Unit 1 to the pre-EPU power level of 2511 MWt over a 3.5-day period. Data was taken at 10 test conditions (TCs) up to 2511 megawatts thermal (MWt). A hold period of approximately 24 hours took place at TC 10 while:

1. An evaluation of the data taken up to that point was performed,

2. A presentation of the results of the evaluation was made to PORC, and

3. Approval is given by PORC and the Plant Manager to proceed with power ascension.

Power was then raised to the maximum achievable as limited by the generator. During this power increase, data was taken at an additional five TCs (TC 11 through TC 15). For power levels both above and below EPU, there were three primary methods to obtain data at each TC.

1. High-speed data recorders captured data from:
   - 3 reactor steam dome pressure sensors
   - 4 pressure measurements at the MSL flow venturis
   - 4 main turbine control valve positions
   - 12 accelerometers on MSL components in the drywell, and
   - 40 strain gauges installed on main steam line (MSL) piping in the drywell.

2. System equipment parameters were obtained by computer points and by Operator round inputs. This data was comprised of approximately 1000 data points.

3. Data was manually gathered using handheld instruments for local vibration levels on small bore piping on the feedwater system and local area

temperatures. This data was taken at only two of the TCs, namely the pre-EPU rated power level and the maximum EPU power level.

Data Acceptance Criteria:
There were three levels of acceptance criteria documented in the Startup Test Procedure:

1. Plant Equipment Acceptance Limits: Normal alarm points or established equipment operating limitations based upon historical performance data.

2. Level 2 Criteria: Exceeding this did not necessarily result in altering plant operation or test plan, but resulted in initiating an Issue Report (IR) to enter the station's Corrective Action Program.

3. Level 1 Criteria: Actions included the initiation of an IR and seeking immediate resolution. Power was held at a known safe level based on prior testing until the condition was resolved.

For Unit 1, acceptance criteria were developed for comparison of the MSL strain gauges on Unit 1 to readings recorded on Unit 2. The readings compared both peak-to-peak values and the comparison of frequency data of power spectral density (PSD) to symmetrical locations on Unit 2. Due to the steam lines not being exactly identical in configuration with respect to the number and placement of safety valves, relief valves, and steam supplies to High Pressure Coolant Injection (HPCI) / Reactor Core Isolation Cooling (RCIC), these comparisons were both a direct reflection (MSL 1A compared to 2A, 1B compared to 2B, etc.) and a mirror reflection (MSL 1A compared to 2D, 1B compared to 2C, etc.)

4. Startup Testing Results

Attachment 1 contains the startup testing timeline for Unit 1. This timeline provides the chronology of the major startup test related events that occurred during startup and provides all the exceptions that were observed.

Figure 1 provides the power ascension profile for Unit 1 and provides a comparison of the planned profile versus the actual ascension.

Figures 2 through 17 provide trends of the comparison of Unit 1 MSL strain gauges to similar locations on Unit 2 (both the directly reflected locations and symmetrical locations). Due to the steam lines not being exactly identical in configuration with respect to the number and placement of safety valves, relief valves, and steam supplies to High Pressure Coolant Injection (HPCI) / Reactor Core Isolation Cooling (RCIC), these comparisons were both a direct reflection (MSL 1A compared to 2A, 1B compared to 2B, etc.) and a mirror reflection (MSL 1A compared to 2D, 1B compared to 2C, etc.) Noteworthy, are Figures 3, 11, 12, and 16. Figure 11 (MSL C at the 651' elevation) and Figure 16 (MSL D

at the 624' elevation) exceeded Level 1 criteria. Figure 3 (MSL A at the 651' elevation) and Figure 12 (MSL C at the 624' elevation) exceeded Level 2 criteria. These locations exceeded their criteria due to piping bending modes and not being able to have this bending subtract out due to failed strain gauges on Unit 1 as the strain gauges are combined. A PORC was held to discuss the issue and to approve TIC-1261. This revision to the startup test procedure allowed power ascension above 2410 MWt (the point where all criteria was satisfied) for up to 12 hours in order to record data at the maximum power level achievable. The procedure change was supported by Engineering Change (EC) 355836, Revision 0.

Figures 18 and 19 provide samples of Power Spectral Density (PSD) comparisons from Unit 1 to Unit 2. Figure 19 is for MSL C at the 651' elevation in which the criteria was not satisfied due to piping bending modes and not being able to have this bending subtract out due to failed strain gauges on Unit 1 as the strain gauges are combined. Note the peak at 80 Hertz, which was not observed on any other data measurement systems.

5. EPU Related Startup Testing Results

Moisture Carryover Data:
Figure 20 shows the Moisture Carryover (MCO) trend on Quad Cities Unit 1 and the time period after startup. The trend has been fairly steady with a tie to reactor thermal power, as expected.

Main Steam Line Flows/Reactor Parameters (Level/Pressure)/Feedwater Flow:
Figure 21 shows the Reactor Water Level trends of the various measurement channels for Unit 1. The trends are consistent with expectations. Step changes of these parameters were used in the past to indicate failure of the old steam dryers. The channels are trending consistent with each other. The refuel level indicator does take step changes, as expected, when recirculation flow is adjusted during power increases. Figure 22 shows the trends for Reactor Pressure and Turbine Throttle Pressure for Unit 1. Figure 23 shows the Main Steam Line flows for Unit 1. Figure 24 shows the Delta Pressure between the reactor and the main turbine, reactor pressure, and reactor power levels for Unit 1. These trends are within expectations with no anomalies detected. Figure 25 shows the Main Steam Line flow deviations from the average steam line flow for Unit 1. Figure 26 shows the feedwater flow/steam flow mismatch for Unit 1. These trends are also as expected and consistent with readings that have been recorded in the past. The indications demonstrate that there is no mismatch between feedwater flow and steam flow. Figure 27 shows the feedwater flows for Unit 1. On the trend indicated on this figure, the change in feedwater flow from starting the idle feedwater pump is evident. No issues are identified by these trends. Figure 28 shows the steam flow and feedwater flow trends for Unit 1.

Data From the Startup After the EHC Malfunction Scram – 06/19/2005
Figures 29 through 44 present frequency plots of peak-to-peak root mean square (RMS) and PSD plots of the Unit 1 Main Steam Line Strain Gauges compared to Unit 2. This data was obtained on Unit 1 on June 19, 2005, after returning to power from the Electro-Hydraulic Control (EHC) scram. During the startup, strain gauge pairs S1/S3 (MSL A-651'), S32/S34 (MSL C-651'), S36/S36A (MSL C-624'), S37/S39 (MSL D-651') failed. Data analysis taken at this power level determined that strain gauge S-31 (MSL C-651') also had failed. Data analysis from Q1F54 startup determined that, due to the number of lost strain gauges on MSL C, an acoustic circuit load definition could not be performed. The data from "B" MSL and remaining pairs on "A" and "D" MSLs were used for comparison purposes and presented to the NRC Staff on June 30, 2005.

Main Steam Line Flows:
The following data was taken on Unit 1 and Unit 2 with the units at maximum thermal power with the old dryer and with the new dryer. The comparisons show that there is no appreciable difference in main steam line flow with the installation of the new steam dryers. Tables 1 and 2 seem to provide reasonable results in that the normalized flow through Main Steam Lines "A" and "D" are higher than "B" and "C" for both units. This is expected since the "A" and "D" Lines are the shorter Main Steam Lines.

Table 1

Comparison of U1 Old Dryer to U1 New Dryer			
3 Hour Average MSL Flows	Old Normalized Flow	New Normalized Flow	Old vs New % Chg
MSL	12/30/2003 14:00 to 12/30/2003 17:00	6/5/2005 14:00 to 6/5/2005 17:00	
A	1.027	1.023	0.40%
B	0.978	0.975	0.28%
C	0.993	0.995	-0.15%
D	1.002	1.007	-0.54%

Table 2

Comparison of U2 Old Dryer to U2 New Dryer			
3 Hour Average MSL Flows	Old Normalized Flow	New Normalized Flow	Old vs New % Chg
	8/11/2004 15:00 to	5/22/2005 3:00 to	
MSL	8/11/2004 18:00	5/22/2005 6:00	
A	1.028	1.033	-0.45%
B	0.986	0.987	-0.05%
C	0.970	0.959	1.12%
D	1.015	1.021	-0.57%

Vibration Measurements

Engineering Change (EC) Evaluation (EVAL) 355773, Revision 0, evaluated in detail, the data and results from the vibration data recorded on Unit 1. Presented below is an excerpt from the detailed evaluation:

Results

The data obtained from the power ascension to 2887 MWth has been assessed against the previously completed evaluations and no concerns were identified. Details of the evaluation are provided below. Previous recommended actions are tracked under AR 194877 and are not changed by this current evaluation.

Detailed Evaluation:

Component Damage Summary (Quad Unit 1)

Walkdowns of MSL affected components were performed during the recently completed Q1R18 (April 2005) to identify any components that exhibited vibration induced degradation. These walkdowns were conducted even though the unit did not operate at EPU power levels since the original walkdowns in 2003. Several IRs were initiated as a result of these walkdowns, for general loose nuts and bolts. The results are documented by the station and will not be repeated here. The MSL drain tie-back supports were found significantly damaged (see IR 315403). A failure analysis by Power Labs determined that the failure was caused by the installation of the c-clamps used to mount the accelerometers at this location combined with the vibration levels. Actions and resolution for that issue can be found in the AR documentation.

The minor discrepancies found on other components were attributed as the result of normal aging or were historical in nature.

Acceptability of ERV Component Operation at EPU Levels

The four ERVs have virtually identical assemblies and are identical to the Unit 2 assemblies, which consist of the main ERV valve body, pilot valve, and solenoid actuator. The pilot valve is connected to the ERV by means of a turnbuckle and a pilot valve tube. Each valve has small diameter leak off piping that is routed back to the ERV discharge line.

Details of the testing and results can be found in the documentation package supporting modification EC 343933. It was determined through testing that an independent structural mode of the actuator plunger assembly was responding to input vibrations, causing premature wear degradation of the bushing, spring and guide rod assembly due to vibration in the frequency range of 70-90 Hz. The valve assemblies installed in Unit 1 were upgraded with hardened components of X750 material for bushings and guide rods and a modified spring, with chamfered edges. These components underwent testing prior to their use to ensure that they would perform at measured vibration levels without experiencing degradation. Comparison of the vibration values used for the modification evaluations are bounding for the Unit 1 measured values in the frequency bands of concern and therefore, these valves are acceptable for full EPU power operation, per Attachment 1.

Evaluation of HPCI 4 Valve Operator

Based on comparison of the current vibration data to the data evaluated under EC 348316, the Unit 2 values in EC 355702 and testing results in EC 350691, the original evaluation and testing remain bounding and there are no concerns for acceptable long term operation of this actuator and limit switch. The maximum measure grms value was in the x direction at 1.3924, from channel 25 at 930 MWe on Unit 2, which bounded the HPCI location from the original component assessments. From page 7, section 4.2.1 of Calc- QDC-0200-M-1392 the testing input used was a grms value of 3.9, which related to a plant input of 0.45 grms equated to 21567 hours of operation. For the measured 1.3924 grms this results in approximately 6970 hours of operation (or just over one year). However, since the principle component in this grms value was at the high frequency of 138 Hz, and no component response except some bolt loosening was seen after this duration, the Limitorque actuator is deemed acceptable for continuous full power operation. Also, the recommended inspections from EC 346515 (documented under ATI 194877-33) will ensure that loosened connections are detected so that appropriate repairs can be made, each outage until sufficient experience allows for extension. The next performance of this inspection on Unit 1 will occur during Q1R19 in Spring 2007.

Evaluation of MSIVs

Comparison of the current measured vibration levels at the B & C ERVs indicates that the original assessment of the MSIV acceptability in EC 346515 for the B, A & D MSIVs remains bounding. For the C MSIV, the currently measured C ERV data is significantly less that the data taken in 2003 with grms value of 1.1007 versus the 2003 grms value of 4.16. Although this value remains higher than the other ERVs, it makes the extrapolation to the MSIV, by reduction factor of 3, produce a value of 0.333 grms. This places the values well below the values from the seismic aging test results used to evaluate these valves in EC 346515. Therefore all MSIVs are considered acceptable, and no further corrective actions are required. Inspections already developed in response to EC 346515 remain as recommendations. The only exception is the need to monitor the C MSIV with accelerometers, which is no longer a requirement.

Evaluation of Target Rock Valves

The Target Rock valve is evaluated in Attachment 1 and comparison to the original evaluation by comparing the measured data to the testing input values documented in EC 350693. Since the frequency domain of concern for valve response is between 20 – 100 HZ and the increased vibration response seen was in the domain of 100 – 200 Hz, there is no concern for long-term acceptability of the modified valve configuration. The hardened upgraded components were used in the replacement value installed during this outage Q1M03.

Conclusions / Findings:

This EC EVAL provides an Engineering Evaluation of MSL components supporting operation up to 2957 MWth. It has been determined that this full EPU power operation will not result in imminent failure or unacceptable degradation levels of any components. The conclusion is provided by evaluation of the measured vibration data, previous evaluations and test reports from laboratory testing.

Small-Bore Piping/Feedwater Sample Probes:

During Unit 1 startup, measuring local vibration data assessed small-bore piping. Vibration data was taken on small bore piping for Feedwater pump suction relief valves and discharge drain lines, Feedwater Reg. Station vents and drains, and HPCI Local Leak Rate Test (LLRT) line. The results were compared to acceptance criteria that was developed based on Exelon Corporation Nuclear Engineering Standard NES-MS-03-04, which utilizes a conservative Electric Power Research Institute (EPRI) model. All locations were satisfactory except for line 1-3417B-1", Feedwater Suction Isolation Bypass Line. The maximum allowable velocity amplitude is 2.70 in/sec and the measured resultant velocity was 2.75 in/sec (exceeds by less than 2%). This is documented in IR 341151. EC 355944, Revision 0, and Action Tracking Item 341151-02 will document the acceptability of the measured vibration levels.

Dresden Condition Report (CR) 190413 generated on 12/12/03 identified a Feedwater sample probe found missing. The probe in question had previously

failed and was replaced in 2001 with a new probe designed per GE Service Information Letter (SIL) 257, which was supposed to fix the problem. Pieces of the probe were found in the feedwater sparger. Quad Cities CR 190513 reviewed the Dresden issue and an Operability Determination was performed even though there was no evidence of the probes breaking at Quad Cities. At subsequent outages, inspections were performed and probes were found to be intact. However, Quad Cities performed similar actions as Dresden. The Feedwater sample probe, 1-0632, was cut out and replaced with a new shorter probe design under Work Order (WO) 00689963. The old probe was inspected and found to be in good condition with 100% of the length intact and no indication of cracking or loss of material to the Reactor vessel. A new probe that is approximately 2" in length as compared to 13" for the old probe was installed. Similar results and actions were performed on Unit 2 under WO 00658382. These actions were performed during Q1R18 and Q2R17.

Operational Issues With Plant Systems/Components:

LLRT of the Drywell Personnel Hatch (X-2)

During startup of the units, operational issues were observed on the Drywell Personnel Hatch Local Leak Rate Test (LLRT) on Unit 1. The issue was documented on Issue Reports (IR) 340591 and IR 340898. Unit 1 Drywell Airlock X-2 Local Leak rate test (LLRT) per QCTS 600-04 exceeded TS (section 5.5.12 d.2.) admin Limit of 22.88 standard cubic feet per hour (scfh) with an indicated leakage of 50.81 scfh. Post-test investigation identified a leak within the test equipment. A retest was re-performed with different test equipment, however, the results still were not acceptable. Initially, a post-test visual inspection of the door gaskets, hand wheels and equalization valves failed to indicate any obvious sources for the indicated leakage. A detailed post-test visual inspection of the door gaskets after the second failed test identified that the inner door gasket had taken a significant permanent set in an area that also had a 6 inch tear outside but parallel the seal area. When closed, each doorframe has one gasket that gets depressed by the doors blunt knife-edge. The Vendor (VETIP) manual C0058 section 2.5.5 states, "The permanent set will increase with time until the door will no longer maintain a pressure tight seal. At this time the gasket will have to be replaced. The expected life of the gasket is a minimum of six months". A formal Apparent Cause Evaluation (ACE) is underway. Final corrective actions will be determined by the ACE, however, these actions will probably include a preventative maintenance predefine to replace the gasket on a periodic basis.

EHC Scram

On 06/17/05 at 1120, the Unit 1 reactor automatically scrammed from 85% power due to a valid high reactor pressure signal. This event is documented under IR 345152 and a formal root cause investigation is in progress. The maximum reactor pressure was approximately 1044 psig

during the event. All control rods inserted to their full-in position. Initial indications are that the reactor pressure increase was caused by a malfunction of the Electro-Hydraulic Control (EHC) system, which resulted in closure of the main turbine control valves. The main turbine bypass valves (nine) opened as expected in response to the pressure increase. No reactor pressure vessel safety or relief valves were required to actuate during the event. Reactor water level decreased to approximately -20 inches, which resulted in automatic Group 2 and 3 isolations as expected. All systems responded properly to the event. A troubleshooting team was assembled to investigate and correct the cause of the event.

Initial corrective actions included the replacement of the circuit boards associated with the three low value gate circuits used in the control valve demand circuit.

(A) Control Valve Amplifier (Circuit Board A48) and Operational Amplifier (Circuit Board A49)
(B) Load Limit (Circuit Board A33) and Operational Amplifier (Circuit Board A34)
(C) Pressure Load Gate Amplifier (Circuit Board A58) and Operational Amplifier (Circuit Board A59)

In addition, there is increased monitoring of the control valve demand circuit. Included in this monitoring is the output of the load limit circuit and the control valve amplifiers. This will provide information on which of the low value gates is in control of the control valve demand signal in the event that this occurs again.

Valve 1-3508B, 1B Moisture Separator Drain Tank (MSDT) to 1D2 Heater Normal Level Control Valve (LCV), stuck greater than 33% open

During the placement of the feedwater (FW) heaters into operation, it was discovered that the 1-3508-B valve is stuck approximately 33% open. The governing procedure (QCOP 3500-02) requires the MSDT normal LCV's to be verified closed prior to unisolating LCV's. This event delayed startup on Unit 1 for six hours while the issue was investigated. It was determined that the startup could continue and the valve will be repaired at the next outage of sufficient duration. The valve is needed to stay nearly full open during normal operation and therefore it being unable to close down below 33% will have no operation impact. The valve will be repaired under Work Order (WO) 00817173.

Overall plant and system performance from personnel interviews and walkdowns

On Unit 1, at TC 15, 2888 MWt (97.6%), locally recorded data was obtained on various ventilation temperatures and area temperatures in the plant. All readings

were acceptable except the Exhaust Air Temperature from the Reactor Feed Pump Motors. The acceptance criterion was 130 deg F and the 1A and 1C Reactor Feed Pump Motor Exhaust temperatures were 132 deg F. The procedure directed notification to the System Manager. The System Manager proposed this criterion to stay below the alarm point of 135 deg F, which was still met. At the present time, actions are underway under IR 348700 to improve the effectiveness of the turbine building ventilation system.

A shift manager made the following statement concerning his observations when Unit 2 was operating at the maximum thermal power:

> "I was on shift during the time U-2 was at 930 MWe and walked down some of the systems I was most concerned about. I am more concerned with the secondary side of the steam plant such as feedwater heating, equipment vibrations etc. more so than the reactor side. I was pleased to see that there were very few concerns identified while at the elevated power. I noted the areas of concern in my parameter review below. The point I tried to make with the flash tanks, is that they are very near full open, but they are still controlling. They are not max'd out. When U-1 was at a higher power (in the past) it seemed to have more problems with vibration and noise so I'll reserve comment on it until I see how it performs. It also remains to be seen how we will cope with the higher power levels when ambient is in the upper 90's and the river is hot, but we are off to a pretty good start. I have been an operator here at Quad since the early 80's when we had ALOT of vibration issues and recall them well. We certainly don't want to go back to those days. My crew and I are optimistic after seeing U-2 at 930 MWe."

The following is a statement made by the Operations Manager:

> "Several things have happened recently to mitigate a large portion of the "uncomfortable" feeling on the part of some Operators. The EPU technical forums allowed them to ask any and all questions related to EPU issues. We made sure that they all had access to the presentations or submitted written questions. Tapes of the forums were run on the ready room TV. They were given clear answers, including "we don't know, but this is how we are going to use the instrumentation to validate our design models". That kind of straightforwardness helped. Several Operators took the opportunity to look at the dryer while it was at JT Cullen. The structure is impressive. The test program was clearly communicated, and the fact that we did what we said, i.e. backed the unit down to within SG #7 criteria (we updated the instrumentation graphs for the control room crews shiftly) showed we have a clear plan. Finally, the fact that the Unit is relatively well behaved right now gives a measure of comfort. "

Attachment 1
Unit 1 Startup Testing Timeline

05/28/2005 00:01 -	Unit 1 is shutdown for Q1M18 to install its new steam dryer.
06/01/2005 17:35 -	Temporary/Interim Changes (TIC) procedure TIC-1252, Quad Cities Unit 1 Power Ascension Test Procedure for the Reactor Vessel Steam Dryer Replacement has all prerequisites complete.
06/02/2005 03:00 -	At Test Condition (TC) 1, Main Steam Line (MSL) strain gauges S6, S11A, and S31 are determined to be non-functional. This is documented in Issue Report (IR) 340618. In addition, recorder channels #1 (pair S1/S3) and #4 (pair S6/S6A) could not be balanced. Troubleshooting is being initiated to get the channels balanced.
06/02/2005 09:30 -	Unit 1 is synchronized to the grid, ending Q1M18.
06/02/2005 11:00 -	After discussions with Yokogawa and Hi-Tec (strain gauge supplier) appropriate resistors are added to balance the troublesome strain gauges. As documented above, main steam line strain gauge S-6 is determined to have failed.
06/03/2005 14:05 -	At TC 5, at 1768 MWt (59.8%), MSL strain gauge S-36 was determined to have failed. This is documented in IR 340929.
06/03/2005 18:05 -	At TC 8, at 2225 MWt (75.2%), MSL strain gauge data is taken.
06/03/2005 21:35 -	At TC 8, at 2225 MWt (75.2%), a Moisture Carryover Sample is taken. The results were later determined to be 0.003%
06/04/2005 00:04 -	At TC 9, at 2414 MWt (81.6%), MSL strain gauge S-3 was determined to have failed. This is documented in IR 340929.
06/04/2005 00:58 -	At TC 10, at 2508 MWt (84.8%), MSL strain gauge data is taken.
06/04/2005 05:35 -	At TC 10, at 2508 MWt (84.8%), a Moisture Carryover (MCO) sample is taken. The results were later determined to be 0.013%.
06/04/2005 05:45 -	The results of the analysis of the MSL strain gauge data indicates that strain gauge pair S32/S34 on C MSL at elevation 651', exceeded the "peak-to-peak" Level 1 acceptance criteria. Per TIC-1252 Section 5.1.1.1, the unit will be placed in a known safe condition based on prior testing. This issue is documented in IR 340961. At Test Condition 9, all data was evaluated as acceptable. Therefore, the unit is being taken to TC 9, 2410 MWt (81.5%) until a formal analysis can be completed.

Attachment 1
Unit 1 Startup Testing Timeline

06/04/2005 06:32 - Began to decrease Unit 1 power to 2410 MWt (81.5%) where all testing data was found to be acceptable.

06/04/2005 06:50 - Holding Unit 1 power at 2410 MWt (81.5%) 750 MWe.

06/04/2005 14:00 - A conference call with the NRC (Region III and NRR) is held at this power level to discuss the data taken and planned actions for the continued power ascension. It is decided that another update will be provided to the NRC on 06/05/2005.

06/05/2005 01:30 - The results have been received from the acoustic circuit analysis of data taken at TC 10, 2508 MWt (84.8%). The results, which are predicted dryer peak-to-peak pressures compared to actual corresponding values measured on Unit 2, showed that level 2 criteria was not met. This is documented in IR 341056.

06/05/2005 06:00 - A PORC is held to discuss the data taken up to this point in the startup and to approve TIC-1261. This revision to the startup test procedure allows power ascension above 2410 MWt (81.5%) for up to 12 hours to allow data to be recorded at the maximum power level achievable. The procedure change is supported by Engineering Change (EC) 355836, Revision 0.

06/05/2005 09:00 - A conference call with the NRC (Region III and NRR) is held at this power level to discuss the data taken and planned actions for the continued power ascension.

06/05/2005 10:08 - Beginning a Unit 1 power increase to above 2511 MWt (84.9%).

06/05/2005 10:15 - Power is increased above 2511 MWt (84.9%).

06/05/2005 10:24 - Holding Unit 1 power at TC 11, 2651 MWt (89.7%) 823 MWe.

06/05/2005 13:48 - Holding Unit 1 power at TC 15, 2887 MWt (97.6%) 910 MWe.

06/05/2005 14:00 - Drywell accelerometer data was taken on Main Steam Line Relief Valves. Structural Evaluation EC 355773, Revision 0, reviewed all the data taken during the startup testing and the EC concludes, "full EPU power operation will not result in imminent failure or unacceptable degradation levels of any components. The conclusion is provided by evaluation of the measured vibration data, previous evaluations and test reports from laboratory testing."

06/05/2005 14:40 - At TC 15, 2887 MWt (97.6%), vibration data was taken on small bore piping for Feedwater pump suction relief valves and discharge drain lines, Feedwater Reg. Station vents and drains, and

HPCI Local Leak Rate Test (LLRT) line. All locations were satisfactory except for line 1-3417B-1", Feedwater Suction Isolation Bypass Line. This is documented in IR 341151. EC 355944, Revision 0, and Action Tracking Item 341151-02 will document the acceptability of the measured vibration levels.

06/05/2005 15:00 - At TC 15, 2888 MWt (97.6%), locally recorded data was obtained on various ventilation temperatures and area temperatures in the plant. All readings were acceptable except the Exhaust Air Temperature from the Reactor Feed Pump Motors. The acceptance criterion was 130 deg F and the 1A and 1C Reactor Feed Pump Motor Exhaust temperatures were 132 deg F. The procedure directed notification to the System Manager. The System Manager proposed this criterion to stay below the alarm point of 135 deg F, which was still met. At the present time, actions are underway under IR 348700 to improve the effectiveness of the turbine building ventilation system.

06/05/2005 16:00 - At TC 15, at 2887 MWt (97.6%), a Moisture Carryover (MCO) sample is taken. The results were later determined to be 0.017%.

06/05/2005 17:17 - Within TC 15, power is increased to 2900 MWt (98.1%), 920 MWe. The power ramp is limited by Main Generator limitations at 920 MWe and MVAR limitations of the grid.

06/05/2005 17:32 - All necessary data has been obtained and a power reduction is begun.

06/05/2005 18:04 - Holding Unit 1 power at 2410 MWt (81.5%).

06/08/2005 07:00 - Power level on Unit 1 is raised to 2511 MWt (84.9%) based upon EC 355874, Revision 0.

06/17/2005 11:20 - Unit 1 scrammed from 2511 MWt (84.9%) due to a failure of an Electro-Hydraulic Control (EHC) card unrelated to the steam dryer and unrelated to EPU. During the subsequent forced outage, an attempt was made to repair the failed MSL strain gauges.

06/19/2005 17:00 - Temporary/Interim Changes (TIC) procedure TIC-1263, Quad Cities Unit 1 Power Ascension Test Procedure for the Reactor Vessel Steam Dryer Replacement has all prerequisites complete. This version of the startup test procedure will re-perform test conditions 10 through 15. EC 355976, Revision 0, supported testing up to full EPU power level for the purpose of recording data. At this time, data is taken for TC 10, 2511 MWt (84.9%). At

	TC 10, strain gauge pairs S1/S3, S32/S34, and S36/S36A would not balance. IR 345443 documents the condition.
06/19/2005 18:41 -	At TC 11, 2657 MWt (89.9%), strain gauge pair S37/S39 would not balance. IR 345443 documents the condition.
06/19/2005 21:02 -	Achieved TC 13, 2902 MWt (98.1%). Power was limited to this power level due to main generator limitations. Data analysis taken at this power level determined that strain gauge S-31 had failed. Data analysis from Q1F54 startup determined that, due to the number of lost strain gauges on MSL C, an acoustic circuit load definition could not be performed. The data from "B" MSL and remaining pairs on "A" and "D" MSLs were used for comparison purposes and presented to the NRC Staff on June 30, 2005.
07/26/2005 10:00	A conference call was held with the NRC Technical Staff, NRR, and the Region to discuss plans to raise Unit 1 to 2642 MWt based upon finite element analysis of data that was gathered at TC 11 on June 5, 2005, during the initial startup with the new dryer.
07/26/2005 12:40	Power was raised to 2642 MWt after EC 356409, Revision 0, authorized operation at 2642 MWt (89.3%). Unit 1 is expected to remain at 2642 MWt until an alternate analysis can be completed in which it is demonstrated that the steam dryer loads are acceptable at full rated power of 2957 MWt.

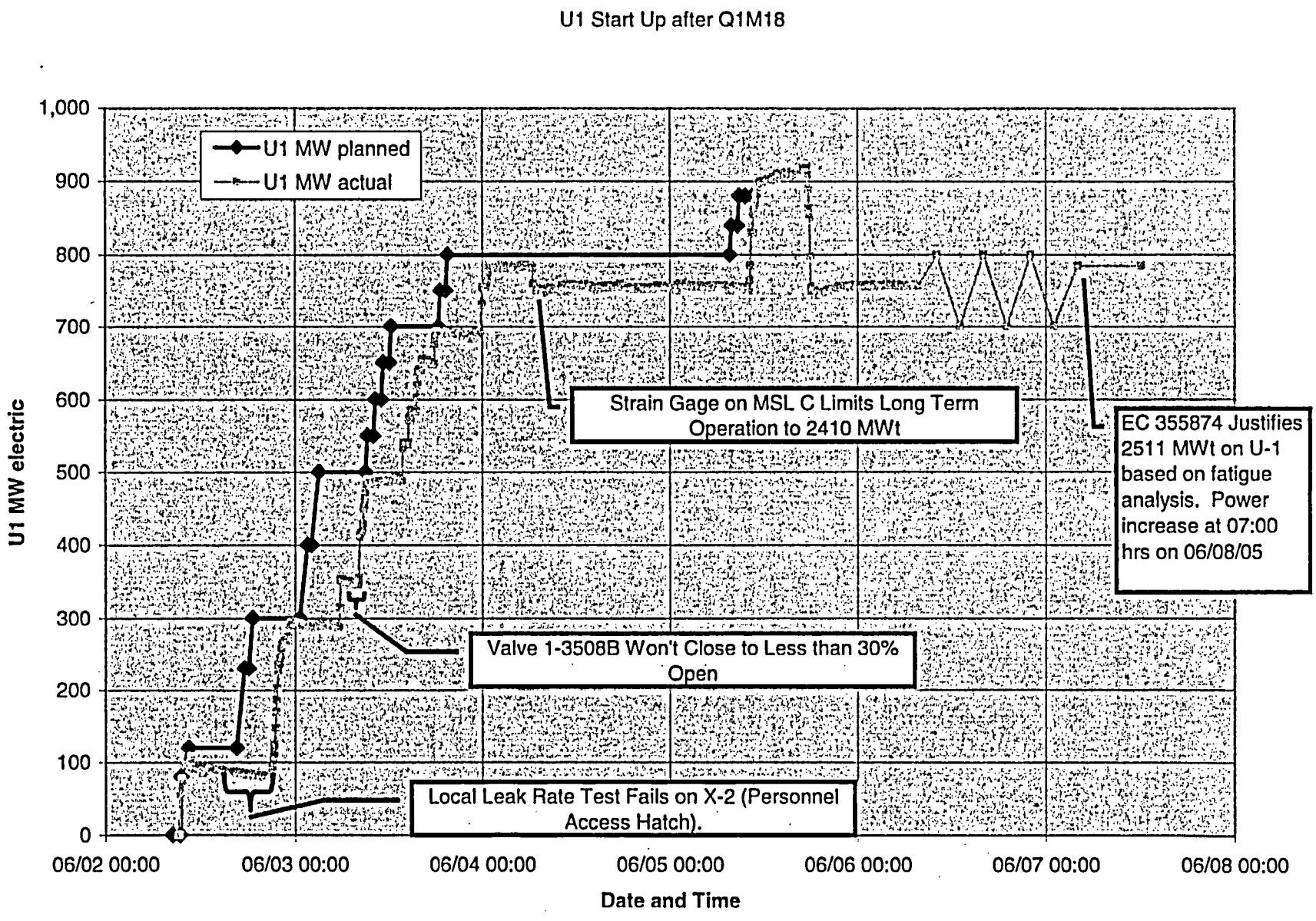
U1 Start Up after Q1M18
U1 MW planned
U1 MW actual
U1 MW electric
1,000
900
800
700
600
500
400
300
200
100
0
06/02 00:00
06/03 00:00
06/04 00:00
06/05 00:00
06/06 00:00
06/07 00:00
06/08 00:00
Date and Time
Strain Gage on MSL C Limits Long Term Operation to 2410 MWt
EC 355874 Justifies 2511 MWt on U-1 based on fatigue analysis. Power increase at 07:00 hrs on 06/08/05
Valve 1-3508B Won't Close to Less than 30% Open
Local Leak Rate Test Fails on X-2 (Personnel Access Hatch).

Figure 2

Unit 1 Startup Results

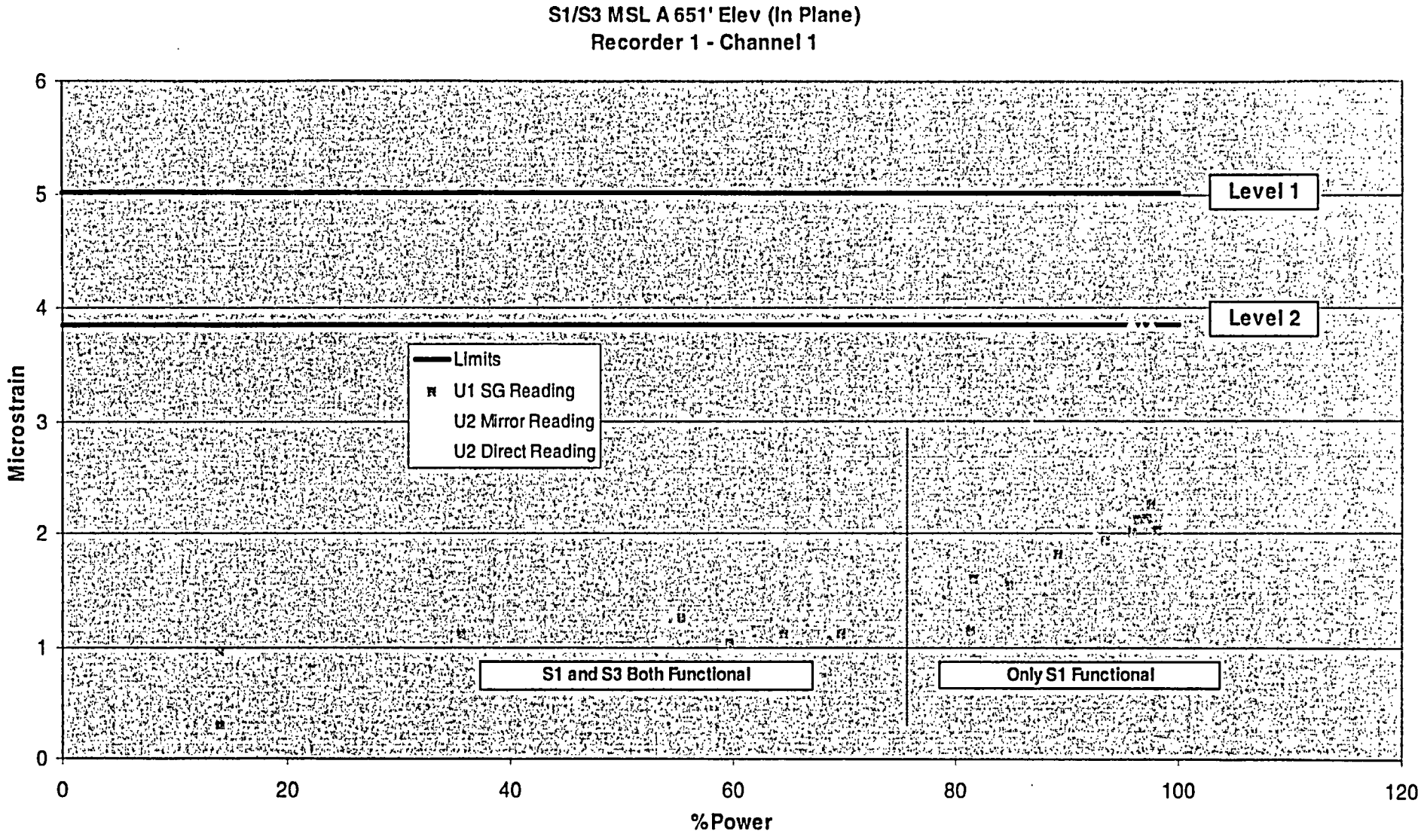

Figure 3

Unit 1 Startup Results

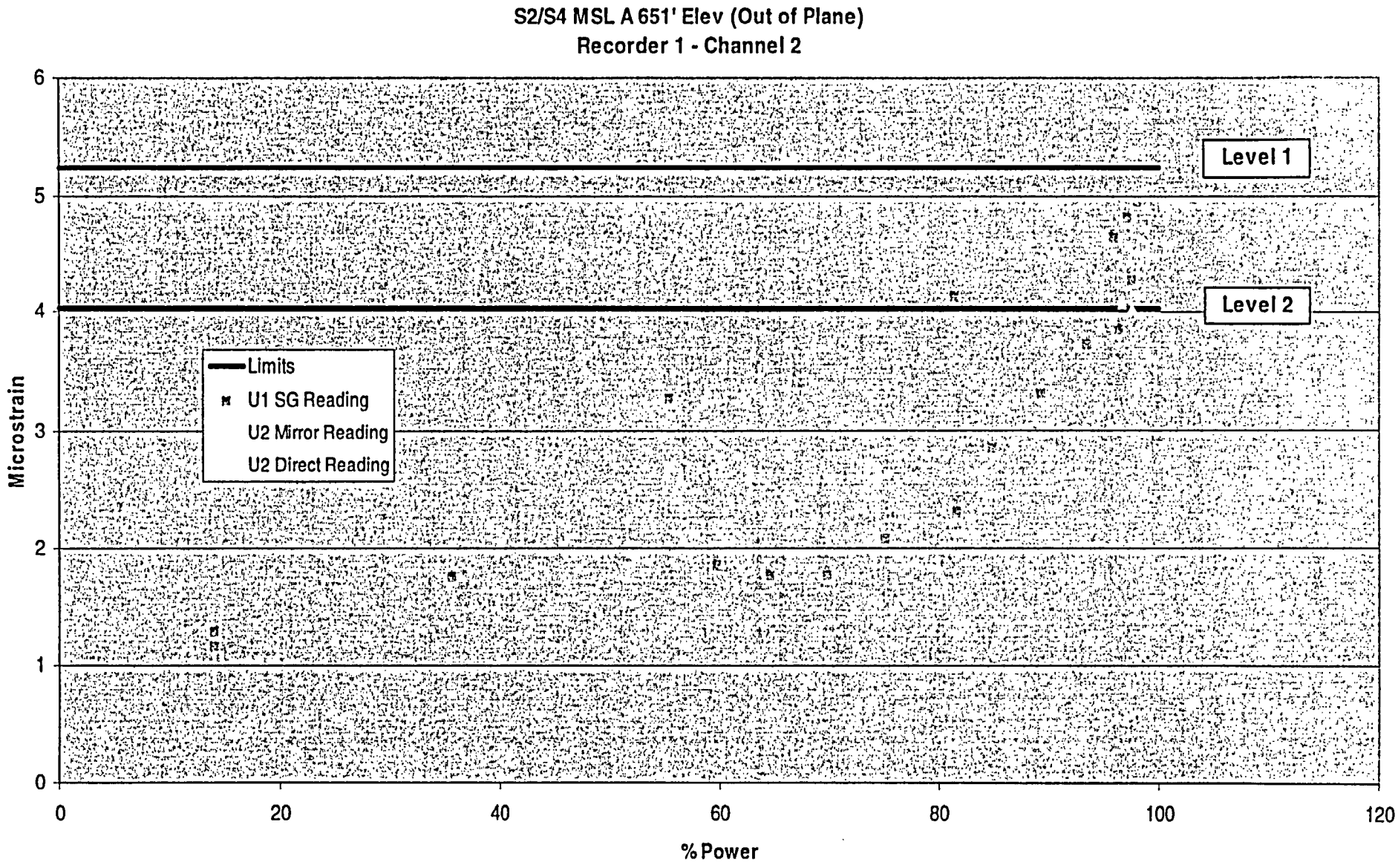

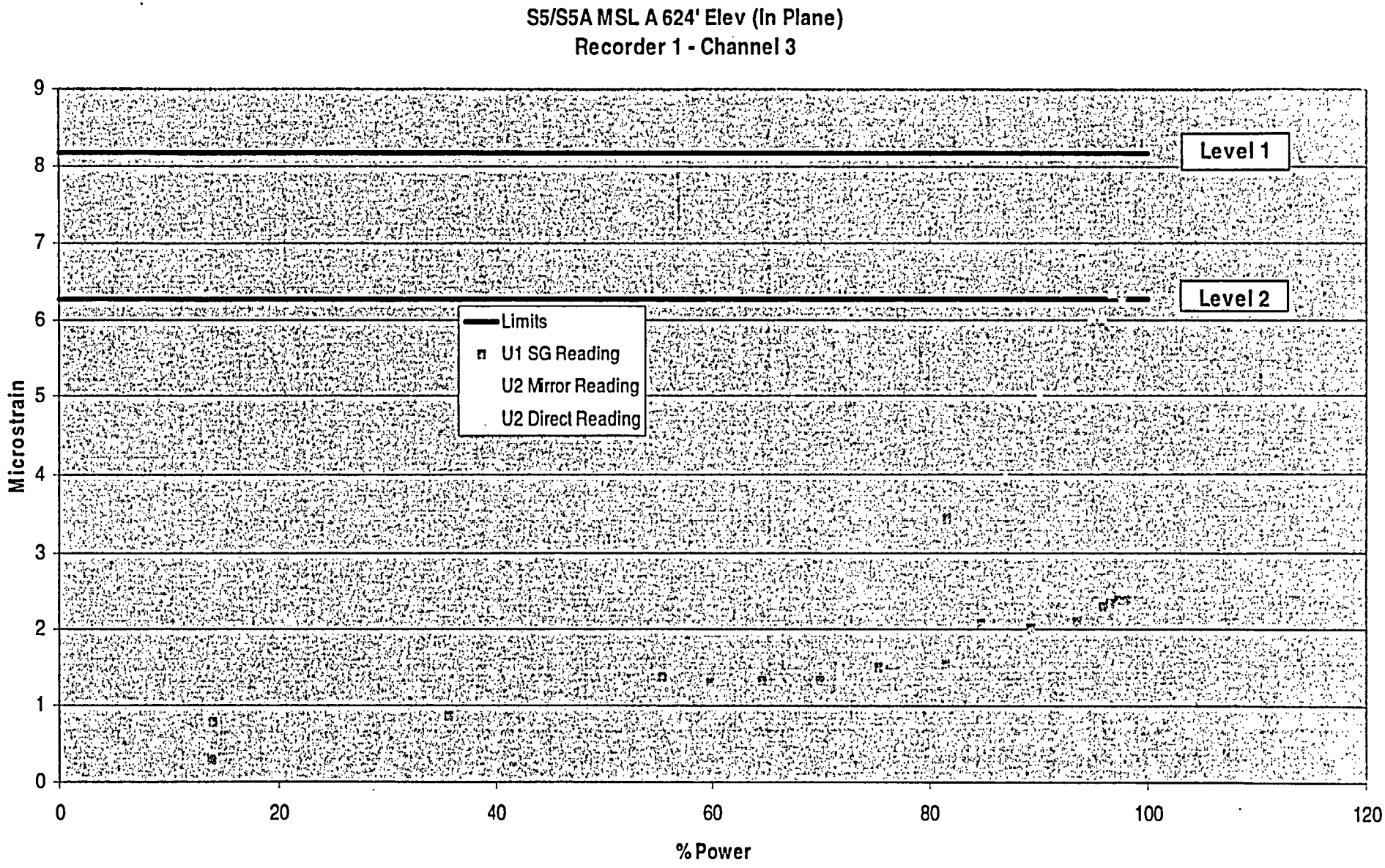
S5/S5A MSL A 624' Elev (In Plane)
Recorder 1 - Channel 3
Level 1
Level 2
Limits
U1 SG Reading
U2 Mirror Reading
U2 Direct Reading
Microstrain
0
1
2
3
4
5
6
7
8
9
0
20
40
60
80
100
120
% Power

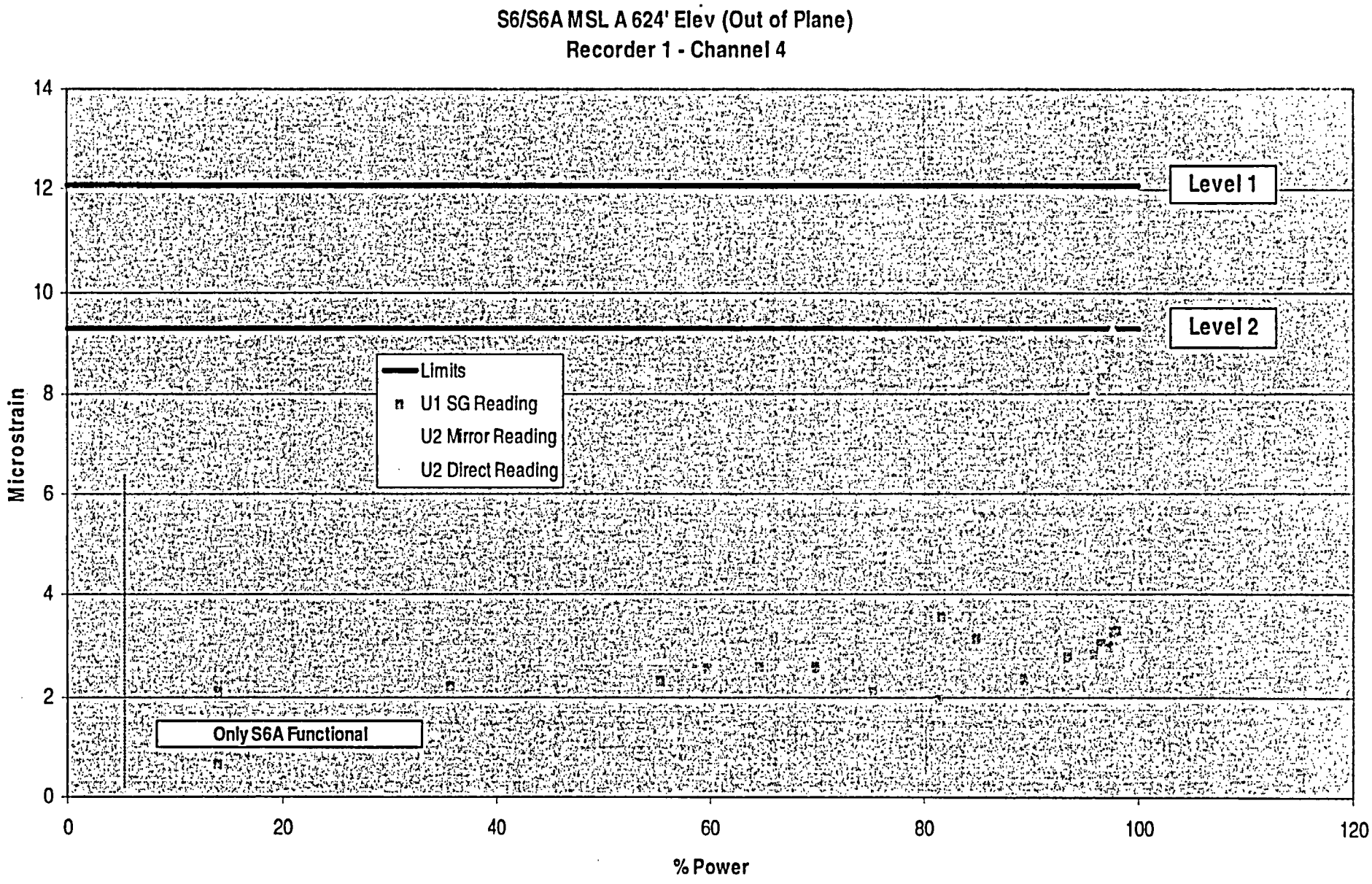
S6/S6A MSL A 624' Elev (Out of Plane)
Recorder 1 - Channel 4
Microstrain
14
12
10
8
6
4
2
0
Level 1
Level 2
Limits
U1 SG Reading
U2 Mirror Reading
U2 Direct Reading
Only S6A Functional
0
20
40
60
80
100
120
% Power

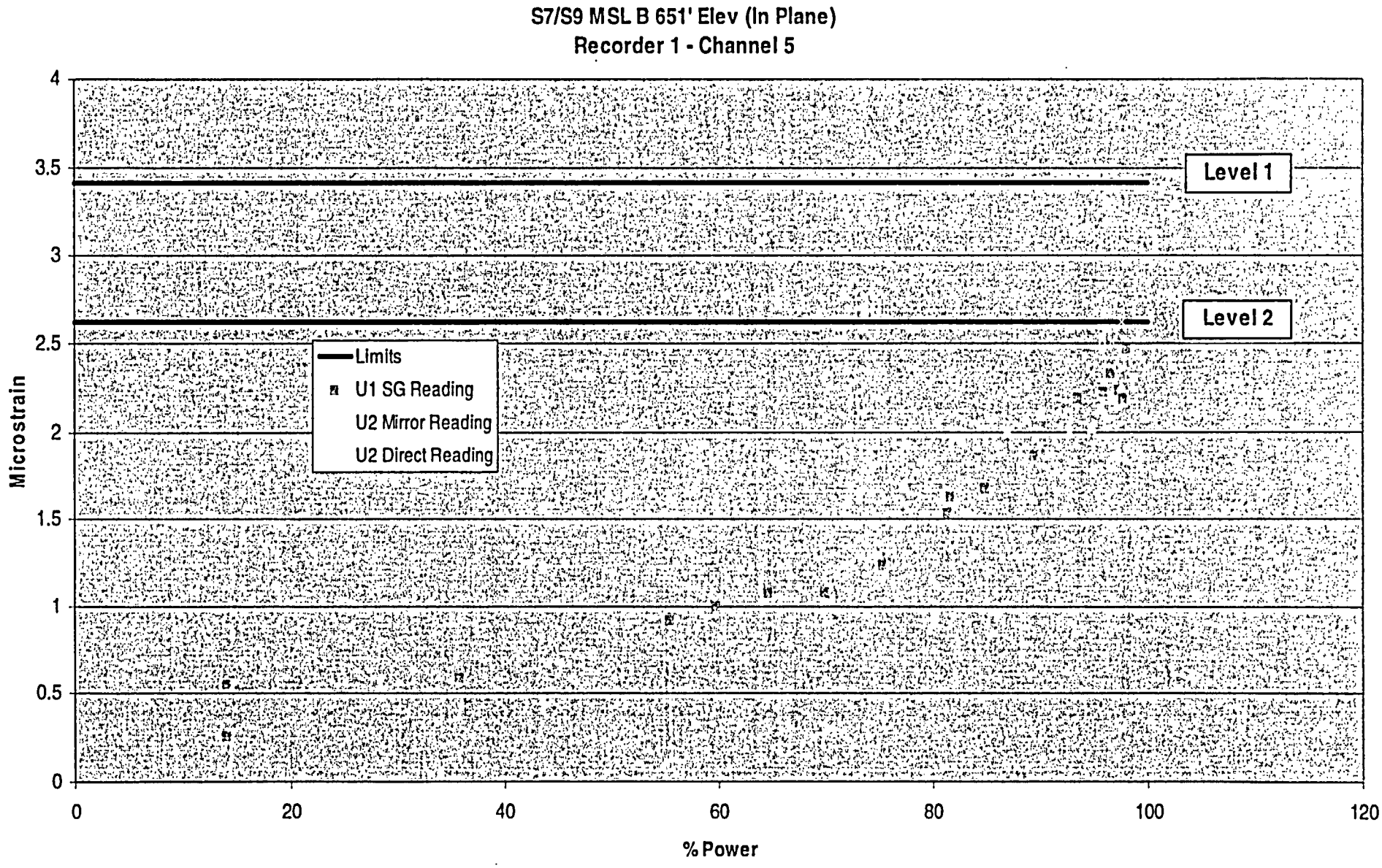
S7/S9 MSL B 651' Elev (In Plane)
Recorder 1 - Channel 5
Microstrain
% Power
Level 1
Level 2
Limits
U1 SG Reading
U2 Mirror Reading
U2 Direct Reading
0
0.5
1
1.5
2
2.5
3
3.5
4
0
20
40
60
80
100
120

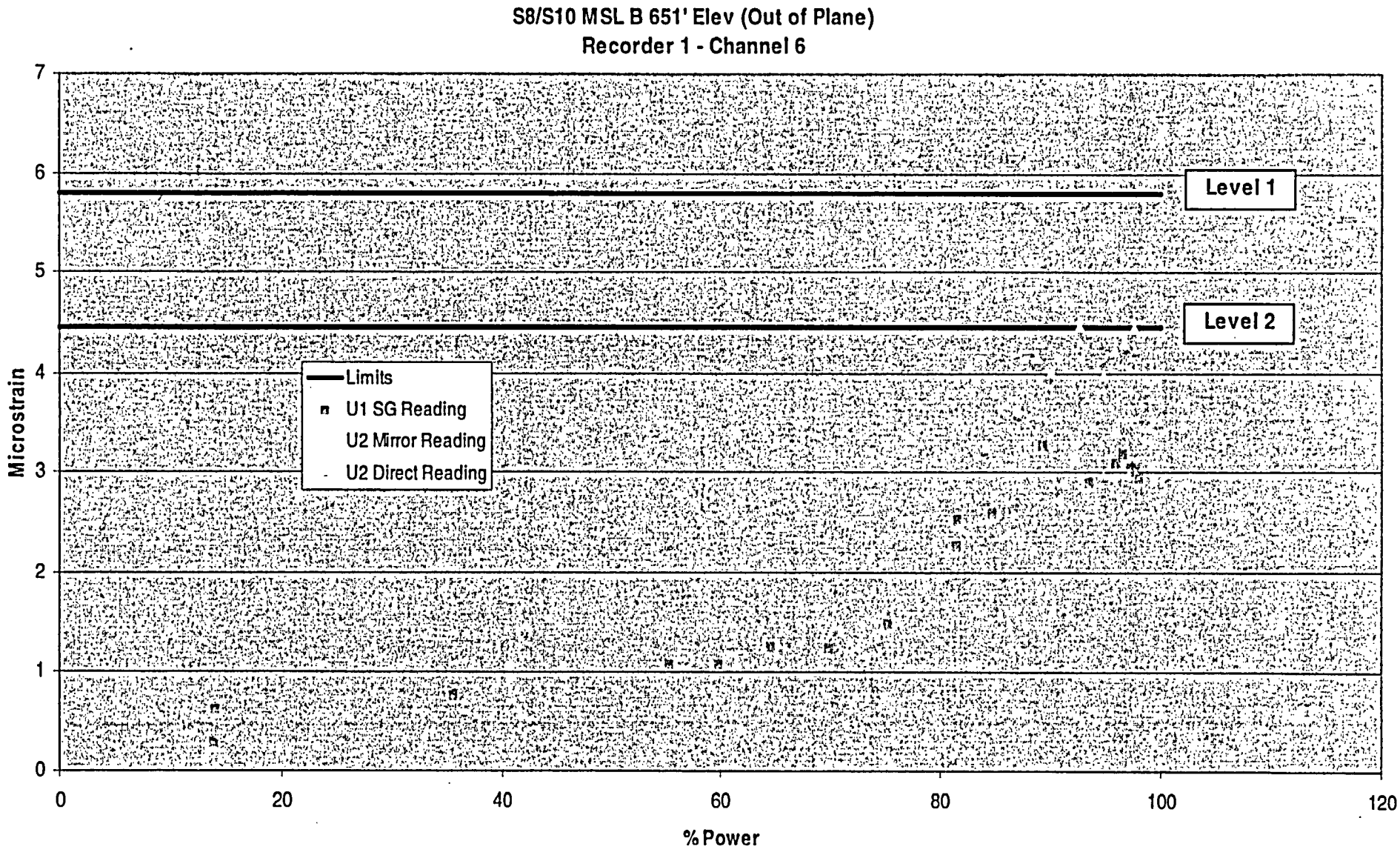
S8/S10 MSL B 651' Elev (Out of Plane)
Recorder 1 - Channel 6
Microstrain
7
6
5
4
3
2
1
0
Level 1
Level 2
Limits
U1 SG Reading
U2 Mirror Reading
U2 Direct Reading
0
20
40
60
80
100
120
% Power

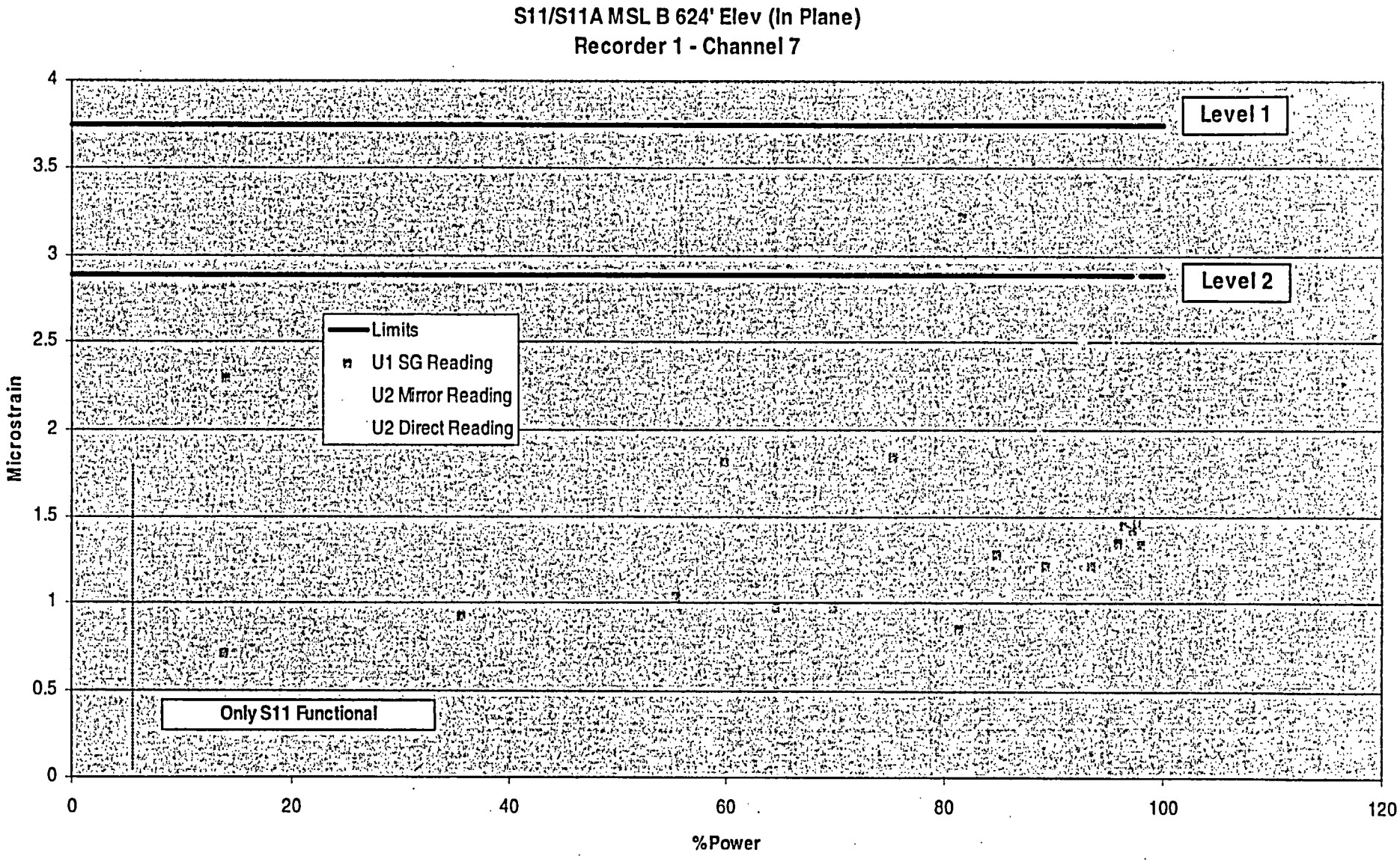
S11/S11A MSL B 624' Elev (In Plane)
Recorder 1 - Channel 7
Level 1
Level 2
Limits
U1 SG Reading
U2 Mirror Reading
U2 Direct Reading
Only S11 Functional
Microstrain
%Power
0
0.5
1
1.5
2
2.5
3
3.5
4
0
20
40
60
80
100
120

Figure 9

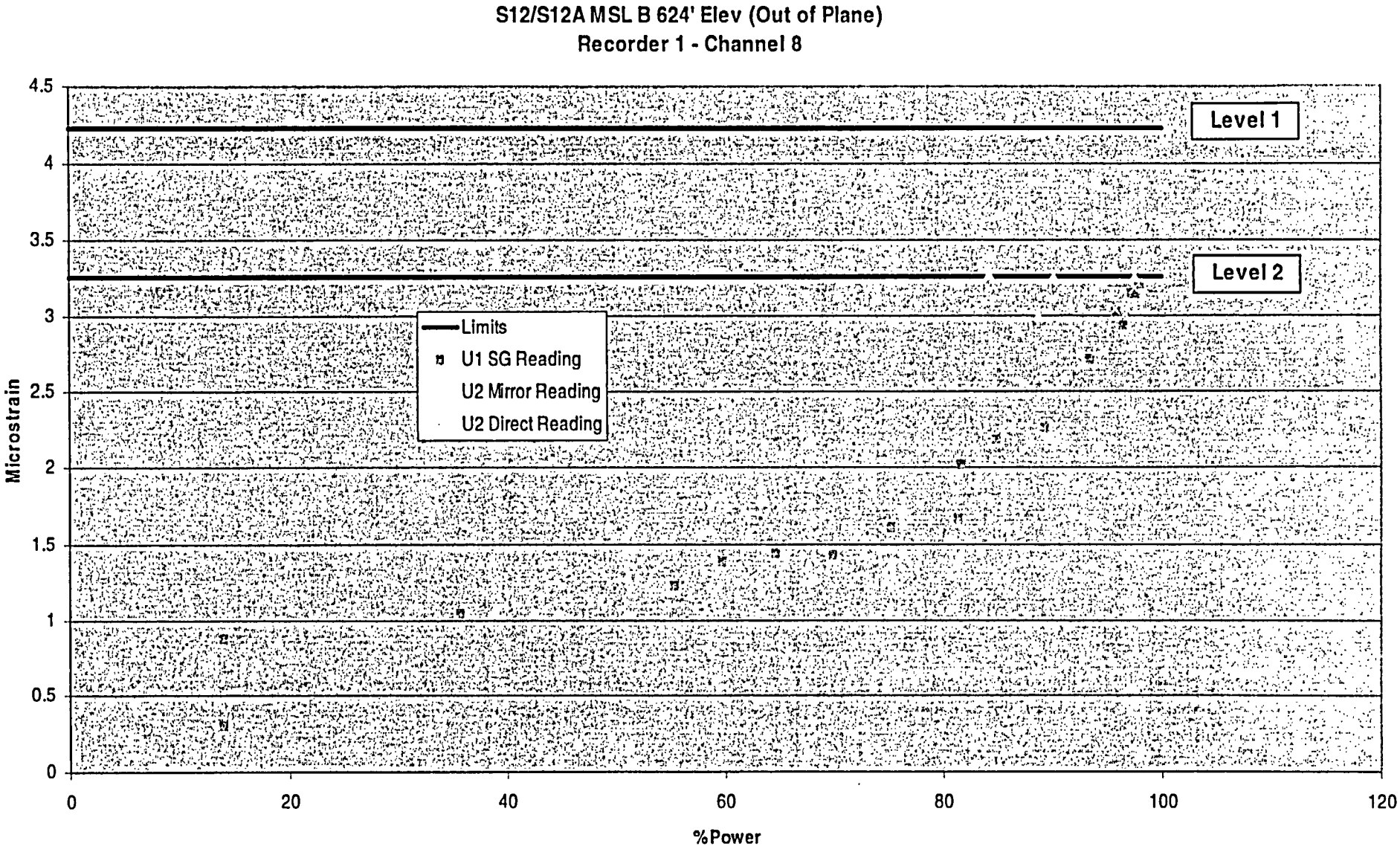
S12/S12A MSL B 624' Elev (Out of Plane)
Recorder 1 - Channel 8
Level 1
Level 2
Limits
U1 SG Reading
U2 Mirror Reading
U2 Direct Reading
Microstrain
%Power
4.5
4
3.5
3
2.5
2
1.5
1
0.5
0
0
20
40
60
80
100
120

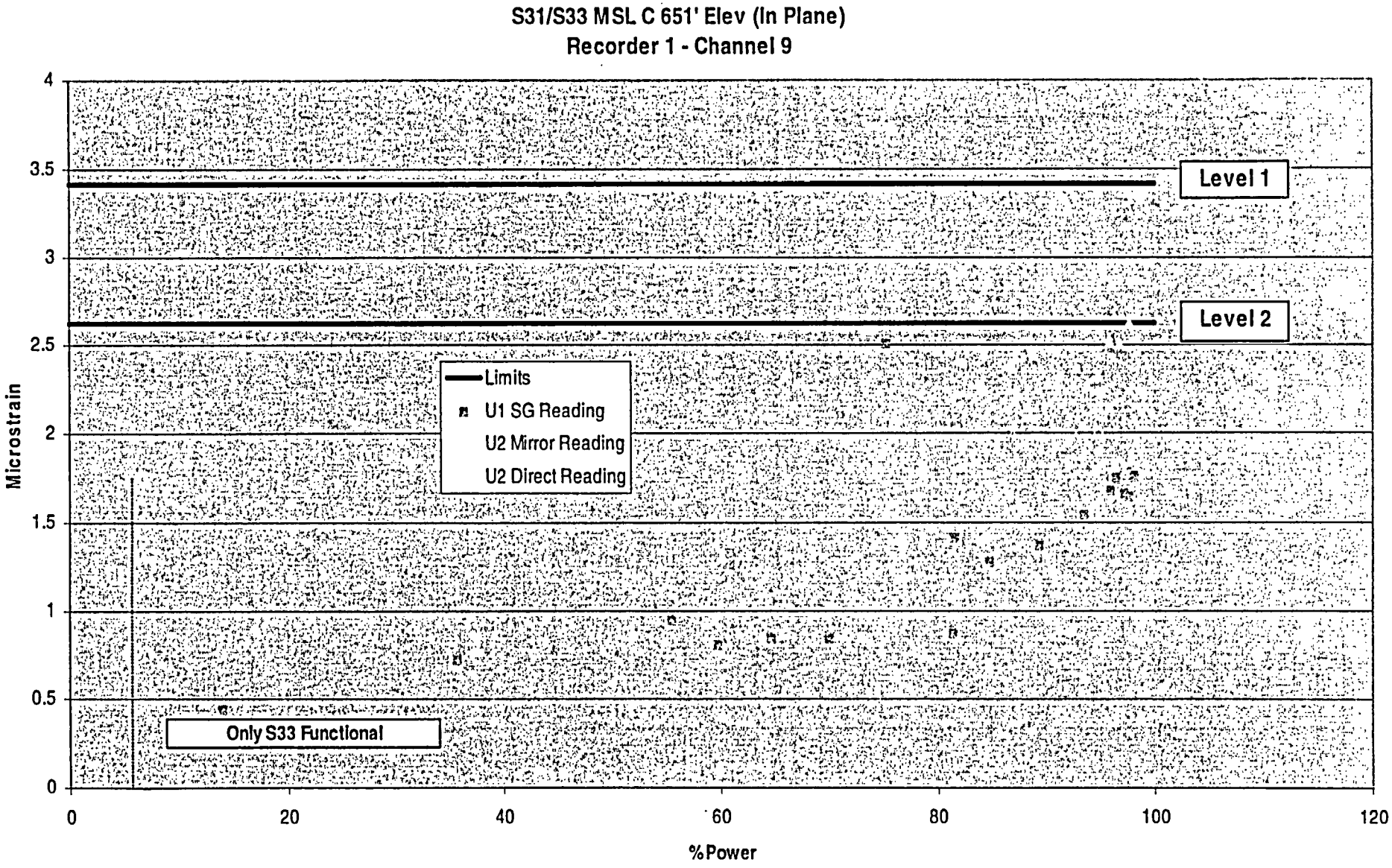
S31/S33 MSL C 651' Elev (In Plane)
Recorder 1 - Channel 9
Microstrain
%Power
Level 1
Level 2
Limits
U1 SG Reading
U2 Mirror Reading
U2 Direct Reading
Only S33 Functional
0
0.5
1
1.5
2
2.5
3
3.5
4
0
20
40
60
80
100
120

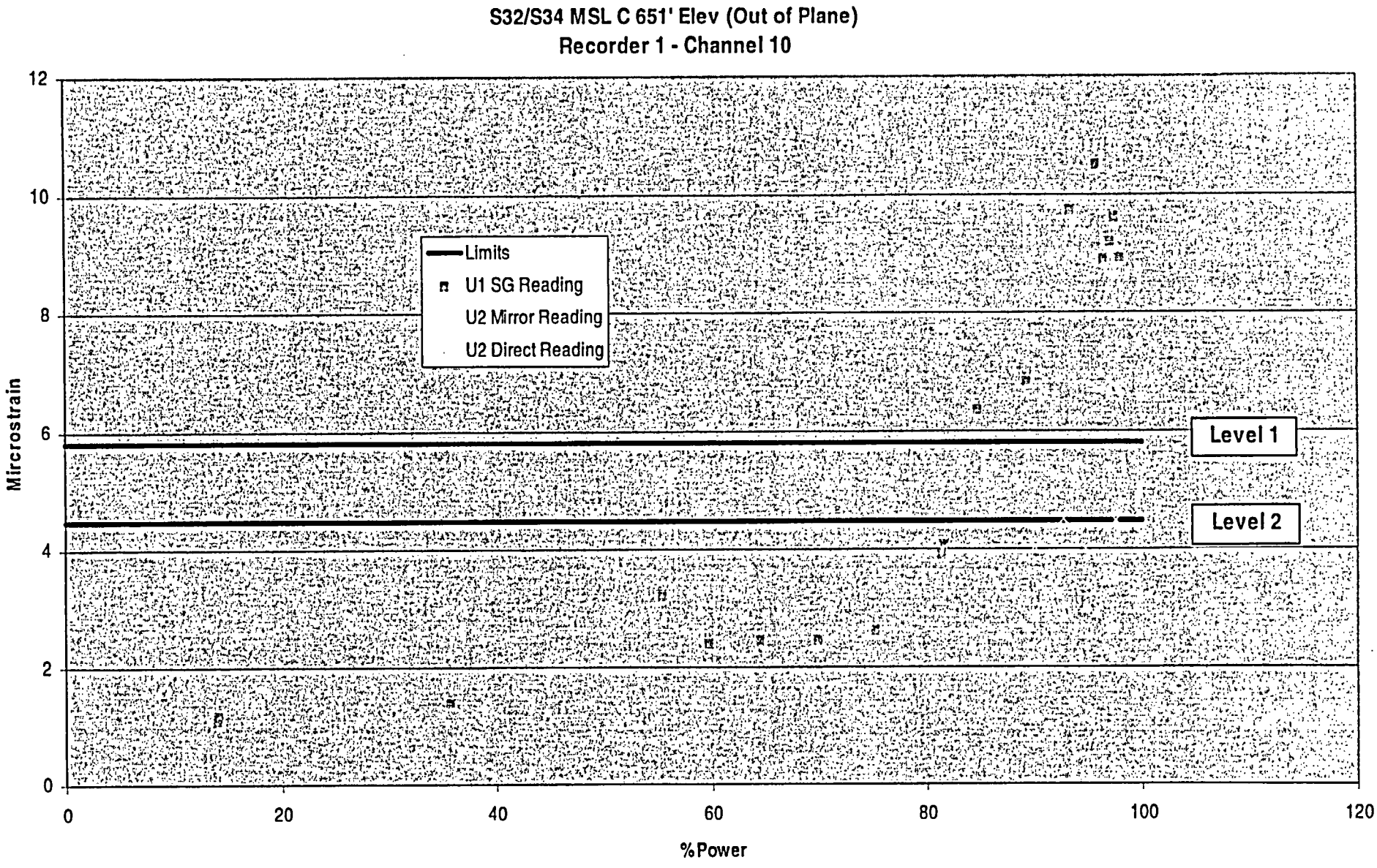
S32/S34 MSL C 651' Elev (Out of Plane)
Recorder 1 - Channel 10
Limits
U1 SG Reading
U2 Mirror Reading
U2 Direct Reading
Level 1
Level 2
Mircrostrain
%Power
0
2
4
6
8
10
12
0
20
40
60
80
100
120

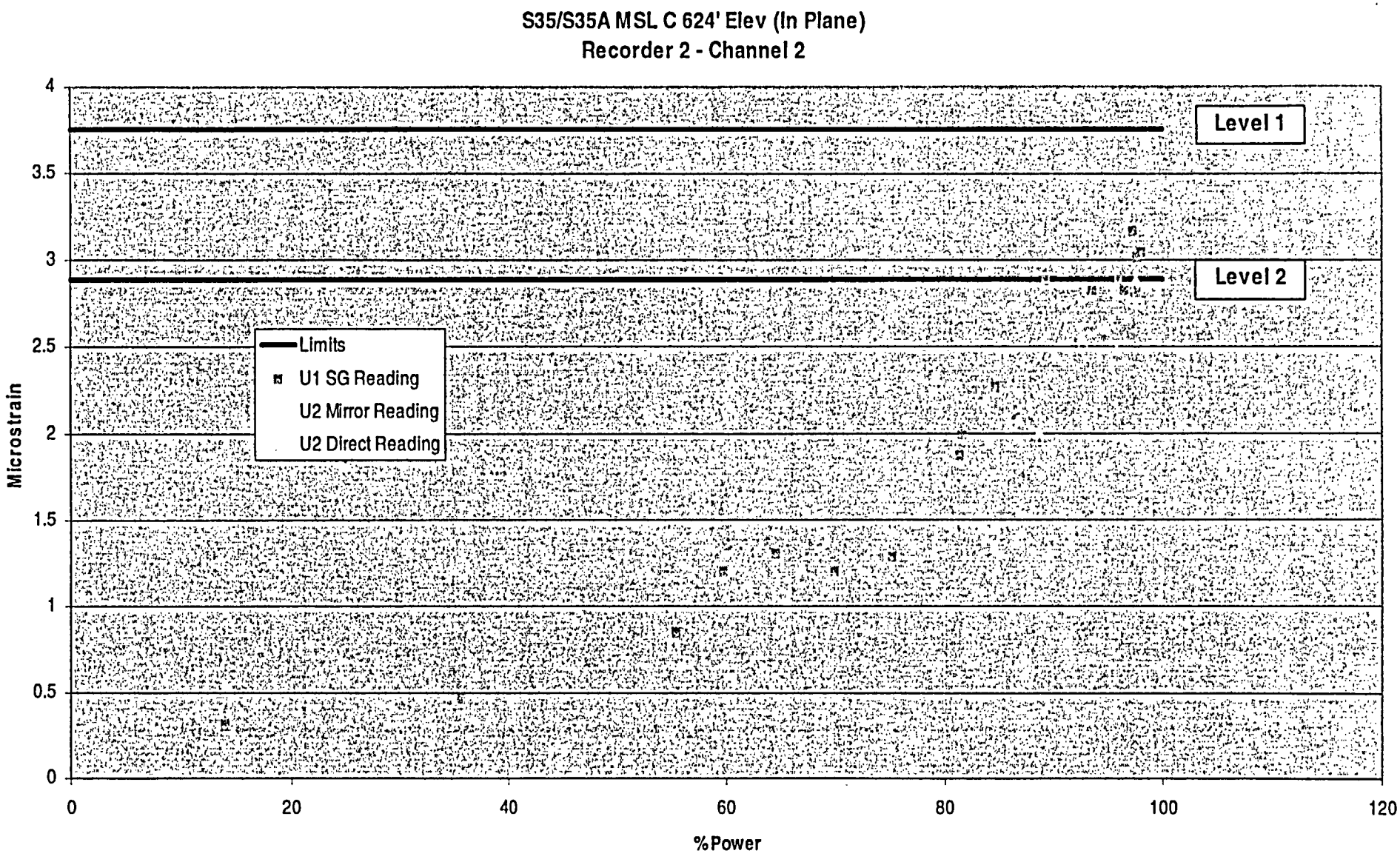
S35/S35A MSL C 624' Elev (In Plane)
Recorder 2 - Channel 2
Level 1
Level 2
Limits
U1 SG Reading
U2 Mirror Reading
U2 Direct Reading
Microstrain
%Power
0
0.5
1
1.5
2
2.5
3
3.5
4
0
20
40
60
80
100
120

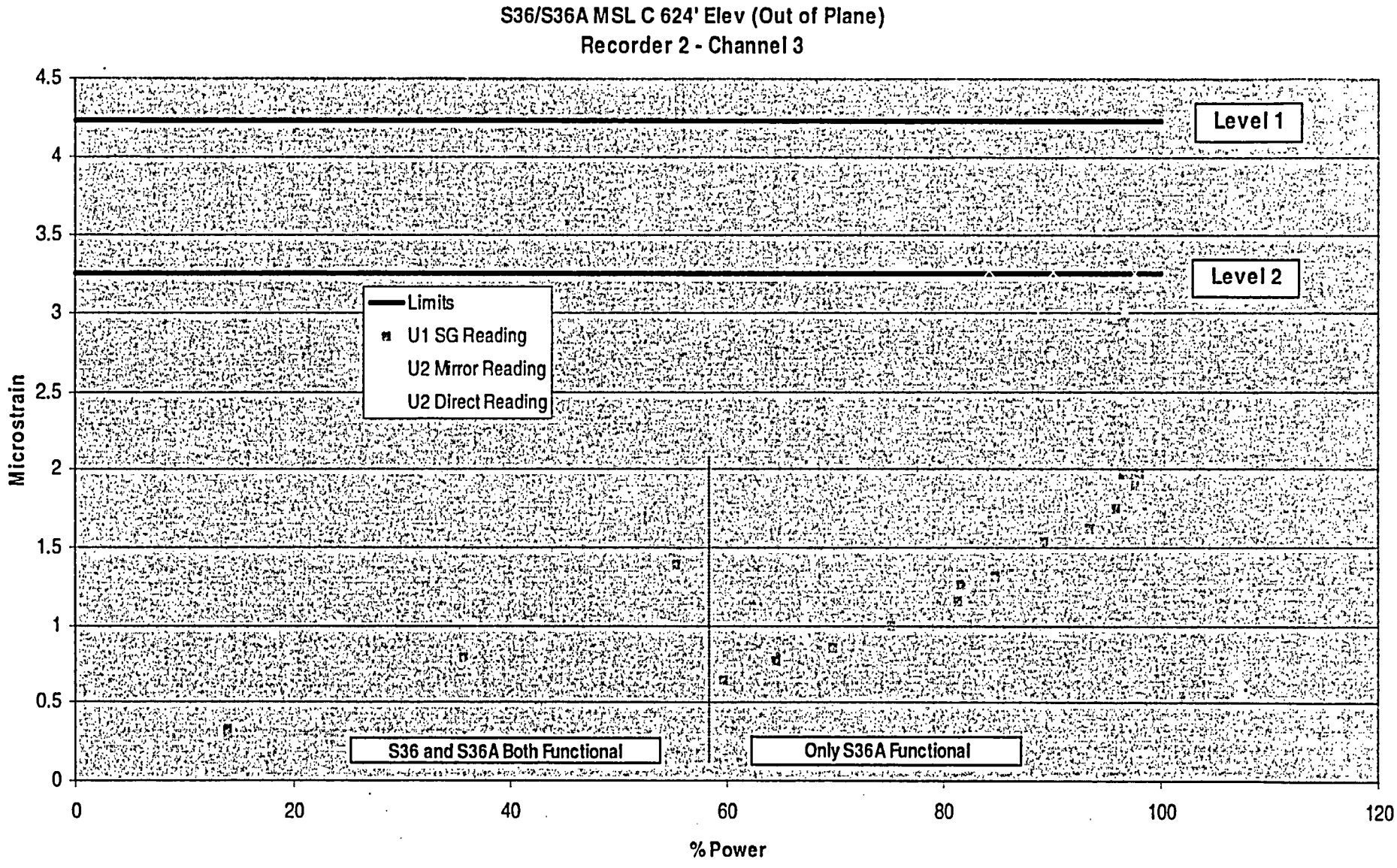
S36/S36A MSL C 624' Elev (Out of Plane)
Recorder 2 - Channel 3
Microstrain
4.5
4
3.5
3
2.5
2
1.5
1
0.5
0
0
20
40
60
80
100
120
% Power
Level 1
Level 2
Limits
U1 SG Reading
U2 Mirror Reading
U2 Direct Reading
S36 and S36A Both Functional
Only S36A Functional

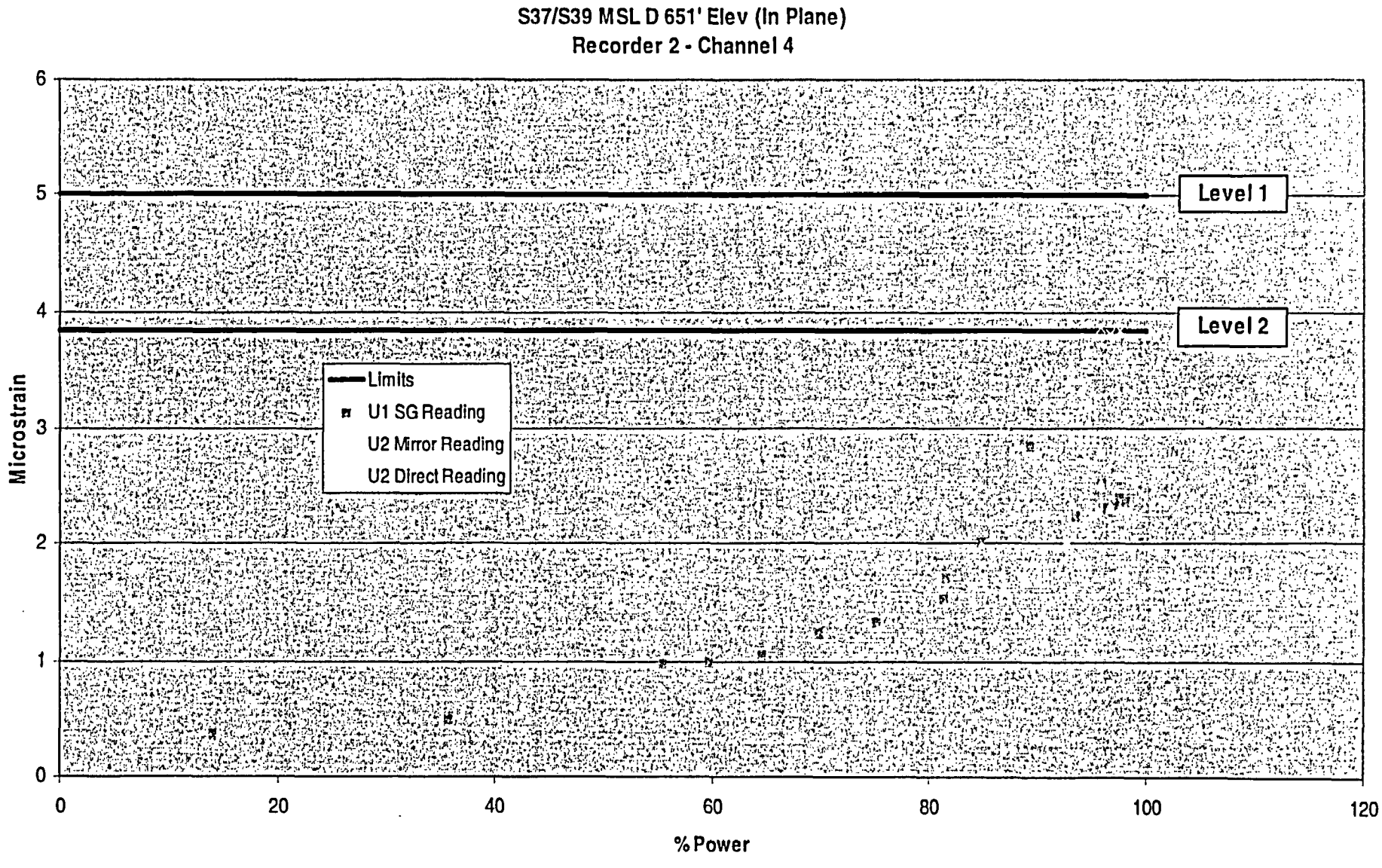
S37/S39 MSL D 651' Elev (In Plane)
Recorder 2 - Channel 4
Microstrain
% Power
Level 1
Level 2
Limits
U1 SG Reading
U2 Mirror Reading
U2 Direct Reading
0
1
2
3
4
5
6
0
20
40
60
80
100
120

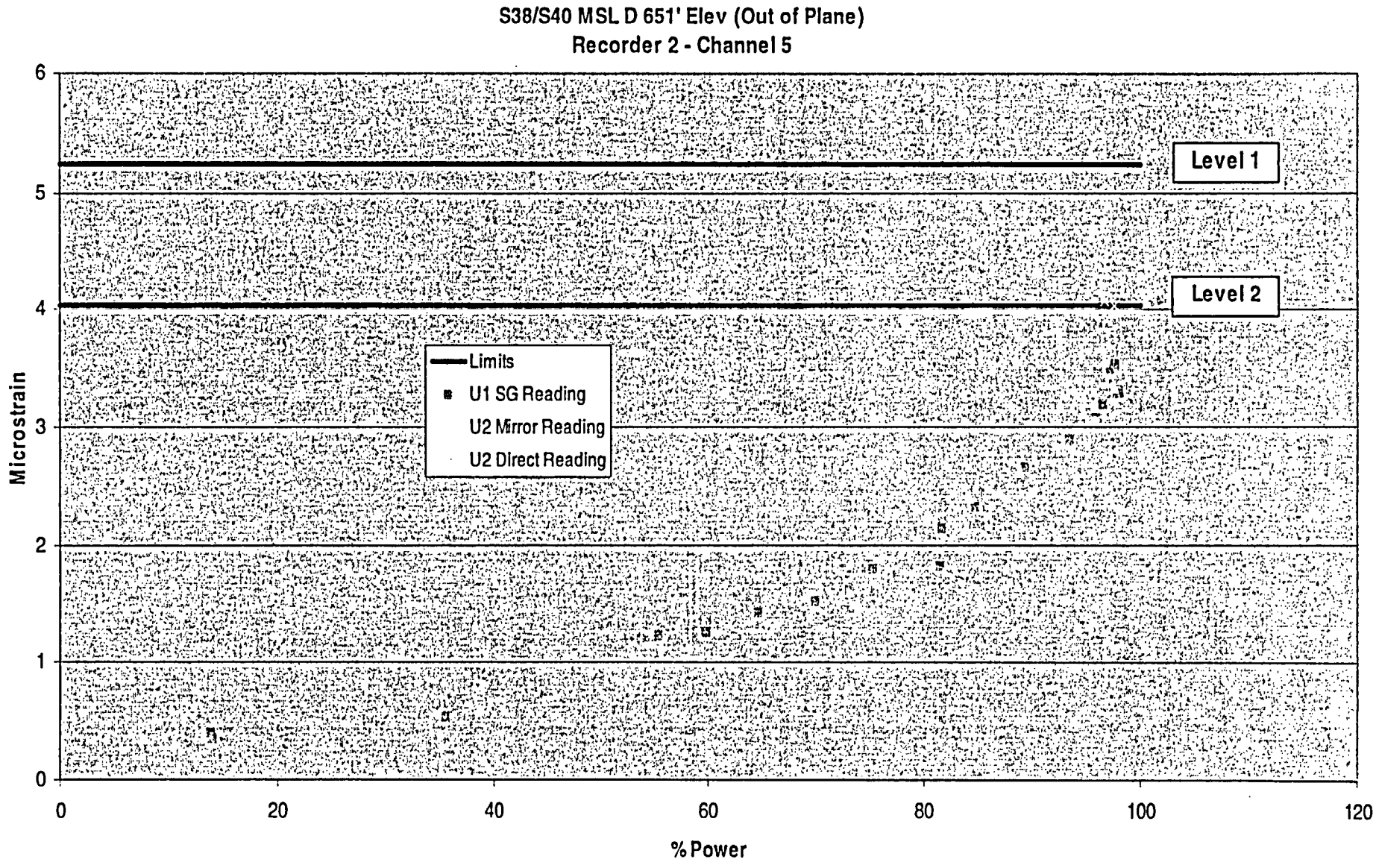
S38/S40 MSL D 651' Elev (Out of Plane)
Recorder 2 - Channel 5
Level 1
Level 2
Limits
U1 SG Reading
U2 Mirror Reading
U2 Direct Reading
Microstrain
0
1
2
3
4
5
6
0
20
40
60
80
100
120
% Power

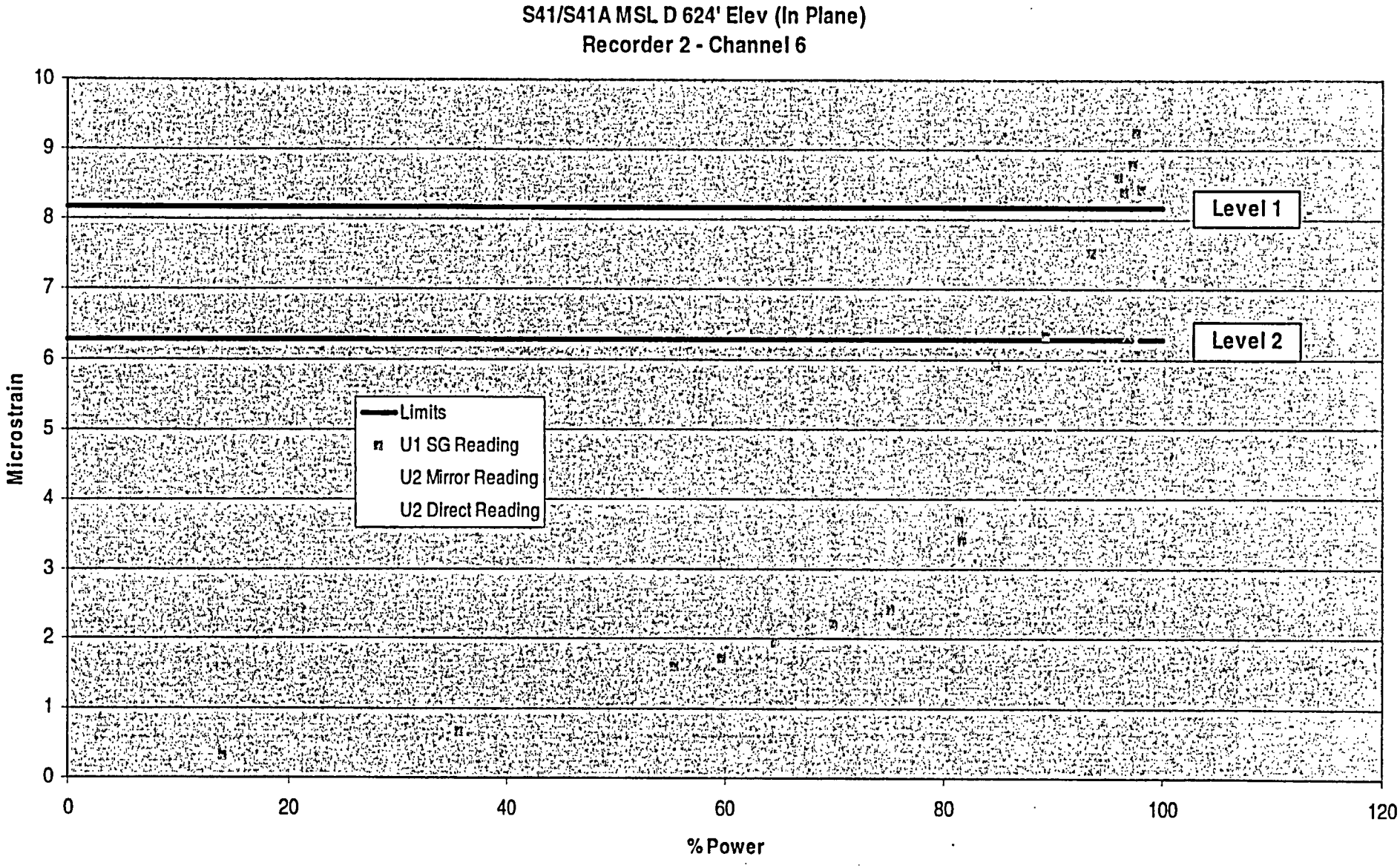
S41/S41A MSL D 624' Elev (In Plane)
Recorder 2 - Channel 6
Microstrain
10
9
8
7
6
5
4
3
2
1
0
0
20
40
60
80
100
120
% Power
Level 1
Level 2
Limits
U1 SG Reading
U2 Mirror Reading
U2 Direct Reading

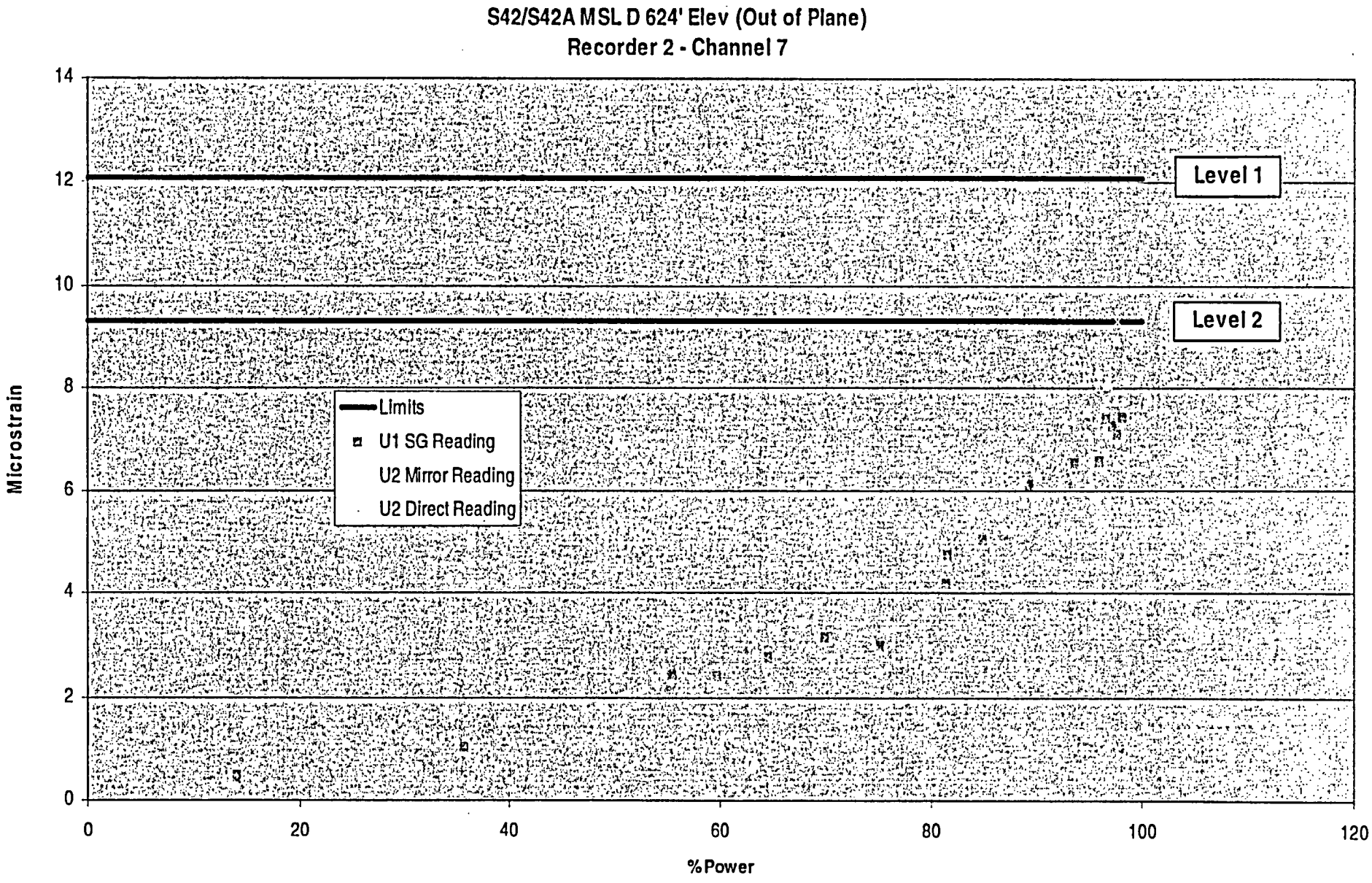
S42/S42A MSL D 624' Elev (Out of Plane)
Recorder 2 - Channel 7
Microstrain
%Power
Level 1
Level 2
Limits
U1 SG Reading
U2 Mirror Reading
U2 Direct Reading
0
2
4
6
8
10
12
14
0
20
40
60
80
100
120

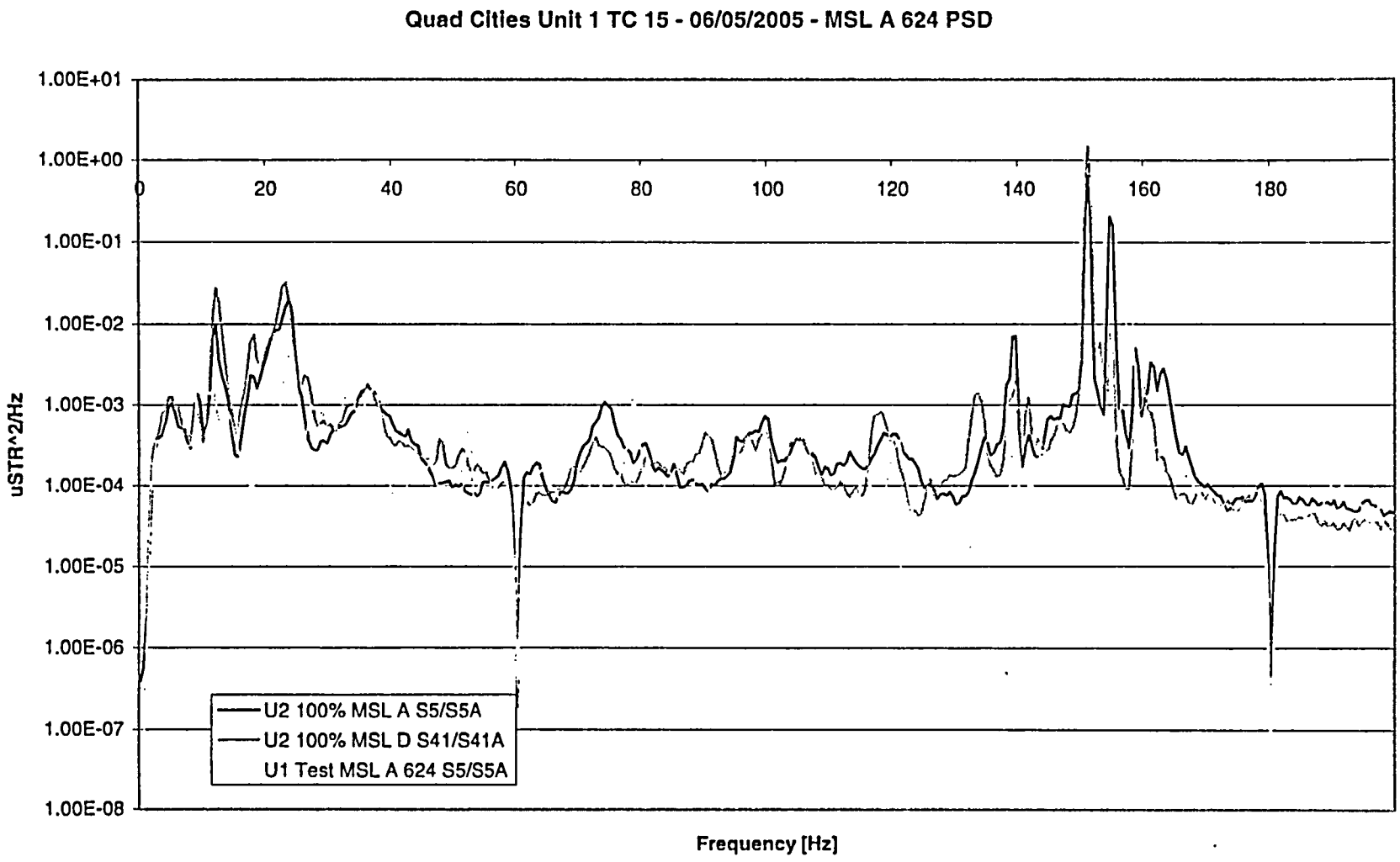
Quad Cities Unit 1 TC 15 - 06/05/2005 - MSL A 624 PSD
1.00E+01
1.00E+00
1.00E-01
1.00E-02
1.00E-03
1.00E-04
1.00E-05
1.00E-06
1.00E-07
1.00E-08
uSTR^2/Hz
0
20
40
60
80
100
120
140
160
180
Frequency [Hz]
U2 100% MSL A S5/S5A
U2 100% MSL D S41/S41A
U1 Test MSL A 624 S5/S5A

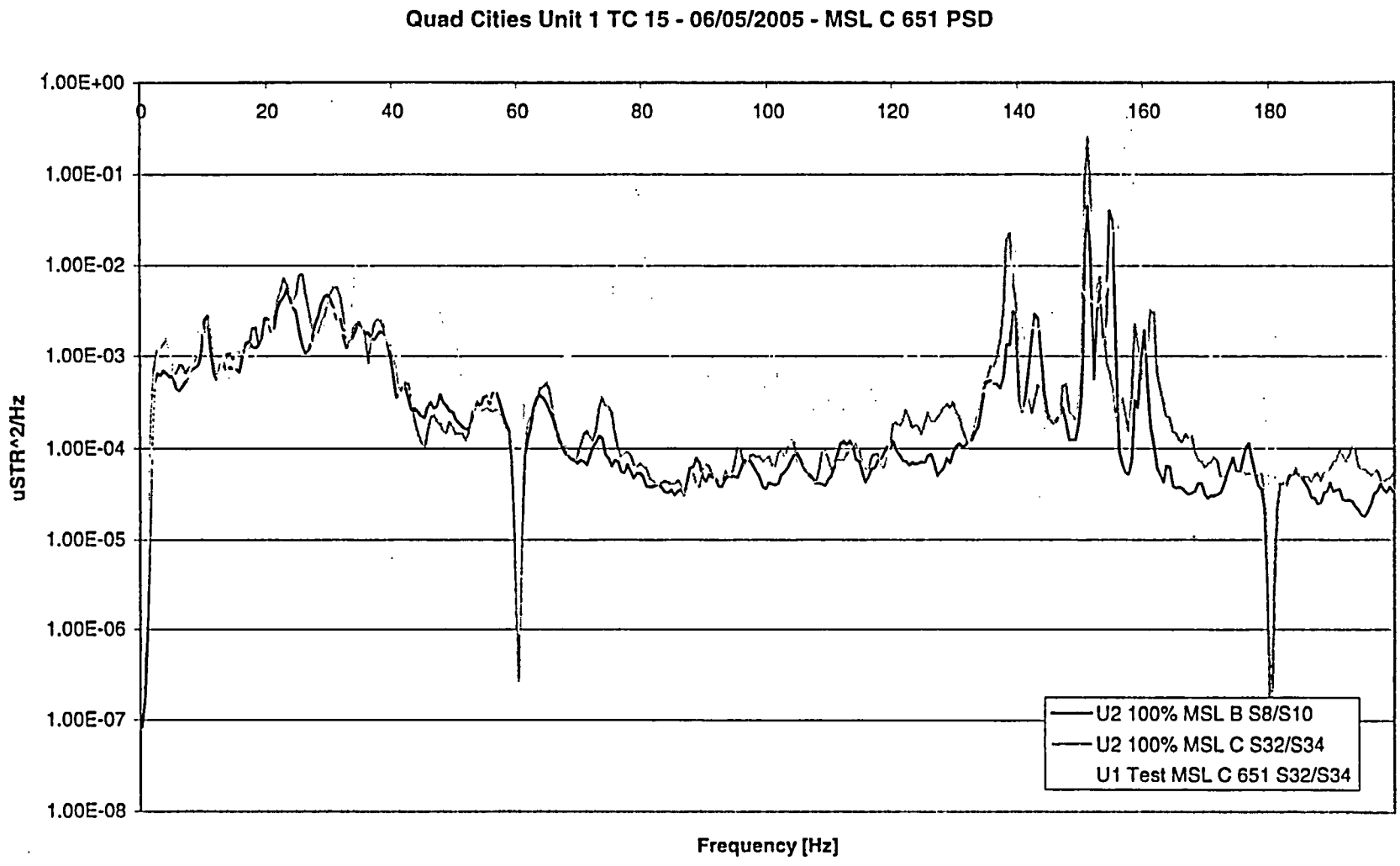
Quad Cities Unit 1 TC 15 - 06/05/2005 - MSL C 651 PSD
1.00E+00
1.00E-01
1.00E-02
1.00E-03
1.00E-04
1.00E-05
1.00E-06
1.00E-07
1.00E-08
uSTR^2/Hz
0
20
40
60
80
100
120
140
160
180
Frequency [Hz]
U2 100% MSL B S8/S10
U2 100% MSL C S32/S34
U1 Test MSL C 651 S32/S34

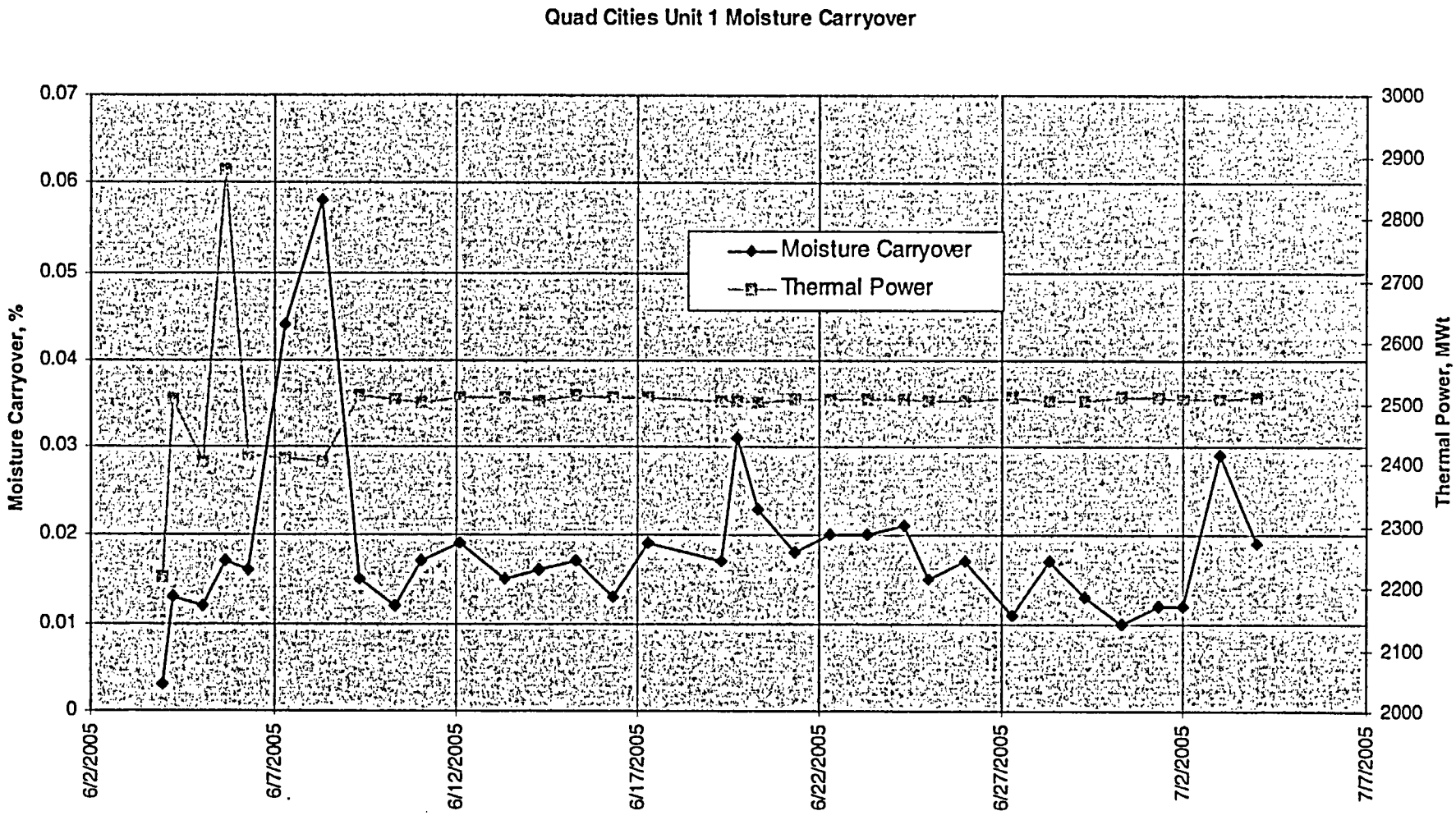
Quad Cities Unit 1 Moisture Carryover
Moisture Carryover, %
Thermal Power, MWt
Moisture Carryover
Thermal Power
0.07
0.06
0.05
0.04
0.03
0.02
0.01
0
3000
2900
2800
2700
2600
2500
2400
2300
2200
2100
2000
6/2/2005
6/7/2005
6/12/2005
6/17/2005
6/22/2005
6/27/2005
7/2/2005
7/7/2005

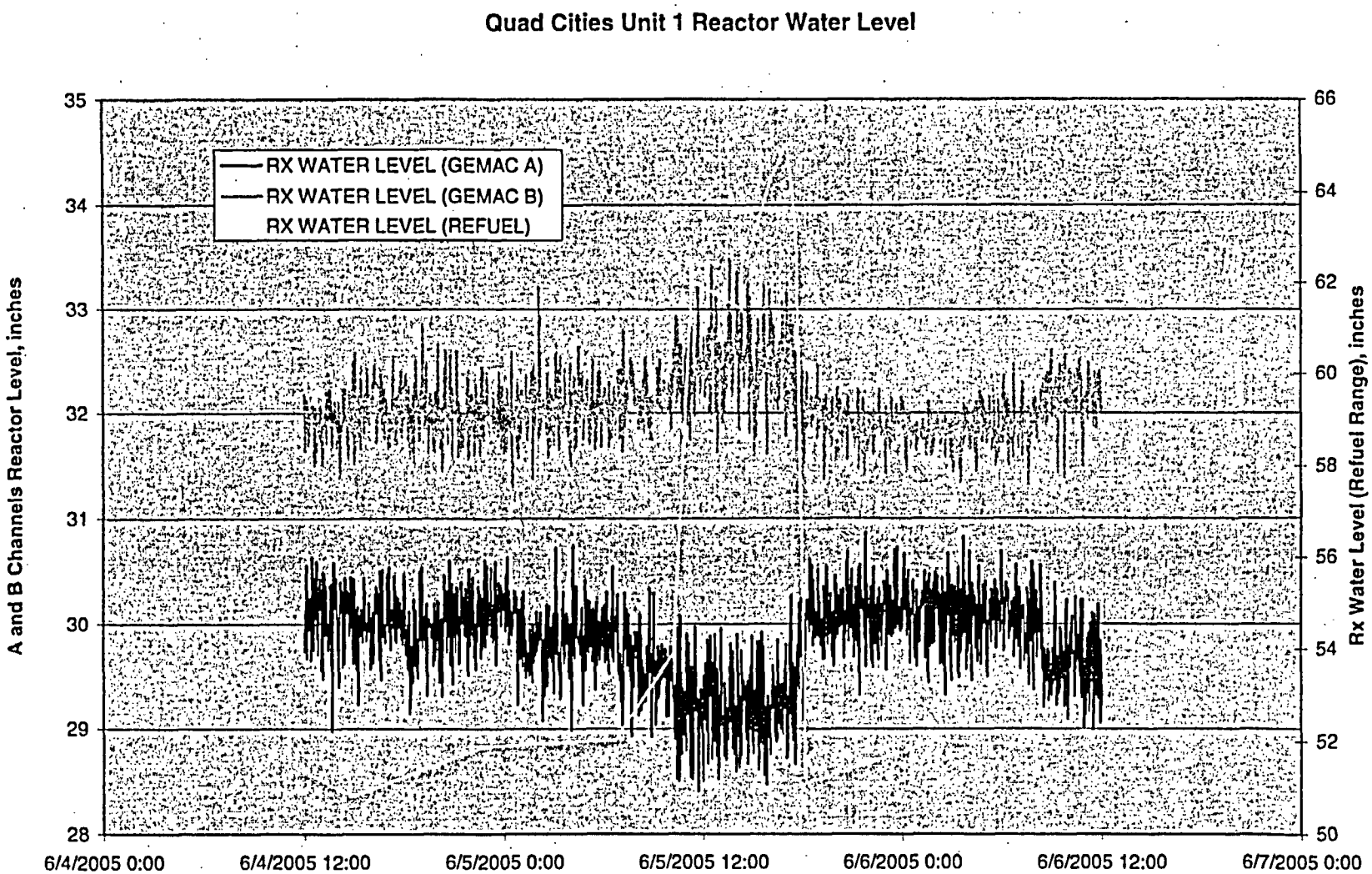
Quad Cities Unit 1 Reactor Water Level
RX WATER LEVEL (GEMAC A)
RX WATER LEVEL (GEMAC B)
RX WATER LEVEL (REFUEL)
A and B Channels Reactor Level, inches
Rx Water Level (Refuel Range), inches
35
34
33
32
31
30
29
28
66
64
62
60
58
56
54
52
50
6/4/2005 0:00
6/4/2005 12:00
6/5/2005 0:00
6/5/2005 12:00
6/6/2005 0:00
6/6/2005 12:00
6/7/2005 0:00

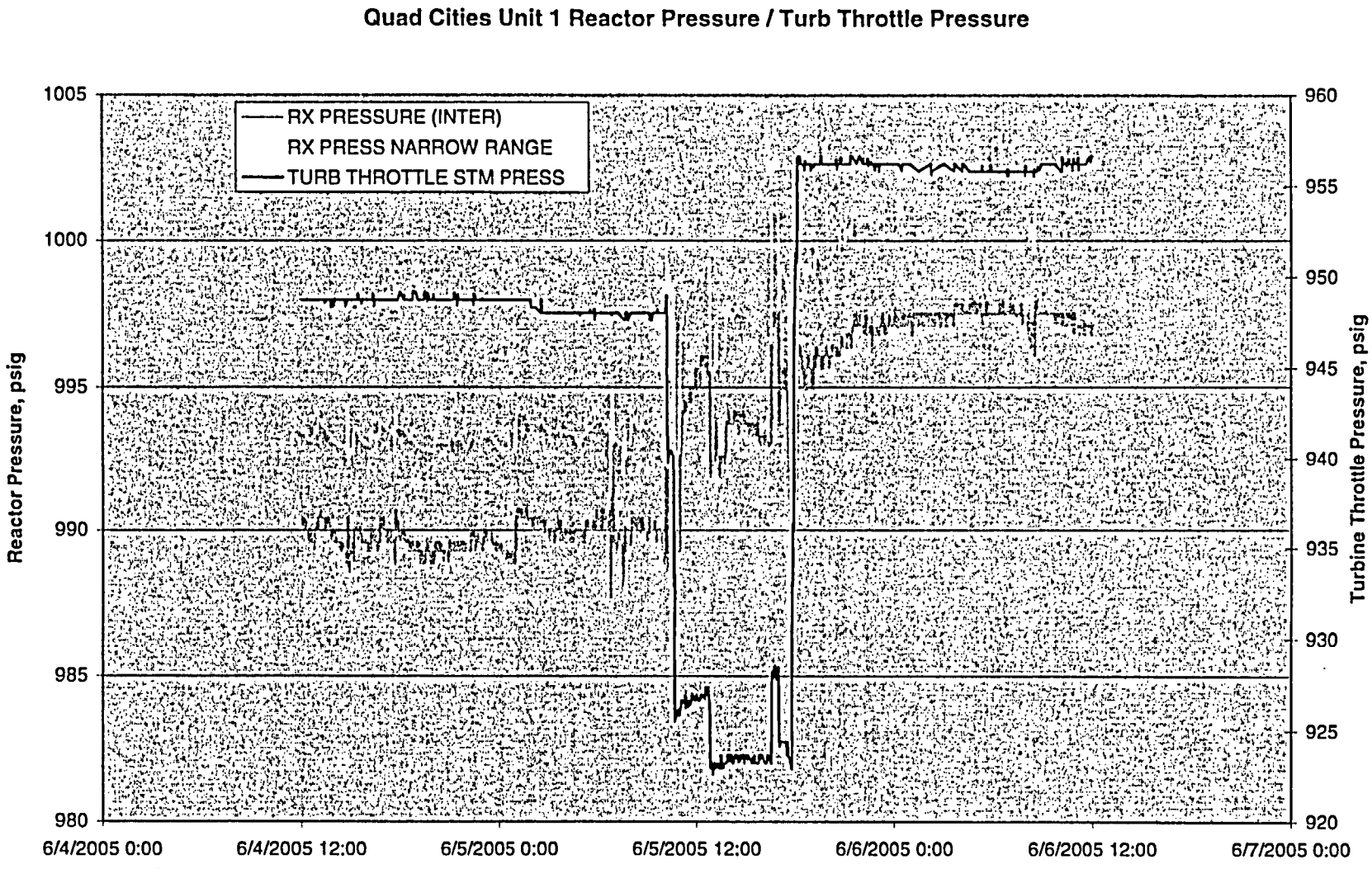
Quad Cities Unit 1 Reactor Pressure / Turb Throttle Pressure
RX PRESSURE (INTER)
RX PRESS NARROW RANGE
TURB THROTTLE STM PRESS
Reactor Pressure, psig
Turbine Throttle Pressure, psig
1005
1000
995
990
985
980
960
955
950
945
940
935
930
925
920
6/4/2005 0:00
6/4/2005 12:00
6/5/2005 0:00
6/5/2005 12:00
6/6/2005 0:00
6/6/2005 12:00
6/7/2005 0:00

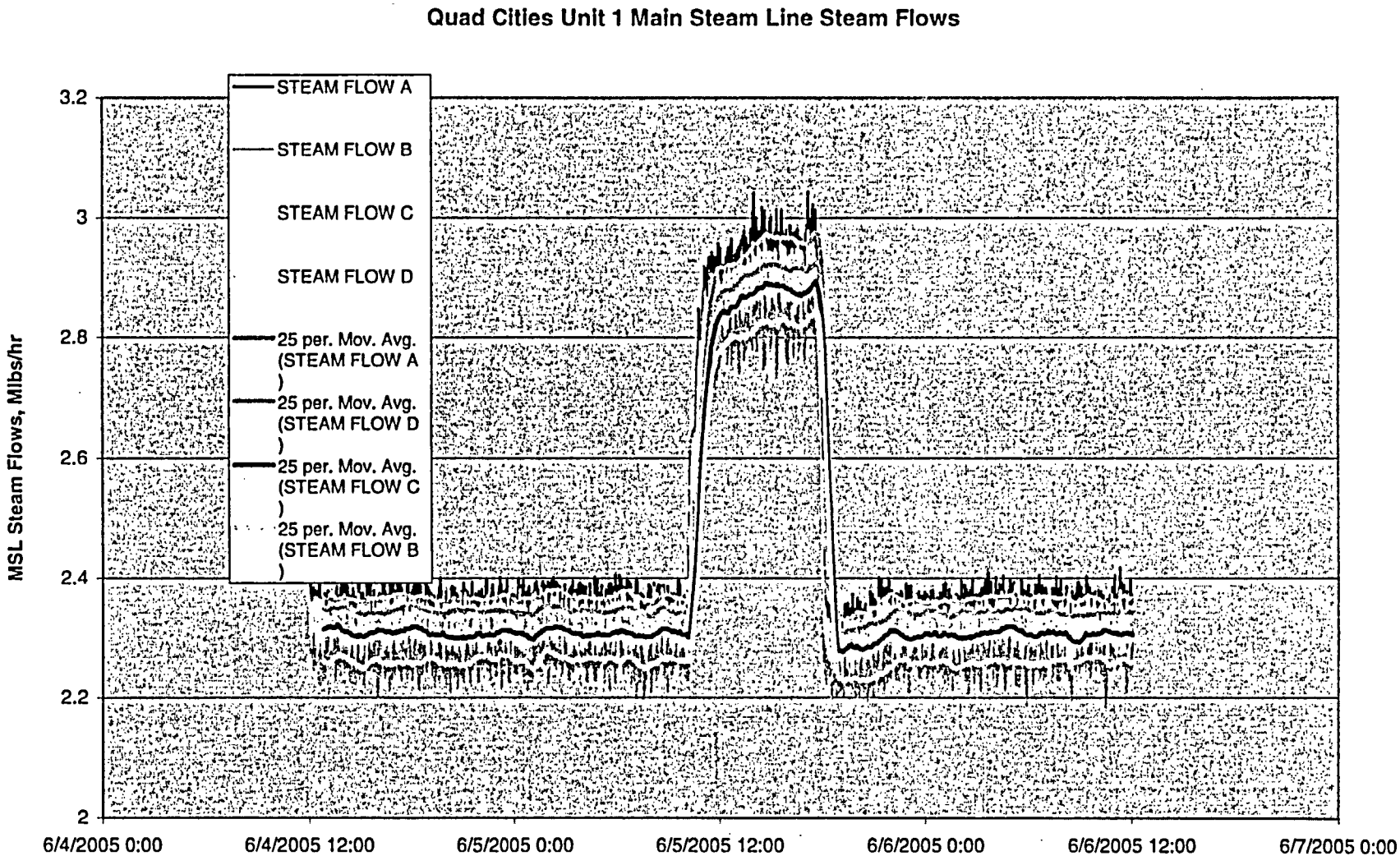
Quad Cities Unit 1 Main Steam Line Steam Flows
STEAM FLOW A
STEAM FLOW B
STEAM FLOW C
STEAM FLOW D
25 per. Mov. Avg. (STEAM FLOW A)
25 per. Mov. Avg. (STEAM FLOW D)
25 per. Mov. Avg. (STEAM FLOW C)
25 per. Mov. Avg. (STEAM FLOW B)
MSL Steam Flows, Mlbs/hr
3.2
3
2.8
2.6
2.4
2.2
2
6/4/2005 0:00
6/4/2005 12:00
6/5/2005 0:00
6/5/2005 12:00
6/6/2005 0:00
6/6/2005 12:00
6/7/2005 0:00

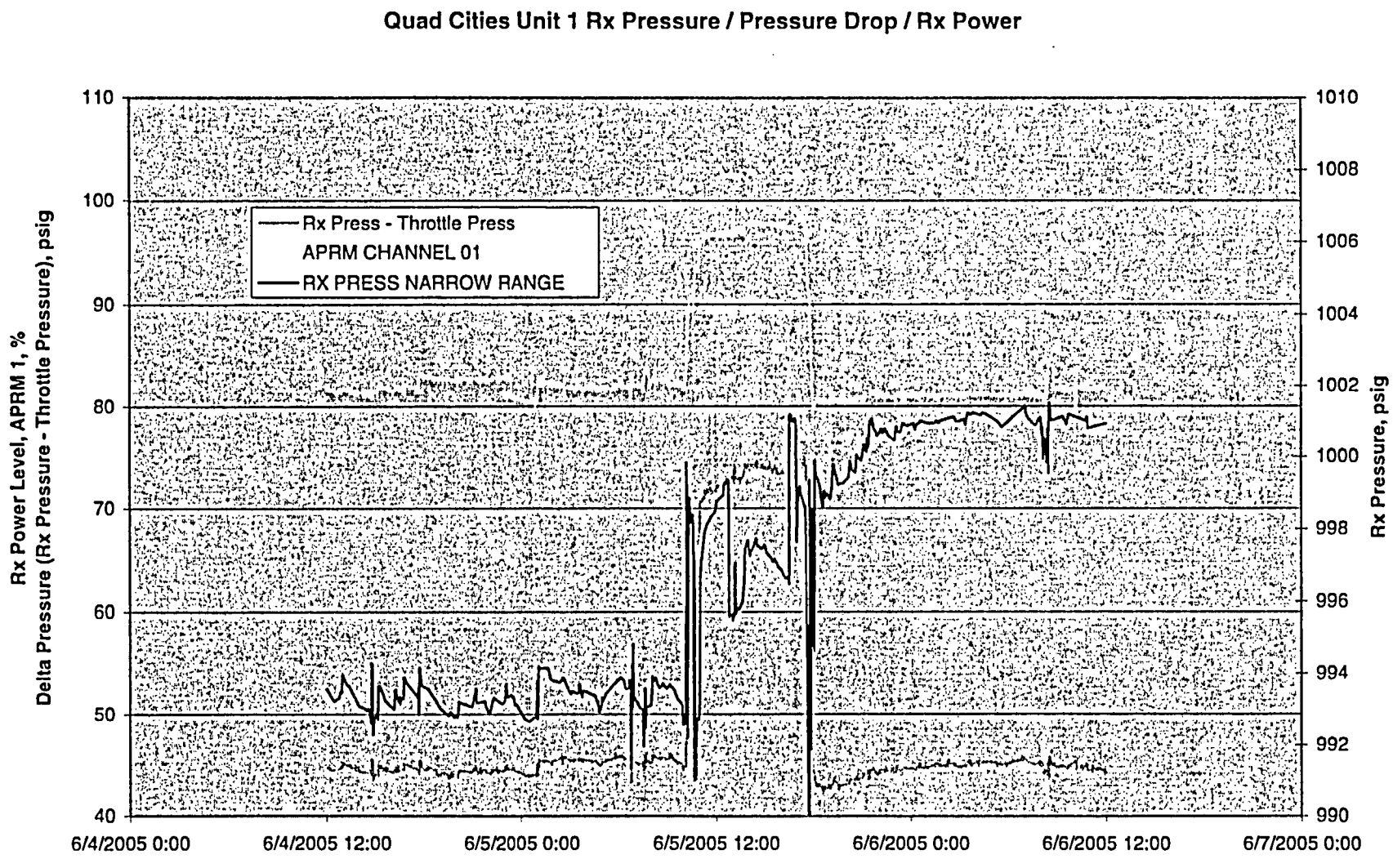
Quad Cities Unit 1 Rx Pressure / Pressure Drop / Rx Power
Rx Press - Throttle Press
APRM CHANNEL 01
RX PRESS NARROW RANGE
Rx Power Level, APRM 1, %
Delta Pressure (Rx Pressure - Throttle Pressure), psig
Rx Pressure, psig
110
100
90
80
70
60
50
40
1010
1008
1006
1004
1002
1000
998
996
994
992
990
6/4/2005 0:00
6/4/2005 12:00
6/5/2005 0:00
6/5/2005 12:00
6/6/2005 0:00
6/6/2005 12:00
6/7/2005 0:00

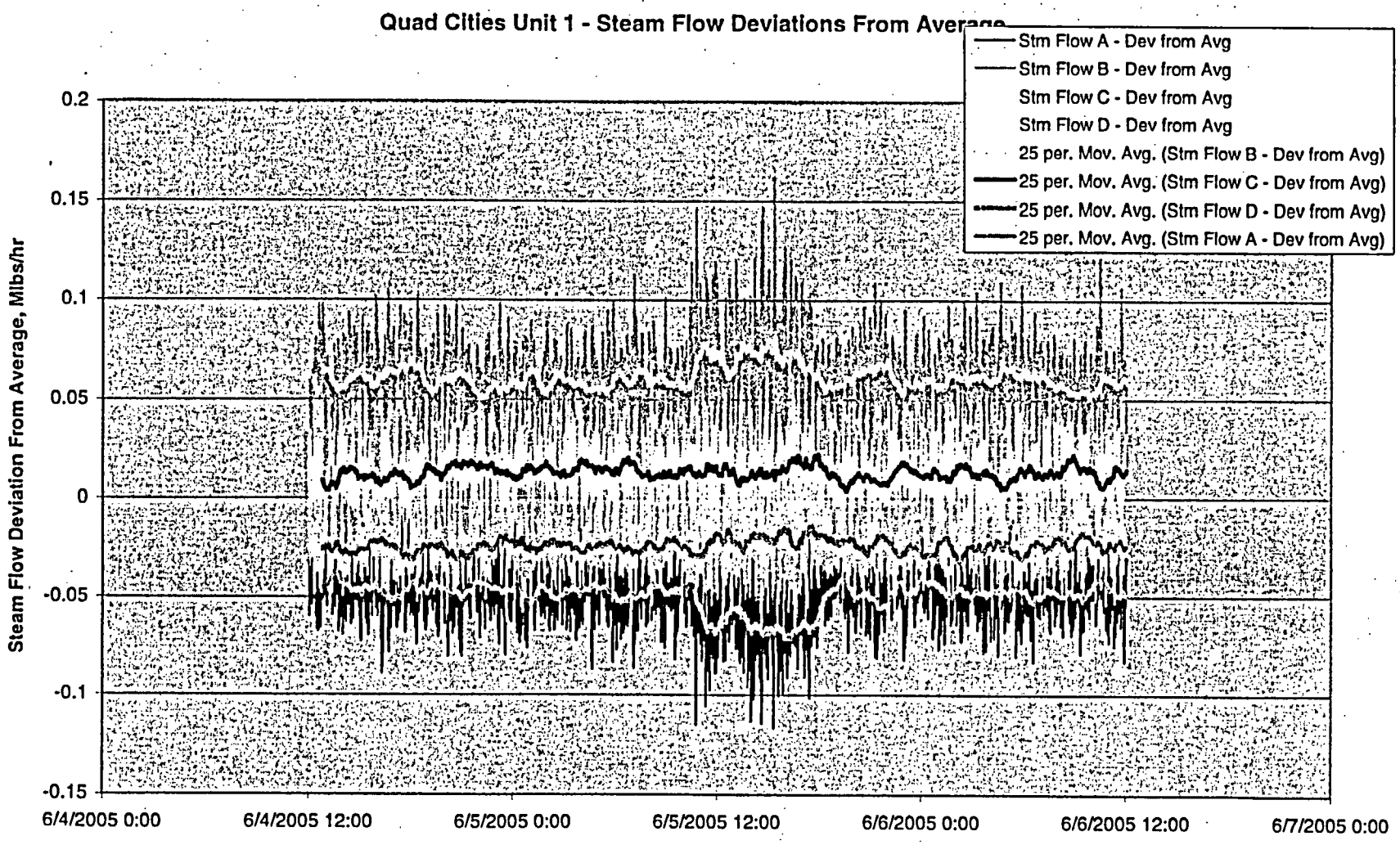
Quad Cities Unit 1 - Steam Flow Deviations From Average
Stm Flow A - Dev from Avg
Stm Flow B - Dev from Avg
Stm Flow C - Dev from Avg
Stm Flow D - Dev from Avg
25 per. Mov. Avg. (Stm Flow B - Dev from Avg)
25 per. Mov. Avg. (Stm Flow C - Dev from Avg)
25 per. Mov. Avg. (Stm Flow D - Dev from Avg)
25 per. Mov. Avg. (Stm Flow A - Dev from Avg)
Steam Flow Deviation From Average, Mlbs/hr
0.2
0.15
0.1
0.05
0
-0.05
-0.1
-0.15
6/4/2005 0:00
6/4/2005 12:00
6/5/2005 0:00
6/5/2005 12:00
6/6/2005 0:00
6/6/2005 12:00
6/7/2005 0:00

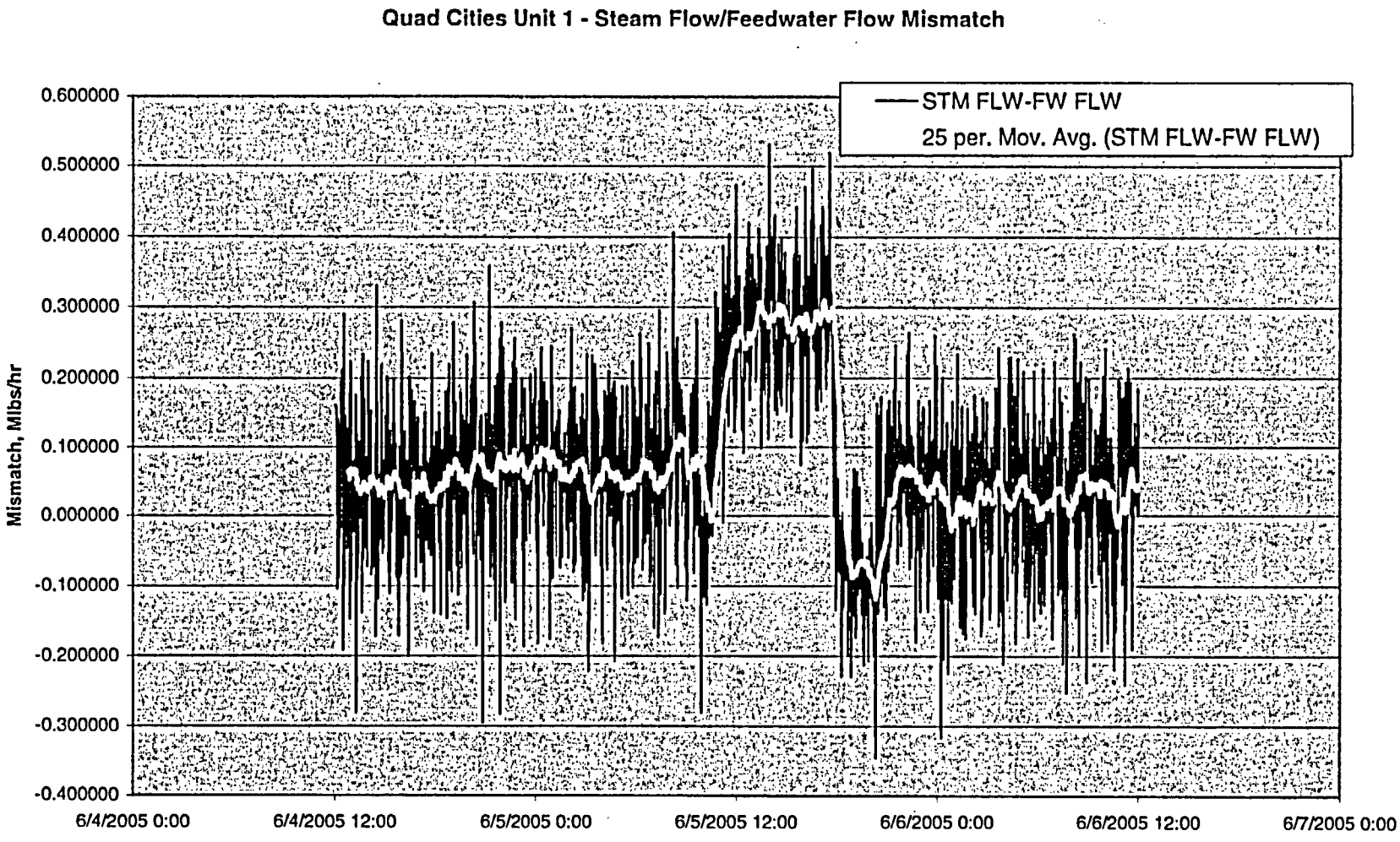
Quad Cities Unit 1 - Steam Flow/Feedwater Flow Mismatch
STM FLW-FW FLW
25 per. Mov. Avg. (STM FLW-FW FLW)
Mismatch, Mlbs/hr
0.600000
0.500000
0.400000
0.300000
0.200000
0.100000
0.000000
-0.100000
-0.200000
-0.300000
-0.400000
6/4/2005 0:00
6/4/2005 12:00
6/5/2005 0:00
6/5/2005 12:00
6/6/2005 0:00
6/6/2005 12:00
6/7/2005 0:00

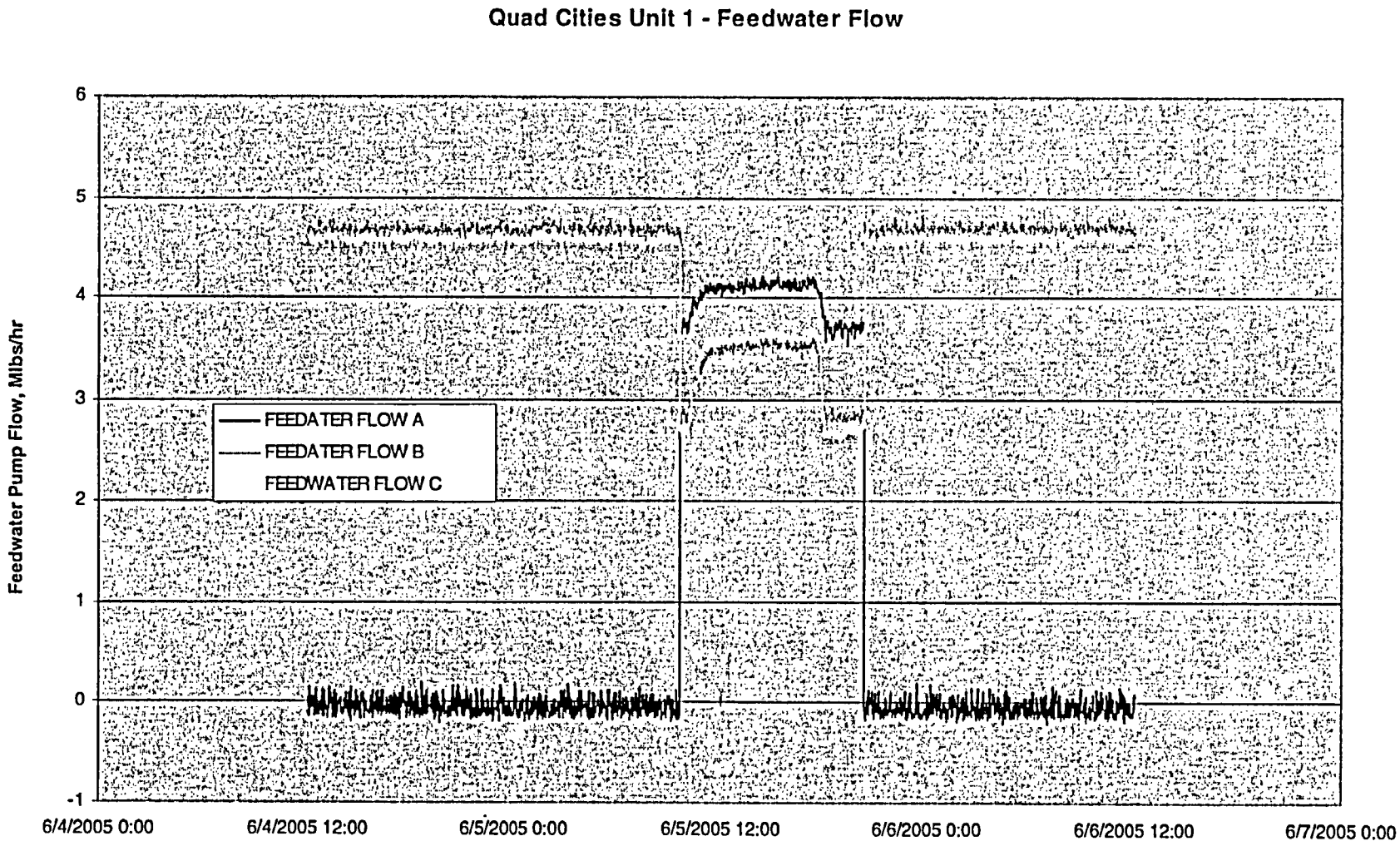
Quad Cities Unit 1 - Feedwater Flow
Feedwater Pump Flow, Mlbs/hr
6
5
4
3
2
1
0
-1
FEEDATER FLOW A
FEEDATER FLOW B
FEEDWATER FLOW C
6/4/2005 0:00
6/4/2005 12:00
6/5/2005 0:00
6/5/2005 12:00
6/6/2005 0:00
6/6/2005 12:00
6/7/2005 0:00

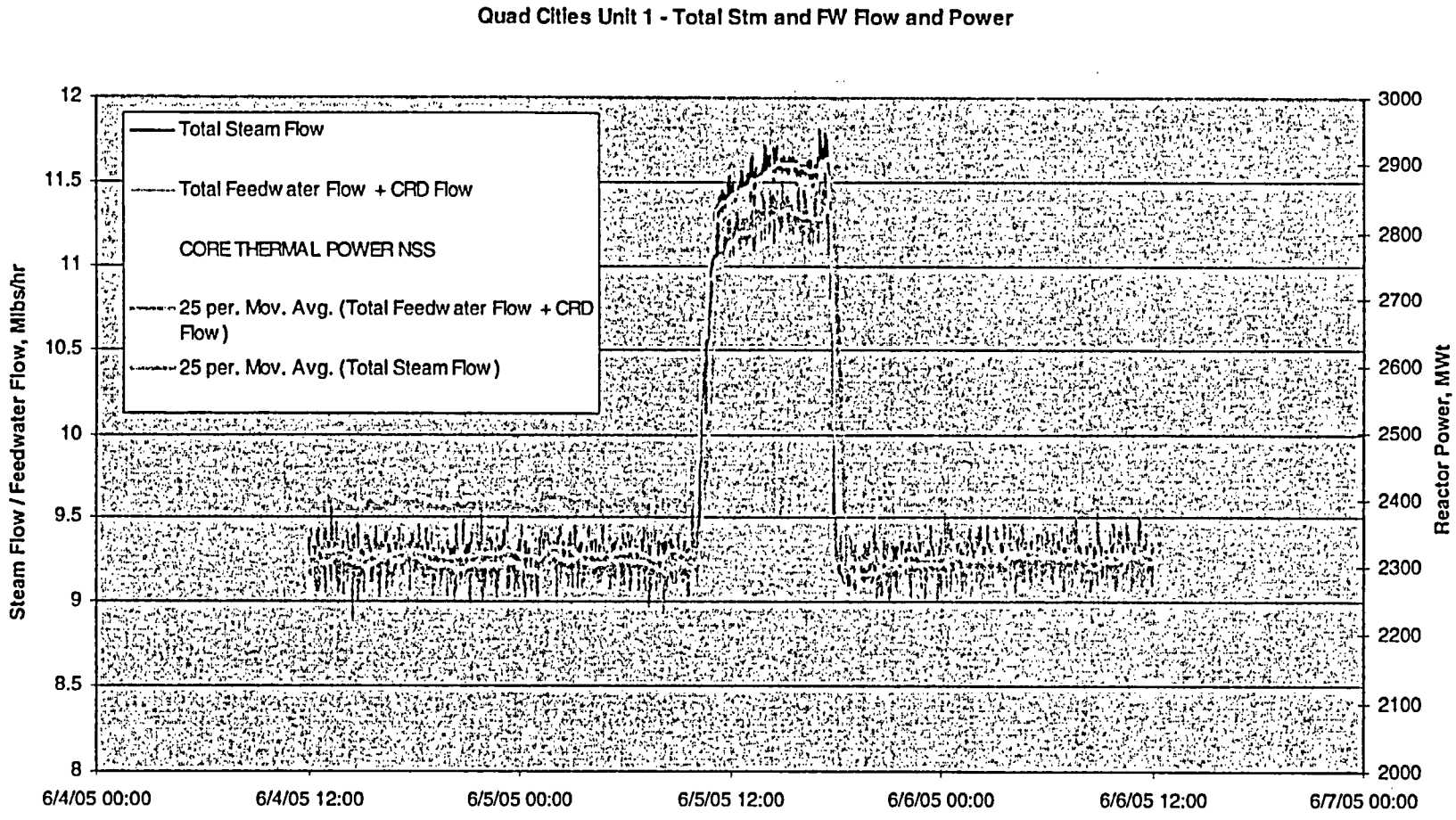
Quad Cities Unit 1 - Total Stm and FW Flow and Power
Total Steam Flow
Total Feedwater Flow + CRD Flow
CORE THERMAL POWER NSS
25 per. Mov. Avg. (Total Feedwater Flow + CRD Flow)
25 per. Mov. Avg. (Total Steam Flow)
Steam Flow / Feedwater Flow, Mlbs/hr
Reactor Power, MWt
12
11.5
11
10.5
10
9.5
9
8.5
8
3000
2900
2800
2700
2600
2500
2400
2300
2200
2100
2000
6/4/05 00:00
6/4/05 12:00
6/5/05 00:00
6/5/05 12:00
6/6/05 00:00
6/6/05 12:00
6/7/05 00:00

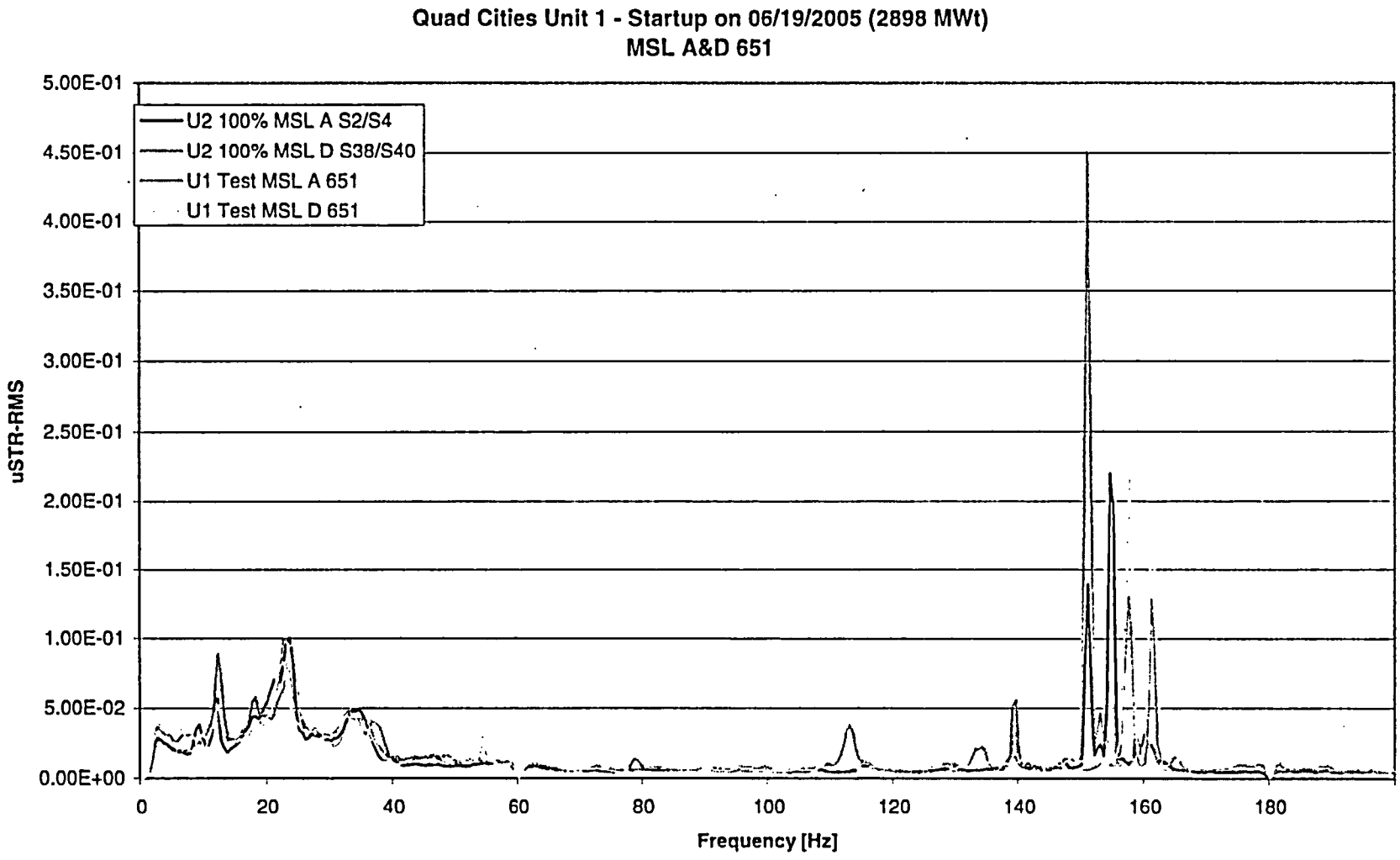
Quad Cities Unit 1 - Startup on 06/19/2005 (2898 MWt)
MSL A&D 651
U2 100% MSL A S2/S4
U2 100% MSL D S38/S40
U1 Test MSL A 651
U1 Test MSL D 651
uSTR-RMS
5.00E-01
4.50E-01
4.00E-01
3.50E-01
3.00E-01
2.50E-01
2.00E-01
1.50E-01
1.00E-01
5.00E-02
0.00E+00
0
20
40
60
80
100
120
140
160
180
Frequency [Hz]

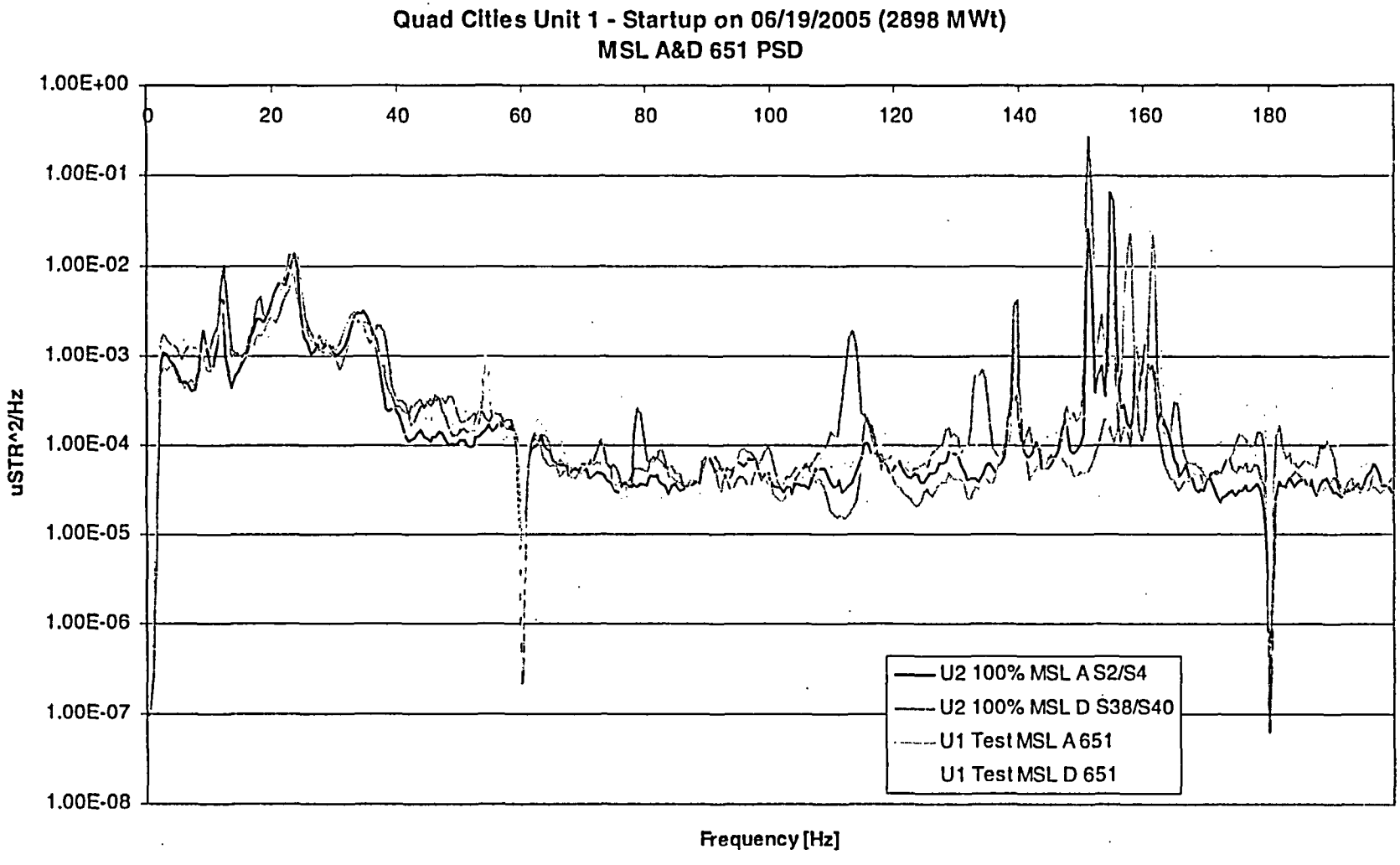
Quad Cities Unit 1 - Startup on 06/19/2005 (2898 MWt)
MSL A&D 651 PSD
1.00E+00
1.00E-01
1.00E-02
1.00E-03
1.00E-04
1.00E-05
1.00E-06
1.00E-07
1.00E-08
uSTR^2/Hz
0
20
40
60
80
100
120
140
160
180
Frequency [Hz]
U2 100% MSL A S2/S4
U2 100% MSL D S38/S40
U1 Test MSL A 651
U1 Test MSL D 651

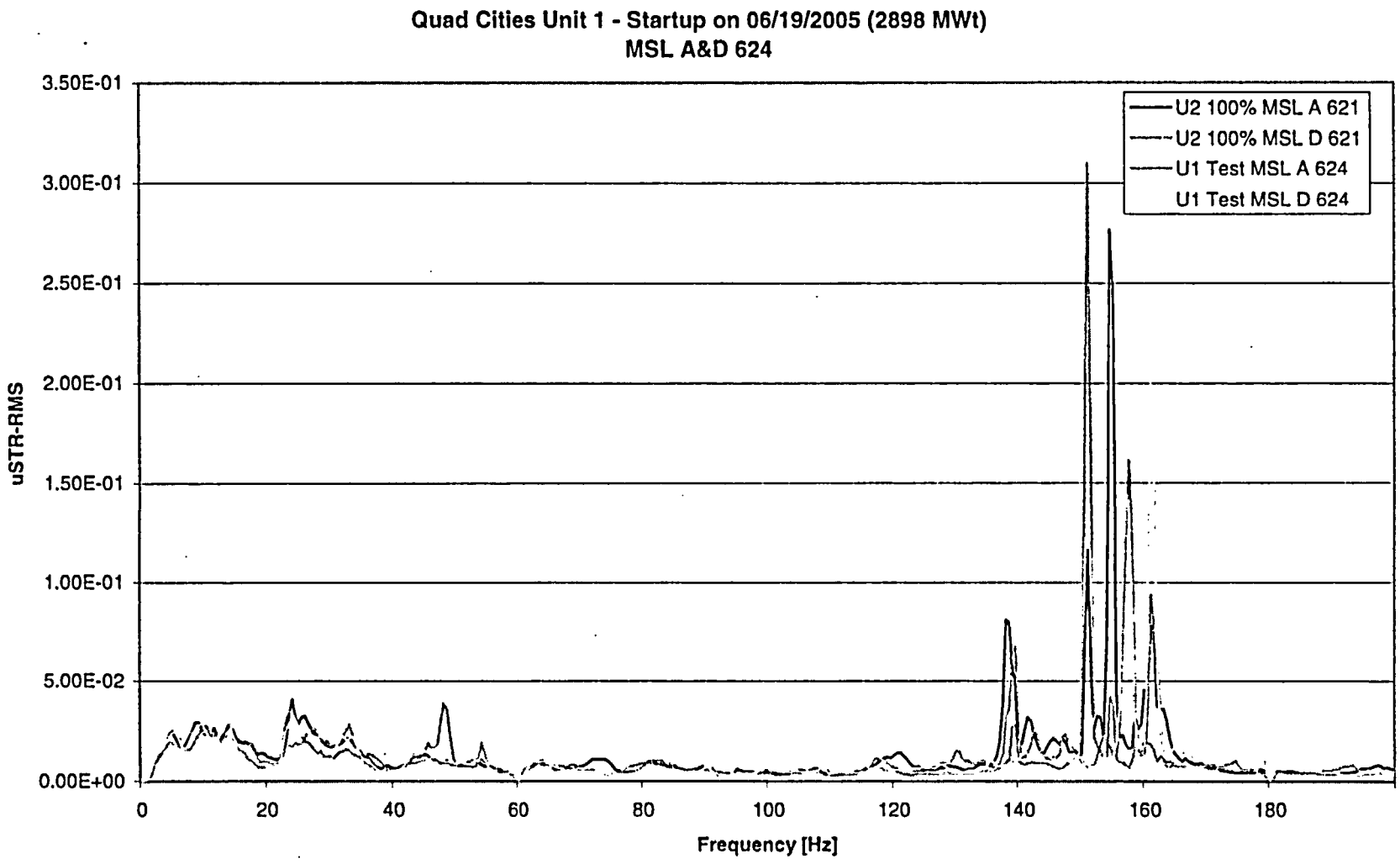
Quad Cities Unit 1 - Startup on 06/19/2005 (2898 MWt)
MSL A&D 624
U2 100% MSL A 621
U2 100% MSL D 621
U1 Test MSL A 624
U1 Test MSL D 624
uSTR-RMS
3.50E-01
3.00E-01
2.50E-01
2.00E-01
1.50E-01
1.00E-01
5.00E-02
0.00E+00
0
20
40
60
80
100
120
140
160
180
Frequency [Hz]

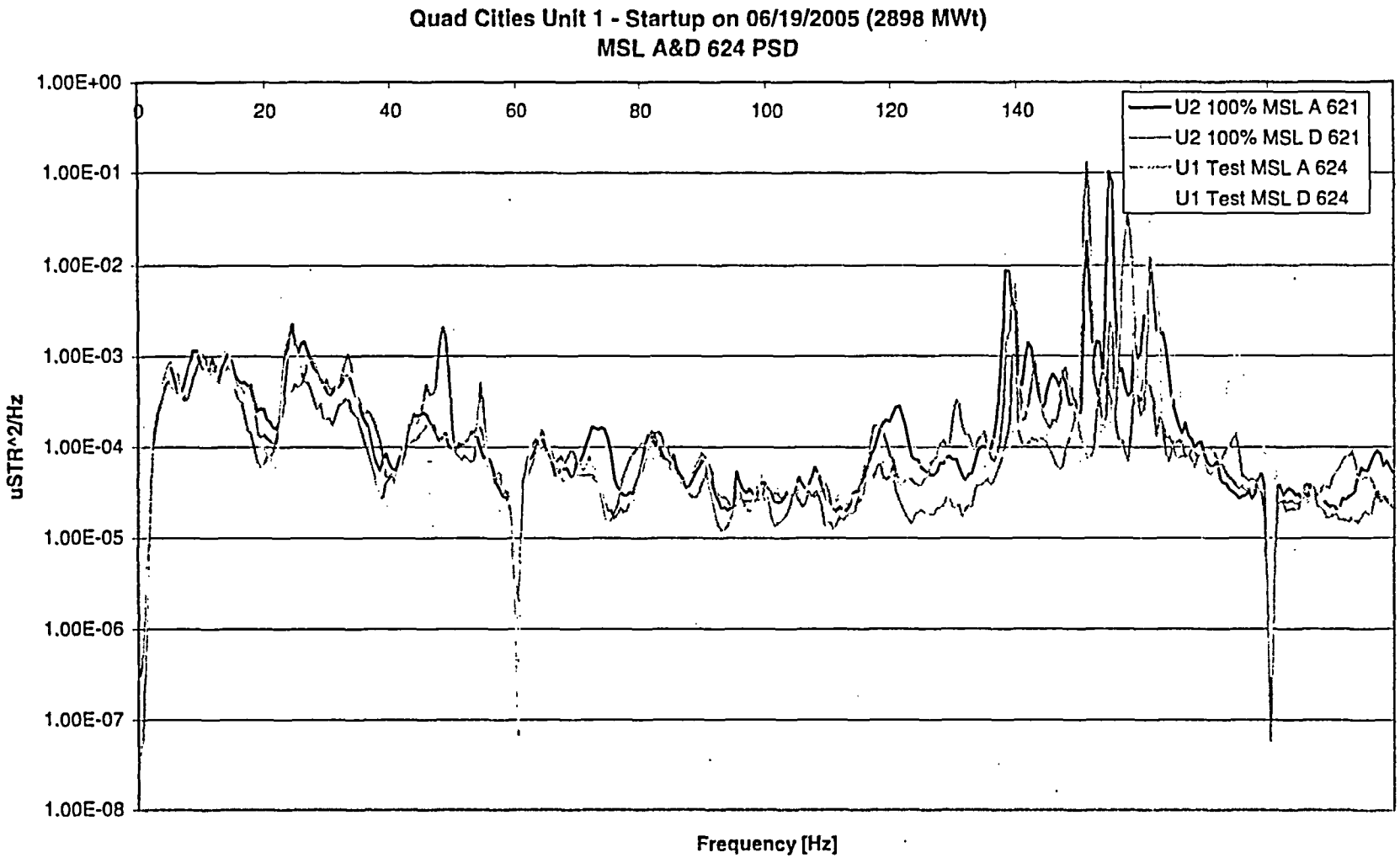
Quad Cities Unit 1 - Startup on 06/19/2005 (2898 MWt)
MSL A&D 624 PSD
1.00E+00
1.00E-01
1.00E-02
1.00E-03
1.00E-04
1.00E-05
1.00E-06
1.00E-07
1.00E-08
uSTR^2/Hz
0
20
40
60
80
100
120
140
Frequency [Hz]
U2 100% MSL A 621
U2 100% MSL D 621
U1 Test MSL A 624
U1 Test MSL D 624

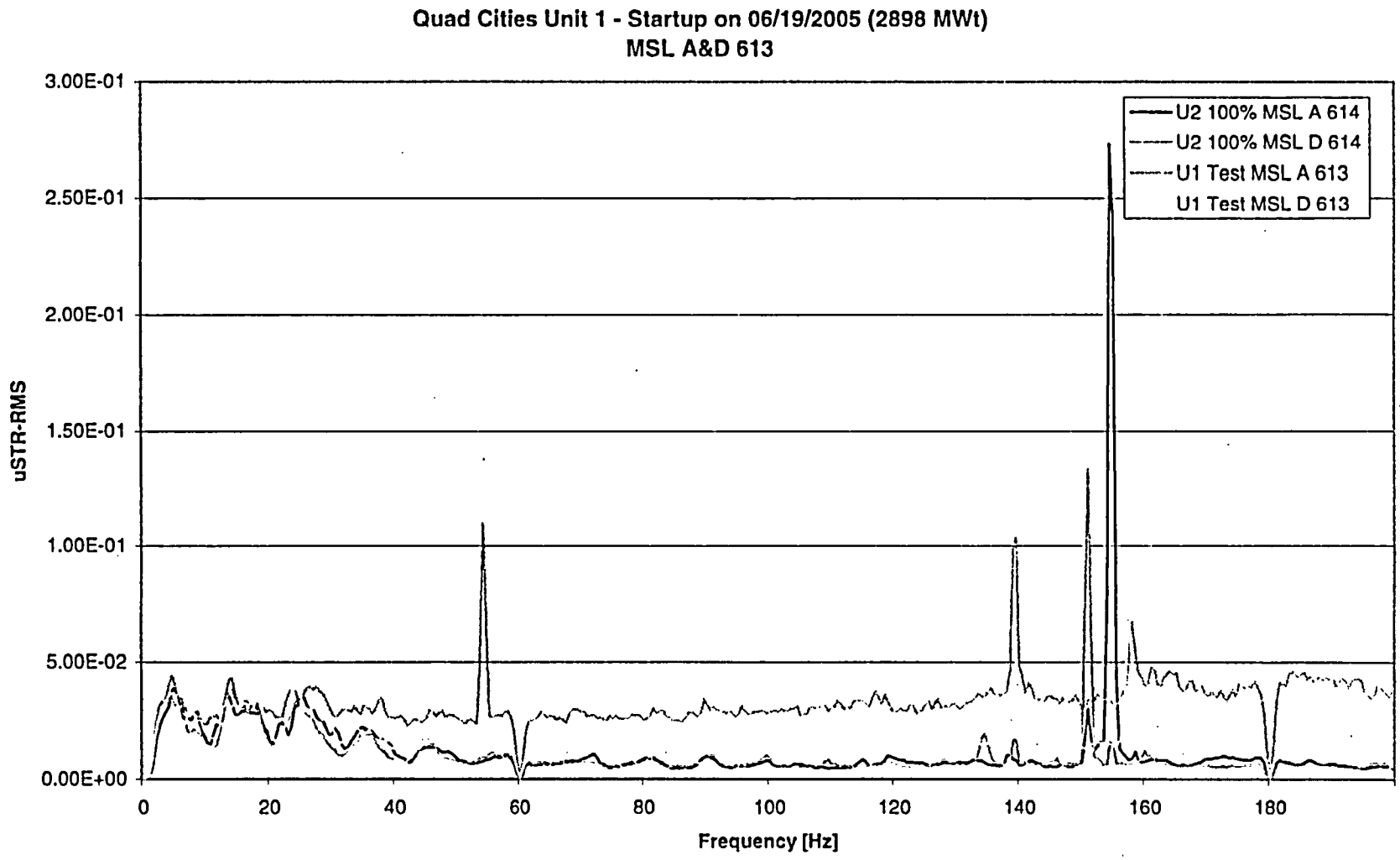
Quad Cities Unit 1 - Startup on 06/19/2005 (2898 MWt)
MSL A&D 613
U2 100% MSL A 614
U2 100% MSL D 614
U1 Test MSL A 613
U1 Test MSL D 613
uSTR-RMS
3.00E-01
2.50E-01
2.00E-01
1.50E-01
1.00E-01
5.00E-02
0.00E+00
0
20
40
60
80
100
120
140
160
180
Frequency [Hz]

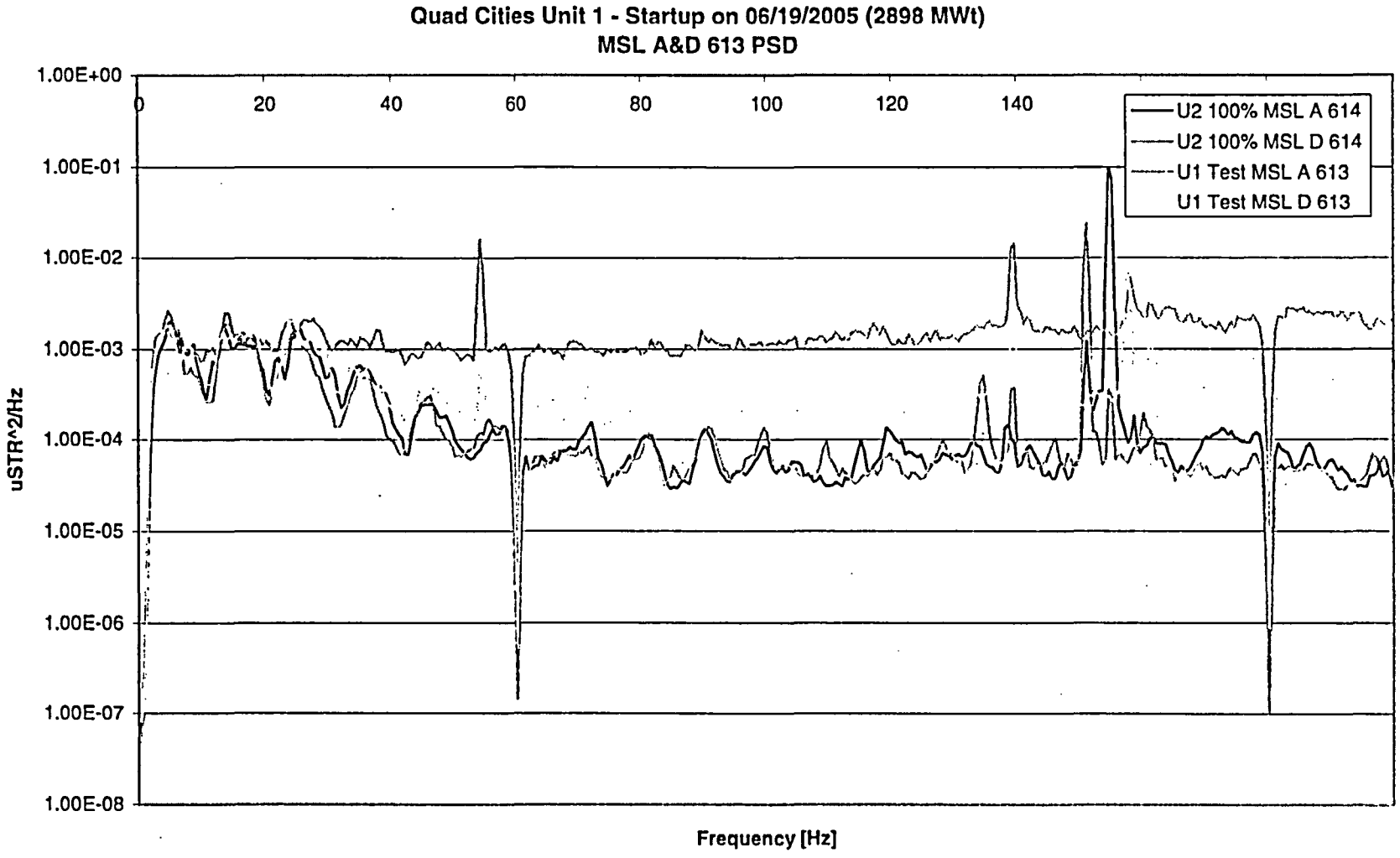
Quad Cities Unit 1 - Startup on 06/19/2005 (2898 MWt)
MSL A&D 613 PSD
1.00E+00
1.00E-01
1.00E-02
1.00E-03
1.00E-04
1.00E-05
1.00E-06
1.00E-07
1.00E-08
uSTR^2/Hz
0
20
40
60
80
100
120
140
Frequency [Hz]
U2 100% MSL A 614
U2 100% MSL D 614
U1 Test MSL A 613
U1 Test MSL D 613

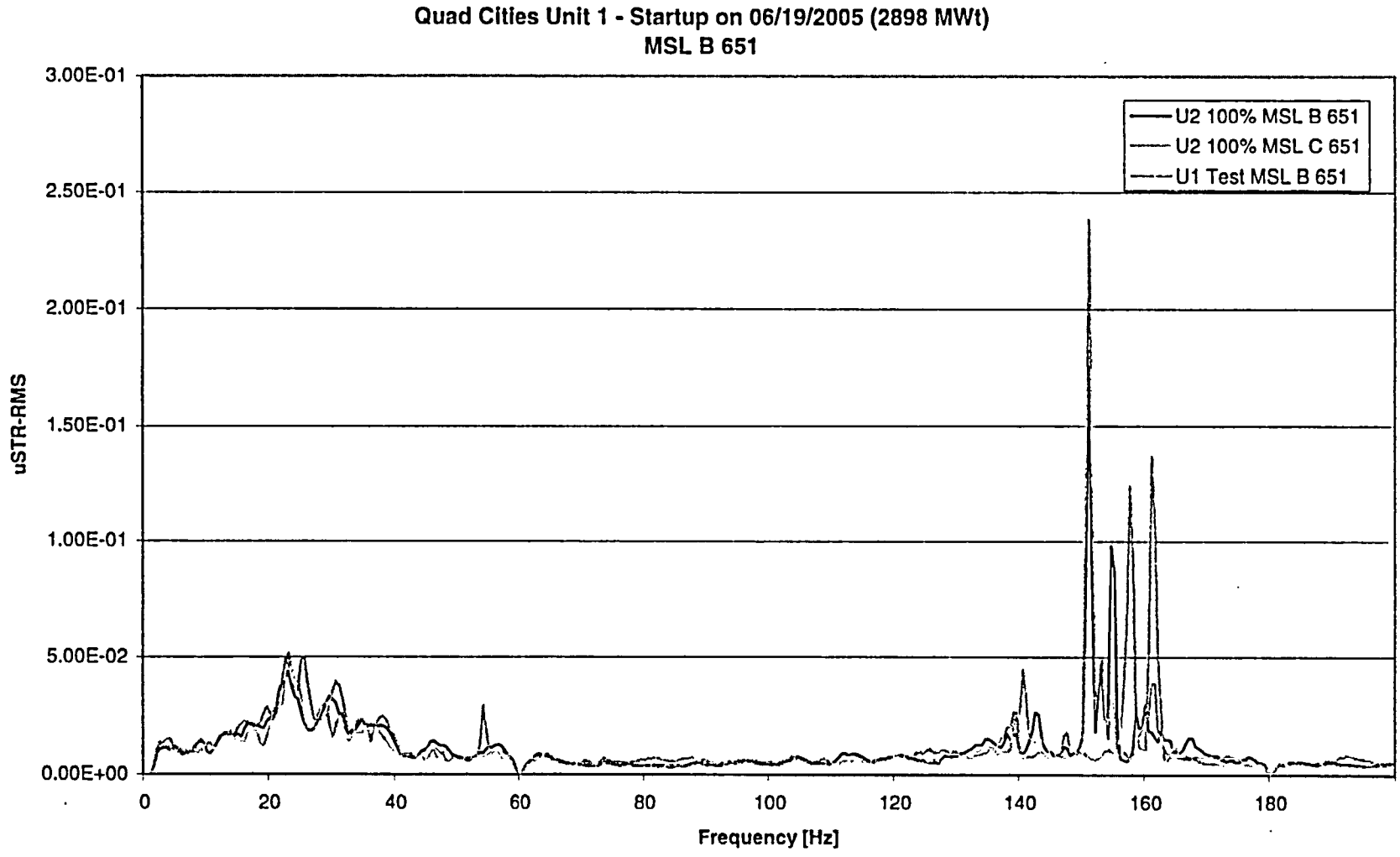
Quad Cities Unit 1 - Startup on 06/19/2005 (2898 MWt)
MSL B 651
U2 100% MSL B 651
U2 100% MSL C 651
U1 Test MSL B 651
uSTR-RMS
3.00E-01
2.50E-01
2.00E-01
1.50E-01
1.00E-01
5.00E-02
0.00E+00
0
20
40
60
80
100
120
140
160
180
Frequency [Hz]

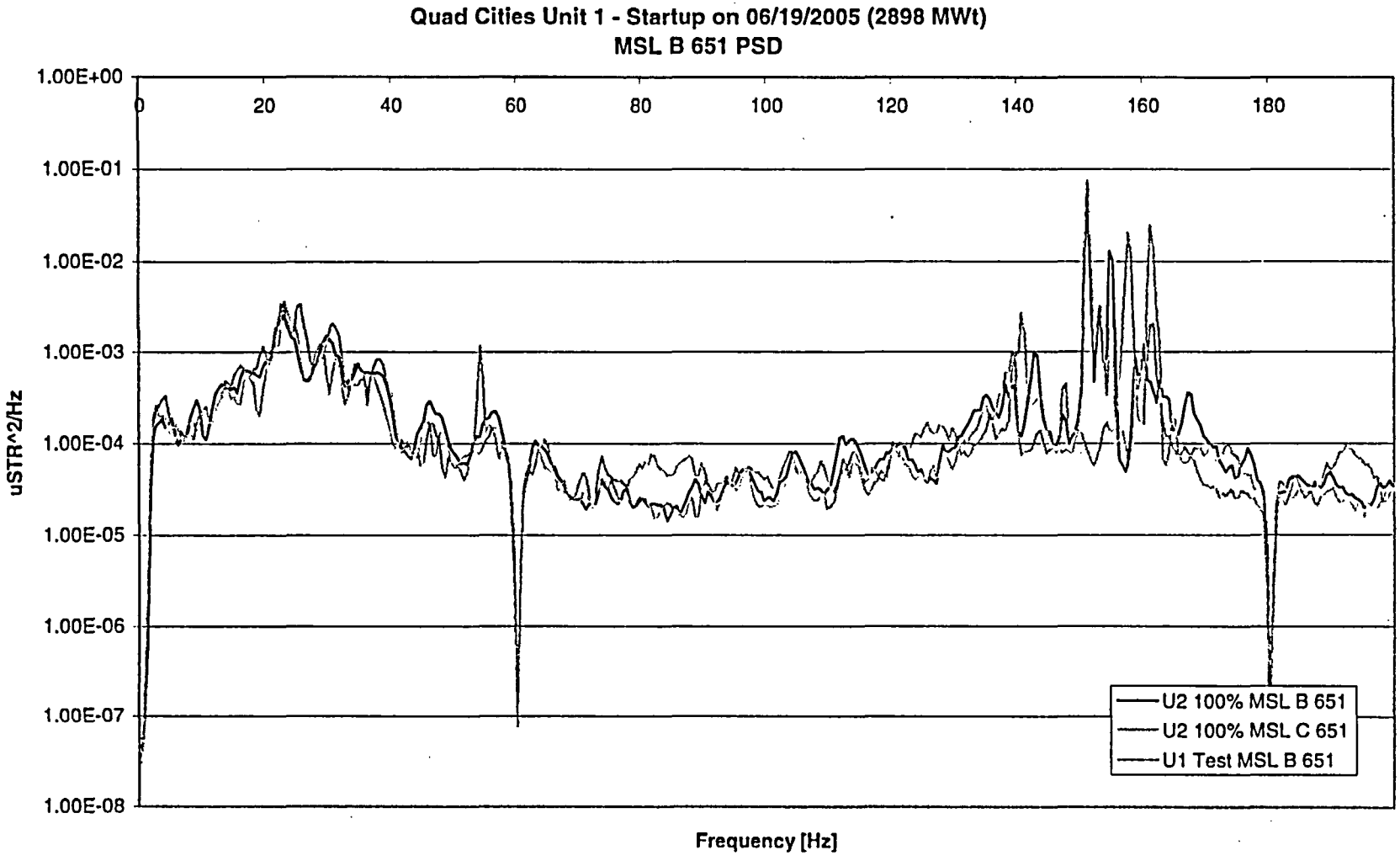
Quad Cities Unit 1 - Startup on 06/19/2005 (2898 MWt)
MSL B 651 PSD
1.00E+00
1.00E-01
1.00E-02
1.00E-03
1.00E-04
1.00E-05
1.00E-06
1.00E-07
1.00E-08
uSTR^2/Hz
0
20
40
60
80
100
120
140
160
180
Frequency [Hz]
U2 100% MSL B 651
U2 100% MSL C 651
U1 Test MSL B 651

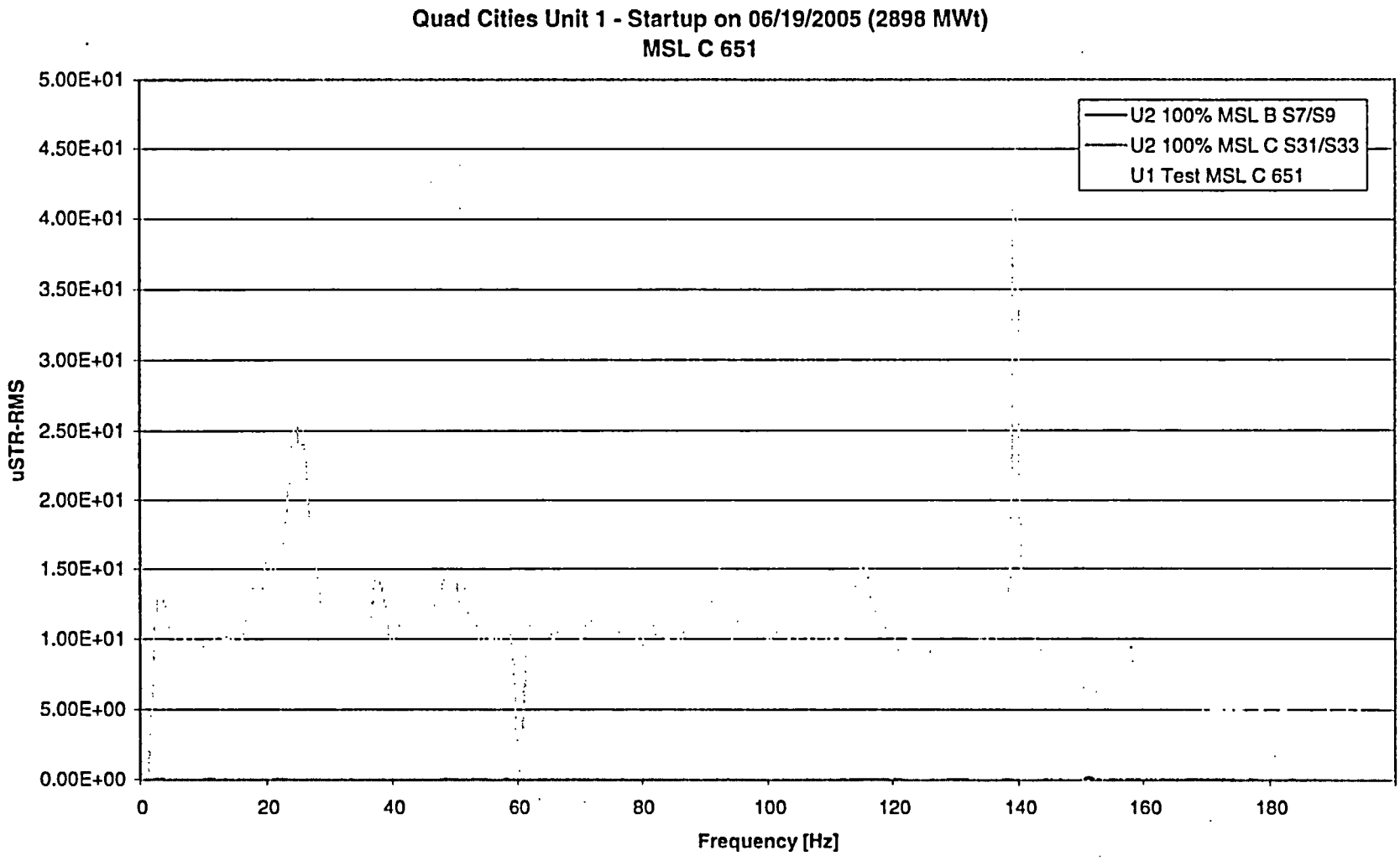
Quad Cities Unit 1 - Startup on 06/19/2005 (2898 MWt)
MSL C 651
U2 100% MSL B S7/S9
U2 100% MSL C S31/S33
U1 Test MSL C 651
uSTR-RMS
5.00E+01
4.50E+01
4.00E+01
3.50E+01
3.00E+01
2.50E+01
2.00E+01
1.50E+01
1.00E+01
5.00E+00
0.00E+00
0
20
40
60
80
100
120
140
160
180
Frequency [Hz]

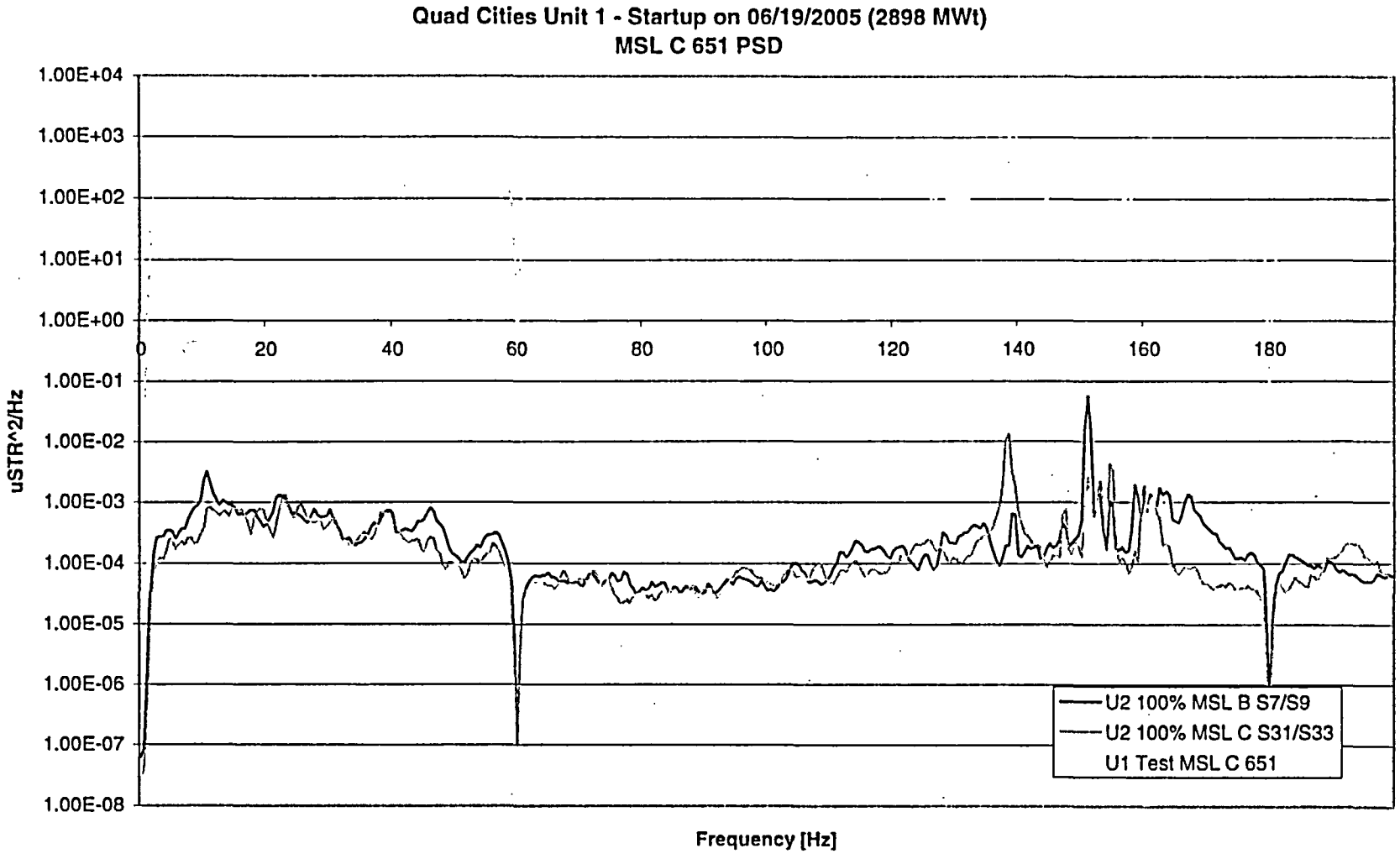
Quad Cities Unit 1 - Startup on 06/19/2005 (2898 MWt)
MSL C 651 PSD
1.00E+04
1.00E+03
1.00E+02
1.00E+01
1.00E+00
1.00E-01
1.00E-02
1.00E-03
1.00E-04
1.00E-05
1.00E-06
1.00E-07
1.00E-08
uSTR^2/Hz
0
20
40
60
80
100
120
140
160
180
Frequency [Hz]
U2 100% MSL B S7/S9
U2 100% MSL C S31/S33
U1 Test MSL C 651

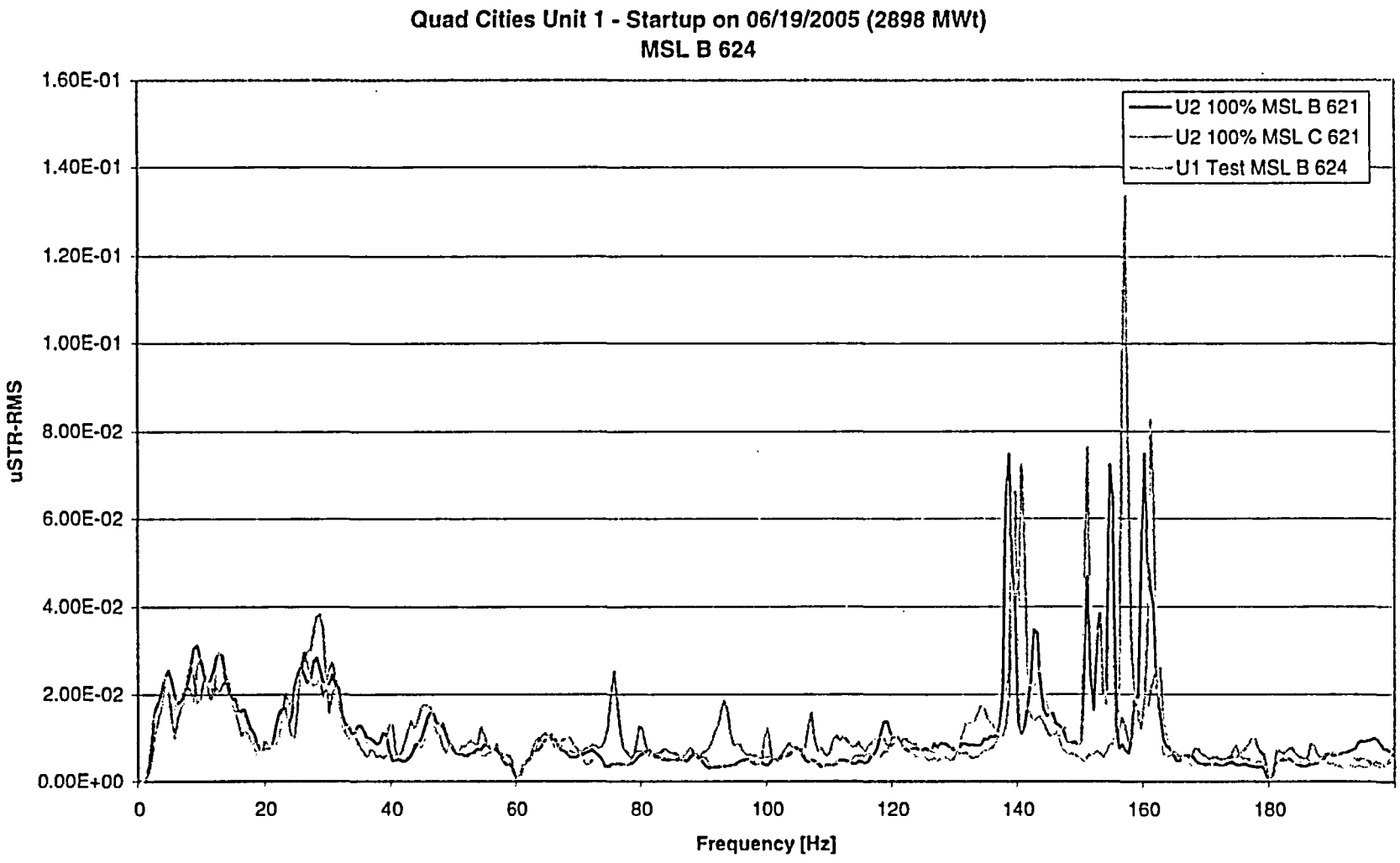
Quad Cities Unit 1 - Startup on 06/19/2005 (2898 MWt)
MSL B 624
U2 100% MSL B 621
U2 100% MSL C 621
U1 Test MSL B 624
uSTR-RMS
1.60E-01
1.40E-01
1.20E-01
1.00E-01
8.00E-02
6.00E-02
4.00E-02
2.00E-02
0.00E+00
0
20
40
60
80
100
120
140
160
180
Frequency [Hz]

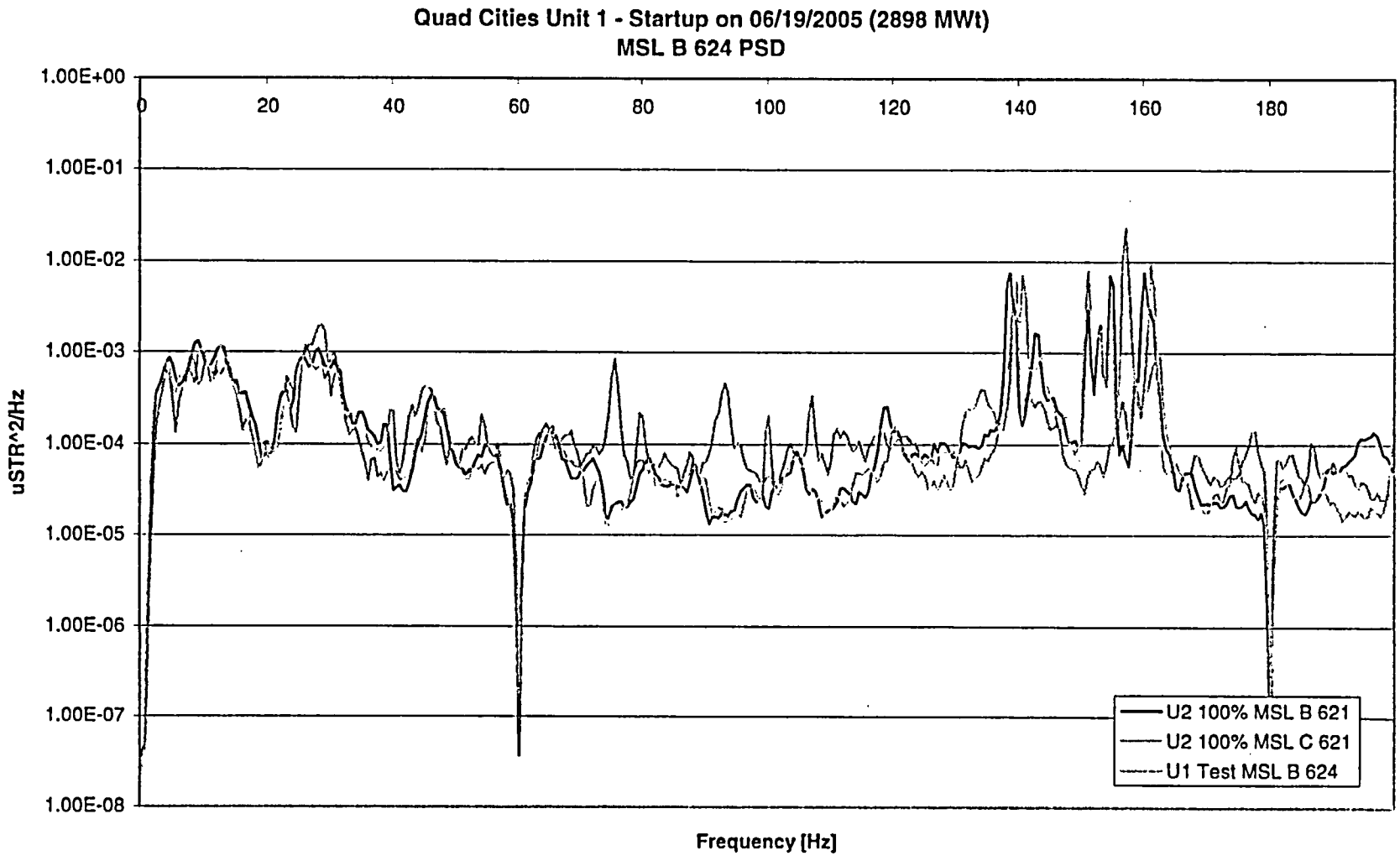
Quad Cities Unit 1 - Startup on 06/19/2005 (2898 MWt)
MSL B 624 PSD
1.00E+00
1.00E-01
1.00E-02
1.00E-03
1.00E-04
1.00E-05
1.00E-06
1.00E-07
1.00E-08
uSTR^2/Hz
0
20
40
60
80
100
120
140
160
180
Frequency [Hz]
U2 100% MSL B 621
U2 100% MSL C 621
U1 Test MSL B 624

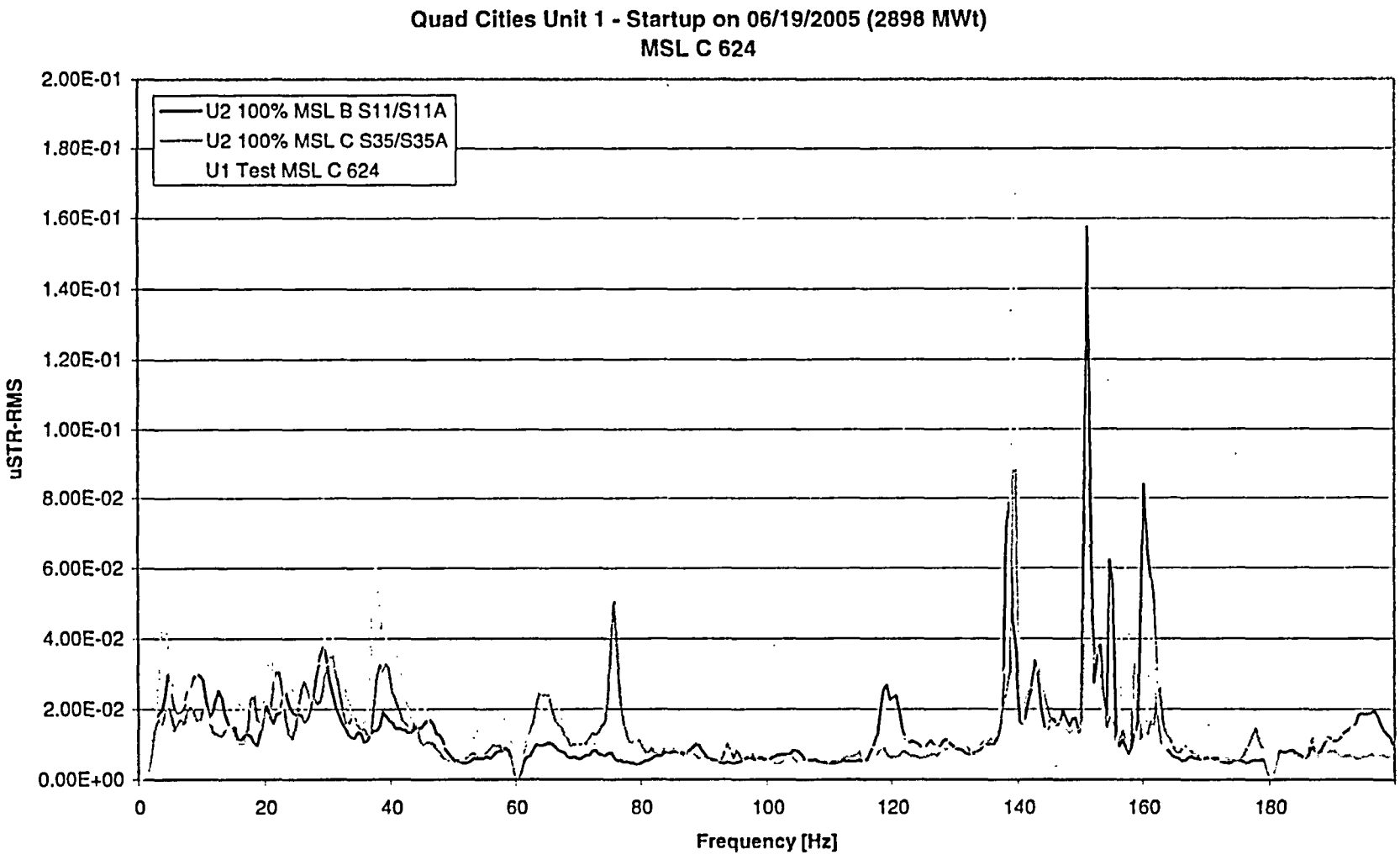
Quad Cities Unit 1 - Startup on 06/19/2005 (2898 MWt)
MSL C 624
U2 100% MSL B S11/S11A
U2 100% MSL C S35/S35A
U1 Test MSL C 624
uSTR-RMS
2.00E-01
1.80E-01
1.60E-01
1.40E-01
1.20E-01
1.00E-01
8.00E-02
6.00E-02
4.00E-02
2.00E-02
0.00E+00
0
20
40
60
80
100
120
140
160
180
Frequency [Hz]

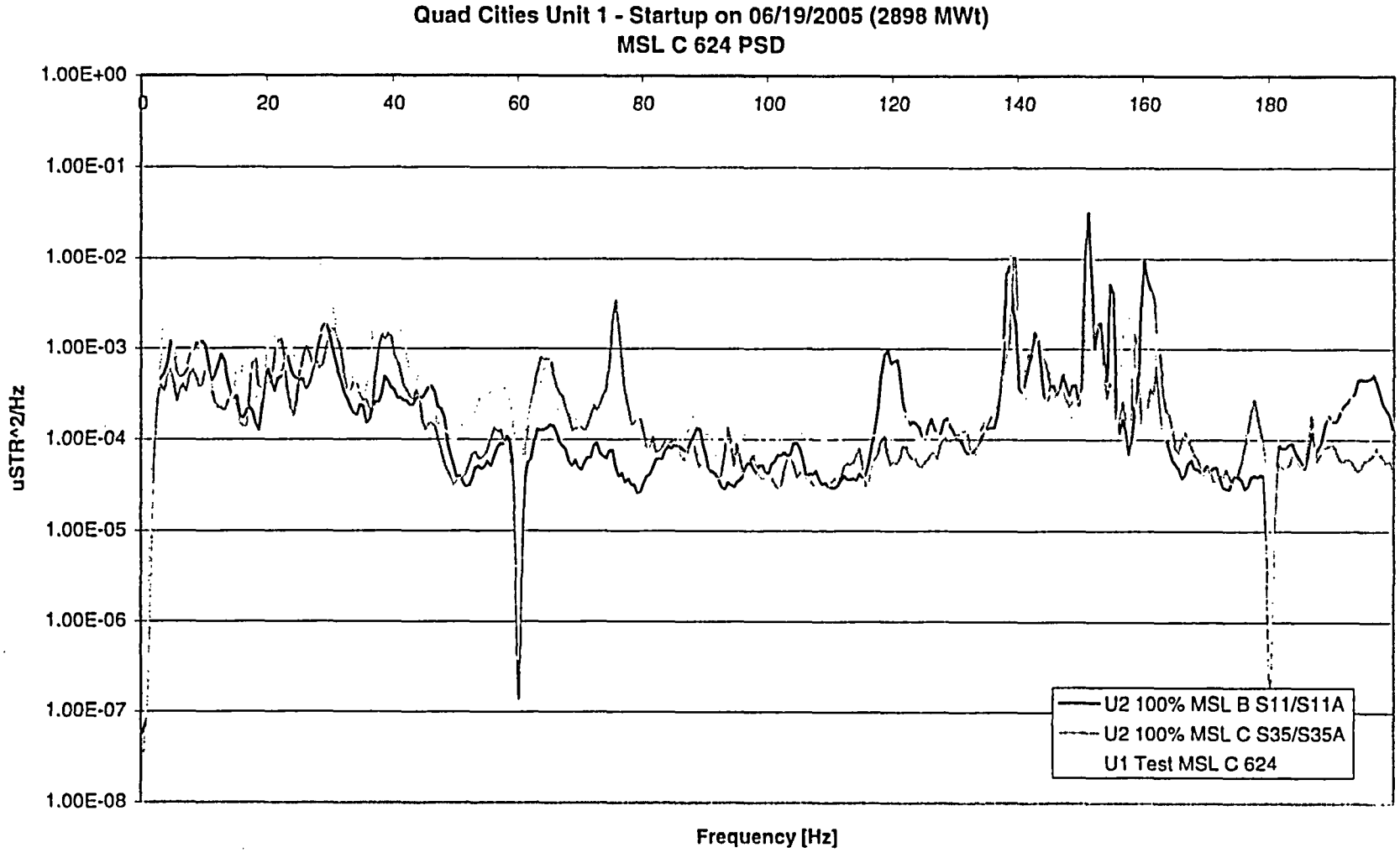
Quad Cities Unit 1 - Startup on 06/19/2005 (2898 MWt)
MSL C 624 PSD
1.00E+00
1.00E-01
1.00E-02
1.00E-03
1.00E-04
1.00E-05
1.00E-06
1.00E-07
1.00E-08
uSTR^2/Hz
0
20
40
60
80
100
120
140
160
180
Frequency [Hz]
U2 100% MSL B S11/S11A
U2 100% MSL C S35/S35A
U1 Test MSL C 624

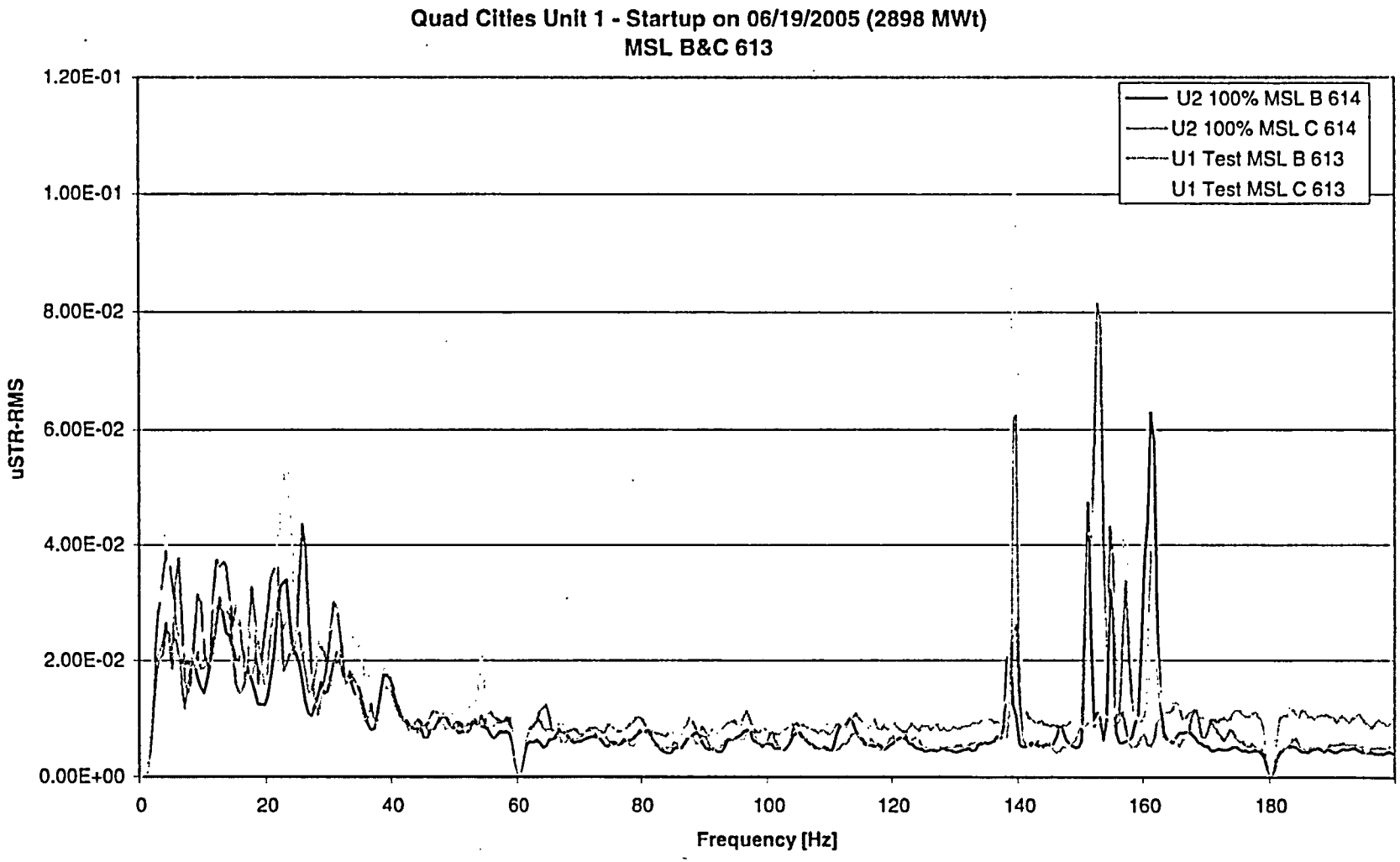
Quad Cities Unit 1 - Startup on 06/19/2005 (2898 MWt)
MSL B&C 613
U2 100% MSL B 614
U2 100% MSL C 614
U1 Test MSL B 613
U1 Test MSL C 613
uSTR-RMS
1.20E-01
1.00E-01
8.00E-02
6.00E-02
4.00E-02
2.00E-02
0.00E+00
0
20
40
60
80
100
120
140
160
180
Frequency [Hz]

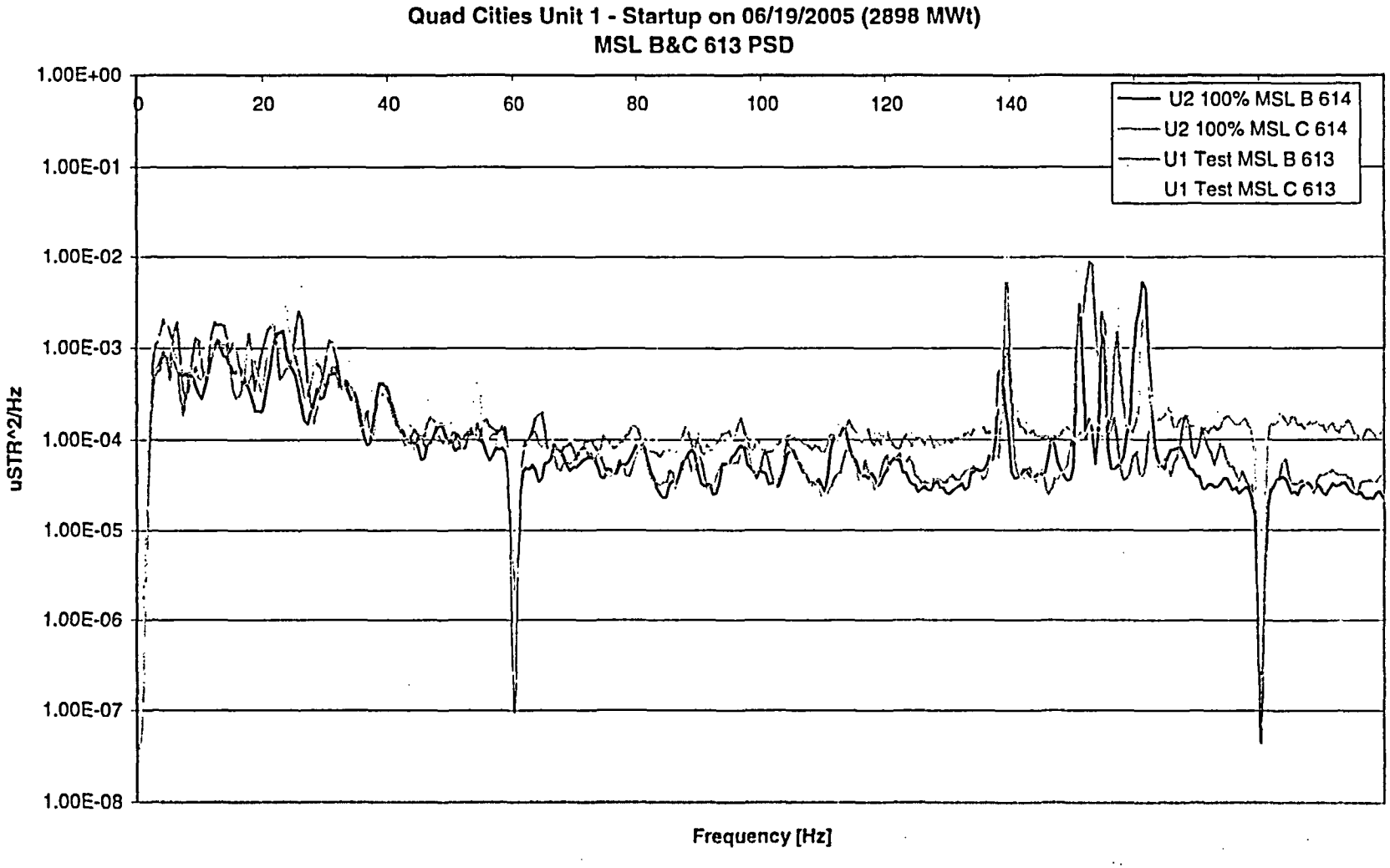
Quad Cities Unit 1 - Startup on 06/19/2005 (2898 MWt)
MSL B&C 613 PSD
1.00E+00
1.00E-01
1.00E-02
1.00E-03
1.00E-04
1.00E-05
1.00E-06
1.00E-07
1.00E-08
uSTR^2/Hz
0
20
40
60
80
100
120
140
Frequency [Hz]
U2 100% MSL B 614
U2 100% MSL C 614
U1 Test MSL B 613
U1 Test MSL C 613

ENCLOSURE 2

Attachment 2

Structural Integrity Associates Letter KKF-05-036, "Quad Cities Unit 1 Main Steam Line Strain Gage Reductions," dated July 6, 2005

Structural Integrity Associates, Inc.

6855 S. Havana Street
Suite 350
Centennial, CO 80112-3868
Phone: 303-792-0077
Fax: 303-792-2158
www.structint.com
kfujikawa@structint.com

July 6, 2005
SIR-05-208 Revision 2
KKF-05-036

Mr. Robert Stachniak
Exelon Nuclear
4300 Winfield Road
Warrenville, IL 60555

Subject: Quad Cities Unit 1 Main Steam Line Strain Gage Reductions

Dear Rob:

This letter report contains an evaluation of the Quad Cities Unit 1 (QC1) main steam line C elevation 651' (MSL C 651) strain gage data obtained during the June 2005 power ascension. In addition, this revision contains the evaluation of the QC1 strain gage locations where one strain gage failed during the June 2005 power ascension.

Background

Main steam line strain gage data was obtained during the June 2005 power ascension at Quad Cities Unit 1 [1]. This data will be used to as input to the acoustic line analysis that determines the forcing function on the steam dryer. Prior to the power ascension, strain gages were installed on each of the four main steam lines (MSLs) at two axial locations. At each axial location two strain gage pairs are formed with two gages 180° apart. The two gages are connected to a Wheatstone bridge in the ½ bridge configuration where the two strain gages will sum to provide higher sensitivity and provide cancellation of the Poisson effect due to pipe bending. Figures 1a and 1b shows sketches of the strain gage locations for Quad Cities Unit 1 MSL A, B, C, and D. In addition, these sketches identify the strain gages that failed during the June 2005 power ascension [2].

The purpose of the strain gage measurement is to obtain an indirect measurement of the dynamic pressure pulsations in the main steam piping. The strain gages are used to measure the hoop strain that can then be converted into internal pressure. Due to the location of the strain gages, each individual gage will contain breathing mode strain as well as additional hoop strains associated with higher order shell responses. Due to the random nature of the pressure in the pipe, the strain bridges were averaged in the two orthogonal planes to provide a representative strain at each location.

The strain data is processed by averaging the time histories of the two orthogonal half bridges (sum and divide by 2) and processing (spectra, rms, maximum, minimum) the data for the averages. In general, the averaging provides a reduction of the rms, maximum and minimum values due to several of the primary frequencies (large amplitude peaks in the spectra) being nearly 180° out of phase between the orthogonal planes.

A problem occurred during the power ascension due to failure of individual strain gages. Specifically, strain gage S31 (located at MSL C 651) failed after test condition TC10 so the half bridge S31/33 data were unavailable for the higher power levels. For this case, an average of the orthogonal bridges was not possible and only the half bridge (S32/34) and the quarter bridge (S33) were available.

A review of the TC15a data at QC1 MSL C 651 where strain gage S31 failed shows that S32/34 provides unusually high peaks (Figures 4 and 5) at 157.7 Hz (0.78 $\mu\varepsilon_{rms}$) and 78.6 Hz (0.26 $\mu\varepsilon_{rms}$). This paper discusses the feasibility of determining a method to combine the strain gages where there is only ¼ and ½ bridge data.

Approach

An approach is to use the actual QC1 plant data obtained during the June 2005 power ascension and combine the ½ bridge (S32/S34) strain gage time history with the ¼ bridge (S33) strain gage time history to obtain the frequency spectra for QC Unit 1 (QC1) MSL C 651. This approach is a reasonable and conservative method for determining the pressure induced measurement at QC1 MSL C 651 and is based on the structural similarities between QC1 and QC Unit 2 (QC2).

The relationship between the pressure loading and the response of the two units at a particular strain location appears to be largely independent of the pressure loading. In other words, the structures respond to pressure loadings based on a set of fixed transfer functions that are the same for both units. The relationship between orthogonal strain measurements, in- and out-of plane at a particular location, is also determined by these transfer functions.

In comparing QC2 MSL C 651 (Figures 2 and 3), where both bridges are functioning as ½ bridges, to QC1 MSL C 651 (Figures 4 and 5), where there is a ½ bridge (S32/34) and a ¼ bridge (S33), the similarity in relative amplitudes between S32/34 to S31/33 is striking. The maximum values in the 140 to 160 Hz range are also comparable per strain gage pair. Figures 1 through 4 are composed of the individual strain measurements in the orthogonal planes and the average (QC1 S31 failed of the strain gage pair S31/33, so only a ¼ bridge is available for that pair).

Another example of similar local strain behavior between QC2 to QC1 strain measurements is found by reviewing the orthogonal amplitudes for QC2 MSL D 624, Figure 6, and QC1 MSL D 624 Figures 7. For QC2 MSL D 624, the amplitudes of the orthogonal pair are similar in magnitude (Figure 6) particularly in the frequency range of 140 to 160 Hz. A comparison of the amplitudes between QC2 MSL D 624 (Figure 6) and QC1 MSL D 624 (Figure 7) shows that the magnitudes of the orthogonal pairs are also similar between the two plants in the frequency range

of 140 to 160 Hz and both yield much lower average amplitudes at these frequencies. In addition, the amplitudes for QC1 and QC2 MSL D 624 (Figures 6 and 7) are greater than the amplitudes in the frequency range of 140 – 160 Hz, for QC1 and QC2 MSL C 651 (Figures 3 and 5). It should be noted that the combined result for QC1 MSL C 651, Figure 5, using S32/34 and S33, reduces the strain amplitudes in the 140 – 160 Hz range less than the reduction for MSL D 624 using two ½ bridges. Based on the amplitude reductions seen from the QC1 and QC2 MSL D 624 averages, it appears that the three strain gages averaged together at QC1 MSL C 651 is still conservative in this frequency range.

Given the structural similarities between the two units in addition to the strain measurement analysis results above and the fact that the strain gages on opposite sides of the piping cross-section should respond similarly (as they do in at least one case where individual gages are available), the combined average of S33 and S32/34 for TC15A (Figures 4 and 5) can be used as a conservative representation of the pressure induced measurement at QC1 MSL C 651. This will provide an overall RMS reduction factor of nearly 1.7 (Table 1) and an individual reduction factor of 1.7 at 157.7 Hz and a reduction factor of 1.7 at 78.6 Hz.

Table 1 contains the rms, peak-peak, and rms spectral values at 157.7 Hz and 78.6 Hz for the ¼ and ½ bridges. The averaged ¼ and ½ bridge rms, peak-peak, and rms spectral values at 157.7 Hz and 78.6 Hz are also listed in Table 1 and are identified as MSL C-651 [avg(S33+S32/S34)]. In addition, the ratio of the ¼ and ½ bridge results divided by the MSL C-651 results are also listed in Table 1.

A review of Table 1 shows the overall reduction of 1.6 to the rms values for S32/34 versus the averaged MSL C-651 rms value. In addition, the spectral peaks at 157.7 Hz and 78.6 Hz are also reduced by factors of 1.7 for both frequencies.

Table 1. QC1 MSL C 651 Strain Gage Data

	TC 15a (1/2 Bridge Data) (με)			
Unit 1 MSL C 651			**157.7 Hz**	**78.6 Hz**
	rms	**pk-pk**	**rms**	**rms**
(S33) In-plane	0.40	3.26	0.13	0.04
Ratio [(S33)]/MSL C-651	**0.58**	**0.56**	**0.32**	**0.28**
(S32/34) Out of plane	1.11	9.63	0.66	0.26
Ratio [(S32/34)]/MSL C-651	**1.60**	**1.66**	**1.67**	**1.72**
MSL C-651 [avg(S33+S32/34)]	0.69	5.80	0.40	0.15

In addition to the failure of strain gage S31, strain gages S3, S6, S11A, and S36 failed during the June 2005 power ascension [2]. These failed strain gages correspond to locations QC1 MSL A 651 (S3), QC1 MSL A 624 (S6), QC1 MSL B 624 (S11A), and QC1 MSL C 624 (S36). Using the same methodology to combine the ¼ and ½ bridge for these locations results in a reduction at 157.7 Hz. Table 2 lists the rms and peak-peak values for these locations for the ¼ and ½ bridges.

Table 2. QC1 MSLs A 651, A 624, B 624, and C 624

	MSL A 651	rms	pk-pk	MSL A 624	rms	pk-pk	MSL B 624	rms	pk-pk	MSL C 624	rms	pk-pk
	(S1) In-plane	0.76	4.81	(S5/5A) In-plane	0.31	3.15	(S11) In-plane	0.38	6.30	(S35/35A) In-plane	0.41	3.50
Ratio	[(S1)]/MSL A-651	1.55	1.31	[(S5/5A)]/MSL A 624	0.58	0.24	[(S11)]/MSL B 624	1.14	1.16	[(S35/35A)]/MSL C 624	1.23	2.76
	(S2/4) Out of plane	0.52	4.93	(S6A) Out of plane	1.02	23.40	(S12/12A) Out of plane	0.41	5.55	(S36A) Out of plane	0.49	4.11
Ratio	[(S2/4)]/MSL A-651	1.06	1.35	[(S6A)]/MSL A 624	1.88	1.81	[(S12/12A)]/MSL B 624	1.22	1.02	[(S36A)]/MSL C 624	1.50	3.24
	MS A-651 avg[S1+S2/4]	0.49	3.66	MSL A 624 avg [S5/S5A+S6A]	0.54	12.90	MSL B 624 avg [S11+S12/S12A]	0.34	5.45	MSL C 624 avg [S35/35A+S36A]	0.33	1.27

There appears to be a minimal reduction for MSL B 624, this is due to a residual amplitude at 60 Hz that still exists after the application of a notch filter.

Raw Data Conversion Factor for CDI

The conversion factor (CF) to be used by CDI to convert from the raw, recorded strain (με) data to pressure (psi) is applied to strain data acquired using a half bridge configuration. The Yokogawa data acquisition system (DAS) was set up to initially record data from ¼ bridges. After the initial DAS setup, the strain gage configuration was modified to two pairs of ½ bridges at each location. The settings on the DAS were not changed so the data was recorded as if each channel was configured as a ¼ bridge. Thus, for this system configuration, if a quarter bridge is used in conjunction with a half bridge, as is the case for MSL C 651, then the following equation must be used to convert this combination to the average pressure ($P_{33+32/34}avg$).

$$P_{33+32/34}avg = \{ [2 * S33 + (S32 + S34)] \div 2 \} \times CF$$

where CF is the conversion factor for MSL C 651(CF=1.94) and $P_{33+32/34}avg$ will be in psi. Table 3 lists the conversion factors for the other main steam line locations that contained ¼ -½ bridge combinations.

Table 3. QC1 Conversion Factors

Location	CF
MSL A 624	1.896
MSL A 651	1.914
MSL B 624	1.821
MSL C 624	1.893

Conclusion

Using actual data obtained during June 2005 for QC1 MSL C 651 where only one ½ bridge (S32/34) and one ¼ bridge (S33) is available; the strain gage measurement can be conservatively determined by averaging the ½ bridge data with the ¼ bridge data. Similarities discussed above in the QC1 and QC2 strain gage data demonstrate that the ¼ and ½ bridge strain gage combination at QC1 MSL C 651 results in conservative pressures for the frequencies of concern. This results in an overall reduction of 1.6 to the overall rms values over the bandwidth of 2 – 200 Hz for S32/34 versus the averaged MSL C-651 rms value. In addition, the spectral peaks at 157.7 Hz and 78.6 Hz are also reduced by factors of 1.7 for both frequencies.

Additionally, for the other locations that had one strain gage fail (QC1 MSL A 624, QC1 MSL A 651, QC1 MSL B 624, and QC1 MSL C 624), the actual measured data for the ¼ and ½ bridges can also be combined which results in an overall reduction of the rms values and spectral peaks.

If you have any questions, please do not hesitate to contact me at (303) 792-0077.

Prepared By:

Lawrence S. Dorfman
Associate

Reviewed By:

Karen K. Fujikawa, P.E.
Associate

Approved By:

Karen K. Fujikawa, P.E.
Associate

kkf

REFERENCES:

1. Exelon Document No. TIC-1252, Revision 0, "Quad Cities Unit 1 Power Ascension Test Procedure for the Reactor Vessel Steam Dryer Replacement," SI File No. EXLN-20Q-201.
2. Exelon TODI No. ODC-05-0225, "Main Steam Line Strain Gauge Failures During Quad Cities Unit 1 Startup Testing," SI File No. EXLN-20Q-201.

cc: EXLN-20Q-401
Chuck Alguire (Exelon)
Guy DeBoo (Exelon)
Brian Strub (Exelon)
Milt Teske (CDI)

Roman Gesior (Exelon)
Keith Moser (Exelon)
Kevin Ramsden (Exelon)

K. Rach (SI)
G. Szasz (SI)

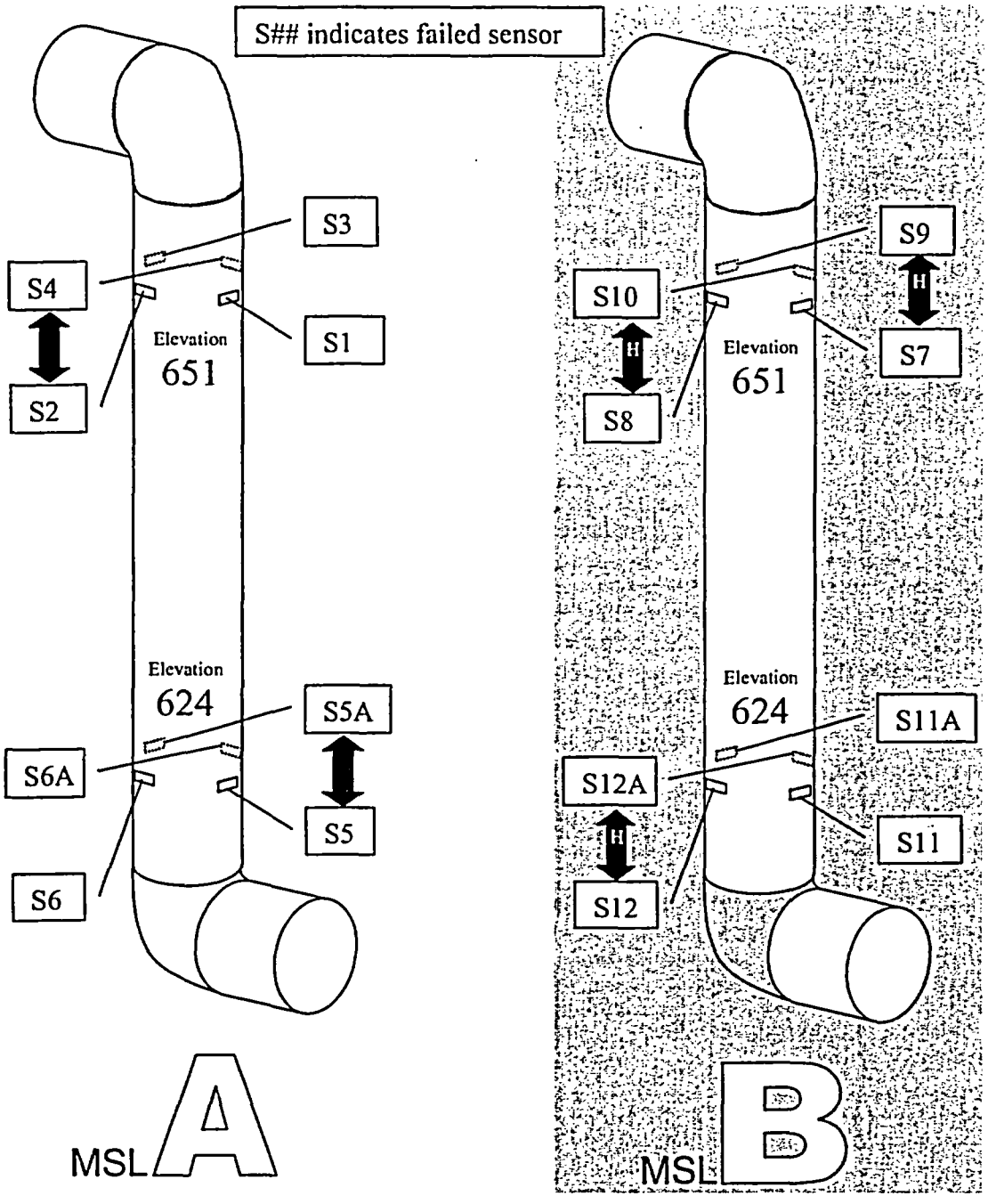

Figure 1a. Location of Failed Strain Gages on QC1 MSLs A and B

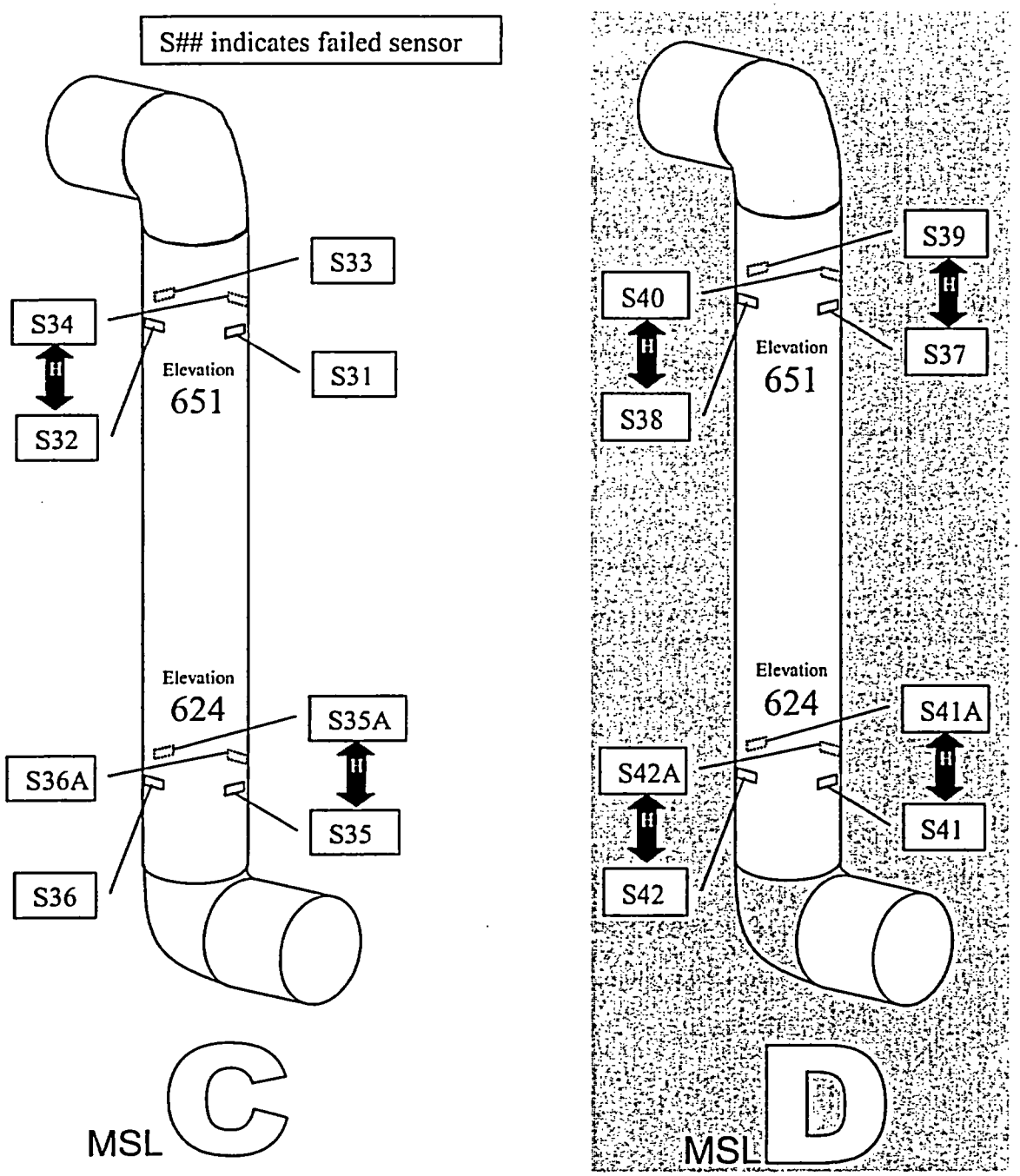

Figure 1b. Location of Failed Strain Gages on QC1 MSLs C and D

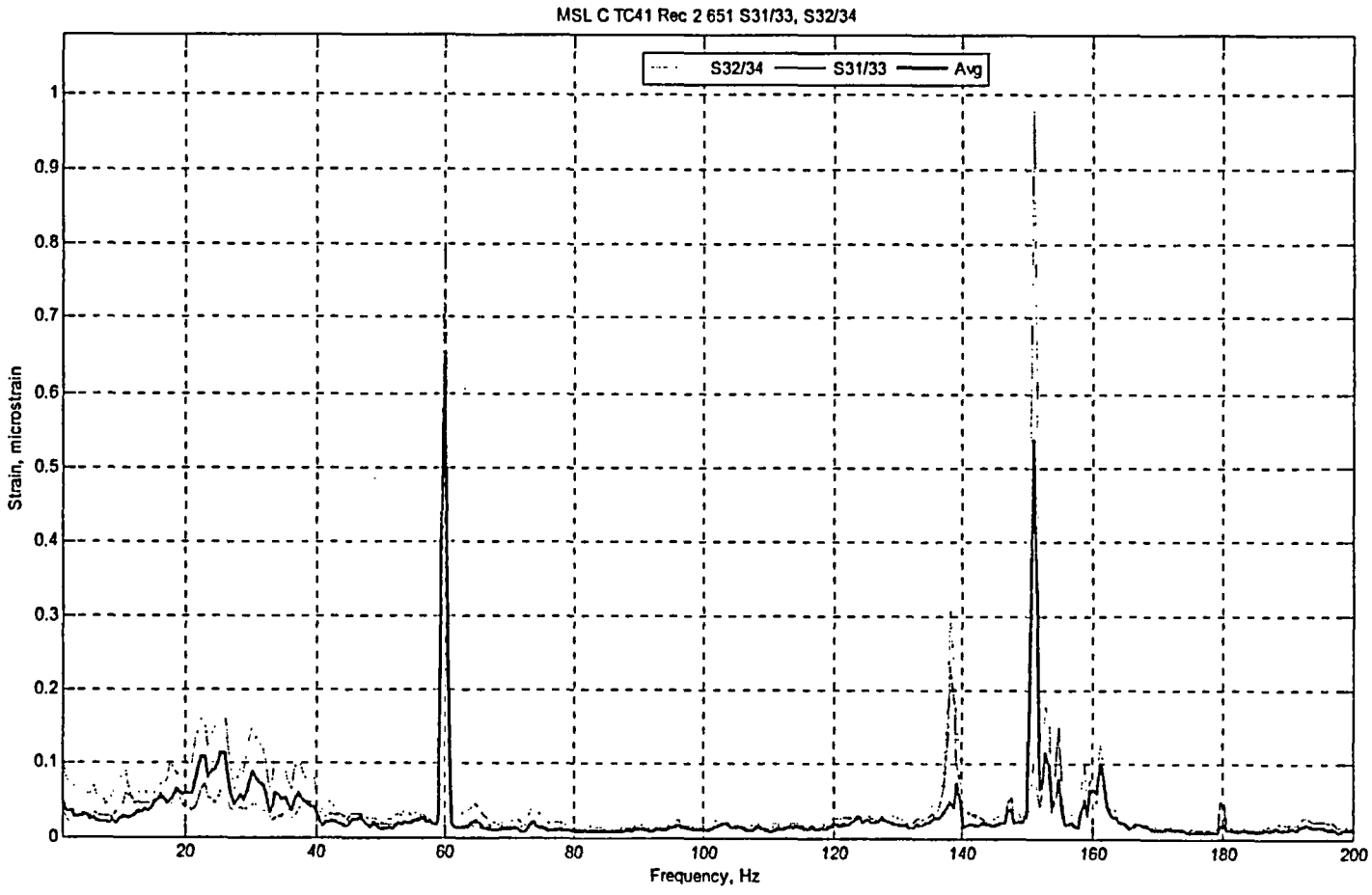

Figure 2. QC2 MSL C 651 Combined

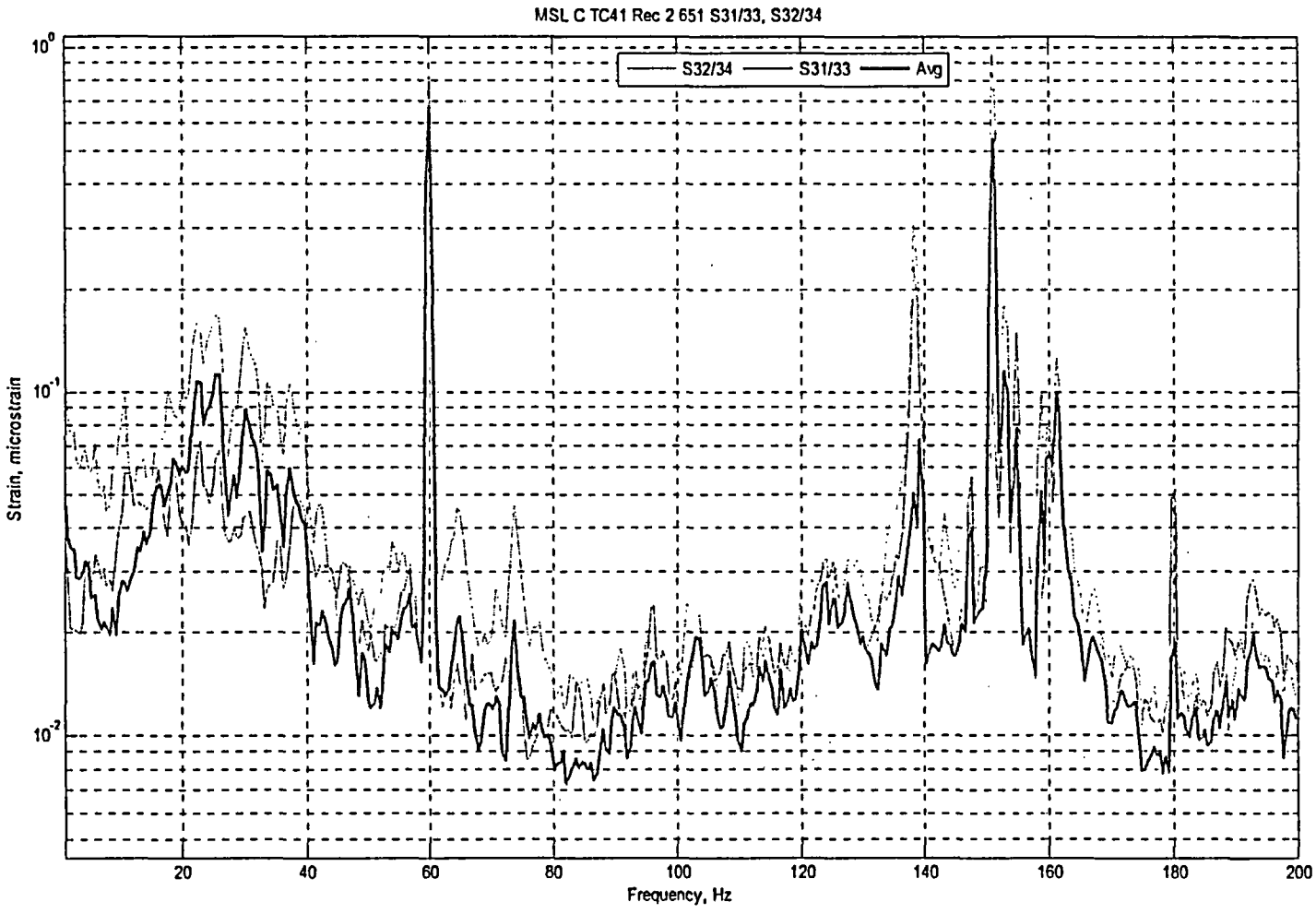

Figure 3. QC2 MSL C 651 Combined

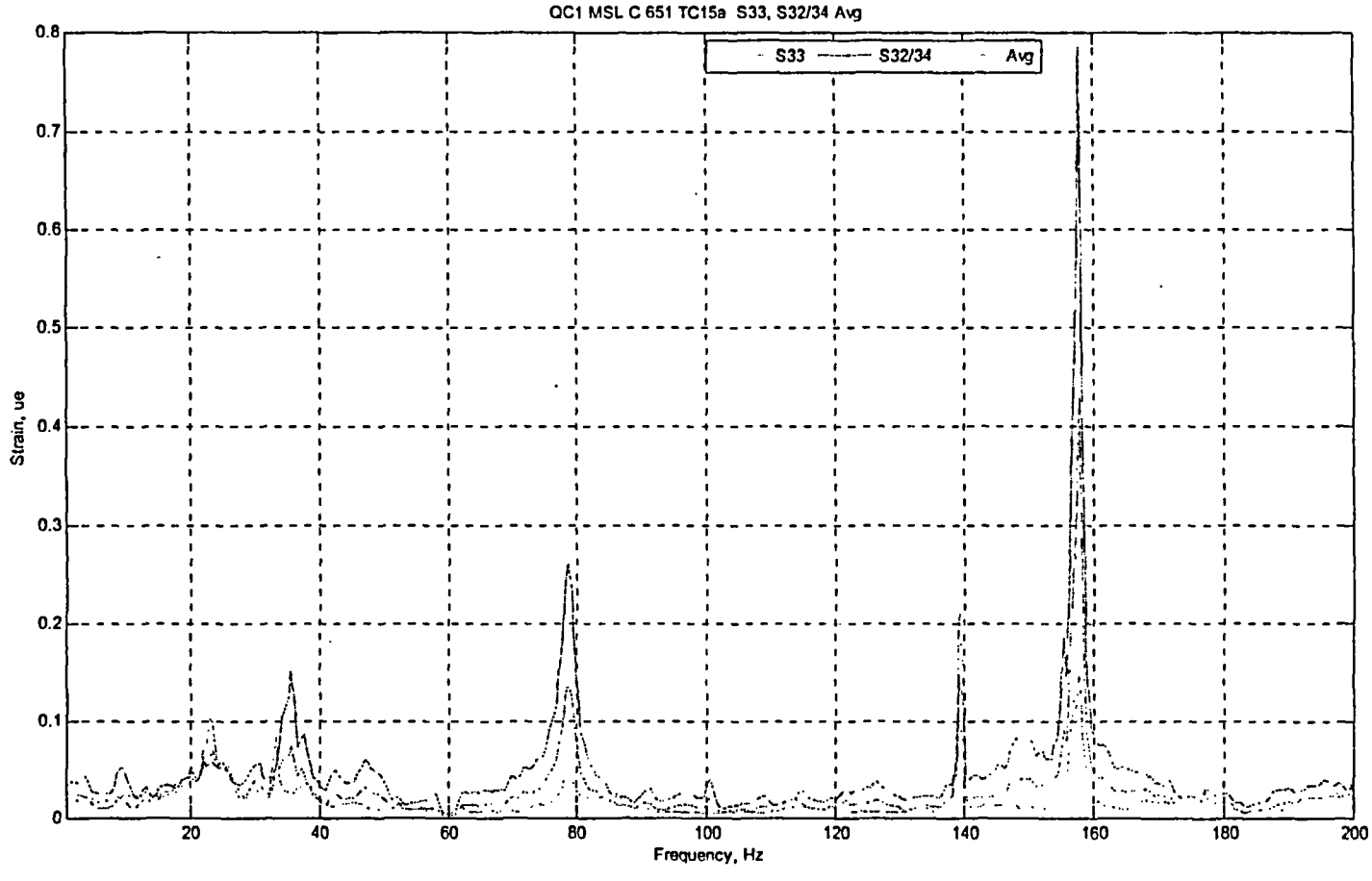

Figure 4. QC1 MSL C 651 S33 & S32/34 Combined

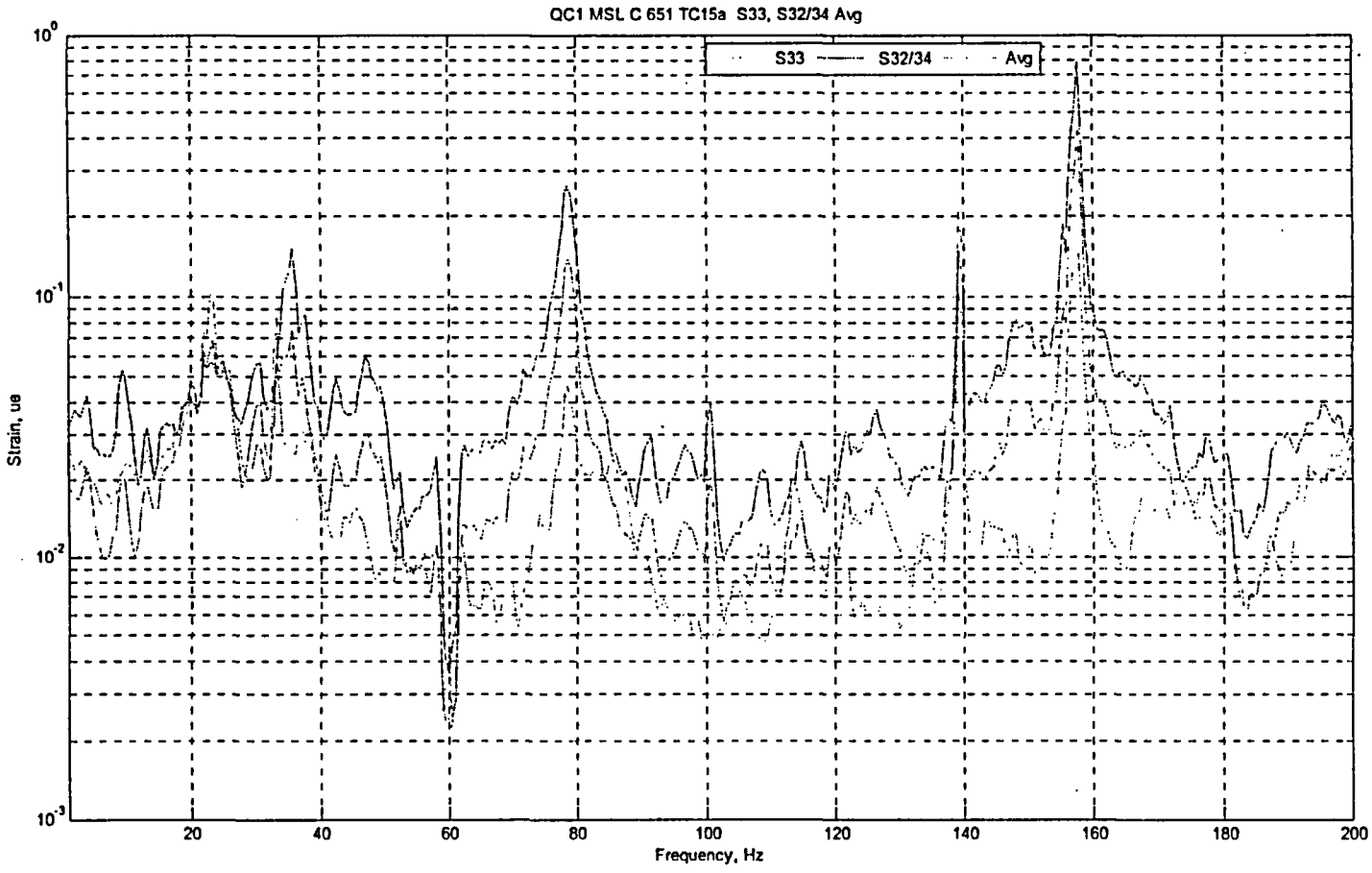

Figure 5. QC1 MSL C 651 S33 & S32/34 Combined

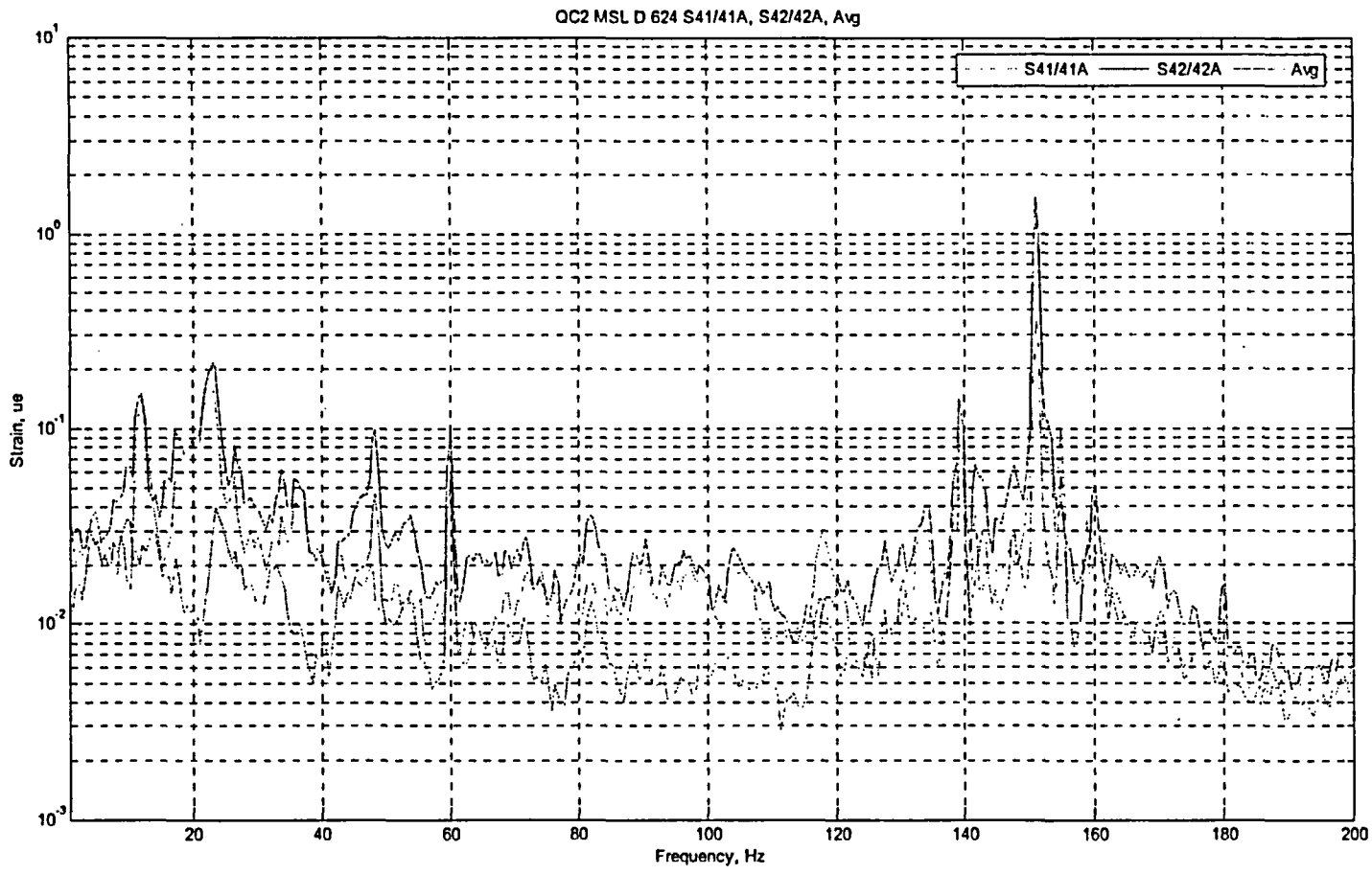

Figure 6. QC2 MSL D 624 Combined (Both ½ Bridges)

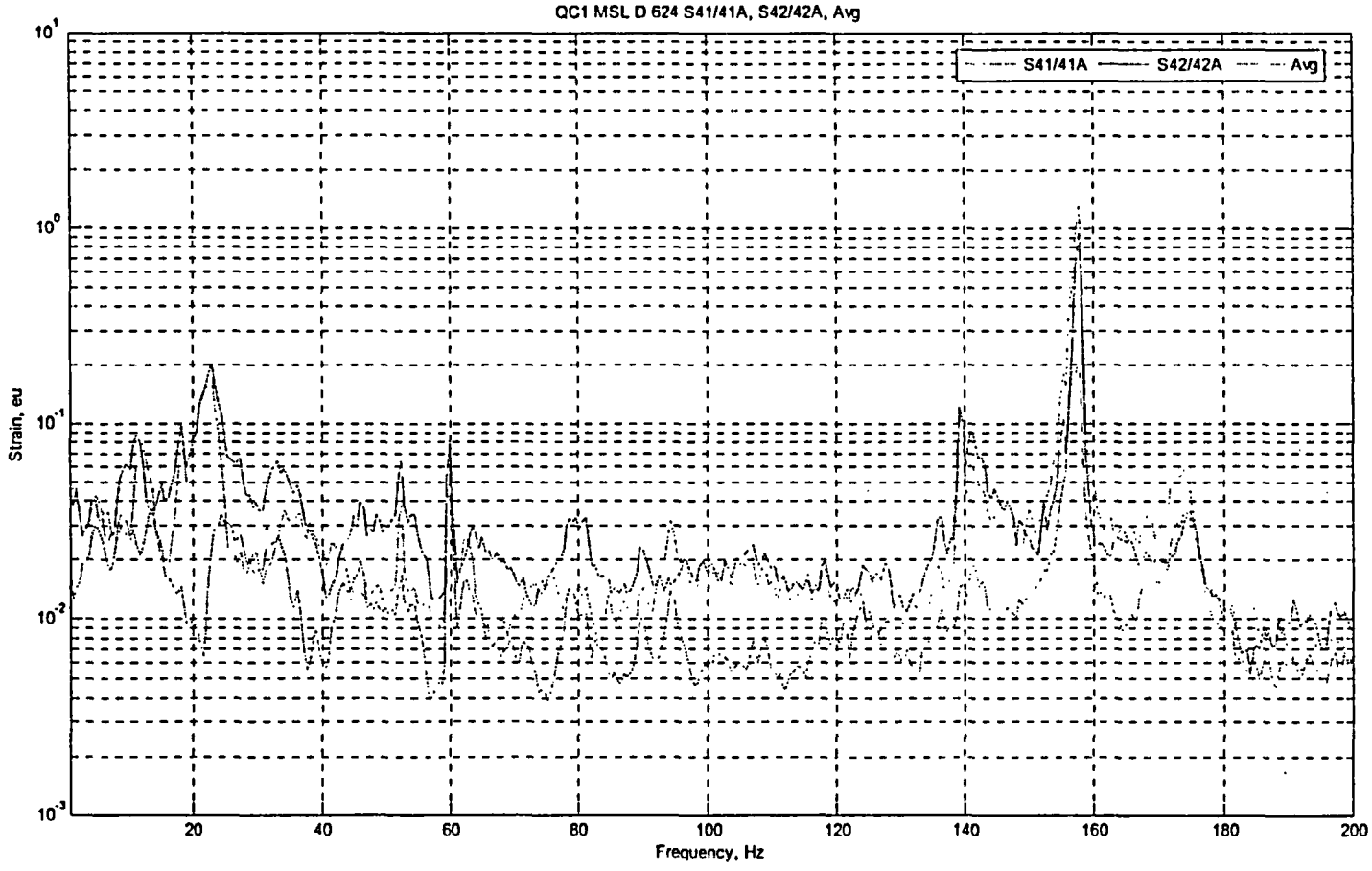

Figure 7. QC1 MSL D 624 Combined (Both ½ Bridges)

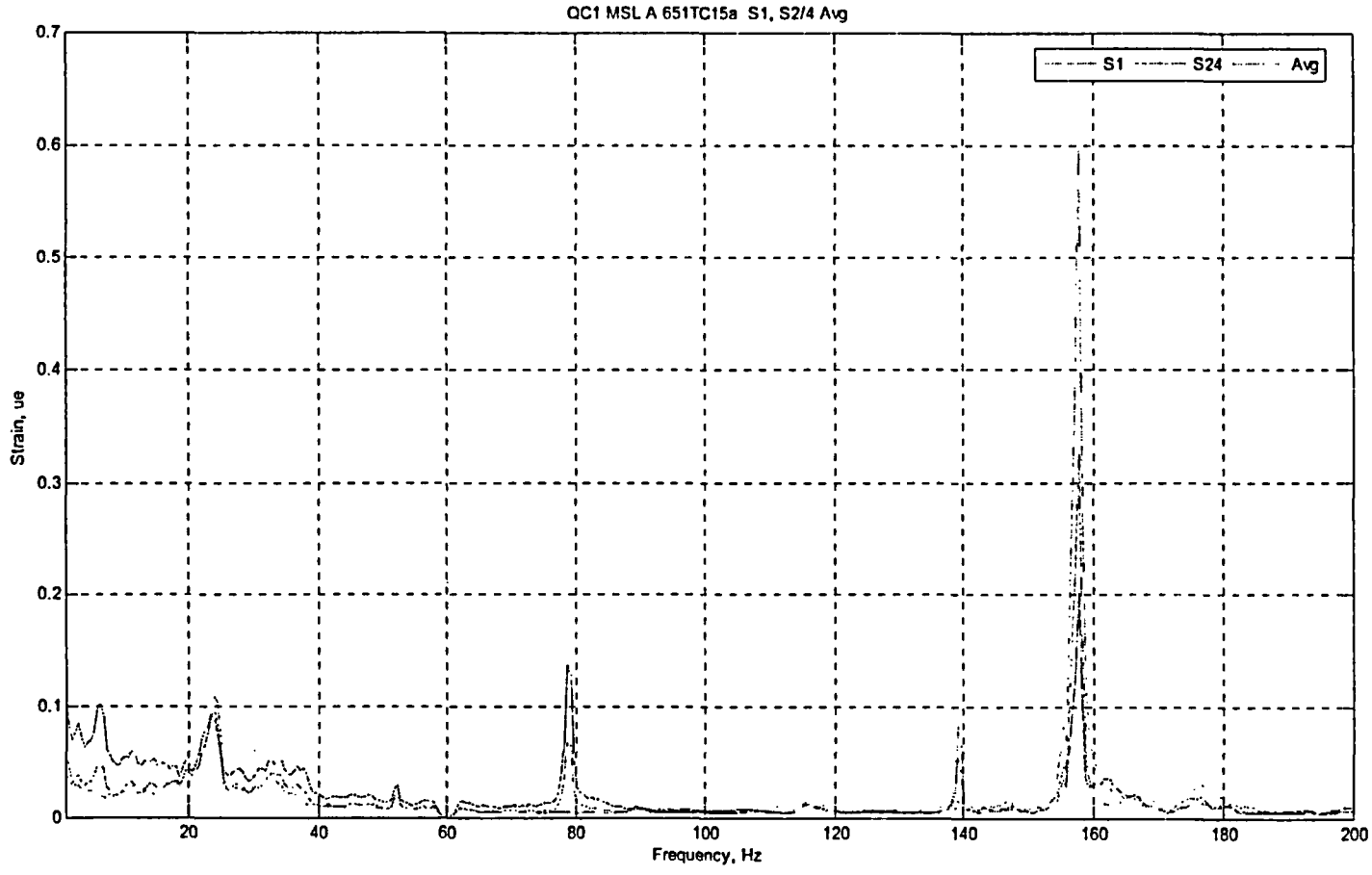

Figure 8. QC1 MSL A 651 S1 & S2/4 Combined

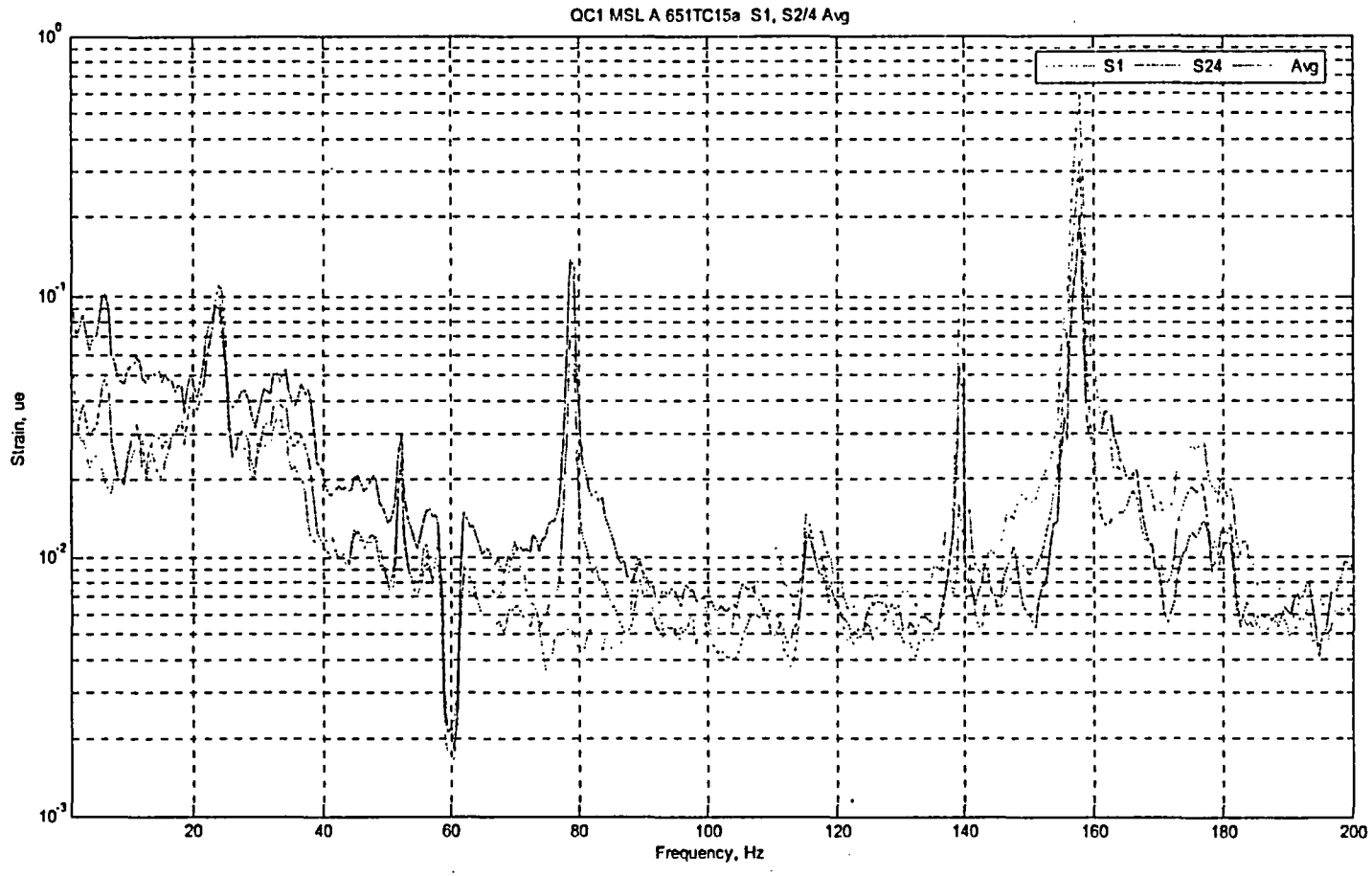

Figure 9. QC1 MSL A 651 S1 & S2/4 Combined

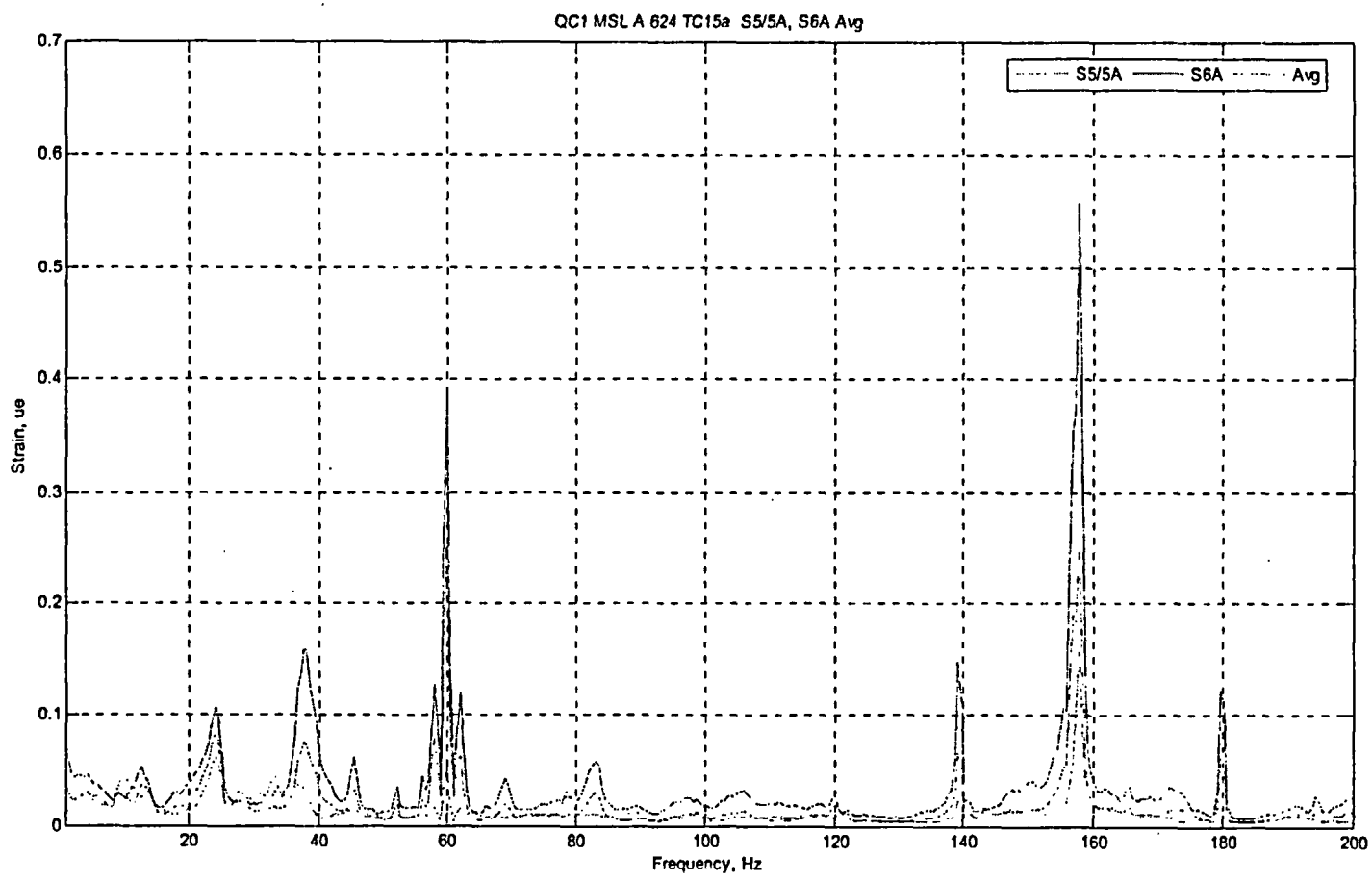

Figure 10. QC1 MSL A 624 S5/5A & S6A Combined

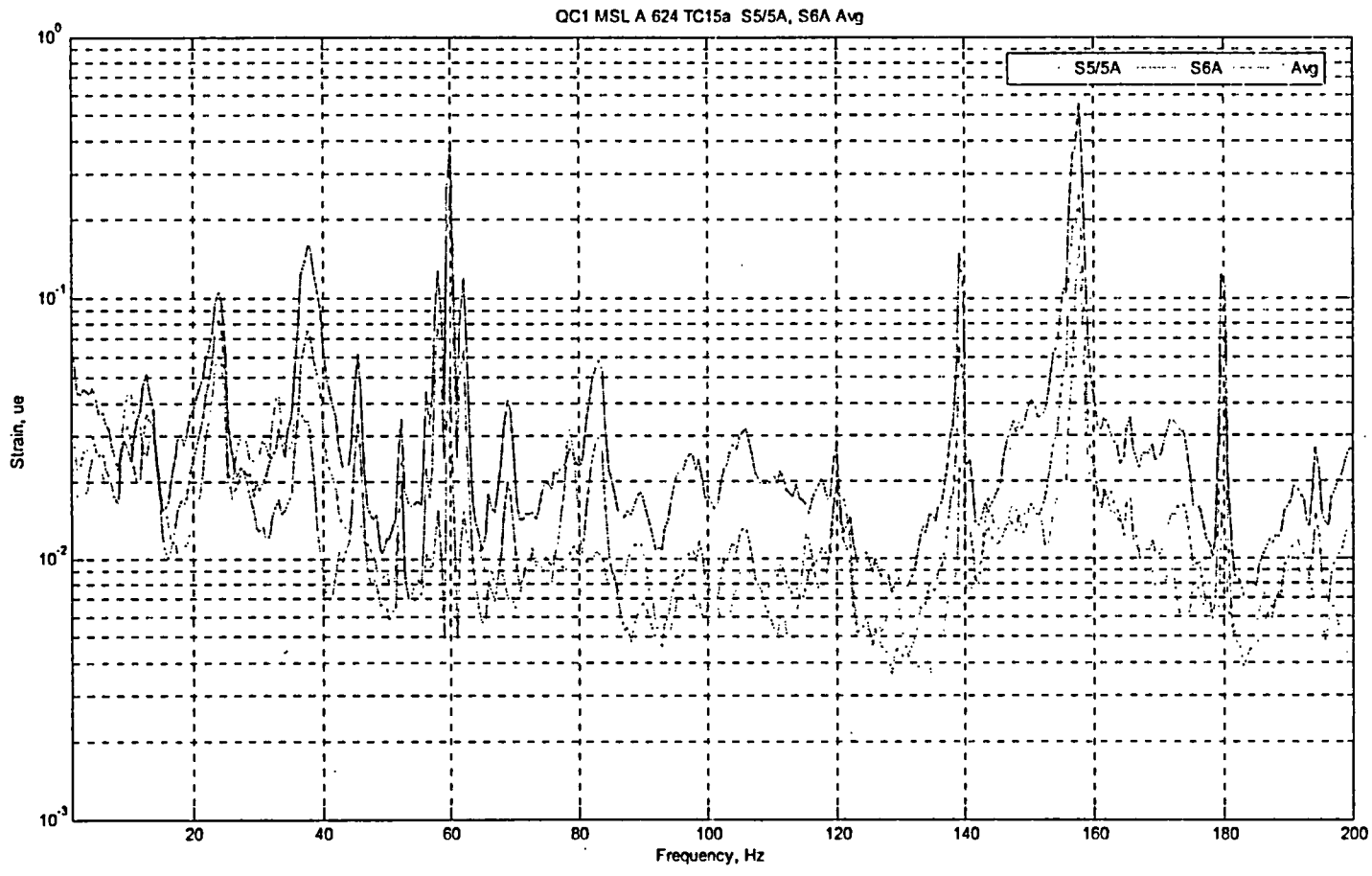

Figure 11. QC1 MSL A 624 S5/5A & S6A Combined

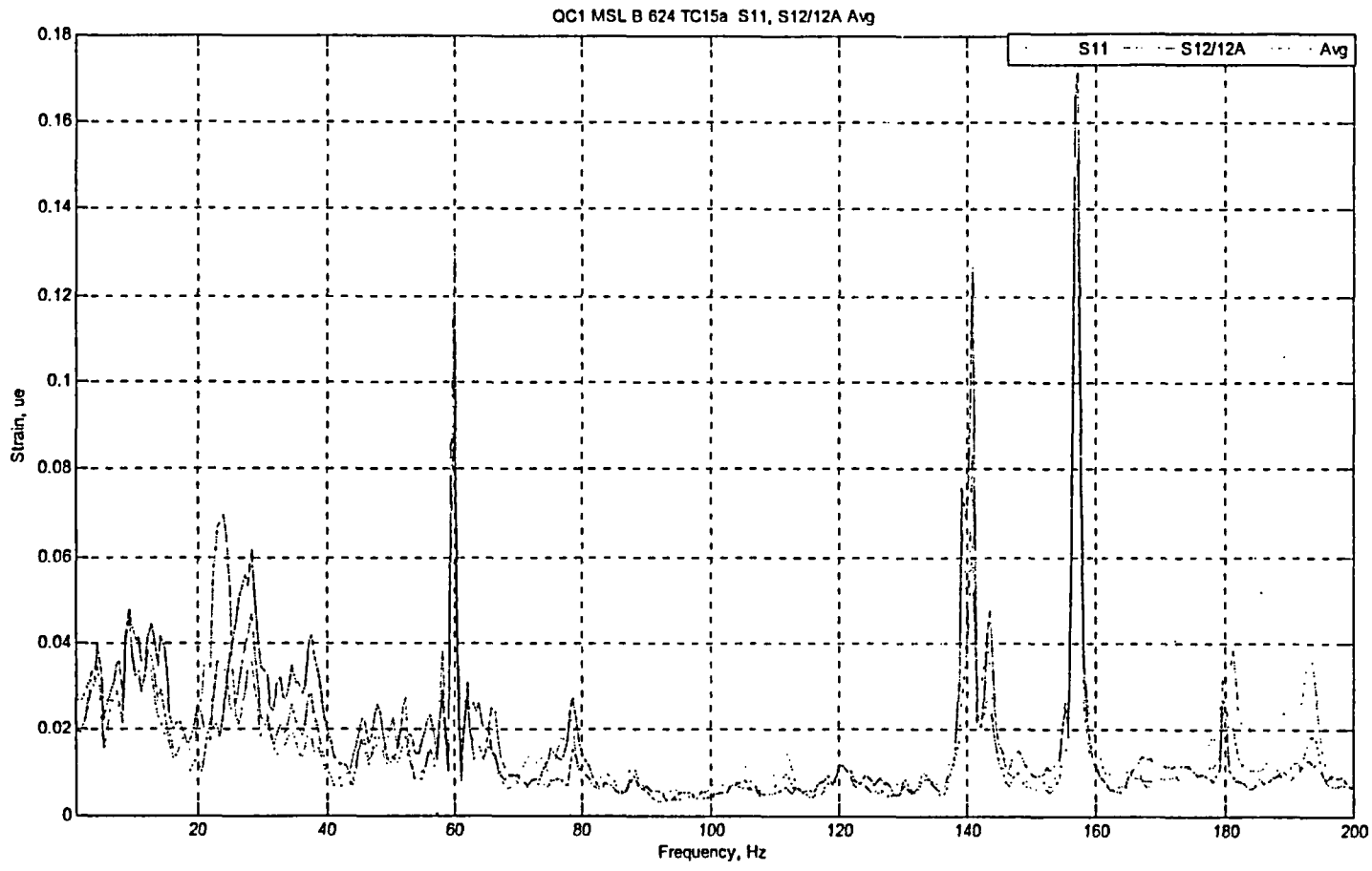

Figure 12. QC1 MSL B 624 S11 & S12/12A Combined

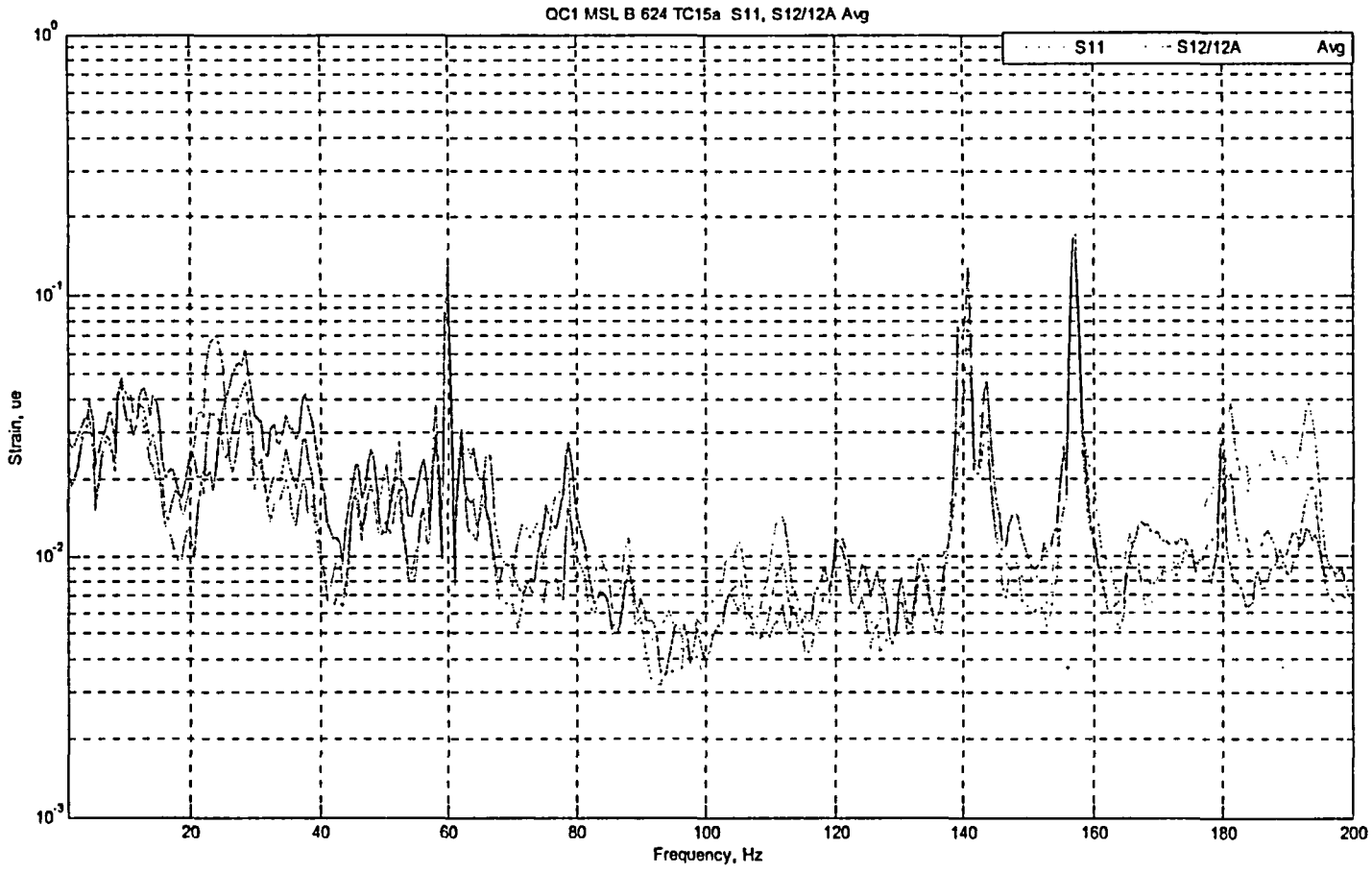

Figure 13. QC1 MSL B 624 S11 & S12/12A Combined

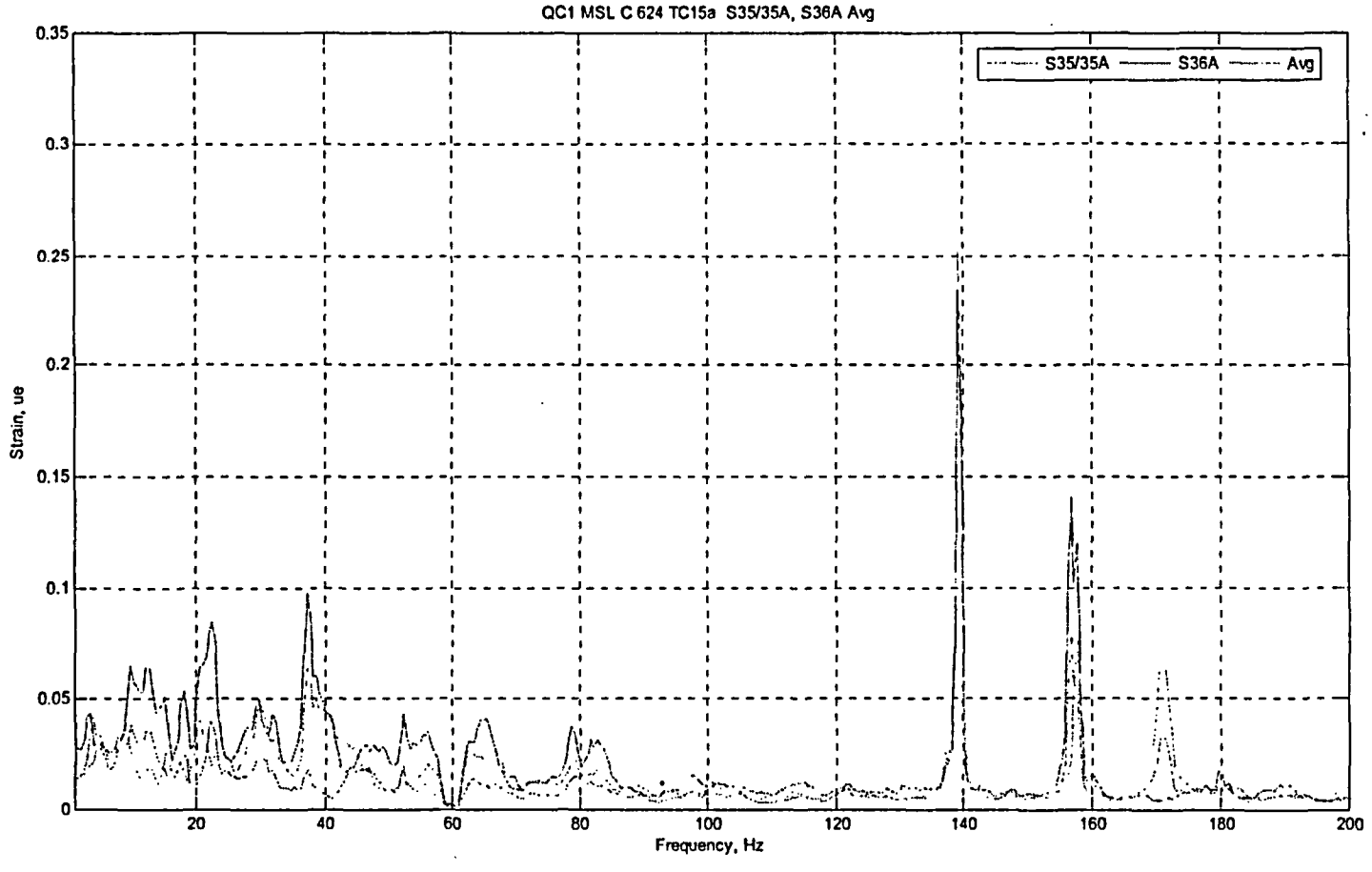

Figure 14. QC1 MSL C 624 S35/35A &S36A Combined

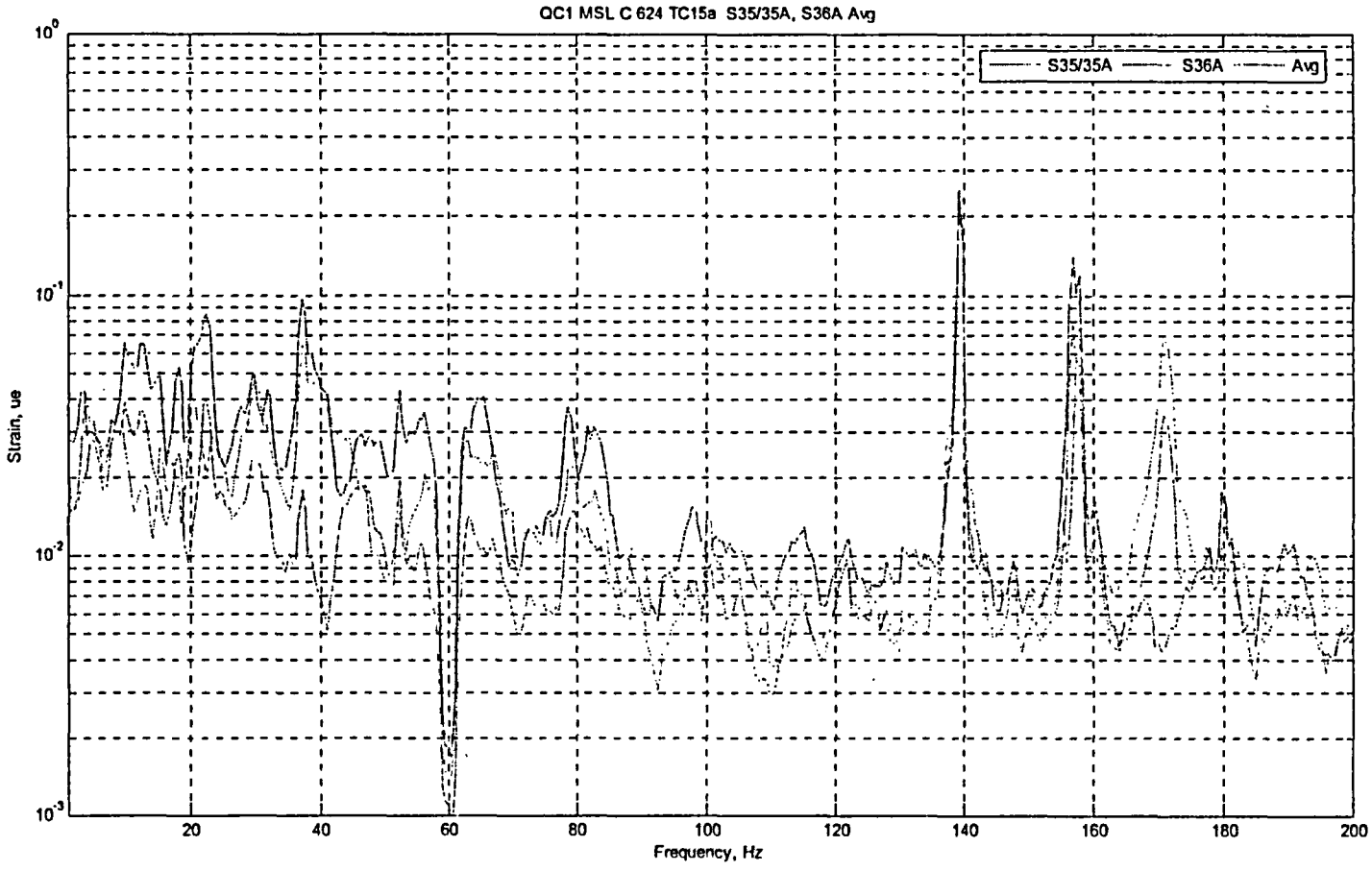

Figure 15. QC1 MSL C 624 S35/35A & S36A Combined

ENCLOSURE 2

Attachment 3

Exelon Report Number AM-2005-003, "Engineering Evaluation of Reduced Strain Gage Data Sets on the Quad Cities Unit 1 Test Condition 15A," dated June 29, 2005

Engineering Evaluation of Reduced Strain Gage Data Sets on the Quad Cities Unit 1 Test Condition 15A

Document Number AM-2005-003

Nuclear Engineering Department
Exelon Nuclear Generating Co.

Prepared by: Kevin B. Ramsden Date: 6/29/05

Reviewed by: Keith Moser Date: 6/29/05

Approved by: Robert Hochmuth Date: 6/29/05
(Date Issued)

Abstract

This report documents the data review and engineering judgments applied to the strain gage data taken at QC1 during Test Condition 15A. The failure of 5 strain gages on 3 steam lines has been determined to have the potential to introduce erroneous pressure information into the Acoustic Circuit Model. The steps taken to confirm and appropriately address this condition are the principal content of this report.

Abstract 1
1. Introduction 3
2. Methodology 4
2.1 CDI Acoustic Circuit Analysis 4
2.2 QC 1 Test Condition 15A Description 4
2.2.1 Power level 4
2.2.2 MSL Strain Gauge Inputs: 4
2.2.3 In-Vessel Instrumentation 5
2.1.1 Additional MSL Instrumentation 5
3. Calculations 6
3.1 Calculation Approach 6
4. Results 7
4.1 Observations from the U-2 790 MWe Blind Comparison and Model Correction 7
4.1.1 Model Configuration 7
4.1.2 Comparison of the Blind to the Revised Case 7
4.2 Unit 1 TC 15A C MSL Single SG Pair Prediction 7
4.3 Vessel Level Sensor Pressure Tap Data 8
4.4 C MSL 624' Elevation Data 8
4.5 C MSL Accelerometer Data 8
5. Conclusions/Discussion 9
6. References 10

1. Introduction

This report documents the evaluation performed and engineering judgments applied to the QC1 Test Condition 15A strain gage data, used as input information to the Acoustic Circuit Models. Specifically, the failure of 5 strain gages in 3 of the steam lines (A,B, and C) yielded a degraded data set that proved to be unusable without modification. The C-line data was the most seriously impacted, relative to the other lines and is the only data that has been determined necessary to be adjusted.

The effect of reducing the numbers of operable strain gages on the collected data was first noted in the first blind benchmark performed on QC 2 at 790 MWe [Reference 1]. The predicted data was based on the use of single pairs of strain gages at each location (2 locations per steam line, 651' and 624' elevations). The comparison to in-vessel measured pressure data showed that the single strain gage pair data yielded the key frequency content of the major acoustic loads (at 155 hz) reasonably. It further showed that significant frequency content not present in the in-vessel data appeared in the predictions. At approximately 80 hz, the prediction included a large magnitude peak that was not reflected in the plant data. Subsequent QC 2 predictions employed the combination of two strain gage pairs at each location, and the results showed that the 80 hz signal was effectively eliminated.

For the QC 1 Test Condition 15A data, a single pair of strain gages is available on the C-line at the 651' elevation. Review of the predicted pressures from this pair shows the same tendency as observed in QC 2, specifically the tendency to include large 80 hz frequency content. Since the opposite strain gage pair is faulted, the only options available are to use the data as is, or to apply correction to produce an appropriate load. The former approach was attempted without success, due to sensitivity of the structural model to excitations in the 80 hz range. Therefore the challenge is to produce a load that is appropriate for use in structural analysis.

2. Methodology

2.1 CDI Acoustic Circuit Analysis

The CDI acoustic circuit analysis methodology employs strain gage data taken at a minimum of two locations on each steam line to establish a boundary condition and then project an inlet condition at the reactor vessel nozzle, using transfer function methods. This approach captures sources in the steam lines as well as any present in the vessel, such as might be expected from a flow vortex entering the steam lines. The pressure field inside the vessel is calculated using a three dimensional Helmholtz equation solution and combining with the boundary conditions established at the nozzles. The output of the CDI analysis is the time dependent acoustic pressure field in the steam space of the reactor vessel. It is important to note that the acoustic circuit analysis is completely dependent on the dynamic pressure data derived from the strain gage data. If non-acoustic pressures are predicted at the strain gage locations, they will be transferred forward and imply false loading conditions on the steam dryer. The CDI methodology is documented in Reference 2.

2.2 QC 1 Test Condition 15A Description

2.2.1 Power level

Test Condition 15A was performed at a power level of 2887 MWt. It represents a maximum observed response achievable at the time of the testing.

2.2.2 MSL Strain Gauge Inputs:

Eight main steam line locations were instrumented with 16 pairs of strain gauge for the acoustic circuit analysis.

- MSL "A" Elevation 651 S1/S3 pair — Elevation 624 S5/S5a pair
- MSL "B" Elevation 651 S7/S9 pair — Elevation 624 S11/S11a pair
- MSL "C" Elevation 651 S31/S33 pair — Elevation 624 S35/S35a pair
- MSL "D" Elevation 651 S37/S39 pair — Elevation 624 S41/S41a pair

- MSL "A" Elevation 651 S2/S4 pair Elevation 624 S6/S6a pair
- MSL "B" Elevation 651 S8/S10 pair Elevation 624 S12/S12a pair
- MSL "C" Elevation 651 S32/S34 pair Elevation 624 S36/S36a pair
- MSL "D" Elevation 651 S38/S40 pair Elevation 624 S42/S42a pair

The failed strain gages in the TC 15A test data condition are:

S3 (MSL "A" Elevation 651)
S6 (MSL "A" Elevation 624)
S11a (MSL "B" Elevation 624)
S31 (MSL "C" Elevation 651)
S36 (MSL "C" Elevation 624)

2.2.3 In-Vessel Instrumentation

No In-vessel instrumentation was employed in the development of the dryer pressure loads on QC 1. High speed pressure data was recorded for the vessel level instrument taps (59A and 59B) located in the dryer skirt region. This data will be used to provide understanding of the acoustic pressure field being experienced in the vessel.

2.1.1 Additional MSL Instrumentation

In addition to the strain gage placements described above, there were accelerometers installed and monitored on the Electromatic Relief Valve on line C. The data from these instruments will be reviewed for frequency content.

3. Calculations

3.1 Calculation Approach

Fast Fourier Transform were generated to allow characterization of the frequency content and power spectral density (PSD) of the strain gage data at both locations on the C MSL, as well as the vessel level tap data. The PSDs were generated using sample groups of 2000 samples per group, based on the data time step. Frequency content up to 200 hz was calculated to coincide with the frequency interval calculated by CDI and applied in the structural loads calculations.

The intent of the comparisons performed at multiple locations is to demonstrate whether non-acoustic loads are being introduced into the strain gage data at the remaining C MSL strain gage pair, and to determine an appropriate reduction factor if justified. The principal criteria applied in this evaluation are:

1. True acoustic pressure signals will be observed to propagate. Evidence of propagation will be sought in the vessel level tap data and the C MSL 624' elevation data.
2. Non-acoustic signals may be reduced to the general background amplitude of adjacent frequencies, but not below comparable data on the fully instrumented D MSL.
3. The frequency range for which a data correction is applied will be minimized to the maximum extent possible.

4. Results

The following section describes the data reviewed and the observations that resulted.

4.1 Observations from the U-2 790 MWe Blind Comparison and Model Correction

4.1.1 Model Configuration

The CDI model for this case applied single strain gage pair data only for the blind comparison. The revised case applied both strain gage pairs at each measurement location. 60 and 180 hz narrowband noise was also filtered.

4.1.2 Comparison of the Blind to the Revised Case

Plots of the predicted vs. measured pressures at sensors P-20 and P-21 for the QC 2 790 MWe blind benchmark and the revised case are shown in Figures 1 through 4. Sensors P-20 and P-21 are on the dryer cover plate adjacent to the C and D MSLs. As noted above, the principal difference in the analytical prediction was the incorporation of both sets of strain gage data at each location measured. The blind comparison, based on a single pair showed significant signal strength at the 80 hz location, that was not reflected in the plant data. The revised calculation, employing both pairs of strain gages, shows a much more appropriate, although still conservative representation of the plant data at the 80 hz range. The following observations are salient:

1) Use of a single strain gage pair in estimating dynamic pressures in the MSL may yield signal frequency content that is not representative of the actual plant acoustic loading.
2) The plant data suggests that there is little or no acoustic loading at the 80 hz frequency range. Indicated pressure loads at this frequency range appear to be in the noise levels of the instrumentation.

4.2 Unit 1 TC 15A C MSL Single SG Pair Prediction

The PSD of the single pair prediction for the 651' location on C MSL is shown in Figure 5. In Figure 6, this data is shown with similar data taken from the B and C MSLs on QC 2 where two pair data combination was performed. What is readily apparent is that the QC 1 C MSL strain gage data shows a large 80 hz signal that is not seen in either of the comparable QC 2 MSL points plotted. The 80 hz signal is large relative to the 157 hz acoustic loads present on all signals. As noted above, initial structural analyses based on the single pair data that utilized only a simplified amplitude correction based on the 157 hz signal strength were performed and showed that the structure was sensitive to 80 hz signal content. Therefore, conservatively ignoring the included signal has been considered and shown not to be a practical approach.

4.3 Vessel Level Sensor Pressure Tap Data

The vessel level taps are located in the dryer skirt region and provide an independent means of confirming the frequency content of the vessel pressure field. The data was taken simultaneous with the strain gage data. Figures 7 and 8 show the PSD plots of the CH59A and CH59B vessel level taps. What is clear from these plots is that the large acoustic load at approximately 157 hz is clearly present and dominant. The figures show that there is little if any signal present in the 80 hz range. This suggests that the 80 hz signal in the C MSL 651' pair is not the result of a propagating acoustic pressure. In contrast the 157 hz signal is clearly a propagating acoustic pressure.

4.4 C MSL 624' Elevation Data

Figure 9 shows the PSD of the response of the functioning strain gage pair at the 624' elevation of the C MSL. Comparison of this plot to the 651' data on the same steam line in Figure 5 is beneficial. The following observations can be made:

1) There is some 80 hz content, but it is very near the background level.
2) The 140 hz signal component is more prominent at this location than the 157 hz signal.

These observations support that there is not a large propagating 80 hz acoustic pressure. The variation in the in the 140 hz vs 157 hz signals suggests that acoustic node points may be a factor. Therefore, this data point does not provide a singularly compelling argument by itself.

4.5 C MSL Accelerometer Data

Figures 10, 11, and 12 provide the x,y, and z direction acceleration vs frequency data for locations at the ERV on the C MSL. The accelerometers clearly show the 140 hz and 157 hz signals. These signals are the only peaks that show in all three axes, which is consistent with the large magnitude of these signals evidenced in other data provided. There is little or no 80 hz signal component in any of the accelerometer data. The lack of 80 hz components suggest that there is no propagating acoustic pressure at this frequency. Since this location is fairly near to the 624' elevation strain gage pair, it supports that the absence of 80 hz signal component in the strain gage data is due to the absence of a propagating signal, and not due to accidental location at an acoustic node point.

5. Conclusions/Discussion

This report has demonstrated the following:

1) Use of a single pair strain gage reading vs multiple pairs can introduce non-acoustic signals into the dynamic pressure time history being developed. This was demonstrated in the QC 2 790 MWe blind benchmark and revised 790 MWe predictions.
2) A large 80 hz signal is present in the single pair data developed from the QC 1 C MSL 651' location.
3) Vessel level tap pressure data suggests that there is no significant 80 hz signal present in the QC 1 dryer skirt region. This is consistent with observations at QC 2.
4) Review of the frequency response at the C MSL 624' elevation does not show evidence of propagating 80 hz signals.
5) The accelerometer data from the C MSL ERV location shows no evidence of 80 hz signal.

These findings support the conclusion that the 80 hz signal in the C MSL 651' elevation is a result of local structural effects and does not reflect a propagating acoustic pressure. Therefore, if the single pair strain gage data must be used for dryer load prediction, it is appropriate to reduce the 80 hz signal to a level comparable to that of adjacent frequencies.

6. References

1. "Acoustic Circuit Benchmark Quad Cities Unit 2 Instrumented Steam Path 790 MWe and 930 MWe Power Levels", Exelon Report AM-2005-002, Dated June 6/15/05

2. "Methodology to Determine Unsteady Pressure Loading on Components in Reactor Steam Domes," CDI Report 04-09, May 2004.

Figure 1 Sensor P-20 CDI 790 MWe Prediction PSD

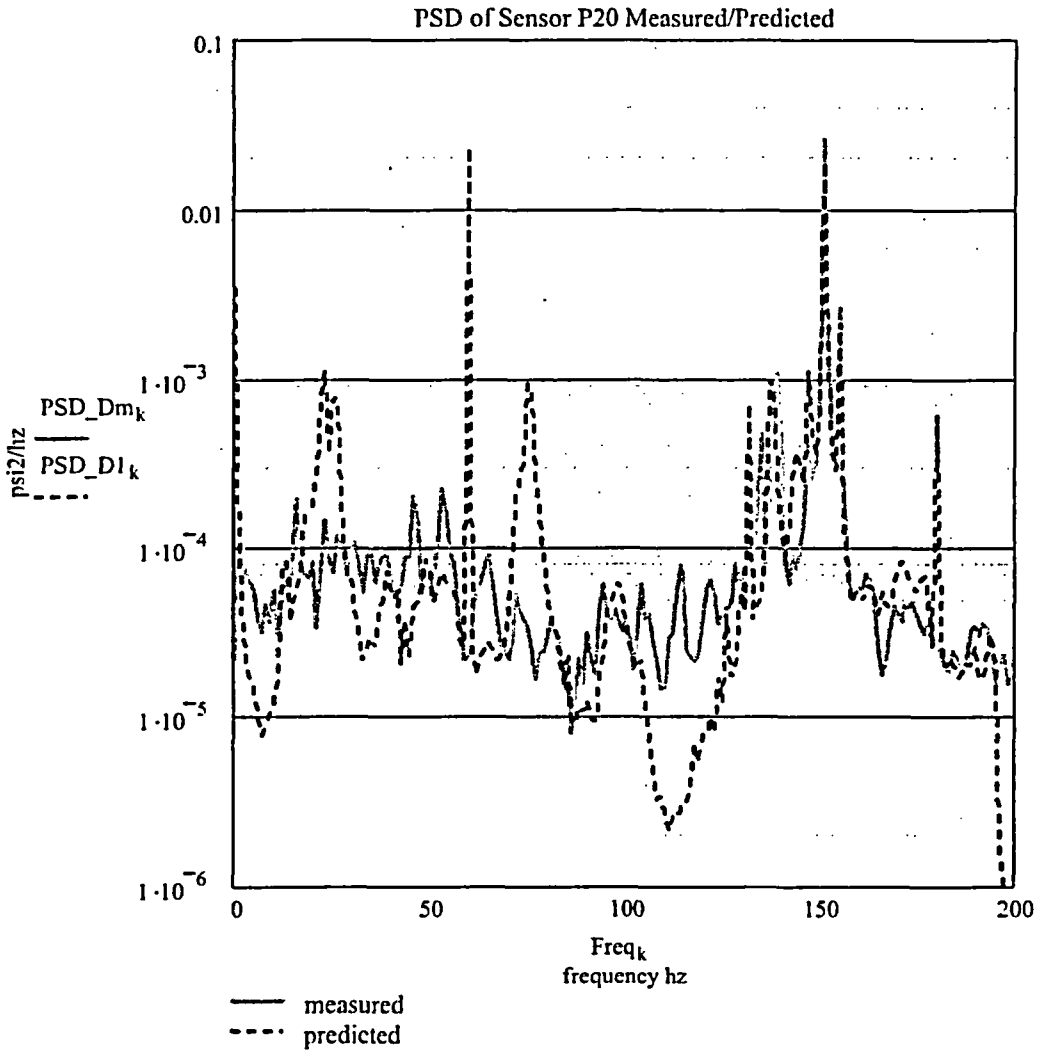

Figure 2 Sensor P-21 CDI 790 MWe Prediction PSD

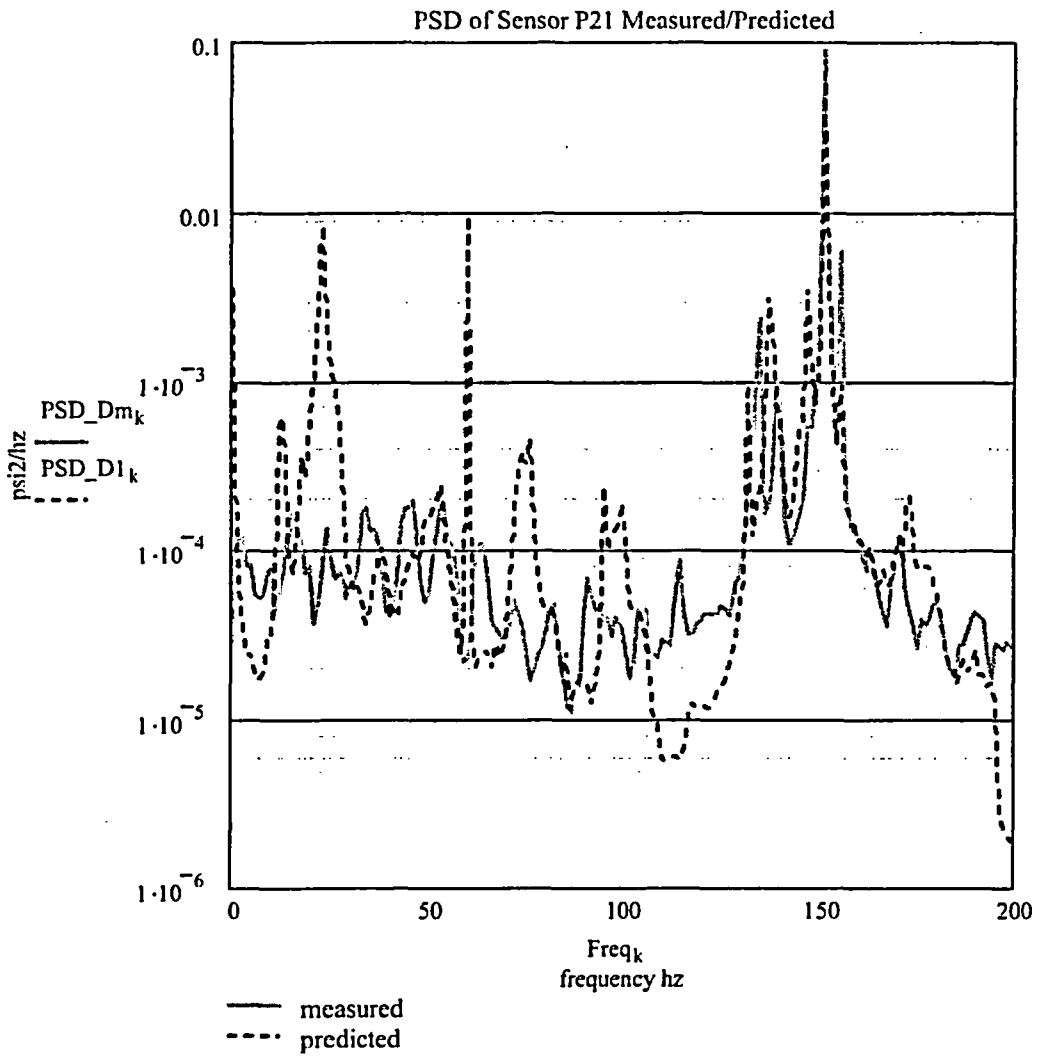

Figure 3 Sensor P-20 CDI 790 MWe Prediction PSD Revised

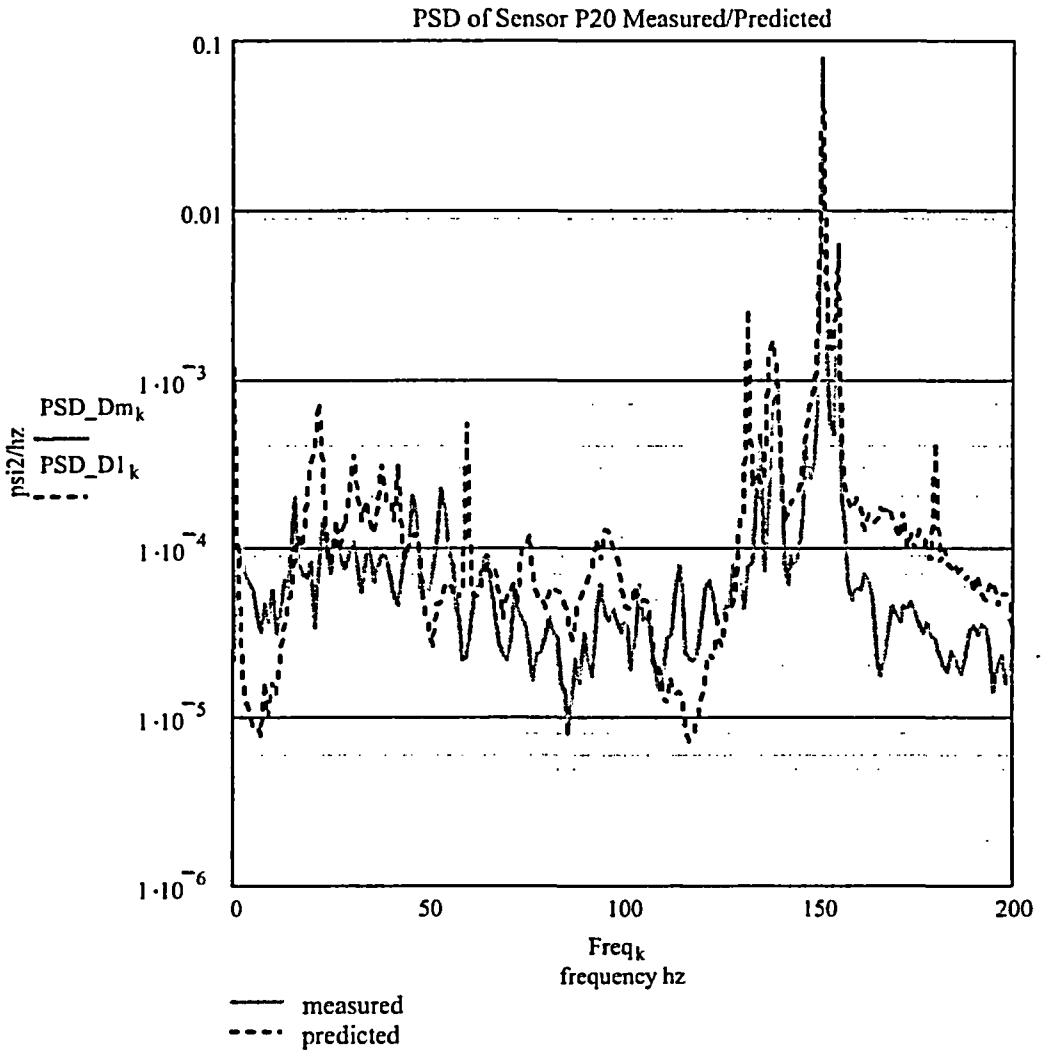

Figure 4 Sensor P-21 CDI 790 MWe Prediction PSD Revised

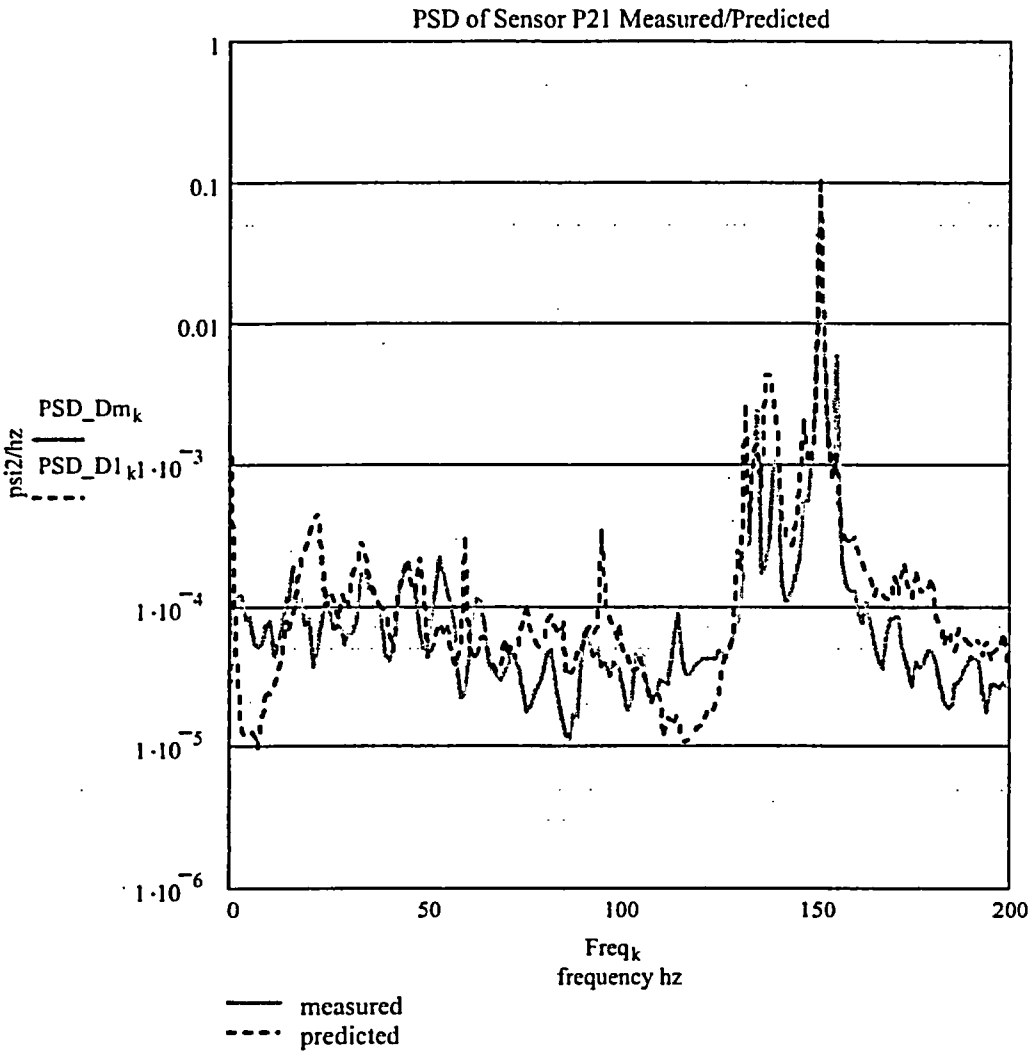

Figure 5 U-1 C MSL 651' Single Pair data

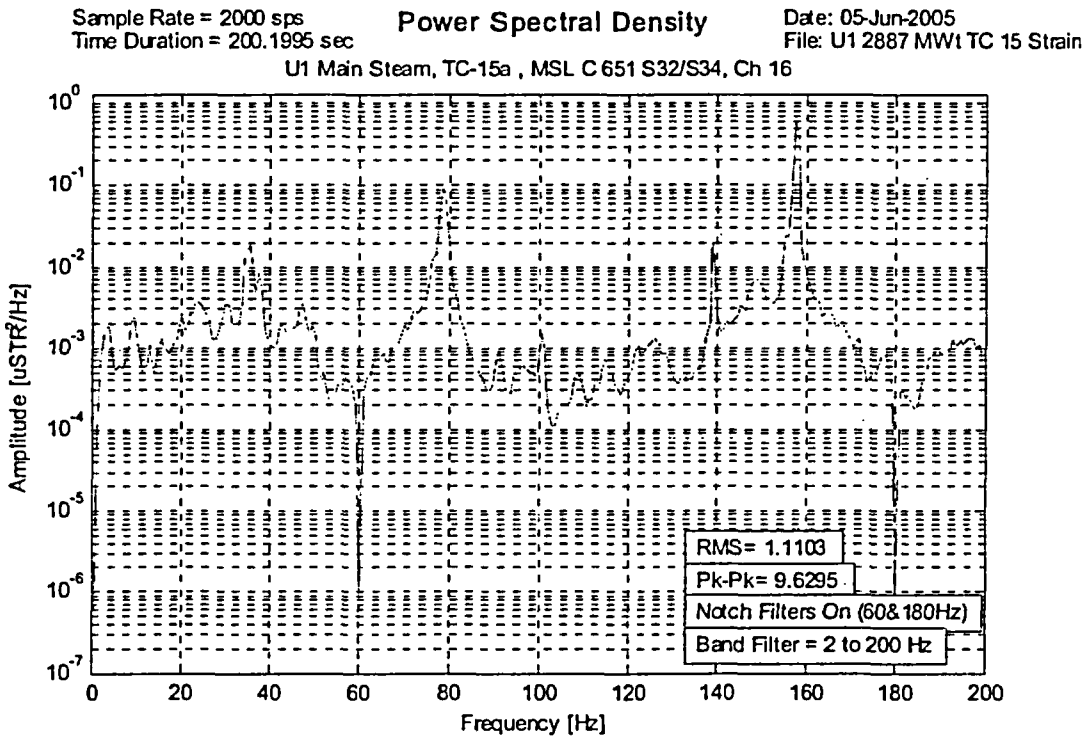

Figure 6 Comparison of QC C MSL Single Pair Data to Q2 Two Pair Based Data

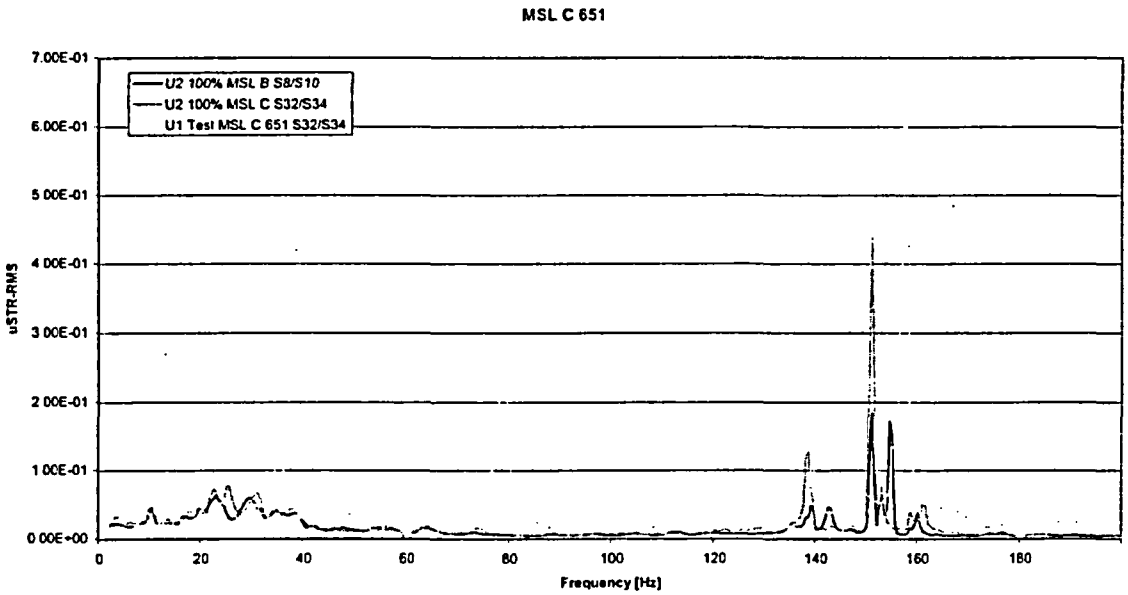

Figure 7 PSD of Vessel Level CH 59A

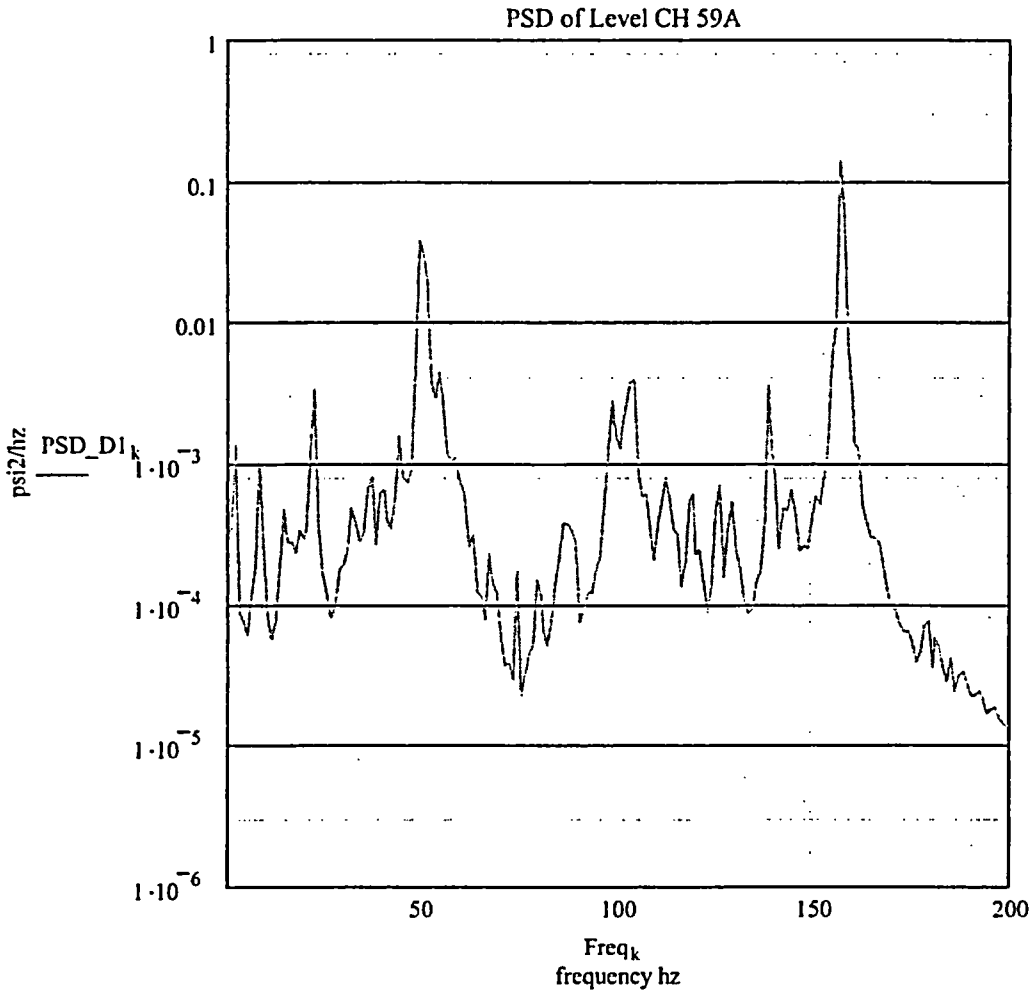

Figure 8 PSD of Vessel Level CH 59B

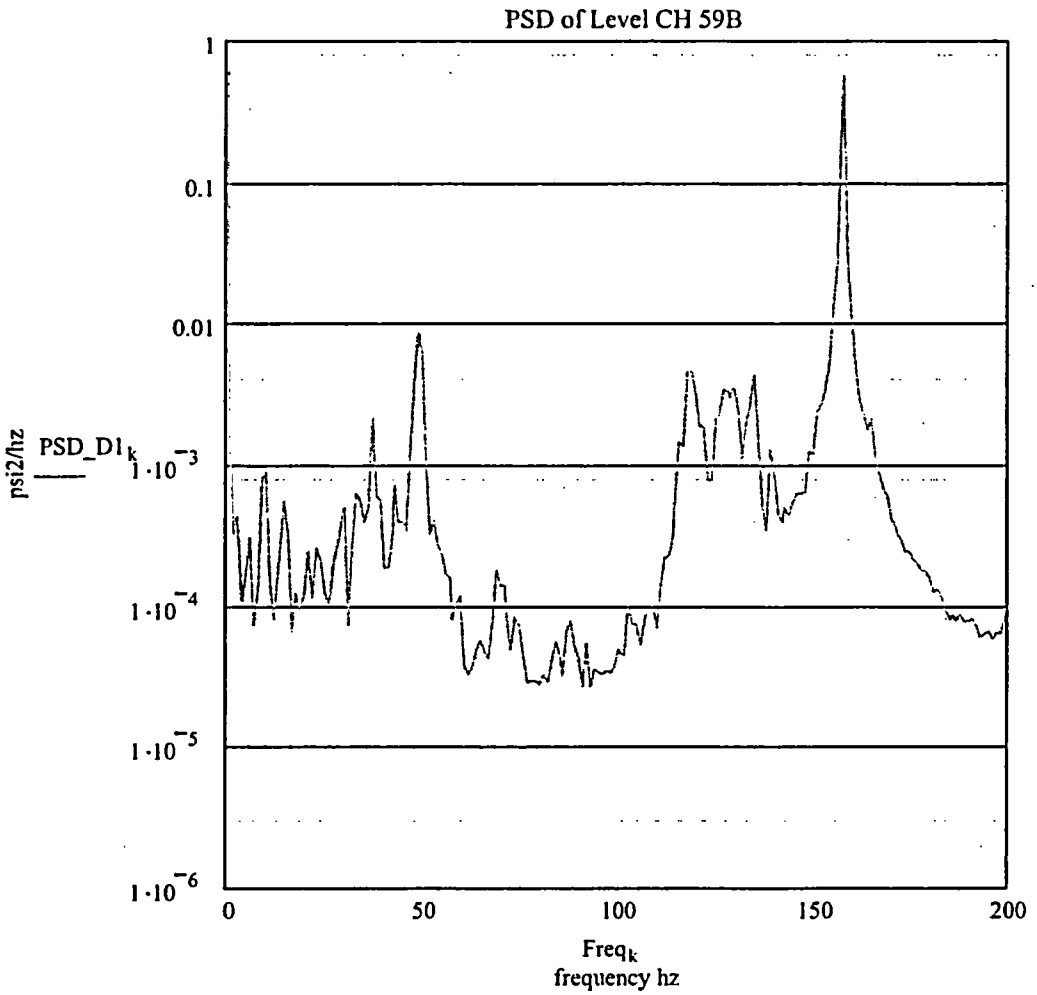

Figure 9 QC 1 C MSL 624' Elevation Single Pair Data

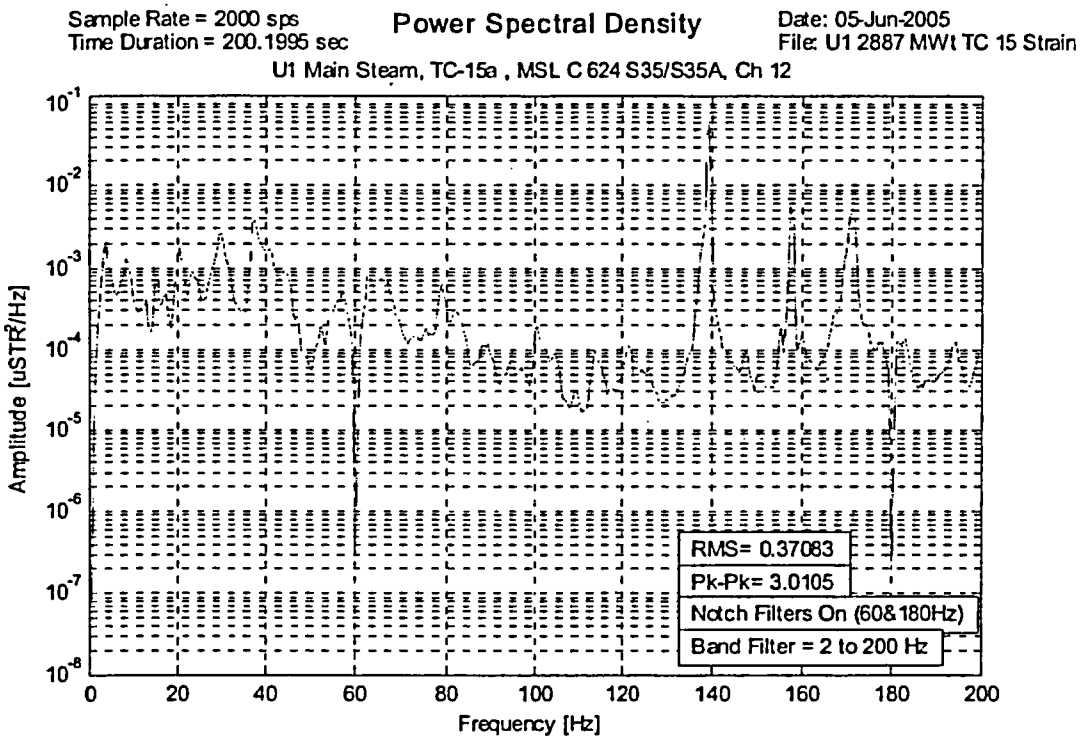

Figure 10 QC 1 C MSL ERV Accelerometer Data (X-direction)

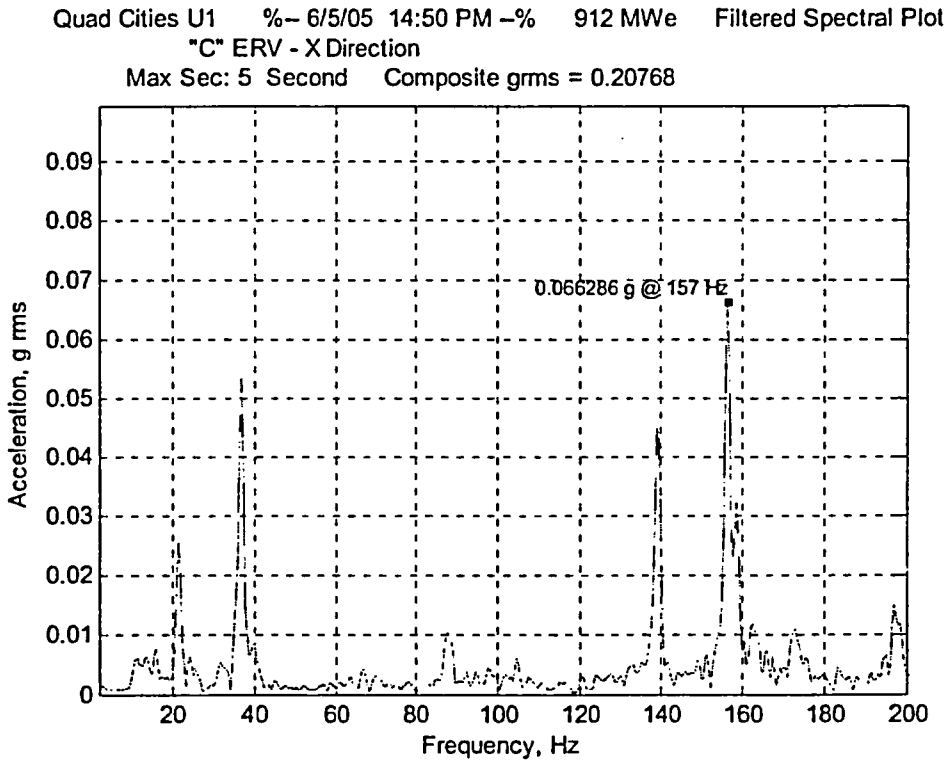

Figure 11 QC 1 C MSL ERV Accelerometer Data (Y-direction)

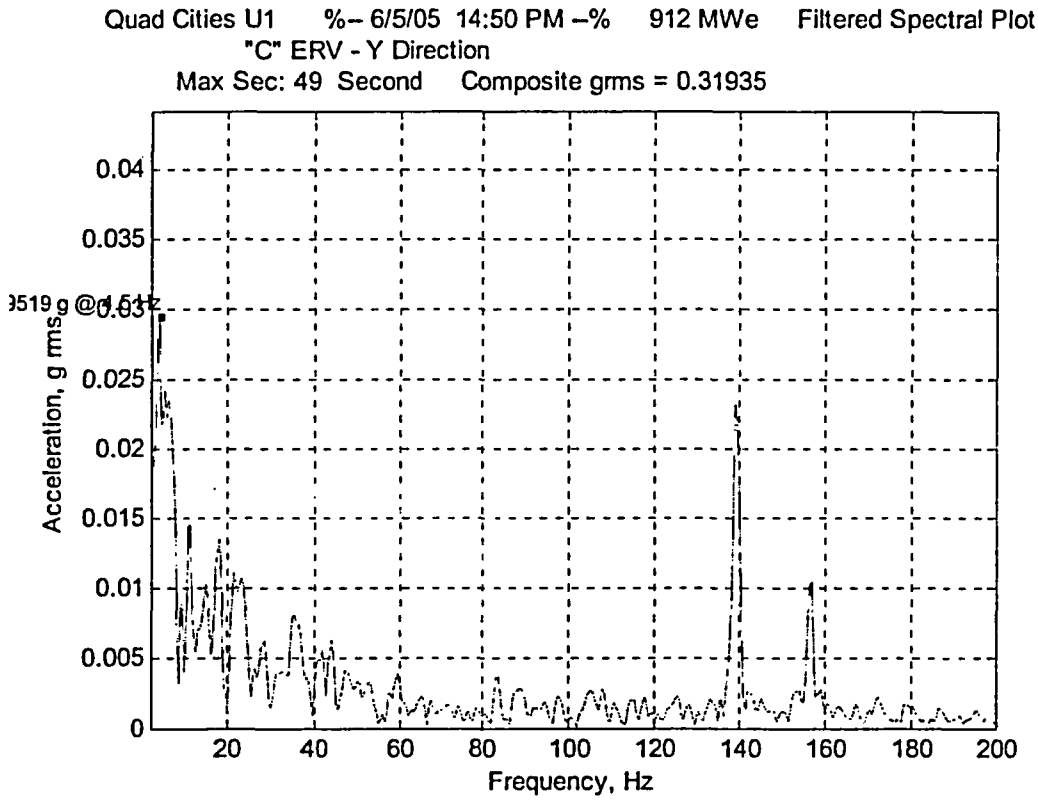

Figure 12 QC 1 C MSL ERV Accelerometer Data (Z-direction)

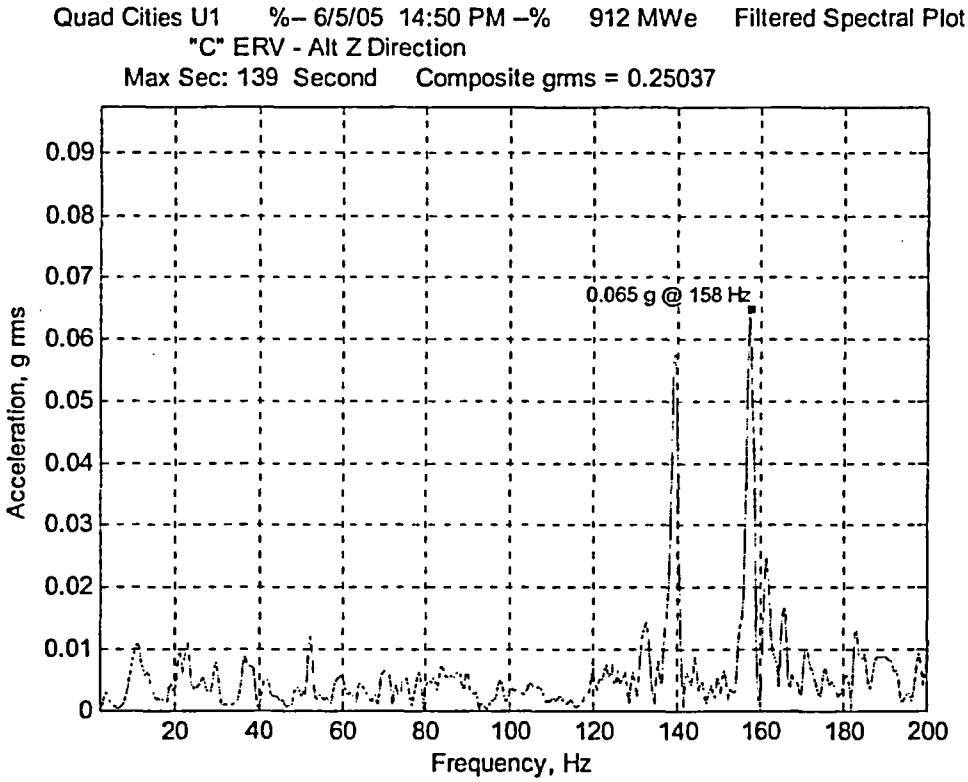

ENCLOSURE 2

Attachment 4

Exelon Report Number AM-2005-006, "Comparison of Acoustic Circuit Dryer Loads for Missing MS Line Strain Gages to Acoustic Circuit Dryer Loads with All MS Line Strain Gages," Revision 0, dated July 19, 2005

Comparison of Acoustic Circuit Dryer Loads for Missing MS Line Strain Gages to Acoustic Circuit Dryer Loads with All MS Line Strain Gages

Document Number AM-2005-006
Revision 0

Nuclear Engineering Department
Exelon Nuclear Generating Co.

Prepared by: Guy DeBoo Date: 7/19/05

Reviewed by: Kevin Ramsden Date: 7/19/05

Approved by: Roman Gesior Date: 7/19/05
(Date Issued)

Abstract

This report documents the comparison of the CDI acoustic circuit steam dryer load predictions using MS line pressure inputs from four hoop direction strain gages at two locations on each steam line to predictions using MS line pressure inputs missing some of the strain gage measurements. This comparison is intended to support the development of engineering judgements regarding the relative acoustic pressures of the QC1 and QC2 steam paths and the resultant loads on the steam dryers at EPU conditions.

Abstract....2
1. Introduction....4
2. Description of Test Data....6
3. Acoustic Circuit Model Calculations....8
4. Acoustic Circuit Model Results....9
5. Conclusions/Discussion....12
6. References....13

1. Introduction

This report documents the comparisons of the steam dryer pressure loads predicted by the CDI acoustic circuit model for MS line pressures that are changed because some of the strain gages used to determine the steam line dynamic pressures failed. Main steam line dynamic pressures at two separate locations on each steam line are required as input to the acoustic circuit model for it to calculate the acoustic pressures acting on the steam dryer. For this purpose, four hoop direction strain gages were mounted at 90° intervals about the circumference of the main steam piping and used to measure the dynamic pressures in the main steam line at that specific location. The location of the strain gages as mounted on the steam lines can be seen in Figure 1.

During the power ascension testing subsequent to replacement of the steam dryers on both units, main steam line strain gage measurements were collected on both units. All of the strain gage data was collected on Quad Cities Unit 2 at 2884 MWt for use in developing the acoustic pressure loads on the dryer. During the start-up test for Quad Cities Unit 1, some of the steam line strain gages failed prior to reaching this power level and collecting strain measurements on all four strain gages at each piping location. The effect of these strain gage failures is to cause an overprediction of the dynamic pressures at these locations in the main steam lines. The higher magnitude pressures and additional frequency content is then transformed into higher predicted loads on the dryer by the acoustic circuit model.

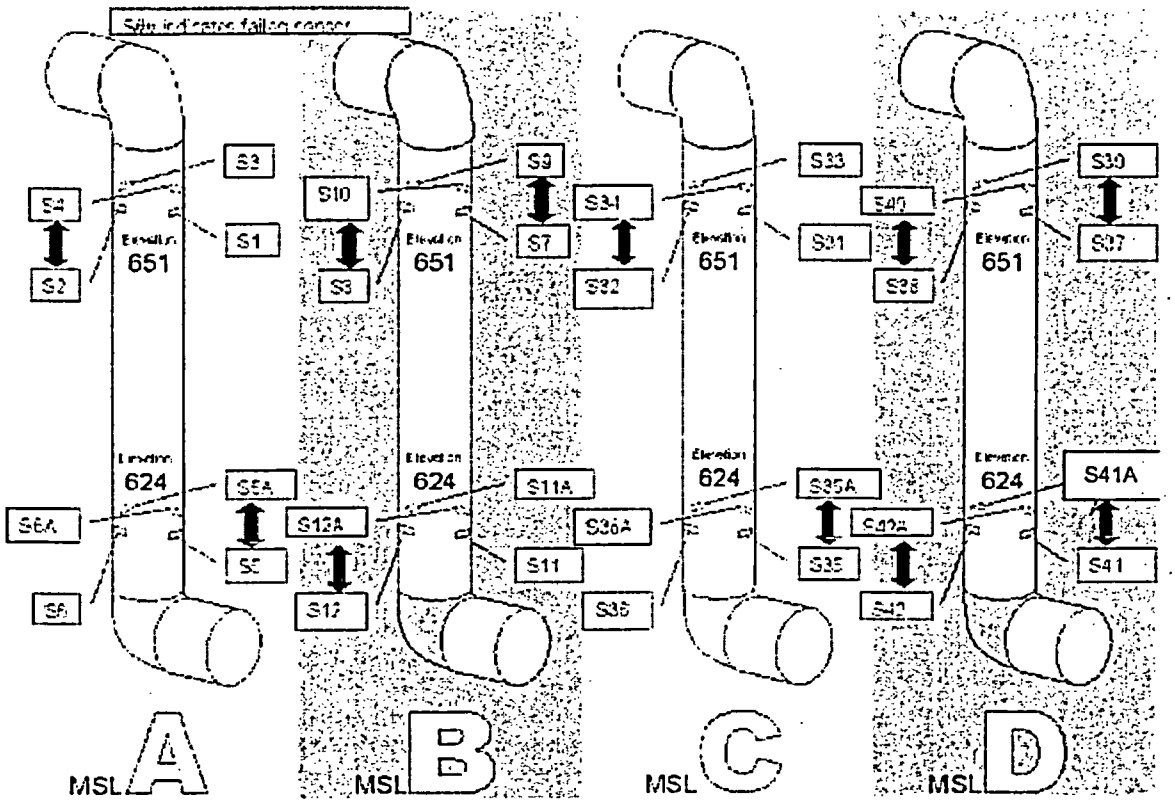

Figure 1: QC1 Main Steam Line Strain Gage Locations and Identification of the Missing Strain Gages

2. Description of Test Data

The power ascension testing was performed at the highest thermal power levels achievable at the time of the testing. The plant electrical output tended to become limiting prior to reaching maximum licensed thermal power. The test conditions being compared in this report are:

1) QC1 Test Condition 15A, performed at 2887 MWt on 6/5/2005.
2) QC2 Test Condition 41, performed at 2884 MWt on 5/23/2005.

To determine the dynamic pressures, the four strain gage measurements at each location were averaged in the time domain to provide the best measure of the breathing mode of the pipe. This combined hoop strain, when converted into pressure, provides the best measure of the dynamic pressure at this location. The strain gages that were 180° apart from each other were connected in half-bridge configurations and the two half-bridge measurements at each location were then averaged.

The main steam line strain gage measurements for these test conditions are summarized in the Table 1 below. This table provides the measured peak to peak strains and RMS strains for the working strain gage pairs on Unit 1 and compares these values to the same strain gage pairs on Unit 2. For the steam line locations on Unit 1 that had all four strain gages working, the combined measurement is compared to the combined measurement from Unit 2. The Quad Cities Unit 1 strain gages that had failed during the start-up are identified on Figure 1.

	RMS Values (με)			Peak to Peak Values (με)		
Description	U1 TC15a 2887 MWt	U2 2884 MWt SG Pair	U2 2884 MWt All SGs	U1 TC15a 2887 MWt	U2 2884 MWt SG Pair	U2 2884 MWt All SGs
MSL A 651 (S2/S4)	0.459	0.422	0.300	4.275	3.334	2.401
MSL B 651 (All)	0.216		0.297	1.849		2.453
MSL C 651 (S32/S34)	1.110	0.593	0.333	9.629	4.462	2.529
MSL D 651 (All)	0.237		0.344	2.166		2.919
MSL A 624 (S5/S5A)	0.275	0.914	0.427	2.358	6.242	3.346
MSL B 624 (S12/S12A)	0.353	0.337	0.251	3.138	3.186	2.274
MSL C 624 (S35/S35A)	0.371	0.272	0.221	3.011	2.236	1.958
MSL D 624 (All)	0.325		0.380	2.529		2.735

Table 1: QC1 and QC2 Main Steam Line Strain Gage Measurements

The strain measurement comparisons, i.e. RMS and peak to peak values at each steam line location, seen in Table 1, show the strain measurements to be very similar for all 651 steam line locations except the C steam line. The most significant difference in strain measurements occurs at this location. The Quad Cities Unit 1 strains (at MSL C 651 (S32/S34)), are 1.87 and 2.16 times greater than the Quad Cities 2 single pair RMS and Peak to Peak strains, respectively. The Table 1 strain measurement comparisons show the 624 steam line strain measurements to be very similar for all locations except the A steam line where the Quad Cities Unit 2 RMS and Peak to Peak strains are greater than Quad Cities Unit 1. For the Quad Cities Unit 2, strain gage data, the net strain results obtained when combining all the strain gages at a location is always less than the individual strain gage pair at that location. For example, the Quad Cities Unit 2 RMS and Peak to Peak strains for MSL C 651 (S32/S34) strain gage pair are 0.593 and 4.462 $\mu\varepsilon$ respectively, and RMS and Peak to Peak strains for all the strain gages at this location are 0.333 and 2.529 $\mu\varepsilon$ respectively. Comparing these strains, the S32/S34 pair strains are 1.78 and 1.76 times greater than the combined strain from all the strain gages at this location for the RMS and Peak to Peak strains, respectively.

3. Acoustic Circuit Model Calculations

The CDI acoustic circuit model was used to predict the steam dryer acoustic pressure loads using the Quad Cities Unit 2 main steam line pressures based on all the strain gage data. To understand the effect of the missing strain gage data, the acoustic circuit model was also used to predict the pressure loads on the steam dryer using the Quad Cities 2 main steam line pressures based on just the strain gage pairs that were functional on Unit1. For this second acoustic circuit model calculation, the strain gages that were used to define the main steam line dynamic pressure are listed in Table 2.

MS Line Location	Strain Gage Pairs
MSL A 651	S2/S4
MSL B 651	S7/S9 & S8/S10
MSL C 651	S32/S34
MSL D 651	S37/S39 & S38/S40
MSL A 624	S5/S5A
MSL B 624	S12/S12A
MSL C 624	S35/S35A
MSL D 624	S41/S41A & S42/S42A

Table 2: Quad Cities 2 Strain Gage Pairs Used to Define the Acoustic Circuit Model Pressure Inputs for the Missing Strain Gage Model

The predictions from these two analyses are then compared to determine impact caused by the missing strain gage data on the dryer acoustic pressure loads.

4. Acoustic Circuit Model Results

The acoustic circuit model pressure predictions for the steam line pressures using all the strain gage data and for the missing strain gage data have been summarized in Reference 1. For this comparison, the predicted dryer pressures opposite the main steam line nozzles are being compared as these are the highest pressures on the dryer and best represent the effect of the line acoustic pressures on the dryer loading. Table 3 provides a summary of the RMS pressures on the dryer for the two acoustic circuit models and also presents the pressures measured at these locations during the start-up test, (TC 41).

Dryer Location	QC2 All Data (psid)	QC2 Missing Data (psid)	QC2 Measured Data (psid)
MSL A – P3	0.682	0.610	0.626
MSL B – P12	0.659	0.657	0.684
MSL C – P20	0.605	1.085	0.493
MSL D – P21	0.804	0.824	0.878

Table 3: Predicted RMS Pressures from Acoustic Circuit Models

The RMS pressure opposite MSL C is significantly greater for the Missing Data case than the All Data case, i.e. factor of 1.79 greater. The RMS pressures for the other nozzles are very similar in magnitude for both cases.

PSD comparisons of the predicted pressures are also provided in Figures 2 through 5. In these figures, the Missing Data case is designated QC2 Fewer SGs. These comparisons also show very similar pressure magnitudes for MSL A, MSL B and MSL D locations for all frequencies. This is especially true for the most predominate frequencies between 135 and 160 Hz. The MSL C comparison shows very similar frequency content for the two cases, but the magnitude of the Missing Data case is significantly higher than the All Data case. At 138 Hz, the Missing Data pressure is approximately 3.5 times greater than the All Data case. At 151 Hz, the Missing Data pressure is approximately 1.8 times greater than the All Data case.

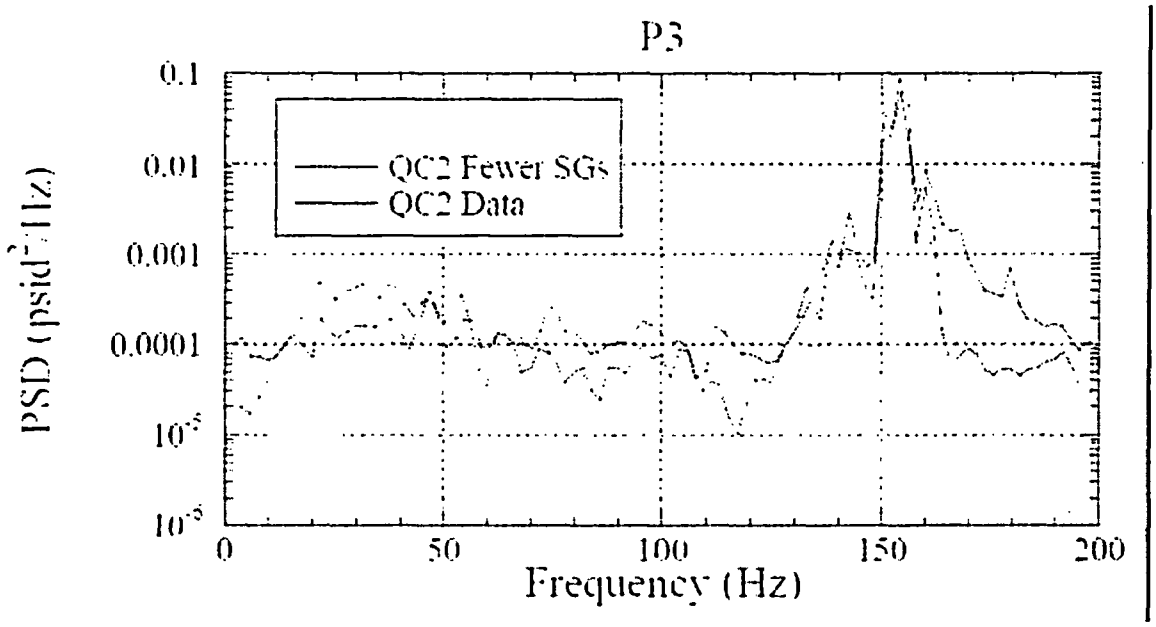

Figure 2: PSD Comparison Opposite MSL A

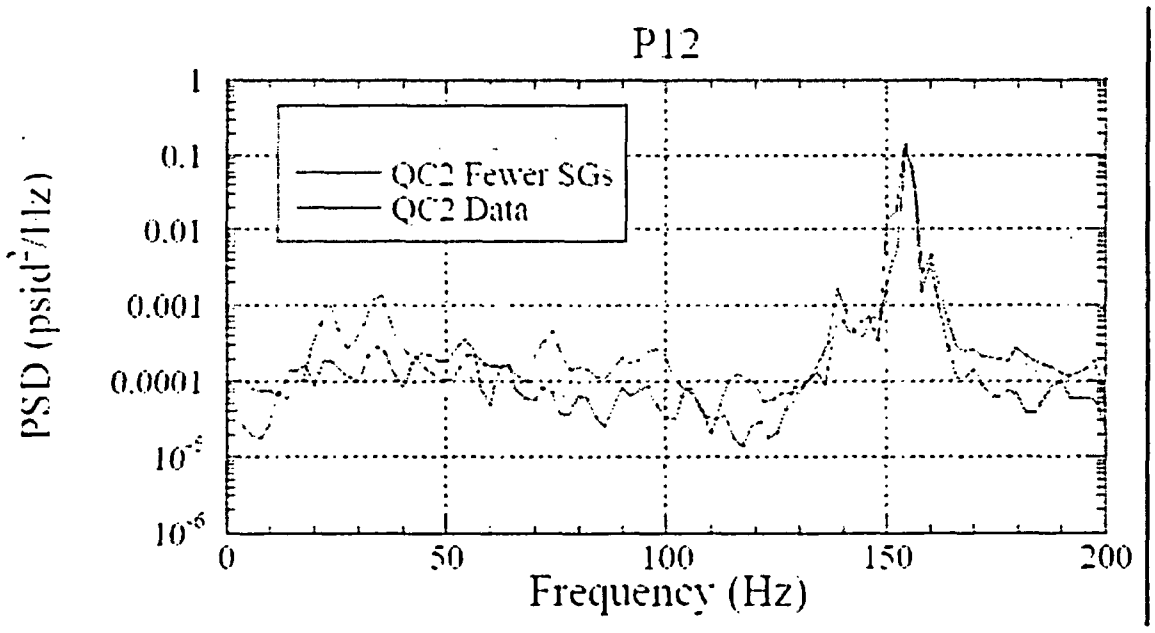

Figure 3: PSD Comparison Opposite MSL B

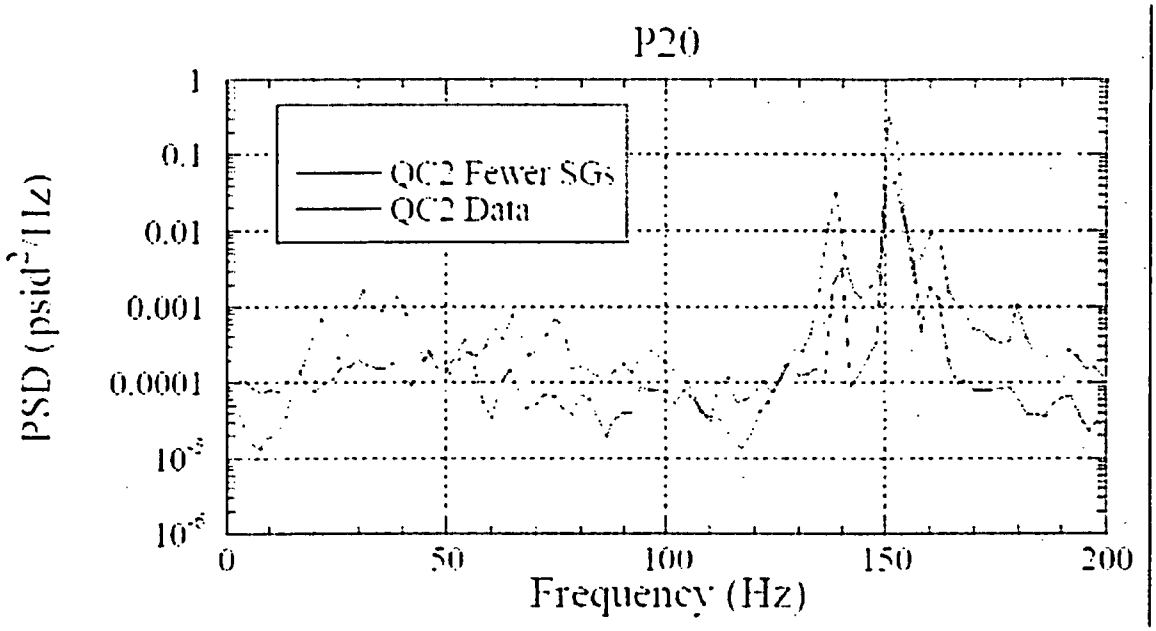

Figure 4: PSD Comparison Opposite MSL C

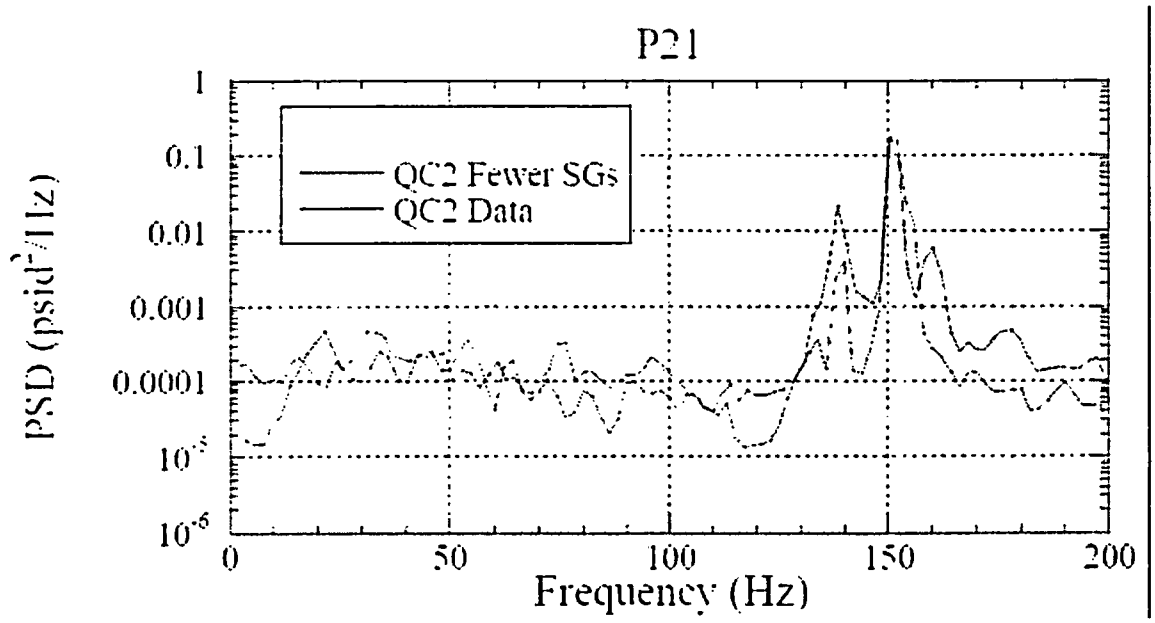

Figure 5: PSD Comparison Opposite MSL D

5. Conclusions/Discussion

The strain gage data taken at comparable power levels on Unit 1 and Unit 2 have been compared. The following observations can be made:

1) In the three locations where all Unit 1 strain gages are operable and direct comparison can be made to Unit 2, (651B, 651D, 624D), the Unit 2 measurements are higher than Unit 1, both in RMS as well as peak strain measurement.
2) Single pair comparisons between the units suggests that comparable phenomena occur in both plants. Use of single pair data introduces a higher RMS and peak strain measurement. The increase in magnitude is not constant at all locations, as would be expected since the differences are due to local pipe modal response.
3) The strain gage data for Unit 1 651C and 624C show considerably higher strain measurements than what would be expected based on comparable Unit 2 single pair data, i.e. 1.8 times higher for the 651 location, and 1.35 times higher for the 624 location. Since the ratios at the two locations differ, it would suggest that the differences are likely the result of localized structural response of the piping and are not indicative of a large acoustic pressure difference. To wit, the Unit 1 C MSL acoustic pressures may in fact be somewhat larger than Unit 2, but are not more than a factor of 2 larger as suggested by the individual strain gage pair measurements. Alternate means of verification, using MSL venturi data are needed to confirm this.

The Acoustic Model for Unit 2 was exercised using equivalent single pair data reflective of the Unit 1 operable strain gage configuration with comparison to actual plant data measured. The following observations can be made:

1) Use of single pair data yields a conservative result when compared against plant data, e.g 1.8 times greater opposite the C main steam nozzle.

Taken in aggregate, the observations above support that the acoustic pressures in QC2 B and D steam lines are clearly higher than in the Unit 1 steam lines. The acoustic pressures in the A steam line are most likely comparable. The acoustic pressures in the Unit 1 C main steam line may be somewhat higher than those observed on Unit 2, but not a factor of 2 larger as is implied by the single strain gage pair measurement.

6. References

1. "Comparison Between QC1 and QC2 at EPU with Five Strain Gages Inoperative," Continuum Dynamics, Inc. Technical Note No. 05-31, Revision 0, dated June 15, 2005.

ENCLOSURE 2

Attachment 5

Exelon Report Number AM-2005-008, "An Assessment of the Effects of Uncertainty in the Application of Acoustic Circuit Model Predictions to the Calculation of Stresses in the Replacement Quad Cities Units 1 and 2 Steam Dryers," Revision 0, dated August 19, 2005

An Assessment of the Effects of Uncertainty in the Application of Acoustic Circuit Model Predictions to the Calculation of Stresses in the Replacement Quad Cities Units 1 and 2 Steam Dryers

Document Number AM-2005-008
Revision 0

Nuclear Engineering Department
Exelon Nuclear Generating Co.

Prepared by: Kevin Ramsden Date: 8/19/05

Reviewed by: Guy DeBoo Date: 8/19/05

Concurred by: Alan Bilanin CDI Date: 8/19/05

Concurred by: GE Date: 8/19/05

Approved by: Roman Gesior Date: 8/19/05
(Date Issued)

Abstract

This report documents the evaluation of uncertainties associated with the prediction and application of unsteady loads to the Quad Cities Units 1 and 2 steam dryers. Elements of the overall uncertainty have been determined and discussed individually in previous reports and calculations. The intent of this report is to compile the various components contributing to the overall uncertainty and provide an assessment of the net uncertainty effects for the evaluation of steam dryers subjected to unsteady pressure loads.

Abstract 2
1. Introduction 4
2. Description of Uncertainties 5
2.1 Strain Gage Measurements 5
2.1.1 Strain Gage Measurement Accuracy 5
2.1.2 Pipe Structural Response Effects on Strain Gages 5
2.2 QC2 Steam Dryer Pressure Measurement Uncertainty 6
2.2.1 Instrument Accuracy 6
2.2.2 Phenomenological Considerations 6
2.3 Uncertainty associated with the ACM 7
2.4 Structural Model Uncertainty 8
3. Calculations/Data Considerations 9
3.1 Software Applications 9
3.2 Comparison of Modified 930 MWe ACM to Minimum Error ACM Predictions 9
3.3 Strain Gage Failure Considerations 11
4. Results 12
5. Conclusions/Discussion 14
6. References 15
Appendix A 16

1. Introduction

This report documents the evaluation of the uncertainty associated with the prediction and application of unsteady pressure loads on the Quad Cities (QC) Units 1 and 2 steam dryers. The Continuum Dynamics, Inc. (CDI) Acoustic Circuit Model (ACM) takes inputs from Main Steam Line (MSL) mounted strain gages and provides a detailed pressure time history for the steam volume of the reactor pressure vessel, with emphasis on the surfaces of the steam dryer. This methodology has been validated against in-plant measurements taken on the QC 2 instrumented steam dryer during power ascension testing. The output of the ACM is used as input to the General Electric (GE) Finite Element Model (FEM), which is used to compute the stresses in the dryer for comparison against code allowable fatigue and stress limits.

Due to the complicated nature of the issue, this process has the possibility to be affected by uncertainties in a number of ways:

1) Measurement accuracy of the strain gages
2) Accuracy of the ACM itself
3) Measurement accuracy of the in-situ QC 2 pressure measurements used for validation of the ACM
4) Accuracy of the FEM

This report examines the individual components of uncertainty, then develops a recommendation for the treatment of uncertainty in the integrated application. The intent is to form a basis for the QC1 and QC2 applications, as well as for future applications of this methodology for the Dresden Unit 2 and Unit 3 steam dryers.

2. Description of Uncertainties

The individual parts of the application will be discussed.

2.1 Strain Gage Measurements

There are two key elements that apply to the results obtained from strain gages to determine breathing mode unsteady pressures for use in the ACM. The first concerns the ability of the strain gage to read the strain measurement correctly and to process the strain measurement into a pressure term. The second involves the potential for strain gage measurements to include local pipe structural response, e.g., bending mode not directly related to internal pressure, in addition to the breathing mode response.

2.1.1 Strain Gage Measurement Accuracy

The MSL pipe strain gage measurement uncertainty is composed of two major components. These are the instrumentation, cabling and data acquisition response and the conversion of hoop strain to pressure, i.e., the wall thickness of the pipe. To minimize uncertainty and yield the most accurate predictions possible, ultrasonic measurements were made of the QC1 and QC2 MSLs at the strain gage locations. Reference 1 provides an assessment of the strain gage measurement accuracy. A value of 5.02% was determined to be the accuracy of the strain gage measurements.

In Reference 2, the error in strain gage readings was applied to the eight sets of strain gage data used to develop the unsteady pressure input into the ACM. The changes in pressure in the four dryer pressure transducers closest to the steam line nozzles was then computed to determine the uncertainty in the minimum error ACM predictions due to strain gage uncertainty. The pressure predictions were determined to be accurate to within +/-3.6%.

2.1.2 Pipe Structural Response Effects on Strain Gages

The underlying premise of using strain gages to measure unsteady pressures in the MSL pipes is the ability to determine the breathing mode (hoop) component of strain and use simple relationships to infer the unsteady internal pressure. Experience with testing at QC2 demonstrated that two perpendicular pairs of strain gages in combination yield more accurate results than a single pair. [Reference 3.] In addition, differences in amplitudes are noted when the strain gage pairs are located in-plane with piping elbows versus out of plane. Both of these effects were noted while processing QC2 790 megawatt-electric (MWe) data. With a single pair of strain gages, introduction of non-acoustic signals was observed, particularly near 80 Hz, which was negated when the second pair of strain gages was combined.

The QC2 steam path was fully instrumented to support the development of loads on the steam dryer based on pressures derived from MSL strain gage data and the use of an ACM. The in-vessel pressure detectors mounted on the QC2 dryer supported the validation of the overall methodology. The QC1 steam path contained MSL strain gages only, supplemented by steam system dynamic pressure measurements taken at selected locations. The failure of some strain gages on QC1 occurred prior to establishment of the steam dryer loads for QC1. Therefore, it is important to understand the implications of loss of strain gages on the establishment of a load definition on the steam dryer. In the work presented in Reference 3, it was shown that pressure calculations based on three strain gages provide very similar results to four strain gage combinations. With three gage combinations, some adjustment at frequencies near 80 Hz is still necessary to approach the four gage pressure prediction.

2.2 QC2 Steam Dryer Pressure Measurement Uncertainty

The uncertainty in dryer pressure measurements consists of two components. The first is the instrument accuracy and calibration results. The second is due to phenomenological effects that may induce error into the steam dryer-mounted pressure instruments.

2.2.1 Instrument Accuracy

Reference 4 provides a detailed discussion of the expected instrument accuracy based on vendor supplied data and calibration results. The testing used two instrument types with differing ranges for each. Two of the instruments used a larger range and had a slightly higher absolute error. The remaining 25 were of a smaller range and had a lower absolute error. The instrument accuracy is developed for both and yields a 3.9% absolute measurement uncertainty and a 2.9% relative measurement uncertainty for the limiting sensor. The relative measurement uncertainty is the most appropriate value to apply for this assessment, since variations from the mean are of interest, rather than the absolute maximum values.

2.2.2 Phenomenological Considerations

There are phenomenological considerations that are salient to the unsteady pressure measurements taken on the QC2 steam dryer. These include:

1) The effects of dome-mounted versus flush-mounted pressure transducers, with respect to measurement of incident acoustic pressure oscillations.
2) The potential for the nozzle entry vortices to induce unsteady velocity fields on the sensors nearest the nozzles.

Item 1 was the subject of considerable analytical work, as well as confirmatory testing in a wind tunnel. The results of this work are contained in Reference 5. There were two important conclusions of this work:

1) The dome-mounted sensors will tend to overpredict the pressures by 3-8%. No correction was recommended in the test data reduction since the overprediction is conservative in application to structural analysis considerations.
2) The sensor domes had an extremely low sound signature as determined by wind tunnel testing. Therefore, the sensor domes could reasonably be expected to yield appropriate frequency content, unaltered by bluff body acoustic noise from the housing. It was also determined that downstream sensors would not be affected by vortex shedding from upstream sensor mounts.

Item 2 is addressed in Appendix A of this report. Based on review of the data collected on QC2, it was determined that there is no need to add a factor to the sensors opposite the steam nozzles to account for uncertainty in dynamic effects.

2.3 Uncertainty Associated with the ACM

The validation of the ACM has been performed against QC2 in-vessel measurements. The initial efforts were directed at comparison predictions to measurements at six sensor locations. Two blind benchmark tests were performed and subsequent model adjustments were made. The resultant model, typically referred to as the "modified 930 MWe model," was then applied to develop dryer loads that were used to qualify the QC2 steam dryer. In this work, it was noted that the model generally overpredicted the loads, particularly in the steam dryer skirt region. The frequency content was found to be accurate, particularly at the dominant acoustic load frequencies (135-160 Hz). This validation is provided in Reference 6.

Recognizing that the ACM validation had been performed for a limited number of sensor locations, and had the tendency to overpredict the loads in the skirt region, an effort was initiated to revise the ACM and perform validation over a larger set of pressure measurements. Specifically, a revised Helmholtz solution was implemented for the vessel that featured more physically representative boundary conditions in the skirt region. In addition, a least squares method was used to adjust the model damping to provide the minimum error for the full set of pressure sensors. Validation of this minimum error ACM was performed by CDI as documented in Reference 2.

Exelon performed additional validation work on the minimum error ACM comparison to test data. The Exelon study (i.e., Reference 7) focused on an assessment of the CDI ACM with respect to the distribution of peak loads.

Statistical evaluations demonstrated that the minimum error model captures sufficient amounts of the pressure distribution to be representative and appropriate for design evaluation without the need for additional multipliers. Specifically, it was concluded that the model was capable of meeting 95-95 criteria on all external surfaces of the steam dryer, with two exceptions; these exceptions would meet 95-90 criteria. It is important to note that the statistical treatments performed, and the associated results, are valid only for the application stated, which is to provide appropriate peak-to-peak pressure response for input to a structural model. Use of the ACM for other applications would require additional evaluation.

2.4 Structural Model Uncertainty

The structural Finite Element Analysis (FEA) model is based on detailed as-built steam dryer geometry. A specific analytical uncertainty associated with the FEA calculation has not been determined, largely because of the complexity of the model. To minimize this uncertainty, separate finite element models of the dryer were independently developed and subjected to identical pressure time histories. Comparing the finite element analysis results, showed both models predicted similar stress analysis results for critical components such as the outer hoods. For design purposes the model producing the more conservative results was used to predict the dryer stresses. Sensitivity analyses were performed by varying the time step by +/- 10%. This interval selection was based on review of the results of the hammer testing performed on the Unit 2 replacement dryer. This sensitivity covers the potential for uncertainty in the structural frequency of the model and the dynamic amplification that would be experienced if a loading frequency approached a structural frequency. The highest responses from the three runs are used to conservatively assess the dryer. To provide additional accuracy, component finite element models constructed with 3 dimensional, solid elements were used to evaluate those dryer components that were not conservatively represented by shell elements in the full dryer model. In addition, steam dryer component critical damping has been verified by in-vessel measurements and by hammer tests to confirm reasonable and conservative damping was considered in the finite element analyses. [References 8 and 9.] These additional models and analyses address the potential uncertainties in the finite element analyses and provide reasonable assurance that the stresses calculated are conservative.

3. Calculations/Data Considerations

3.1 Software Applications

The Mathcad-11 software package was used to support this evaluation. The statistical analysis features were used to calculate standard deviation (rms pressure) along with minimum, maximum, and mean values. The spectral analyses presented were performed using complex Fast Fourier Transforms, to allow characterization of the frequency content and power spectral density (PSD) of the measured data. The data sets were reviewed to determine the data trigger point. All data after the trigger point was used from each data set. The PSDs were generated using sample groups of 2048 samples per group, based on the data time step.

3.2 Comparison of Modified 930 MWe ACM to Minimum Error ACM Predictions

Comparison of the modified 930 MWe ACM results to the minimum error ACM results for QC2 test data is provided in the following table, based on data calculated in References 6 and 7.

Table 1 Statistical Comparison of Minimum Error and Modified 930 MWe ACM

Sensor	*RMS pressure psi*	*Min pressure psi*	*Max pressure psi*
P-3 min err	0.603	-1.894	1.971
P-3 mod 930	0.682	-2.262	2.193
P-12 min err	0.625	-1.94	1.906
P-12 mod 930	0.659	-1.751	1.848
P-20 min err	0.541	-1.648	1.738
P-20 mod 930	0.605	-1.977	1.994
P-21 min err	0.638	-1.974	2.026
P-21 mod 930	0.804	-2.289	2.337
P-24 min err	0.288	-1.129	1.016
P-24 mod 930	0.251	-1.034	0.986

The data above demonstrates that the modified 930 MWe ACM generally overpredicts both RMS and peak values compared to the minimum error ACM results. It can be readily seen that the peak values in the 930 MWe ACM are greater than 1.96 times the RMS. This suggests that the modified 930 MWe ACM provides comparable capture of the peak pressure distribution as the minimum error ACM. What is not apparent is why the skirt sensor location P-24

is more conservative in the modified 930 MWe ACM than the minimum error ACM. The reasons for this are subtle, and depend more on the frequency content of the load than on the absolute magnitude. In addition, the skirt is more responsive to low frequency loads. The following figure compares the predicted frequency content of the modified 930 MWe ACM and the minimum error ACMs for the P-24 skirt location.

Figure 1 PSD of Load Predictions at P-24

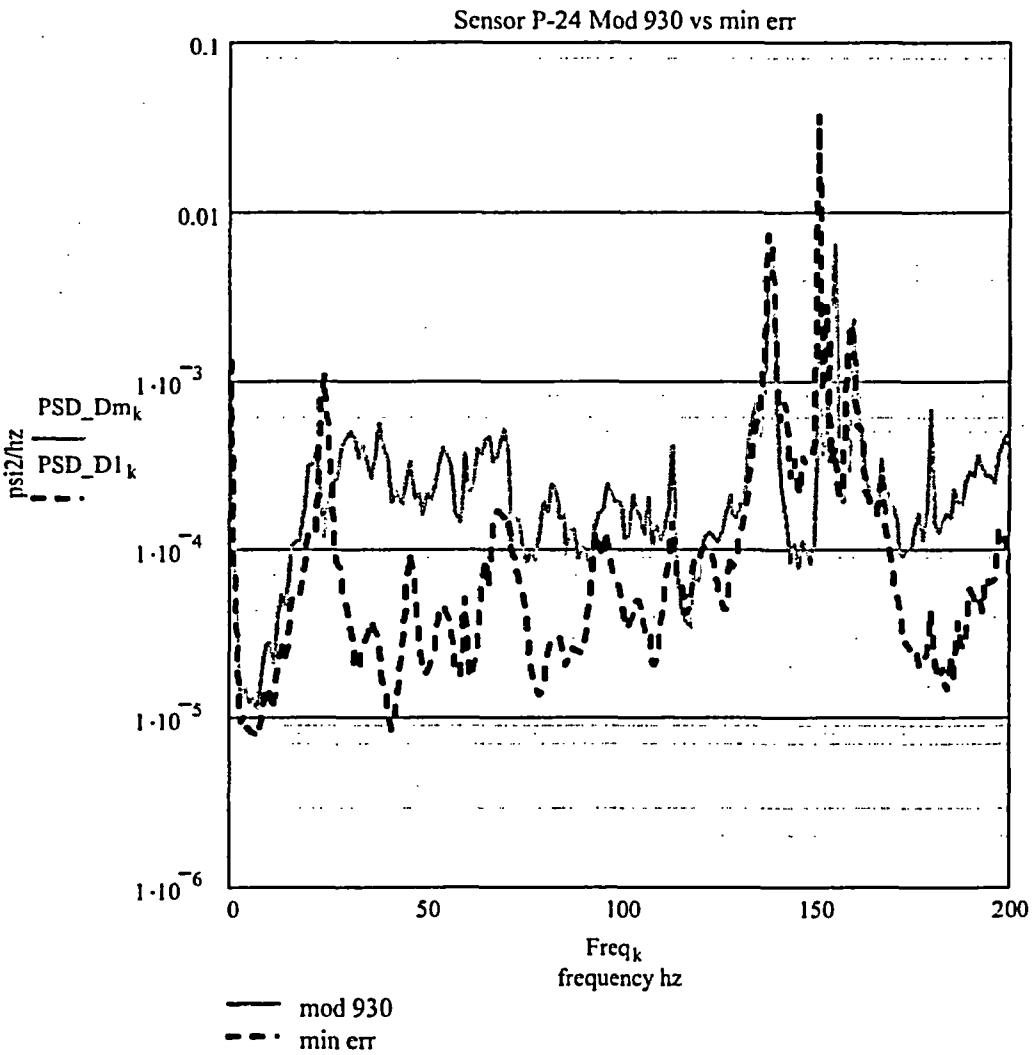

The figure illustrates that the minimum error load prediction produces significantly less frequency content in the 30-120 Hz range. This is a direct consequence of the refined Helmholtz solution employed in the minimum error load set, and explains why the modified 930 MWe ACM produces higher predicted skirt response.

3.3 Strain Gage Failure Considerations

As noted in Section 2, the failure of strain gages can have a considerable impact on the resulting pipe internal pressures used as input to the ACM. Specifically, the loss of strain gages tends to cause over-prediction of pressures and also to introduce non-acoustic frequency content due to non-breathing mode piping structural responses. Reference 10 investigated the effects of strain gage failure on QC1 and documented comparisons to calculated single pair response on Unit 2. The conclusion that can be drawn is that loss of in-plane strain gages, particularly at the 651' elevation can have dramatic effects on the predicted pressure and frequency content. Subsequent efforts to include the remaining strain gage into the pressure calculation have been performed, along with selected adjustment of 80 Hz (approximate) signal content. [Reference 3] This was performed in a manner that will overpredict the response applied to the ACM.

4. Results

Based on the discussion in Sections 2 and 3, an overall assessment of uncertainties and conservative applications was generated. Separate tables are provided for each unit to reflect differences in the analysis. The uncertainty summaries are contained in the following tables.

Table 2 Uncertainty Terms in Unit 1 Dryer Analysis

Uncertainty Term	*Absolute Effect %*	*Effect on Analysis*
Strain Gage Measurement	5.02	+/-3.6% based on minimum error model sensitivity
Strain Gage Failure Impact	In-plane failures yield conservative pressure predictions	Conservative results occur (magnitude and frequency content)
Pressure Sensor Measurement	3.9 Absolute 2.9 Relative	+/-2.9%
Pressure Sensor Phenomenological	N/A	+3 to +8%
ACM Uncertainty		ACM captures 95% of peak-peak pressure distribution with high confidence levels (95%).
Structural FEA		Bounding values selected based on +/- 10% time step sensitivity cases, plus other attributes of FEA noted in section 2.4.
Net Effect		Range: underpredict by 3.5% to overpredict by 14.5% plus conservatism introduced by strain gage failure, and use of modified 930 MWe ACM for upper dryer loads

Table 3 Uncertainty Terms in Unit 2 Dryer Analysis

Uncertainty Term	*Absolute Effect %*	*Effect on Analysis*
Strain Gage Measurement	5.02	+/- 3.6% based on minimum error model sensitivity
Strain Gage Failure Impact	N/A	N/A
Pressure Sensor Measurement	3.9 Absolute 2.9 Relative	+/- 2.9%
Pressure Sensor Phenomenological	N/A	+3 to +8%
ACM Uncertainty		Modified 930 MWe ACM used for Unit 2 analysis is conservative compared to minimum error model, particularly in skirt region and front hood
Structural FEA		Bounding values selected based on +/-10% time step sensitivity cases, plus other attributes of FEA noted in section 2.4
Net Effect		Range: underpredict by 3.5% to overpredict by 14.5% plus conservatism introduced by use of modified 930 MWe ACM

5. Conclusions/Discussion

A summary of the key uncertainties and deliberate conservatism included in QC1 and QC2 steam dryer analyses was prepared. The following conclusions are made based on this work.

1) The best estimate of the overall uncertainty for dryer analysis methodology is that it would range from a maximum under-prediction of 3.5% to an over-prediction of 14.5%.
2) This uncertainty is supplemented by conservatism in the application of the ACM. For QC1, the effect of strain gage failure yields conservative load development. For QC2, the modified 930 MWe ACM produces conservative load predictions when compared to the minimum error ACM.
3) The results of the analyses for both units are conservative as currently developed. The conservatism in the load development compared with the maximum under-prediction anticipated, provides confidence in the analyses as being appropriate for validation of the structural margin of the steam dryers in both Quad Cities units.
4) The application of these methods to other plants will require careful examination of the key inputs. The uncertainty associated with the test instrumentation and model validation can be expected to remain applicable. The quality of the information (i.e., from MSL strain gages) used as input to the ACM is a key contributor to the overall determination of conservatism.

Based on the development and consideration of uncertainties presented, no additional factors are required to compensate for potential uncertainties in the various elements of the replacement steam dryer evaluation.

6. References

1. Structural Integrity Associates, Inc. 2005. Quad Cities Strain Gage Evaluation. Calculation Package File No. EXLN-20Q-301, Project No. EXLN-20Q. Revision 0.
2. C.D.I. Report No. 05-10 - Benchmarking of Continuum Dynamics, Inc. Steam Dryer Load Methodology Against Quad Cities Unit 2 In-Plant Data, Revision 0.
3. SIA letter report, SIR-05-223 Revision 1, "Comparison of Quad Cities Unit 1 and Quad Cities Unit 2 Main Steam Line Strain Gage Data," July 18, 2005.
4. GE-NE-0000-0037-1951-01, Revision 0, "Dryer Vibration Instrumentation Uncertainty," April, 2005.
5. GE-NE-0000-0038-2076-01-Revision 0, Summary of the Effects of the Sensor Cover Plates on Dynamic Pressure Measurement," April, 2005.
6. "Acoustic Circuit Benchmark, Quad Cities Unit 2 Instrumented Steam Path, 790 MWe and 930 MWe Power Levels," AM-2005-002, June 2005.
7. "Acoustic Circuit Model Validation, Quad Cities Unit 2 Instrumented Steam Path, Final Model Revision 930 MWe Power Level," AM-2005-004, Revision 0, July 2005.
8. GE letter report, GE-NE-0000-0039-4749, Revision 1, "Exelon Steam Dryer Replacement Program-2% Structural Damping for Seismic and Non-Seismic (FIV) Dynamic Analysis for Quad Cities 1 and 2," June 22, 2005.
9. LMS Report, "Test and Analysis Report. Quad Cities New Design Steam Dryer. Dryer #1 Experimental Modal Analysis and Correlation with Finite Element Results," Revision 1, May 12, 2005.
10. "Comparison of Acoustic Circuit Dryer Loads for Missing MS Line Strain Gauges to Acoustic Circuit Dryer Loads with All MS Line Strain Gages," AM-2005-006, Revision 0, July 2005.

Appendix A- Consideration of Dynamic Effects on Pressure Sensors Near the MSL Nozzles

Purpose

The purpose of this appendix is to document the investigation performed to assess the need for additional dynamic compensation terms on the sensors nearest the vessel steam nozzles. As noted in Reference 4, the effect of placing the pressure sensors in dome housings was anticipated to result in a conservative bias of 3 to 8% overall, compared to mounting the sensors flush with the surfaces of the steam dryer. One concern with respect to the sensors located closest to the steam nozzles was that turbulence due to vortex behavior might affect the measured pressures at these locations. The complexity of the geometry precluded simple calculation of these effects, and it was determined that the best way to address this concern would be to review the test data to identify if this behavior were evidenced.

Review Method

Turbulence near the vortex entering the steam nozzle would be expected to be fairly low frequency (i.e., below 100 Hz). The vortex itself would be expected to produce a frequency of about 20-25 Hz, based on the formulas governing vortex whistles. The review of the plant data focused on two elements that would indicate a reason for concern.

1) There would be a significant spike in the lower frequency 0-100 Hz data for sensors near the nozzles.
2) This spike would not be reflected in other sensors further from the nozzles since it is a local turbulence effect and not a propagating acoustic phenomena.

PSD plots were prepared for sensor locations P-3 and P-12 (the sensors nearest the nozzles on the 90 degree side of the dryer). Similar PSDs were generated for sensor locations P-2 and P-11, which are adjacent to P-3 and P-12, but higher up on the dryer face.

Results

The PSD plots are shown in Figures A-1 through A-4. The frequency content between P-3 and P-2 is virtually identical, as is the case for P-12 and P-11. The magnitudes are lower at P-2 and P11, which is expected. Therefore, it can be concluded that the sensors closest to the vortex are not subject to significant

turbulent behaviors. As such, no correction factor is necessary to modify the sensors closest to the nozzles.

Figure A-1 PSD of Sensor P-3 Test Data 930 MWe

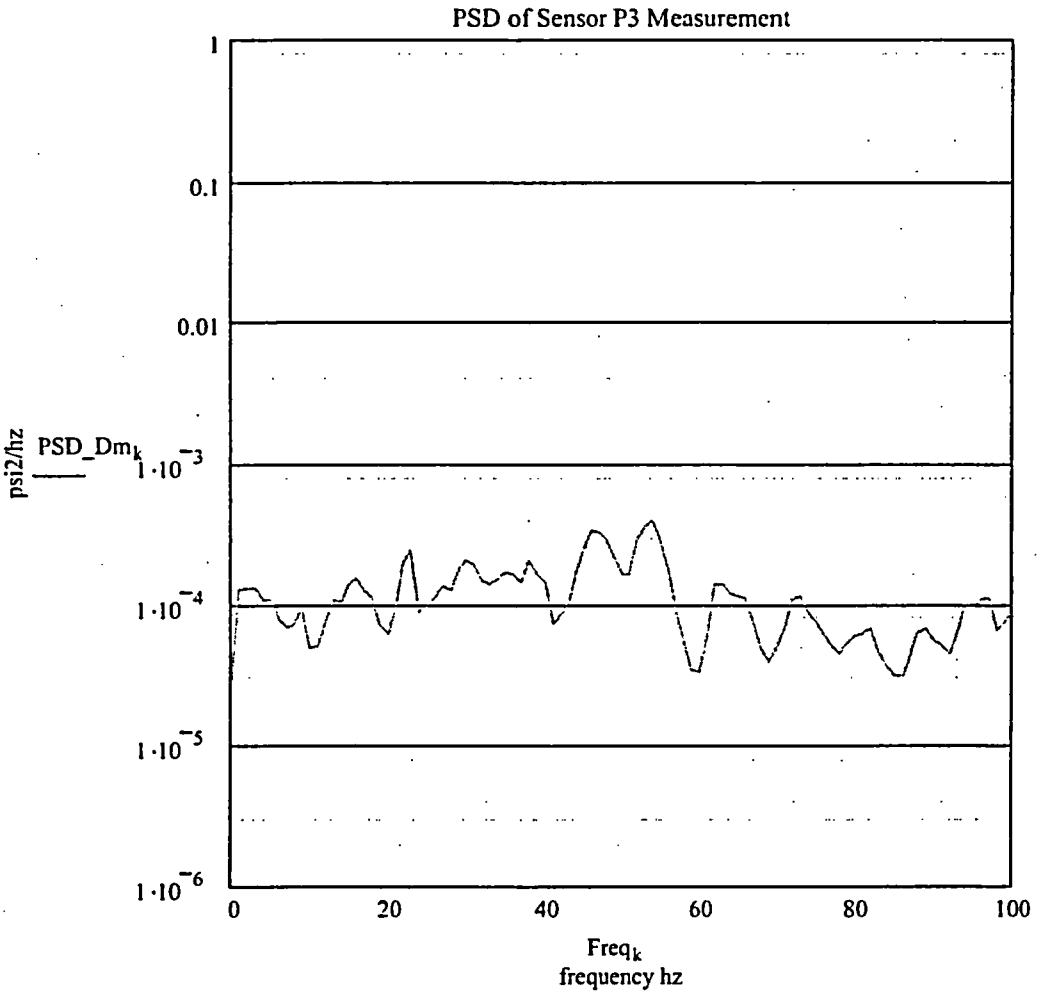

Figure A-2 PSD of Sensor P-2 Test Data 930 MWe

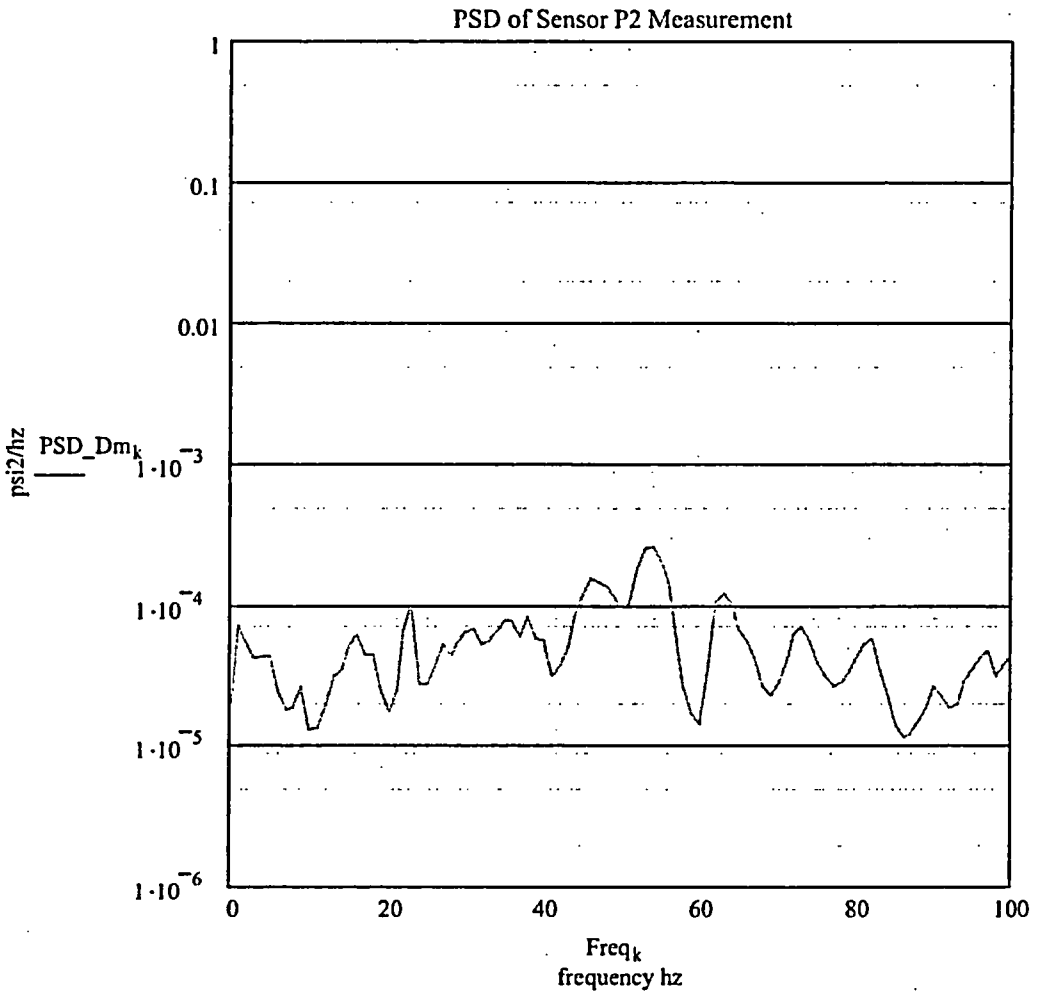

Figure A-3 PSD of Sensor P-12 Test Data 930 MWe

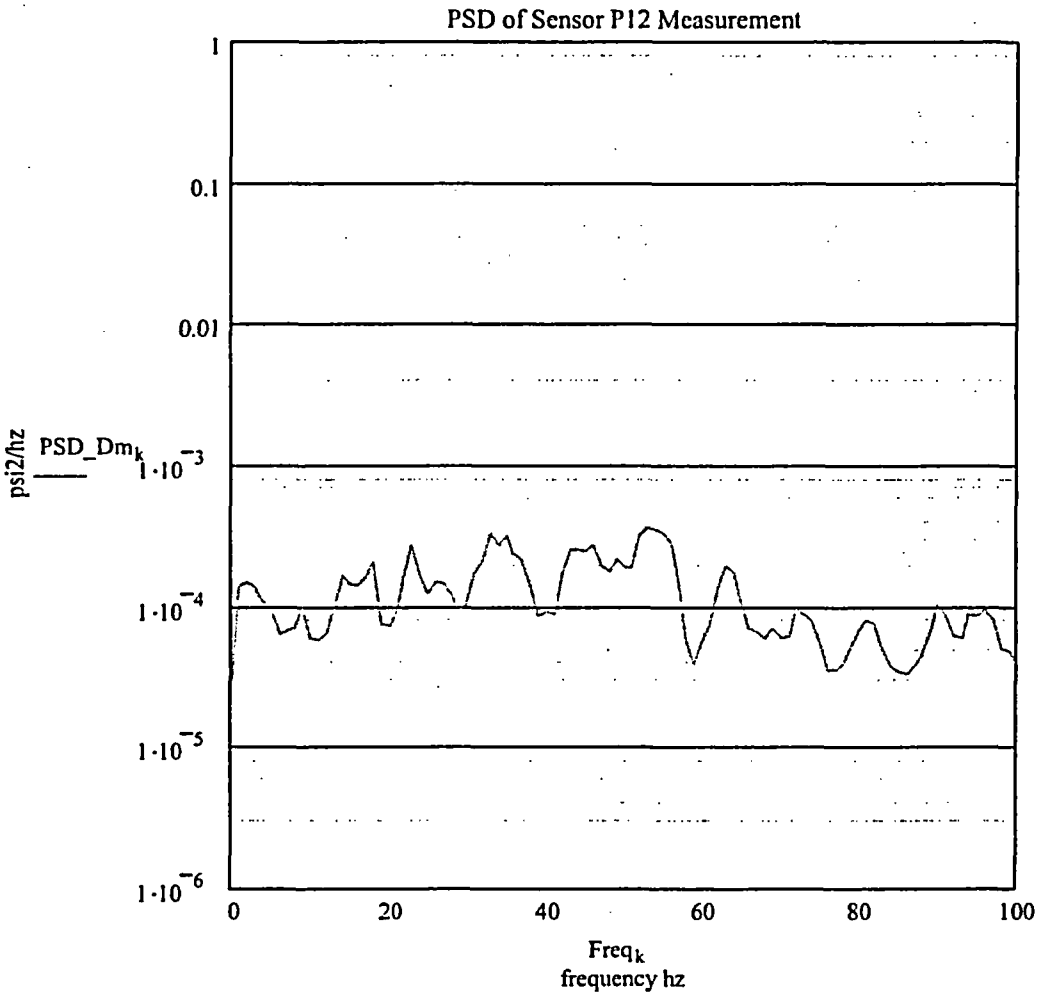

Figure A-4 PSD of Sensor P-11 Test Data 930 MWe

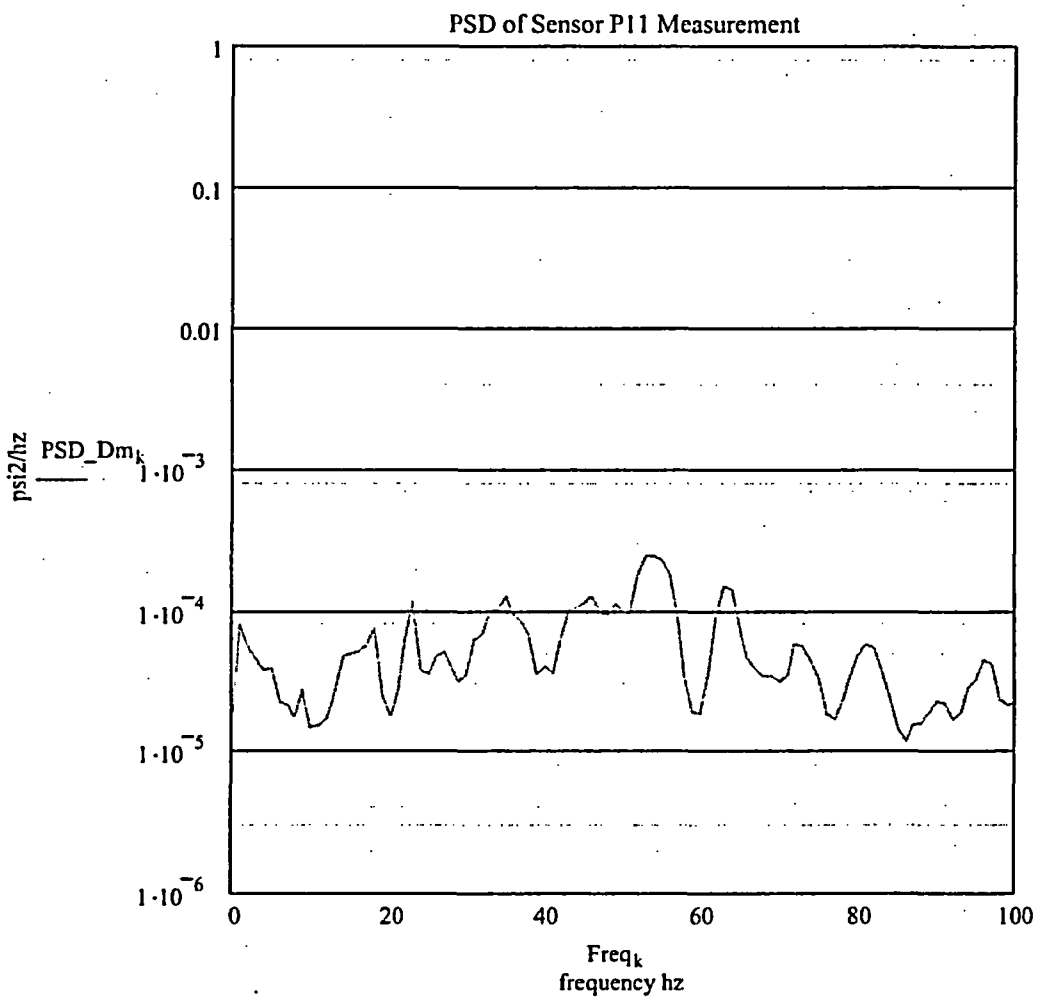

ENCLOSURE 2

Attachment 6

Exelon Report Number AM-2005-007, "AM-2005-007 Assessment of the Revised QC1 Minimum Error ACM Loads Using All Main Steam Line Strain Gages," Revision 0, dated August 2, 2005

AM-2005-007 Assessment of the Revised QC1 Minimum Error ACM Loads Using All Main Steam Line Strain Gages

Document Number AM-2005-007
Revision 0

Nuclear Engineering Department
Exelon Nuclear Generating Co.

Prepared by:	Guy DeBoo	Date:	8/2/05
Reviewed by:	Kevin Ramsden	Date:	8/2/05
GE Confirmation by:	Daniel C. Pappone	Date:	AUG 2, 2005
Approved by:	Roman Gesior	Date:	8/2/05 (Date Issued)

Abstract

This report documents an assessment of the minimum error acoustic circuit model loads that were developed by CDI using different main steam (MS) line pressure inputs. The assessment examines the differences between these two load cases to determine which would produce bounding dryer stresses.

Abstract 2
1. Introduction 4
2. Description of Assessment Criteria 5
3. Assessment of TC15a and TC15a_3 Load Cases 6
Table 1: Pressure Comparisons for TC15a and TC15a_3 Load Cases 6
Figure 1: P22 PSD – Black Curve is TC15a & Blue Curve is TC15a_3 7
Figure 2: P24 PSD – Black Curve is TC15a & Blue Curve is TC15a_3 8
4. Conclusions and Recommendations 13
5. References 14

1. Introduction

This report assesses the magnitudes and frequency content of the steam dryer pressure loads predicted by the CDI minimum error acoustic circuit model (ACM) for Quad Cities Unit 1 (QC1) as reported in Reference 1. Two sets of dryer pressure loads developed using the same acoustic circuit model with different main steam line pressure inputs were compared and assessed to determine which load case is bounding. Details of the CDI minimum error acoustic circuit model are found in Reference 2, Section 5.6. The difference between the two pressure load cases being compared is the treatment of the failed strain gage data used to develop the main steam line pressures. A detailed description of the differences in the main steam line pressures used to develop these two load cases is found in Reference 1.

The load case identified as TC15a in Reference 1 has been used in the finite element analysis of the dryer to qualify the dryer skirt. The GE finite element analysis results are designated as QC1B. The load case identified as TC15a_3 in Reference 1 represents the dryer loads that best represent the pressures acting on the Unit 1 dryer. This is based on the conclusions developed in References 2 and 3 for the acoustic circuit model, and the recommendations for defining the QC1 main steam line pressure input to these models given in Reference 4.

The purpose of this assessment is to determine which of the two load cases would produce bounding dryer stresses. It will examine the differences in pressures at specified locations on the dryer to determine changes in pressure magnitudes and frequencies. The pressure loads on the dryer skirt and outer hoods are the specific locations to examine, as these are the locations of the largest pressures and highest stresses on the dryer.

2. Description of Assessment Criteria

The purpose of this assessment is to determine the relative magnitudes and frequencies of the two load cases. The locations of primary interest are:

1) Skirt Locations P22, P24, and P25
2) Dryer external locations P3, P12, P20, and P21 (these are the highest load points opposite the nozzles)
3) Other external dryer locations may also be reviewed as necessary
4) Internal pressures at P13, P14 will be compared in combination with P3 and P20 to establish hood differential pressure behavior.

These locations were chosen because they best represent the pressure loads acting on the skirt (i.e., P22, P24 andP25) and the largest pressure loads acting on the outer hoods (i.e., P3, P12, P20 and P21).

The following criteria were applied for the initial comparison:

1) Root mean square (RMS) pressures – TC15a case should be within -5% or greater than the TC15a_3 load case.
2) Peak pressures – TC15a case should be within -3% or greater than the TC15a_3 load case.
3) Differential pressure indications should be conservative for TC15a case relative to TC15a_3 load case.
4) Power Spectral Densities (PSDs) will be compared at critical structural frequencies for the elements in question: For the skirt, this frequency is 33 Hz +/- 5Hz. For the hood, the frequencies of interest are 80-110 Hz, 140 Hz +/- 5Hz, and 155 Hz +/- 5hz. The expectation is that the TC15a case will show comparable or conservative PSD amplitude values compared to the TC15a_3 load case.

If these criteria are satisfied, the TC15a load case is considered to be an acceptable load definition for determining the FIV stresses in the dryer.

3. Assessment of TC15a and TC15a_3 Load Cases

The summary pressures and PSDs for the two load cases are documented in Reference 1. To assess these results, Table 1 below provides the minimum, maximum, and RMS pressures for both load cases at each of the QC2 dryer pressure transducer locations.

Pressure Sensor Number	TC15a: Minimum psi	TC15a_3: Minimum psi	% Change Minimum	TC15a: Maximum psi	TC15a_3: Maximum psi	% Change Maximum	TC15a: RMS psi	TC15a_3: RMS psi	% Change RMS
P1	-1.342	-1.355	-0.959	1.341	1.440	-6.875	0.438	0.464	-5.603
P2	-1.028	-1.121	-8.296	1.010	1.140	-11.404	0.224	0.270	-17.037
P3	-1.938	-1.776	9.122	1.830	1.688	8.412	0.504	0.467	7.923
P4	-0.723	-0.777	-6.950	0.755	0.728	3.709	0.177	0.182	-2.747
P5	-1.038	-0.766	35.509	0.813	0.799	1.752	0.199	0.194	2.577
P6	-1.301	-1.164	11.770	1.267	1.171	8.198	0.347	0.312	11.218
P7	-1.054	-1.125	-6.311	1.038	1.179	-11.959	0.338	0.386	-12.435
P8	-0.837	-0.678	23.451	0.809	0.713	13.464	0.182	0.161	13.043
P9	-1.674	-1.550	8.000	1.695	1.562	8.515	0.510	0.518	-1.544
P10	-1.322	-1.361	-2.866	1.364	1.393	-2.082	0.436	0.458	-4.803
P11	-0.946	-0.789	19.899	0.866	0.848	2.123	0.209	0.193	8.290
P12	-2.335	-2.069	12.856	2.231	2.116	5.435	0.678	0.741	-8.502
P13	-0.549	-0.355	54.648	0.403	0.343	17.493	0.106	0.087	21.839
P14	-0.461	-0.452	1.991	0.512	0.489	4.703	0.114	0.106	7.547
P15	-2.027	-2.012	0.746	1.896	1.882	0.744	0.569	0.572	-0.524
P16	-0.366	-0.304	20.395	0.289	0.262	10.305	0.078	0.063	23.810
P17	-1.160	-1.112	4.317	1.135	1.014	11.933	0.275	0.287	-4.181
P18	-1.691	-1.617	4.576	1.696	1.701	-0.294	0.501	0.517	-3.095
P19	Not functional								
P20	-3.342	-3.503	-4.596	3.621	3.781	-4.232	1.075	1.124	-4.359
P21	-1.641	-1.503	9.182	1.461	1.462	-0.068	0.407	0.395	3.038
P22	-1.439	-1.407	2.274	1.527	1.351	13.027	0.435	0.445	-2.247
P23	-0.332	-0.251	32.271	0.257	0.204	25.980	0.073	0.056	30.357
P24	-1.138	-1.029	10.593	1.193	1.125	6.044	0.280	0.257	8.949
P25	-1.342	-1.260	6.508	1.348	1.258	7.154	0.328	0.295	11.186
P26	-0.294	-0.238	23.529	0.280	0.245	14.286	0.077	0.064	20.313
P27	-0.335	-0.242	38.430	0.285	0.231	23.377	0.074	0.059	25.424
Average	-1.218	-1.147	6.168	1.189	1.159	2.646	0.332	0.334	-0.450
P3-P13	-1.984	-1.928	2.905	1.952	1.973	-1.064	0.553	0.511	8.219
P20-P14	-3.660	-3.821	-4.214	3.877	4.096	-5.347	1.148	1.204	-4.651

Skirt pressures for assessment

Outer Hood pressures for assessment

Table 1: Pressure Comparisons for TC15a and TC15a_3 Load Cases

The table contains the percent difference of the TC15a load case to the TC15a_3 load case. Positive percentages indicate that TC15a pressures are greater than the TC15a_3 pressures for the RMS and maximum pressures. A positive percentage also indicates that TC15a minimum pressures are smaller than the TC15a_3 minimum pressures. Positive percent changes indicate that TC15a bounds the TC15a_3 load case for the pressure being evaluated.

The percent changes at the skirt locations, P22, P24, and P25, meet the assessment criteria provided in Section 2. The minimum pressures for the TC15a load case are smaller than the minimum pressures for the TC15a_3 load case by approximately 2% to 10%. The maximum pressures for TC15a are larger than the maximum pressures for the TC15a_3 load case by approximately 6% to 13%. The RMS pressures for TC15a are generally larger than the maximum pressures for the TC15a_3 load case by approximately 8% to 11%, however one location is less by 2.2%.

Reviewing the frequency content of the skirt pressures at the P22, P24 and P25 locations in Figures 1 through 3 below, the TC15a load case clearly envelops all frequencies at these three locations with one minor exception at approximately 180 Hz.

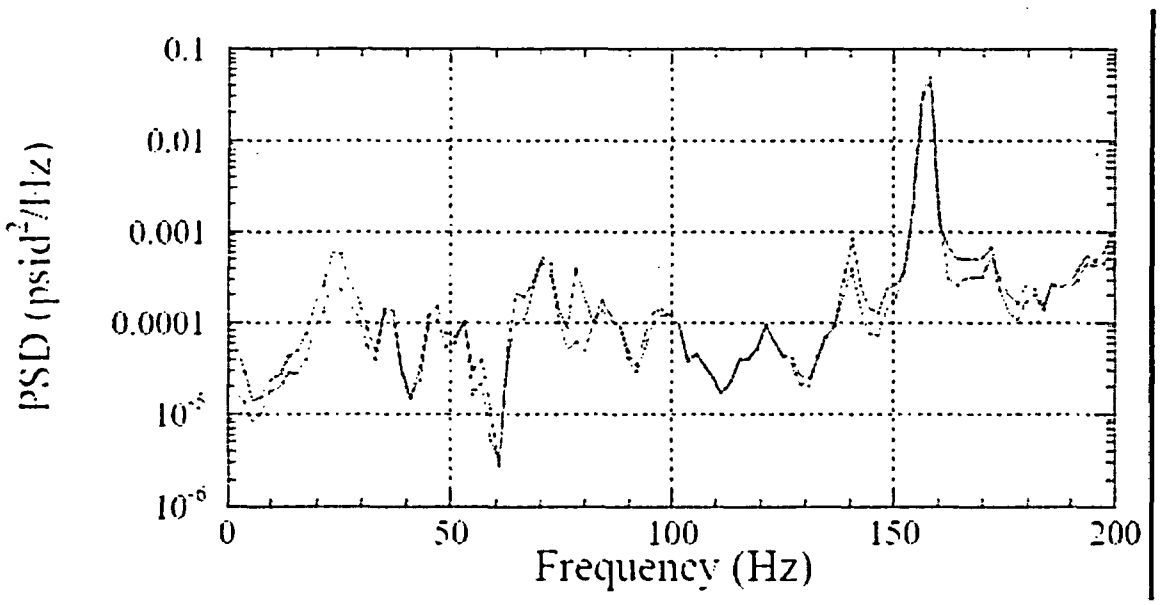

Figure 1: P22 PSD – Black Curve is TC15a & Blue Curve is TC15a_3

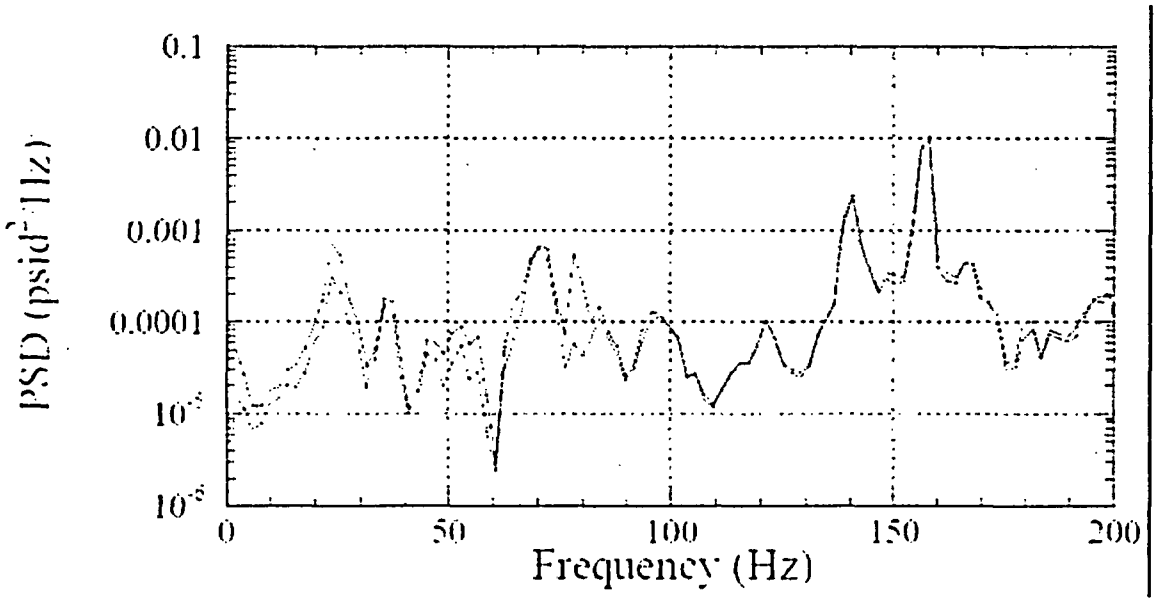

Figure 2: P24 PSD – Black Curve is TC15a & Blue Curve is TC15a_3

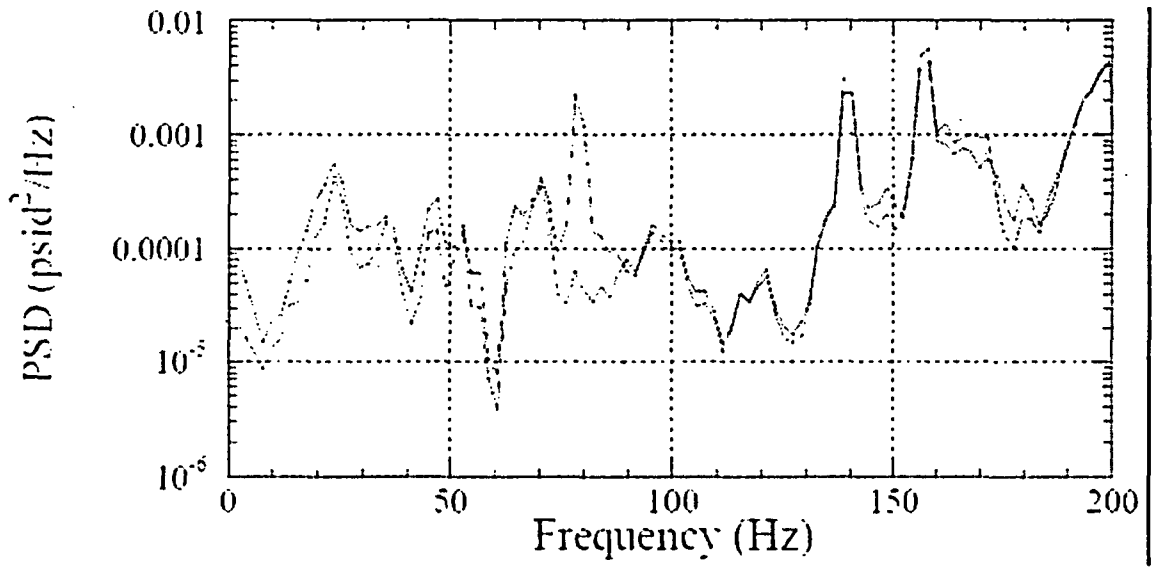

Figure 3: P25 PSD – Black Curve is TC15a & Blue Curve is TC15a_3

For the outer hood pressure comparisons, the assessment is not as conclusive as it was for the skirt comparisons. The TC15a maximum and minimum pressures for the P3, P12, and P21 locations are clearly bounding the pressures from the TC15a_3 load case. The TC15a maximum, minimum and RMS pressures for the P20 location are less than the TC15a_3 by approximately 5% for each. The P3-P13 differential pressure satisfies the assessment criteria and is bounding for the minimum and RMS pressures. The TC15a maximum, minimum and RMS pressures for the P20-P14 differential pressure are less than the TC15a_3 pressures by approximately 5% for each. With the exception of the TC15a_3 pressures at the P20 nozzle, the TC15a pressures at the other nozzles and generally for the rest of the dryer locations bound the TC15a_3 pressures.

The frequency comparisons for the outer hood locations opposite the main steam nozzles are presented in Figures 4 through 7 below. Reviewing these figures the following conclusions are drawn.

1. P3 – TC15a bounds the TC15a_3 pressures at all frequencies except a minor difference at approximately 180 Hz. This has not been a frequency of concern for the design of the dryer and magnitudes are greater at other frequencies that are more significant to the dryer.
2. P12 – TC15a bounds the TC15a_3 pressures at all frequencies except minor differences at approximately 150 Hz and 180 Hz. These have not been frequencies of concern for the design of the dryer and magnitudes are greater at other frequencies that are more significant to the dryer.
3. P20 – TC15a bounds the TC15a_3 pressures at all frequencies except minor differences at approximately 15 Hz and 50 Hz. These have not been frequencies of concern for the design of the dryer and magnitudes are greater at other frequencies that are more significant to the dryer.
4. P21 – TC15a bounds the TC15a_3 pressures at all frequencies.

The frequency content comparisons for the P3-P13 and P20-P14 differential pressures are presented in Figures 8 and 9 below. Reviewing these figures the following conclusions can be drawn:

1. P3-P13 – TC15a bounds the TC15a_3 pressures at all frequencies except minor differences at approximately 80 Hz and 180 Hz. The 180 Hz has not been a frequency of concern for the design of the dryer and magnitudes at other more significant frequencies to dryer are greater. The 80 Hz difference is very minor and would be enveloped by a much larger pressure at approximately 78 Hz.
2. P20-P14 – TC15a bounds the TC15a_3 pressures at all frequencies except a minor difference at approximately 10 Hz to 15 Hz. This has not been a frequency range of concern for the design of the dryer and magnitudes are greater at other frequencies that are more significant to the dryer.

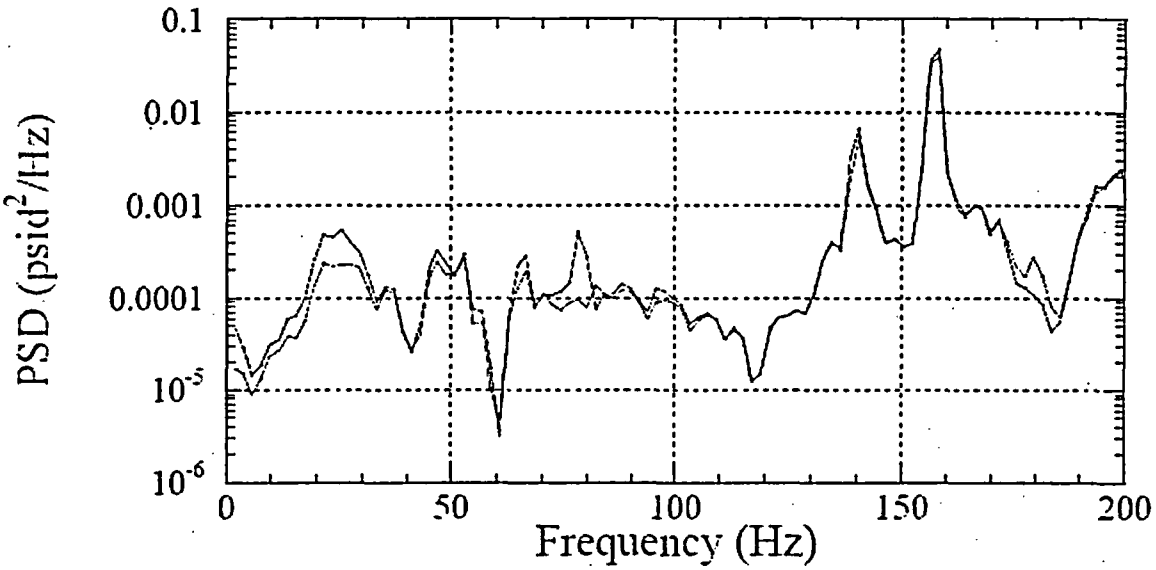

Figure 4: P3 PSD – Black Curve is TC15a & Blue Curve is TC15a_3

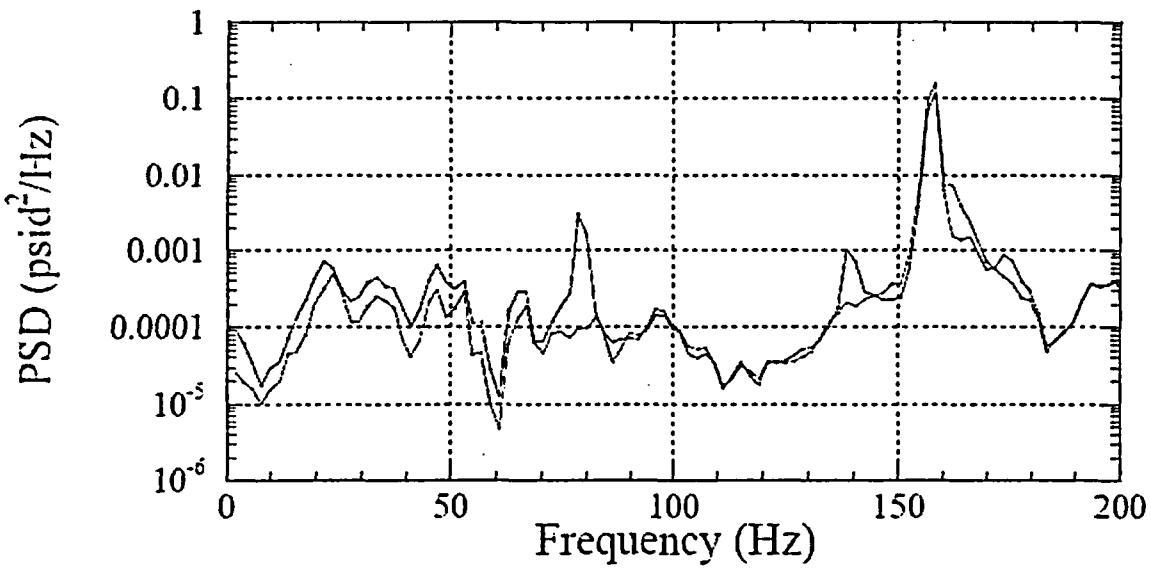

Figure 5: P12 PSD – Black Curve is TC15a & Blue Curve is TC15a_3

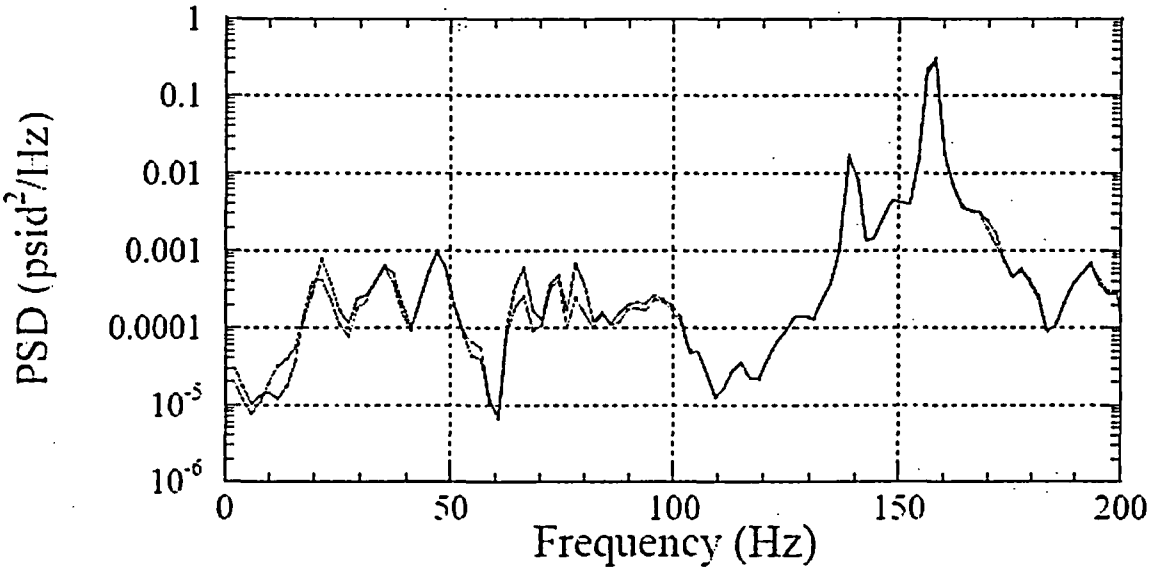

Figure 6: P20 PSD – Black Curve is TC15a & Blue Curve is TC15a_3

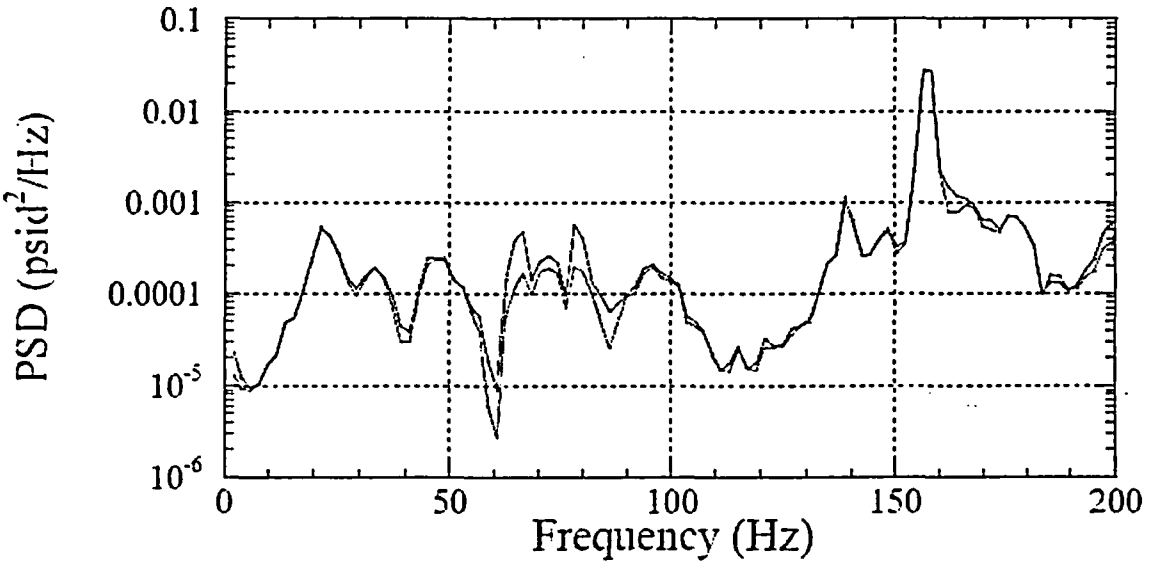

Figure 7: P21 PSD – Black Curve is TC15a & Blue Curve is TC15a_3

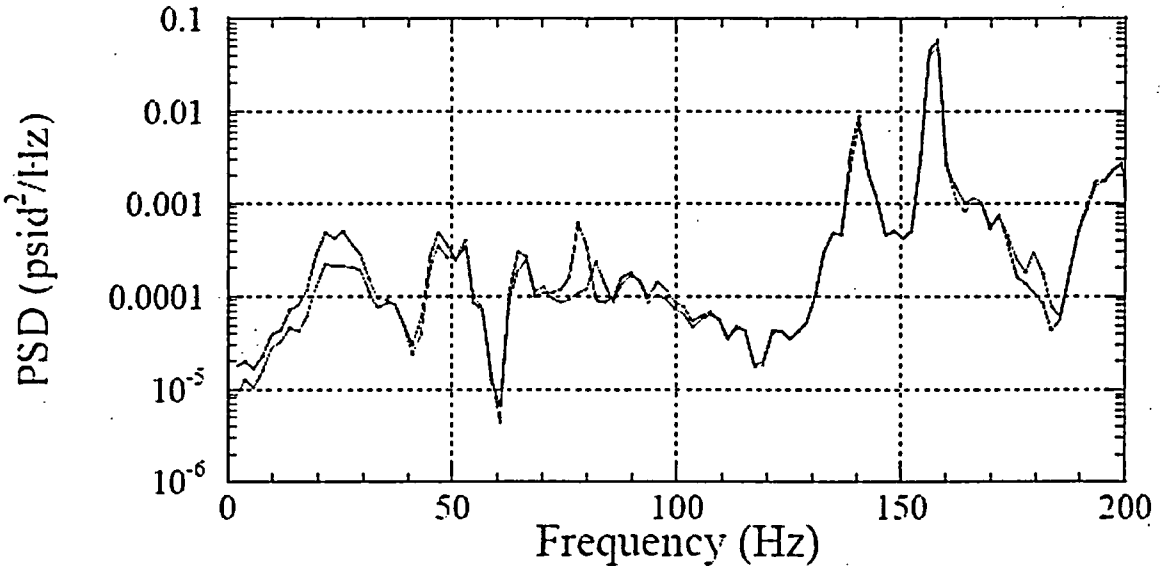

Figure 8: P3-P13 PSD – Black Curve is TC15a & Blue Curve is TC15a_3

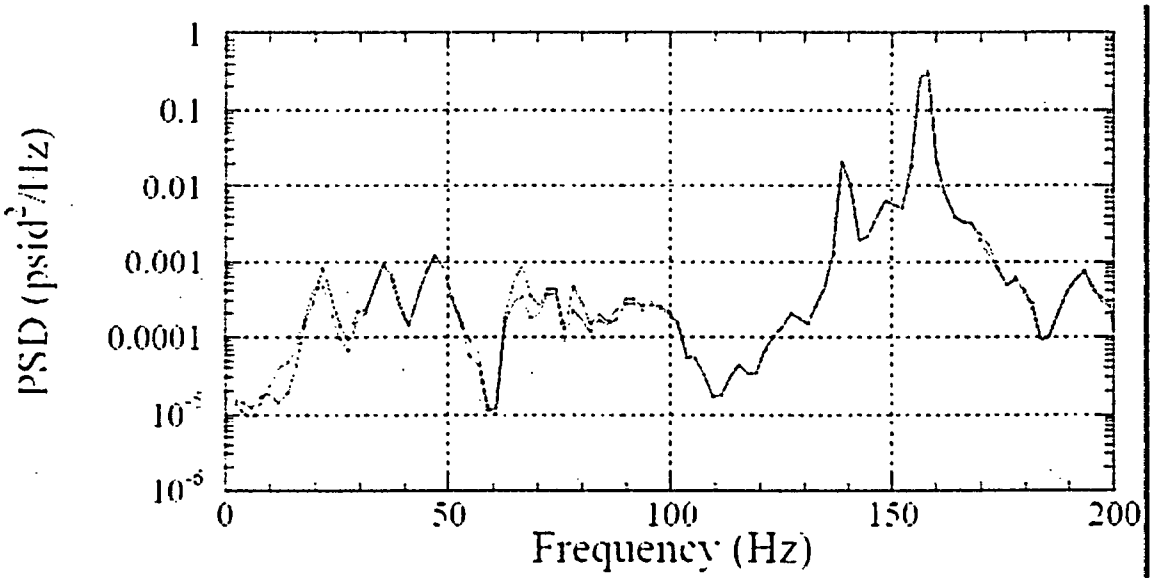

Figure 9: P20-P14 PSD – Black Curve is TC15a & Blue Curve is TC15a_3

4. Conclusions and Recommendations

Based on the results of this assessment, the following conclusions are drawn.

1. The TC15a load case is bounding for the loading on the skirt when compared to the TC15a_3 load case. The pressures are bounding and the frequency content envelops that of TC15a_3 frequency content.

2. The TC15a load case is representative but not necessarily bounding for the loading on the outer hoods when compared to the TC15a_3 load case. The pressures generally bounding those from the TC15a_3 load case and the frequency content generally envelops that of TC15a_3 frequency content.

Based on these conclusions, it is recommended to qualify the skirt using the QC1B FEA results. All other dryer components should be qualified using the QC1D FEA results since that acoustic circuit model load case was developed using a validated acoustic circuit model, Reference 2 and Reference 3, with main steam line pressure inputs equivalent to those used in the TC15a_3 load case and satisfied the recommendations specified in Reference 4.

An additional recommendation is to perform a finite element analysis using the TC15a_3 load case. This load case is based on a validated acoustic circuit model using the best representation of main steam line pressure data as input, Reference 4; and it is less conservative than the load case used in the QC1D FEA.

5. References

1. "Test Condition TC15a Load Comparison for Quad Cities Unit 1," Continuum Dynamics, Inc. Technical Note No. 05-34, Revision 0, dated August 1, 2005.

2. "Evaluation of Continuum Dynamics, Inc. Steam Dryer Load Methodology Against Quad Cities Unit 2 In-Plant Data," Continuum Dynamics, Inc. Report No. 05-10, Revision 0, July 2005.

3. "Acoustic Circuit Benchmark Quad Cities Unit 2 Instrumented Steam Path Final Model Revision 930 MWe Power Level," Exelon Nuclear Asset Management Report AM-2005-004, Revision 0, July 2005.

4. "Comparison of Quad Cities Unit1 and Quad Cities Unit 2 Main Steam Line Strain gage Data," SIA Letter Report KKF-05-037, SIR-05-223 Revision 1, July18, 2005.

ENCLOSURE 2

Attachment 7

Structural Integrity Associates Letter KJO-05-004, "Vibration Comparison of Quad Cities Units 1 and 2 Power Ascension Accelerometer Spectra Data," dated July 14, 2005

Structural Integrity Associates, Inc.

6855 S. Havana Street
Suite 350
Centennial, CO 80112-3868
Phone: 303-792-0077
Fax: 303-792-2158
www.structint.com
kohara@structint.com

July 14, 2005
SIR-05-219 Rev. 0
KJO-05-004

Mr. Rob Stachniak
Exelon Nuclear
4300 Winfield Road
Warrenville, IL 60555

Subject: Vibration Comparison of Quad Cities Units 1 and 2 Power Ascension Accelerometer Spectra Data

Dear Rob,

The intent of this review is to compare the amplitude and frequency of ERV-3B and ERV-3C accelerometer vibration data between Quad Cities Unit 1 (QC1) and Quad Cities Unit 2 (QC2). Data comparisons were made at common, higher power levels where frequency content is representative of full power operation. Additionally, frequency content will be compared to known acoustic frequencies present within the main steam (MS) piping systems.

INTRODUCTION

QC1 and QC2 completed their maintenance outages and subsequent power ascensions in May and June 2005, respectively. During their 2005 outages, accelerometers were installed and/or reconnected and during each power ascension accelerometers were monitored at two ERV locations (ERV-3B and ERV-3C). Only ERV-3B and ERV-3C were common to both QC1 and QC2 (QC1 had accelerometers on ERV-3B and ERV-3C only, whereas, QC2 had accelerometers on all ERVs). Data monitoring consisted of recording accelerometer time histories at several power levels during power ascension. These accelerometer time histories were then converted to acceleration frequency spectra by Exelon.

This review provides a detailed assessment of both the amplitude and frequency content of these accelerometer spectra.

INSTRUMENT TYPES AND LOCATIONS

The accelerometer spectra comparisons were limited to two locations; QC1 had accelerometers at two locations (ERV-3B and ERV-3C), whereas, QC2 had accelerometers at all ERVs, including ERV-3B and ERV-3C. This limited the frequency spectra comparisons to the two valve locations only.

QC1 – Power Ascension, June 2005

The vibration levels of two ERVs (ERV-3B and ERV-3C) were monitored during the June 2005 power ascension. These locations were selected because they had the highest amplitudes observed during the December 2003 power ascension. Six accelerometers were mounted on each valve inlet in the x, y, and z axes (two tri-axial mounts on either side of the valve inlet flange, Table 1 and Figures 1 through 3). QC1 accelerometers were in approximately the same locations as the QC2 accelerometers.

Vibration data was captured and processed by Exelon personnel and Structural Integrity Associates received frequency spectra for each of 10 power levels [1]. Spectra data was captured from 0-2887 MWth (87.3 – 910.7 MWe) [8], but only power levels greater than 85% power level (Table 3) were used in this comparison. Amplitude and frequency content for these spectra plots are more representative of full power operation.

QC2 – Power Ascension, April 2005

The vibration levels of four ERVs (ERV-3B, ERV-3C, ERV-3D, and ERV-3E) were monitored during the April 2005 power ascension. All locations had three accelerometers mounted on each valve inlet in the x, y, and z axes (one tri-axial mount on the valve inlet flange, Table 2 and Figures 1 and 2). QC1 accelerometers were in approximately the same locations as the QC2 accelerometers. Due to the fact, that QC1 had accelerometers at only two ERV locations, then the QC2 comparison was also limited to these two locations (even though more accelerometer data was available).

Vibration data was captured and processed by Exelon personnel and Structural Integrity Associates received frequency spectra for each of 17 power levels [2]. Spectra data was captured from 0-2887 MWth (119.7 – 930.4 MWe) [8], but only power levels greater than 85% power level (Table 3) were used in the comparison (as explained above).

AMPLITUDE AND FREQUENCY COMPARISONS

The spectra plots for QC1 and QC2 at 2887 MWth are shown in Figures 4 through 15. Spectra plots were compared for each individual axis for ERV-3B and ERV-3C on both units (QC1 and QC2). Discrete frequency RMS amplitudes are shown in Table 4, whereas, overall composite amplitudes are shown in Table 5. The detailed assessments are provided below.

ERV-3B Spectra Assessment

Figures 4 through 9 show the acceleration spectra plots for ERV-3B for 2887 MWth. Inspection of each plot (x, y, and z axes), for Units 1 and 2, shows only two "significant" discrete frequencies that were common to both units; 139-140.5 Hz and 157 Hz (Table 4). These frequencies are very similar to the Quad Cities data taken during the last power ascensions (QC1 in December 2003 [3] and QC2 in April 2004 [4]) and are indicative of an acoustic phenomenon within the MS lines near the valves.

QC2 did show some frequency content between 140 and 160 Hz. These frequencies were sharp and had comparable amplitudes. Frequencies were observed at 151.5 and 160.5 Hz. These frequencies are believed to be associated with the modifications to the steam dryer, since they were not observed during the 2003/2004 power ascension spectra plots. No other "significant" frequency content was observed in these spectra plots.

The maximum QC1 composite amplitude was 0.48 grms for ERV-3B y-axis; whereas, the maximum QC2 composite amplitude was 0.54 grms for ERV-3B z-axis. The maximum discrete frequency amplitudes are shown in Table 4. These amplitudes do not exceed 0.25 grms and 0.44 grms at any discrete frequency for QC1 and QC2, respectively. Amplitudes at other frequencies (other than the discrete frequencies) were less than 0.02 grms (basically noise floor responses). Amplitudes below 0.1 grms are considered low, whereas, amplitudes between 0.1 and 0.5 grms are considered low-to-moderate. These amplitudes are not high enough to cause excessive wear.

ERV-3C Spectra Assessment

Figures 10 through 15 show the frequency spectra for ERV-3C for 2887 MWth. In general, inspection of each plot for each axes (x, y, and z), for Units 1 and 2, showed only two "significant" discrete frequencies that were common to both units; ~139 Hz and ~157 Hz (Table 4). These frequencies are similar to the Quad Cities data taken during the last power ascensions (QC1 in December 2003 [3] and QC2 in April 2004 [4]) and are indicative of an acoustic phenomenon within the MS lines near the valves. QC2 did show some low frequency content between 140 and 160 Hz; at 151.5 and 160.5 Hz. These frequencies were sharp and had comparable amplitudes. These frequencies are believed to be associated with the modifications to the steam dryer, since they were not observed during the 2003/2004 power ascension. Additionally, QC1 ERV-3C showed two discrete frequencies at 21 and 36 Hz. These frequencies were only observed on the x-axis. These frequencies are low and may be associated with a structural response of the valve. No other "significant" frequency content was observed in the spectra plots. Amplitudes at other frequencies were less than 0.02 grms (basically noise floor responses).

The maximum QC1 composite amplitude was 0.32 grms for ERV-3B y-axis; whereas, the maximum QC2 composite amplitude was 0.78 grms for ERV-3B z-axis (Table 5). The maximum discrete frequency amplitudes are shown in Table 4. These amplitudes do not exceed 0.066 and 0.358 grms at any discrete frequency for QC1 and QC2, respectively. Amplitudes at other frequencies (other than the discrete frequencies) were less than 0.02 grms (basically noise floor responses). Amplitudes below 0.1 grms are considered low, whereas, amplitudes between 0.1 and 0.5 grms are considered low-to-moderate. These amplitudes usually are not high enough to cause excessive wear. The maximum composite amplitude of 0.78 grms is concentrated at 139 and 157 Hz frequencies and based upon Wyle Labs testing [7], no valve responses were observed in this frequency range.

RESULTS AND CONCLUSIONS

A review of the acceleration frequency spectra for the most recent QC1 and QC2 power ascensions (June 2005 and May 2005, respectively), resulted in the following observations between QC1 and QC2 MS piping and their associated valve dynamic response:

1) Frequency content between QC1 and QC2 are similar.
   a. A comparison of the frequency spectra between QC1 and QC2 showed similar frequency responses in the 0-200 Hz frequency range. In general, the frequency spectra were comparable and had similar frequency content (Figures 4 through 15). Additionally, data from the previous QC1 and QC2 power ascensions [3, 4] appeared to be dynamically similar with respect to frequency content.
   b. In the 139-160 Hz frequency range for both QC1 and QC2, there are slight differences in the frequency of the spectral peaks. These frequency differences were ~2-5 Hz and most likely attributed to the steam dryer modifications, since they were not present in the previous power ascensions. Per References 5 and 6, most valve components have natural frequencies below this frequency range and would not respond.
   c. QC1 ERV-3C x-axis had two discrete frequencies (21 and 36 Hz) that were not observed on QC2 ERV-3C x-axis. Again these frequency differences were minor in that they occurred only on one vibration axis and based on frequency seemed to be unique to the valve.
2) The acceleration amplitudes (RMS) are similar in magnitude for both units, based on the maximum composite amplitudes (Table 5). The maximum composite amplitudes observed were 0.54 and 0.78 grms for QC1 and QC2, respectively. In general, both units had most of this energy concentrated at 139 and 157 Hz.

Based on this acceleration data and the resultant spectra plots, the dynamic behavior of QC1 and QC2 MS piping, and the responses of ERV-3B and ERV-3C valves are similar, both in amplitude and frequency content. Thus, the structural responses of the MS lines are similar between QC1 and QC2.

If you have any questions, please do not hesitate to contact me at (303) 792-0077.

Prepared By:

K. J. O'Hara
Senior Consulting Engineer

Reviewed By:

Karen K. Fujikawa, P.E.
Associate

Approved By:

Karen K. Fujikawa, P.E.
Associate

REFERENCES:

1. Frequency spectra received from Exelon via ibackup.com, SI File No. QC-28Q-203.
2. Frequency spectra received from Exelon via ibackup.com, SI File No. QC-28Q-201.
3. Structural Integrity Associates Calculation No. QC-11Q-302, Revision 0, "Quad Cities Unit 1 Main Steam Line Vibration Data Reduction," SI File No. QC-11Q-302.
4. Structural Integrity Associates Calculation No. QC-16Q-303, Revision 0, "Quad Cities Unit 2 ERV Vibration Data Reduction," SI File No. QC-16Q-302.
5. Structural Integrity Associates Report No. SIR-05-198, Revision 0, "Assessment of Quad Cities Unit 1 Power Ascension Main Steam Line Vibration Frequency Spectra," SI File No. QC-28Q-402.
6. Structural Integrity Associates Report No. SIR-05-192, Revision 0, "Assessment of Quad Cities Unit 2 Power Ascension Main Steam Line Vibration Frequency Spectra," SI File No. QC-28Q-401.
7. Wyle Test Report No. 50584-01, dated 2/23/04, "Test Report – Vibration Endurance Test Program for a Dresser Electromatic Relief Valve Type 6" 1525-VX for Exelon Nuclear," SI File No. QC-16Q-202.
8. Exelon Transmittal of Design Information (TODI) No. QDC-05-031, Revision 0, "Quad Cities Startup Testing Test Conditions," SI File No. QC-28Q-204.

cc: Guy Deboo (Exelon)
Roman Gesior (Exelon)
Kevin Ramsden (Exelon)
Roy Hunnicutt (Exelon)
K. Rach (SI)
K. J. O'Hara (SI)
QC-28Q-403

Table 1: QC1 Accelerometer Types and Location

Channel Number	Type	Direction	Location
1, 4	Accelerometer	Parallel to MS flow (X)	Inlet Flange ERV 3B
2, 5	Accelerometer	Vertical (Y)	Inlet Flange ERV 3B
3, 6	Accelerometer	Perpendicular to MS flow (Z)	Inlet Flange ERV 3B
7, 10	Accelerometer	Parallel to MS flow (X)	Inlet Flange ERV 3C
8, 11	Accelerometer	Vertical (Y)	Inlet Flange ERV 3C
9, 12	Accelerometer	Perpendicular to MS flow (Z)	Inlet Flange ERV 3C

Table 2: QC2 Accelerometer Types and Location

Channel Number	Type	Direction	Location
7	Accelerometer	Parallel to MS flow (X)	Inlet Flange ERV 3B
8	Accelerometer	Vertical (Y)	Inlet Flange ERV 3B
9	Accelerometer	Perpendicular to MS flow (Z)	Inlet Flange ERV 3B
13	Accelerometer	Parallel to MS flow (X)	Inlet Flange ERV 3C
14	Accelerometer	Vertical (Y)	Inlet Flange ERV 3C
15	Accelerometer	Perpendicular to MS flow (Z)	Inlet Flange ERV 3C

Table 3: QC1 and QC2 Accelerometer Data – Power Levels of Comparison

Quad Cities Power Levels	
Unit 1 [8]	**Unit 2 [8]**
MWth (MWe)	MWth (MWe)
2887 (911) TC15a	2887 (930) TC41
	2831 (912) TC39
2854 (901) TC14	2800 (900) TC38
2765 (871) TC12	2754 (882) TC37
2642 (829) TC11	2573 (821) TC34
2508 (788) TC10	2493 (792) TC33

Table 4: QC1 and QC2 Discrete Frequency and Amplitude Comparison

Accelerometer Location	Axis	QC-1		QC-2		QC-1		QC-2	
		Frequency (Hz)	Amplitude (grms)	Frequency (Hz)	Amplitude (grms)	Frequency (Hz)	Amplitude (grms)	Frequency (Hz)	Amplitude (grms)
ERV-3B Inlet Flange	X	140.5	0.043	Bad Channel		157	0.092	Bad Channel	
	Y	140.5	0.116	139	0.049	157	0.189	160.5	0.130
	Z	140.5	0.036	139	0.170	157	0.149	151.5	0.202
ERV-3C Inlet Flange	X	139.5	0.042	139	0.125	157	0.066	160	0.045
	Y	139.5	0.023	Bad Channel		157	0.011	Bad Channel	
	Z	139.5	0.057	140	0.358	158	0.065	150.2	0.256

Table 5: QC1 and QC2 Composite Amplitude Comparison

Accelerometer Location	Axis	Composite Amplitude	
		QC1 (grms)	QC2 (grms)
ERV-3B Inlet Flange	X	0.19	---
	Y	0.48	0.330
	Z	0.41	0.540
ERV-3C Inlet Flange	X	0.21	0.310
	Y	0.32	---
	Z	0.25	0.780

Date: 5/19/2003 Time : 10:43:31 AM

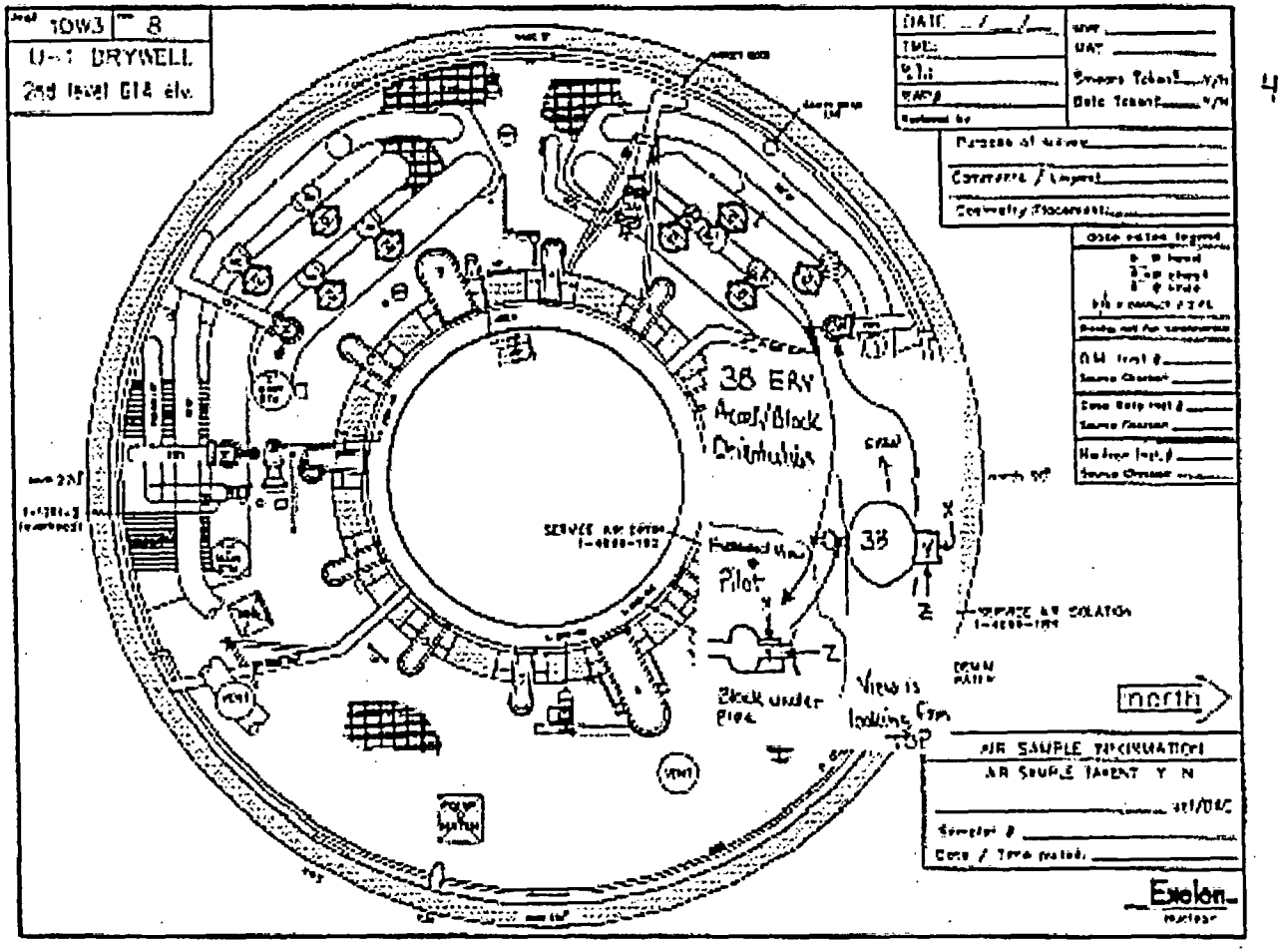

Title: K:\RPDRAW\DW1\2nd level\1DW3-8.dwg

Figure 1: Accelerometer Locations for ERV-3B

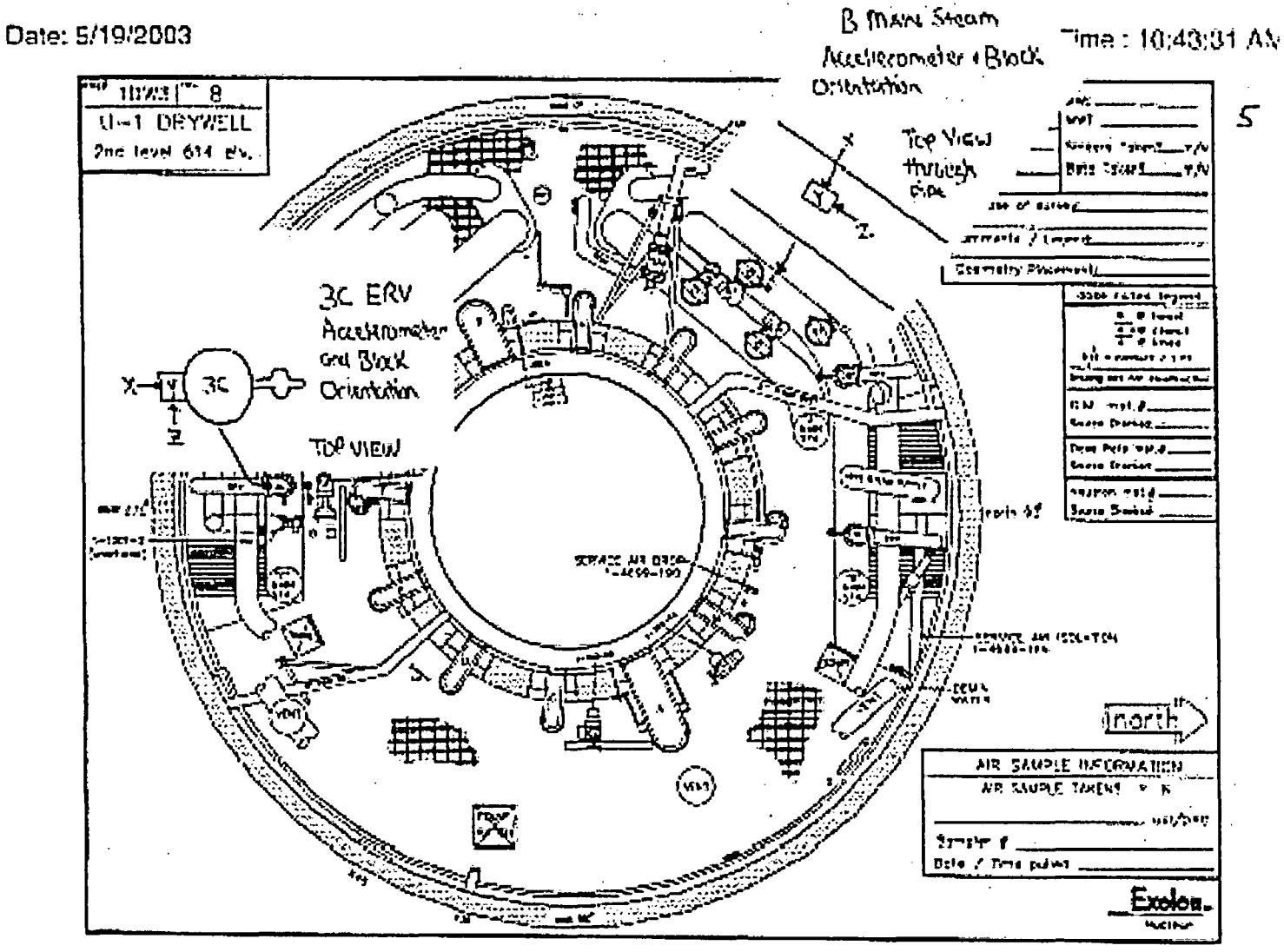

Title: K:\RPDRAW\DW1\2nd level\1DW3-8.dwg

Figure 2: Accelerometer Locations for ERV-3C

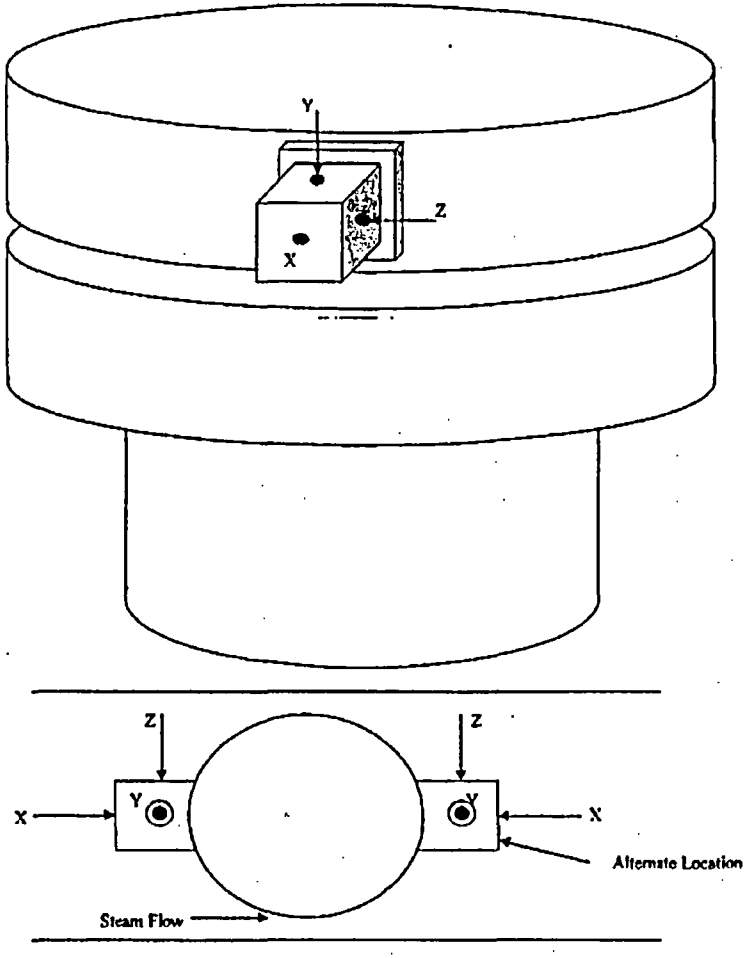

B ERV			
Direction	Label	Cable	Accel S/N
X	BX	TOD06 Pair 1	10537
Y	BY	TOD06 Pair 2	10533
Z	BZ	TOD13 Pair 1	10445
Alt X	BAX	TOD13 Pair 2	10532
Alt Y	BAY	TOD12 Pair 1	10598
Alt Z	BAZ	TOD12 Pair 2	10564

C ERV			
Direction	Label	Cable	Accel S/N
X	CX	TOD03 Pair 1	10539
Y	CY	TOD03 Pair 2	10565
Z	CZ	TOD15 Pair 1	10557
Alt X	CAX	TOD05 Pair 1	10550
Alt Y	CAY	TOD05 Pair 2	10558
Alt Z	CAZ	TOD16 Pair 1	10562

X = Parallel To Flow

Y = Vertical

Z = Perpendicular To Flow

Figure 3: QC1 ERV Accelerometer Location/Orientation – Tri-Axial Accelerometer Blocks

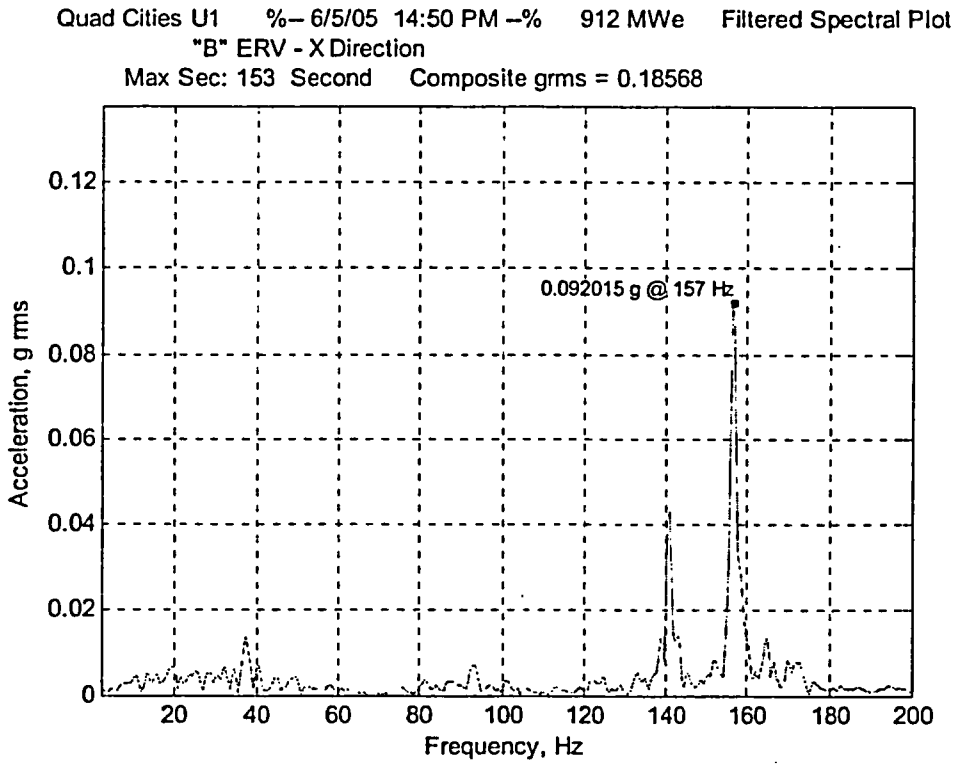

Figure 4: QC1 ERV-3B Accelerations – X-Axis (June 2005)

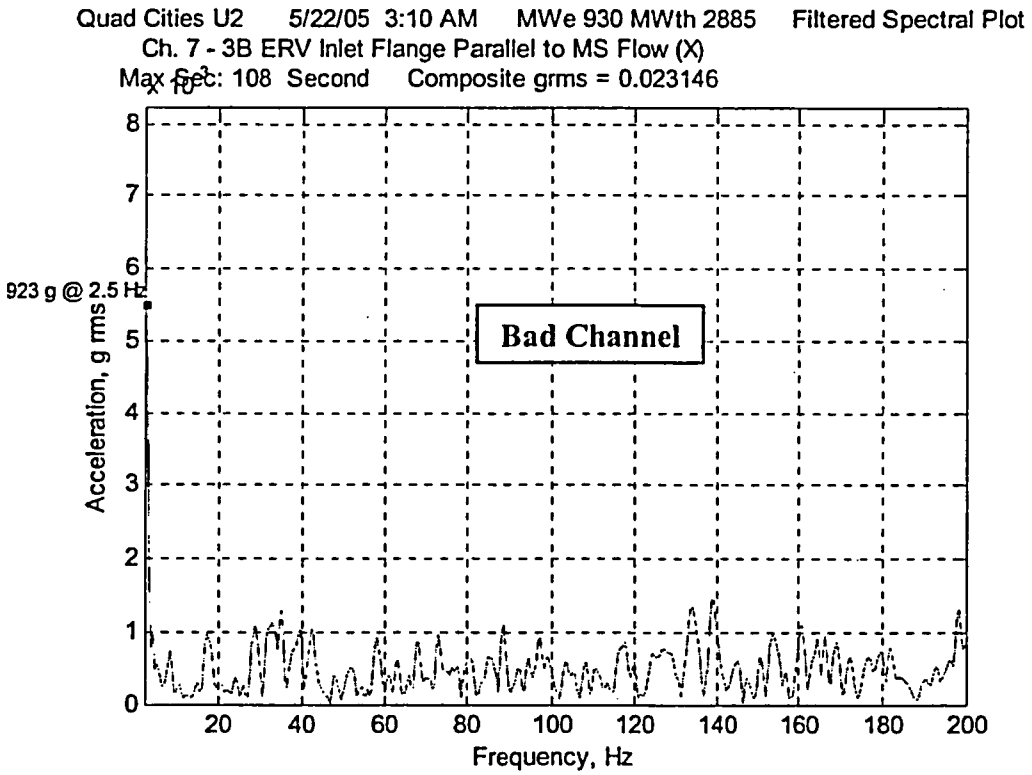

Figure 5: QC2 ERV-3B Accelerations – X-Axis (May 2005)

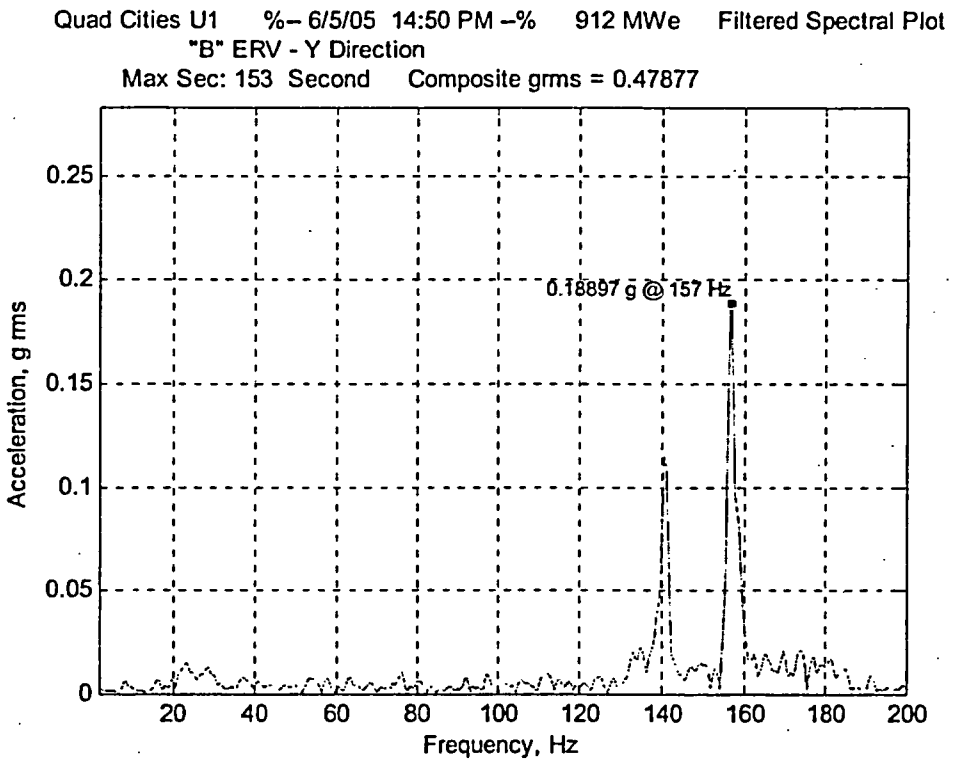

Figure 6: QC1 ERV-3B Accelerations – Y-Axis (June 2005)

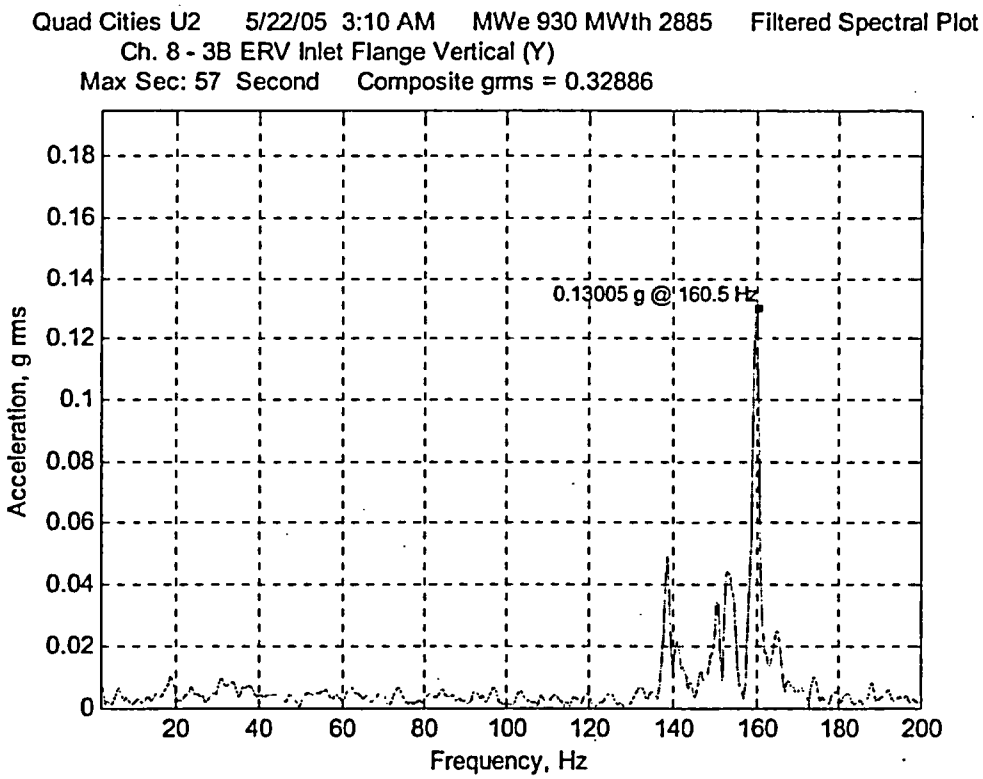

Figure 7: QC2 ERV-3B Accelerations – Y-Axis (May 2005)

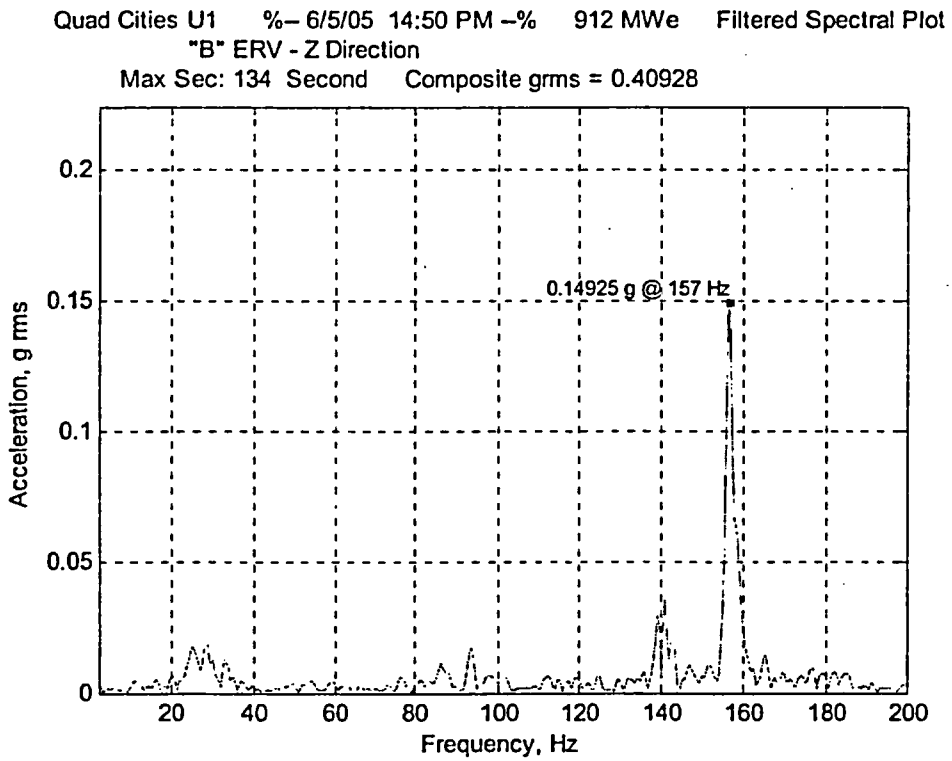

Figure 8: QC1 ERV-3B Accelerations – Z-Axis (June 2005)

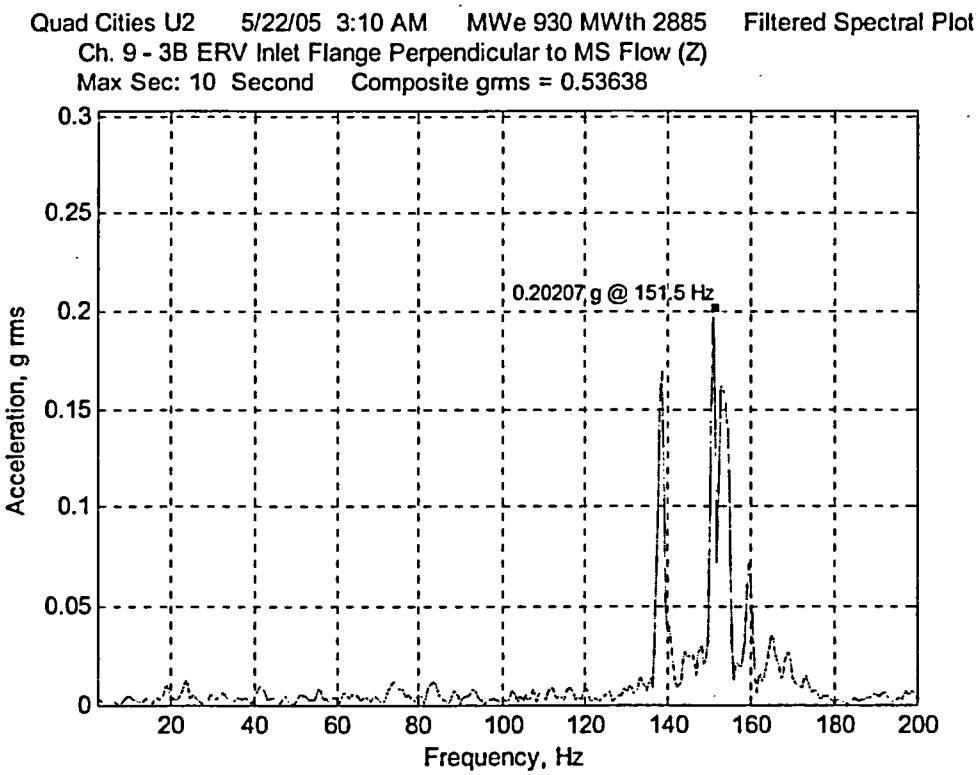

Figure 9: QC2 ERV-3B Accelerations – Z-Axis (May 2005)

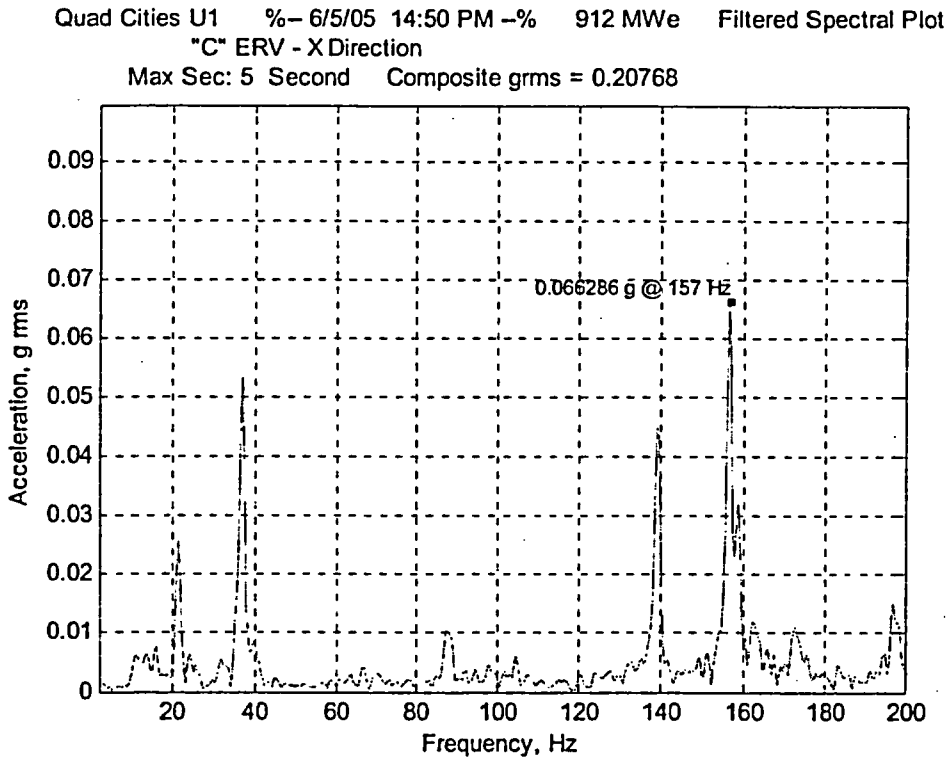

Figure 10: QC1 ERV-3C Accelerations – X-Axis (June 2005)

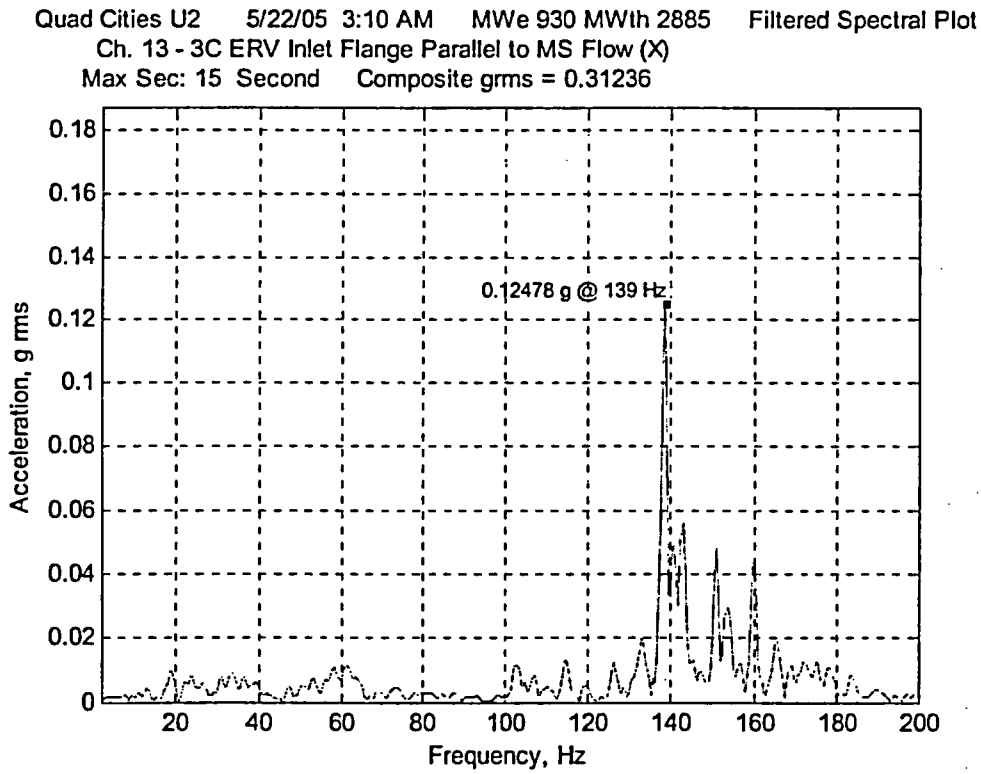

Figure 11: QC2 ERV-3C Accelerations – X-Axis (May 2005)

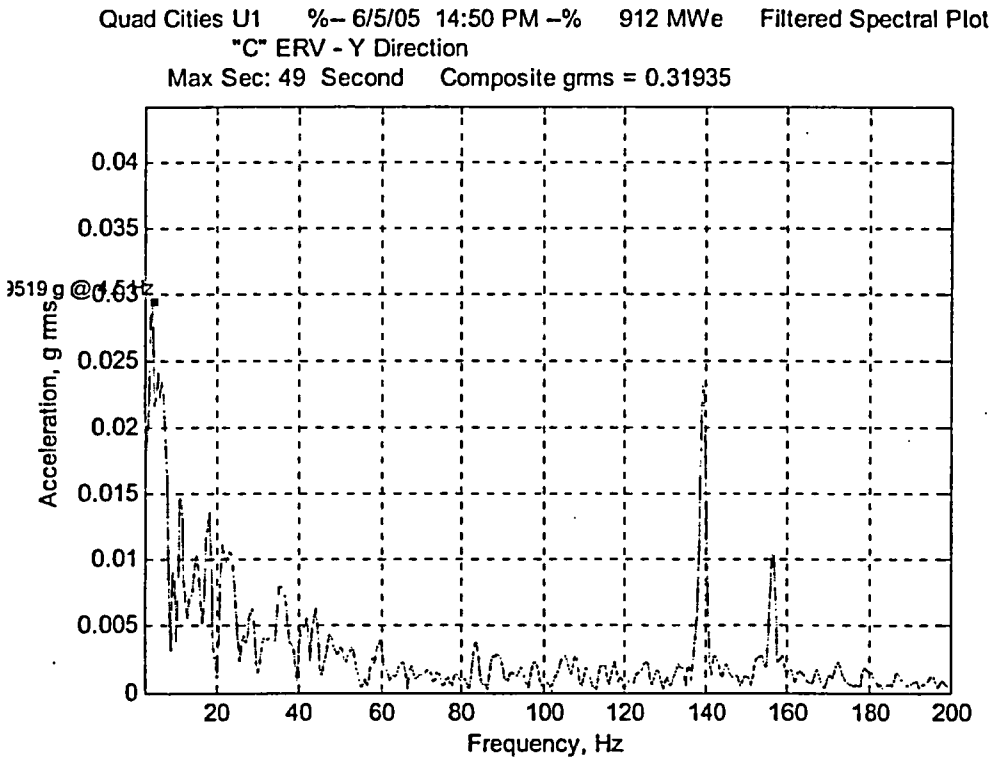

Figure 12: QC1 ERV-3C Accelerations – Y-Axis (June 2005)

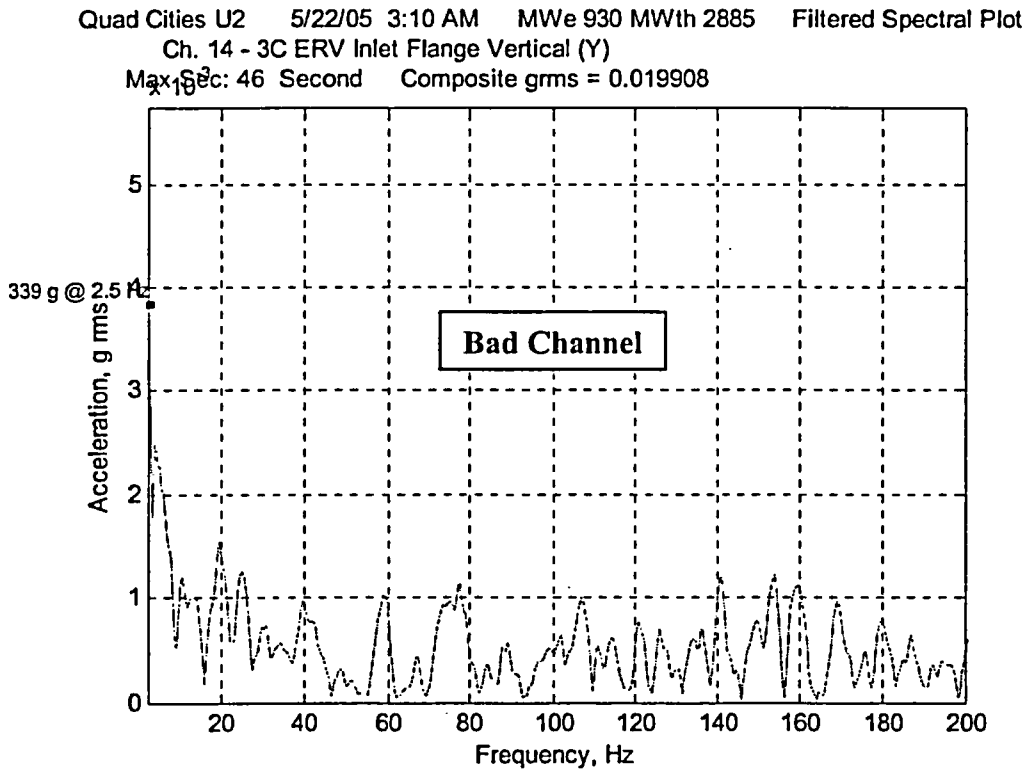

Figure 13: QC2 ERV-3C Accelerations – Y-Axis (May 2005)

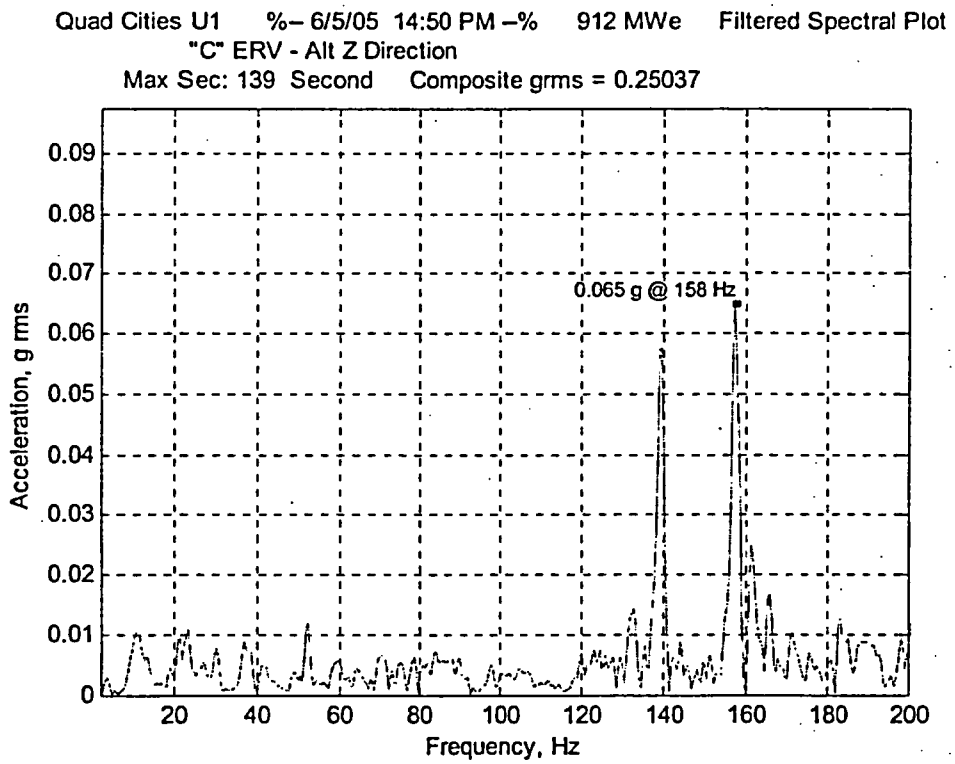

Figure 14: QC1 ERV-3C Accelerations – Z-Axis (June 2005)

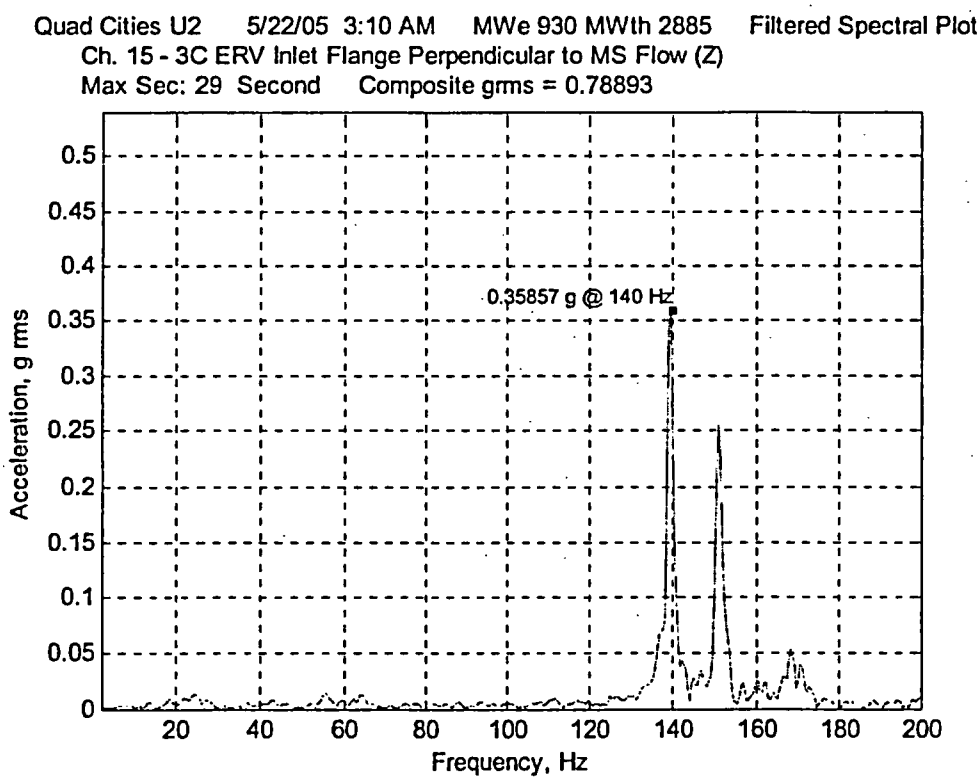

Figure 15: QC2 ERV-3C Accelerations – Z-Axis (May 2005)

ENCLOSURE 2

Attachment 8

C.D.I. Technical Note No. 05-34,"Test Condition TC15a Load Comparison for Quad Cities Unit 1," Revision 0, dated August 2005

C.D.I. Technical Note No. 05-34

Test Condition TC15a Load Comparison for Quad Cities Unit 1

Revision 0

Prepared by

Continuum Dynamics, Inc.
34 Lexington Avenue
Ewing, NJ 08618

Prepared under Purchase Order No. 85758 for

Exelon Generation LLC
4300 Winfield Road
Warrenville, IL 60555

Approved by

Alan J. Bilanin

August 2005

SUMMARY

To date, two high resolution loads have been developed for Quad Cities Unit 1 (QC1) at Test Condition TC15a, as shown below.

Test Condition Identifier	Strain Gage (SG) Correction Technique	Acoustic Circuit Model Used
TC15a	Reduced 80 Hz on C main steam line, averaged single SG S32/S34 with SG pair S31/S33 on C main steam line only	Minimum Error Model
TC15a_2	Reduced 80 Hz on A and C main steam lines, averaged single SG with SG pairs for all failed strain gage locations	Modified Benchmark Model

Justification for reducing the 80 Hz frequency peak (± 4 Hz on either side) may be found in [1], while justification for averaging a single strain gage with a corresponding strain gage pair may be found in [2]. A description of the Modified Benchmark and the Minimum Error models may be found in [3].

C.D.I. has been asked by Exelon to develop the QC1 high resolution load

Test Condition Identifier	Strain Gage (SG) Correction Technique	Acoustic Circuit Model Used
TC15a_3	Reduced 80 Hz on A and C main steam lines, averaged single SG with SG pairs for all failed strain gage locations	Minimum Error Model

and compare its predictions against TC15a, the other Minimum Error model. This report summarizes the low resolution results for TC15a_3 compared against TC15a, in preparation for delivery of a high resolution load for structural analysis.

MODELING RESULTS

Table 1 compares the minimum, maximum, and RMS pressure levels for TC15a_3 and TC15a at 27 locations on the QC1 dryer. Also included in this table is the comparison for two sensor differences from the outside to the inside of the outer bank hoods at the same location: P3 - P13 (the A-B side of the dryer) and P20 - P14 (the C-D side of the dryer). Figure 1 plots the values presented in Table 1.

A comparison of these values at the 27 locations shows that the differences between the two load cases translate into an average reduction of the minimum pressure by 0.066 psid (the average minimum pressure in TC15a_3 is less minimum than the average minimum pressure in TC15a),

an average reduction of the maximum pressure by 0.027 psid (the average maximum pressure in TC15a_3 is less maximum than the average maximum pressure in TC15a), and an average increase of the RMS pressure of 0.002 psid (the RMS pressure in TC15a_3 is slightly larger than the RMS pressure in TC15a).

Correspondingly, for the pressure difference P3 - P13, the minimum pressure in TC15a_3 is less minimum than the minimum pressure in TC15a (by 0.056 psid), the maximum pressure in TC15a_3 is larger than the maximum pressure in TC15a (by 0.021 psid), and the RMS pressure in TC15a_3 is smaller than the RMS pressure in TC15a (by 0.042 psid). For the pressure difference P20 - P14, the minimum pressure in TC15a_3 is more minimum than the minimum pressure in TC15a (by 0.161 psid), the maximum pressure in TC15a_3 is larger than the maximum pressure in TC15a (by 0.219 psid), and the RMS pressure in TC15a_3 is larger than the RMS pressure in TC15a (by 0.056 psid).

Figures 2 to 28 show the PSD comparisons for locations P1 to P27. Figures 29 and 30 show the PSD comparisons for P3 - P13 and P20 - P14, respectively. It is seen that the two load cases are very similar, with a noticeable, yet slight, 80 Hz signal in TC15a (possibly resulting from the fact that no adjustment was made to the A main steam line strain gage data).

REFERENCES

1. Exelon Generation Company. 2005. QC1 Evaluation to Remove 80 Hz from Strain Gage Data. White Paper.

2. Structural Integrity Associates, Inc. 2005. Quad Cities Unit 1 Main Steam Line Strain Gage Reductions. Letter Report No. SIR-05-208 Revision 2 (draft), KKF-05-034.

3. Continuum Dynamics, Inc. 2005. Evaluation of Continuum Dynamics, Inc. Steam Dryer Load Methodology Against Quad Cities Unit 2 In-Plant Data. C.D.I. Report No. 05-10.

Table 1. Summary of pressure predictions at 27 sensors on the QC1 dryer, based on the first 65 seconds of data collected.

Pressure Sensor Number	TC15a Minimum (psid)	TC15a Maximum (psid)	TC15a RMS (psid)	TC15a_3 Minimum (psid)	TC15a_3 Maximum (psid)	TC15a_3 RMS (psid)
P1	-1.342	1.341	0.438	-1.355	1.440	0.464
P2	-1.028	1.010	0.224	-1.121	1.140	0.270
P3	-1.938	1.830	0.504	-1.776	1.688	0.467
P4	-0.723	0.755	0.177	-0.777	0.728	0.182
P5	-1.038	0.813	0.199	-0.766	0.799	0.194
P6	-1.301	1.267	0.347	-1.164	1.171	0.312
P7	-1.054	1.038	0.338	-1.125	1.179	0.386
P8	-0.837	0.809	0.182	-0.678	0.713	0.161
P9	-1.674	1.695	0.510	-1.550	1.562	0.518
P10	-1.322	1.364	0.436	-1.361	1.393	0.458
P11	-0.946	0.866	0.209	-0.789	0.848	0.193
P12	-2.335	2.231	0.678	-2.069	2.116	0.741
P13	-0.549	0.403	0.106	-0.355	0.343	0.087
P14	-0.461	0.512	0.114	-0.452	0.489	0.106
P15	-2.027	1.896	0.569	-2.012	1.882	0.572
P16	-0.366	0.289	0.078	-0.304	0.262	0.063
P17	-1.160	1.135	0.275	-1.112	1.014	0.287
P18	-1.691	1.696	0.501	-1.617	1.701	0.517
P19	-1.986	1.894	0.589	-2.031	1.941	0.613
P20	-3.342	3.621	1.075	-3.503	3.781	1.124
P21	-1.641	1.461	0.407	-1.503	1.462	0.395
P22	-1.439	1.527	0.435	-1.407	1.351	0.445
P23	-0.332	0.257	0.073	-0.251	0.204	0.056
P24	-1.138	1.193	0.280	-1.029	1.125	0.257
P25	-1.342	1.348	0.328	-1.260	1.258	0.295
P26	-0.294	0.280	0.077	-0.238	0.245	0.064
P27	-0.335	0.285	0.074	-0.242	0.231	0.059
Average	-1.246	1.215	0.342	-1.180	1.188	0.344
P3 - P13	-1.984	1.952	0.553	-1.928	1.973	0.511
P20 - P14	-3.660	3.877	1.148	-3.821	4.096	1.204

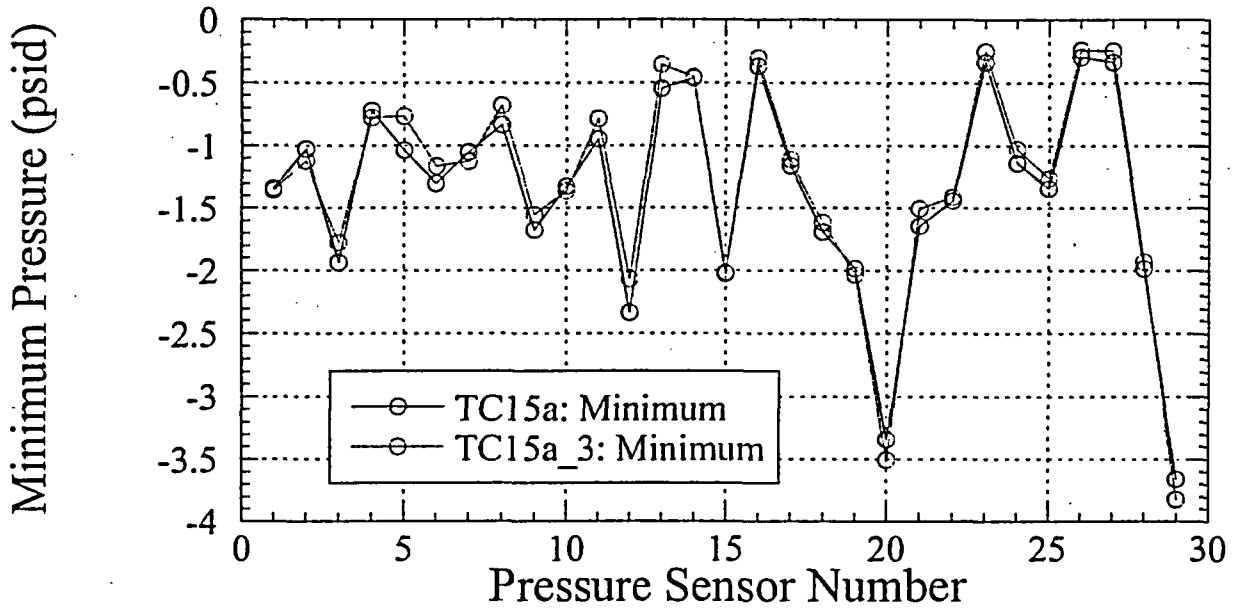

Figure 1a. Comparison between TC15a and TC15a_3 (minimum pressure). Pressure sensor number P28 = P3 - P13, while pressure sensor number P29 = P20 - P14.

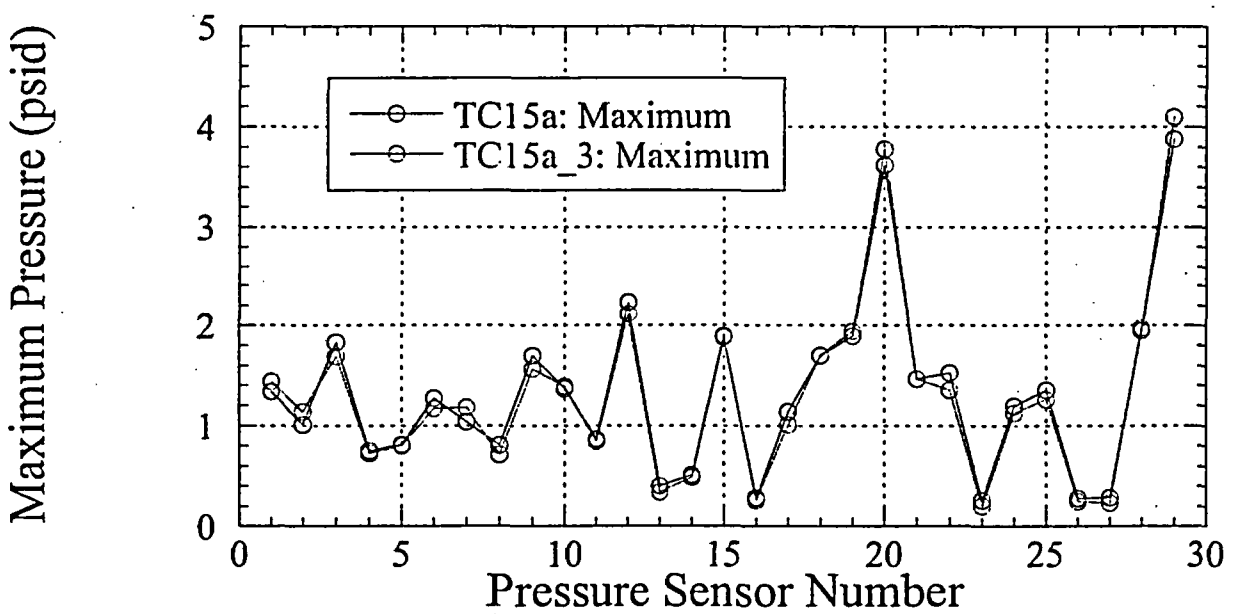

Figure 1b. Comparison between TC15a and TC15a_3 (maximum pressure). Pressure sensor number P28 = P3 - P13, while pressure sensor number P29 = P20 - P14.

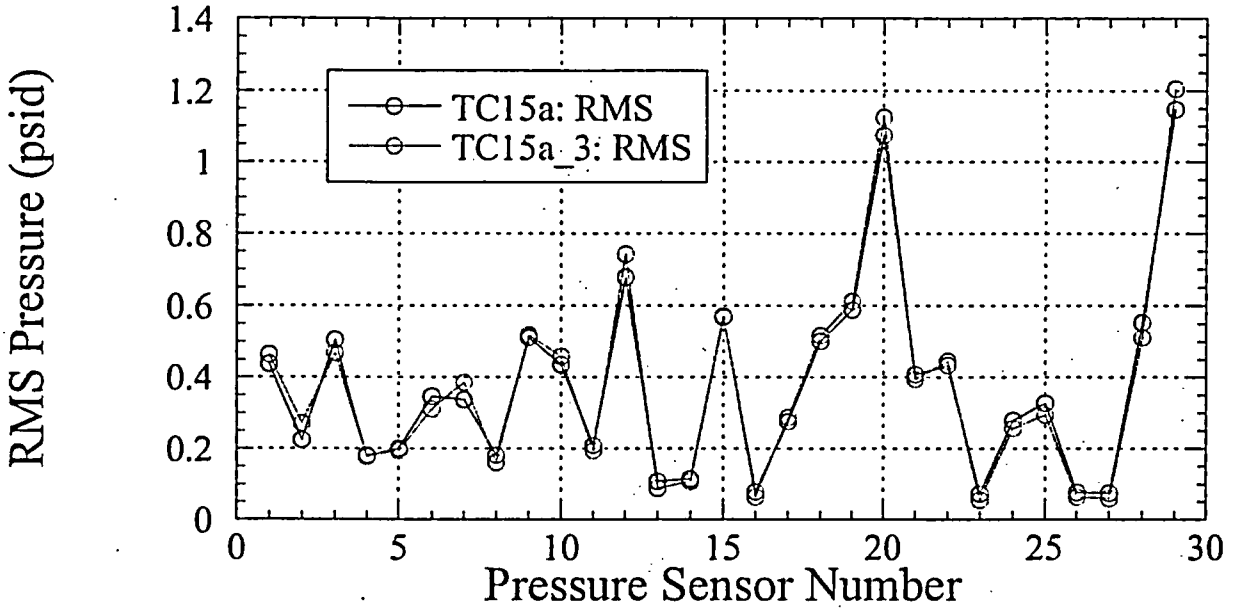

Figure 1c. Comparison between TC15a and TC15a_3 (RMS pressure). Pressure sensor number P28 = P3 - P13, while pressure sensor number P29 = P20 - P14.

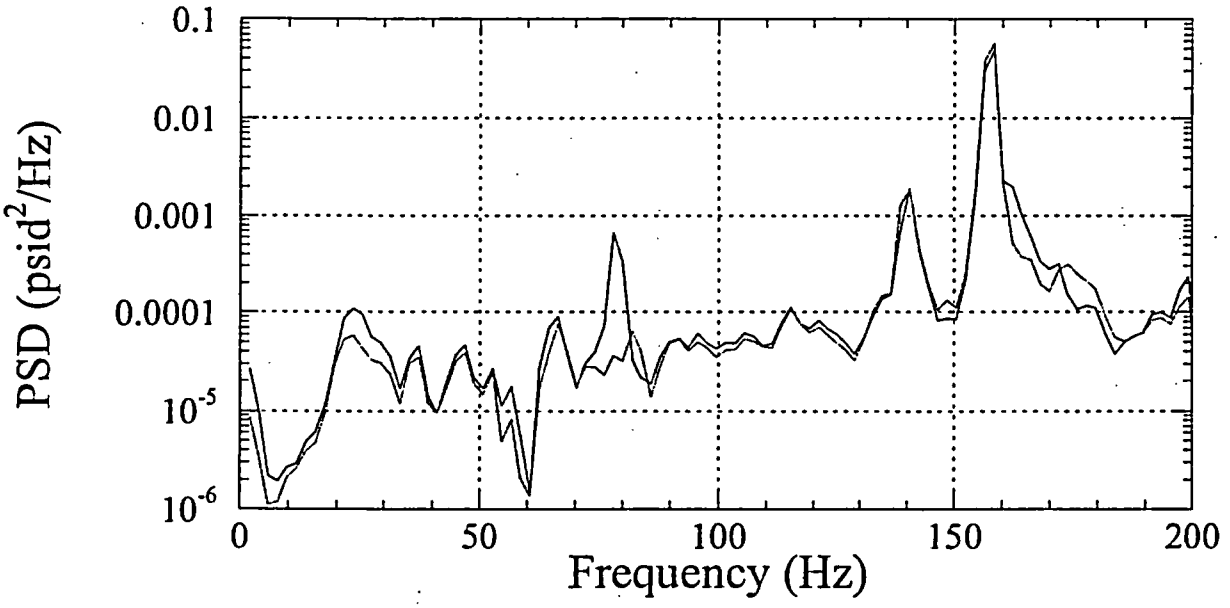

Figure 2. PSD comparison between TC15a (black curve) and TC15a_3 (blue curve) for pressure sensor number P1.

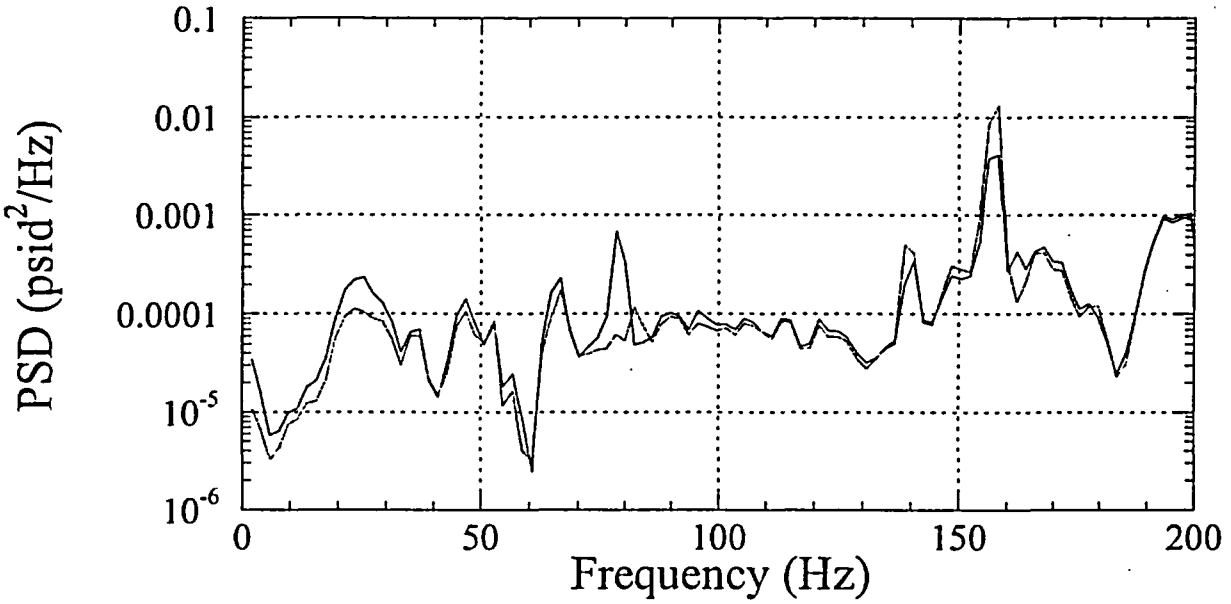

Figure 3. PSD comparison between TC15a (black curve) and TC15a_3 (blue curve) for pressure sensor number P2.

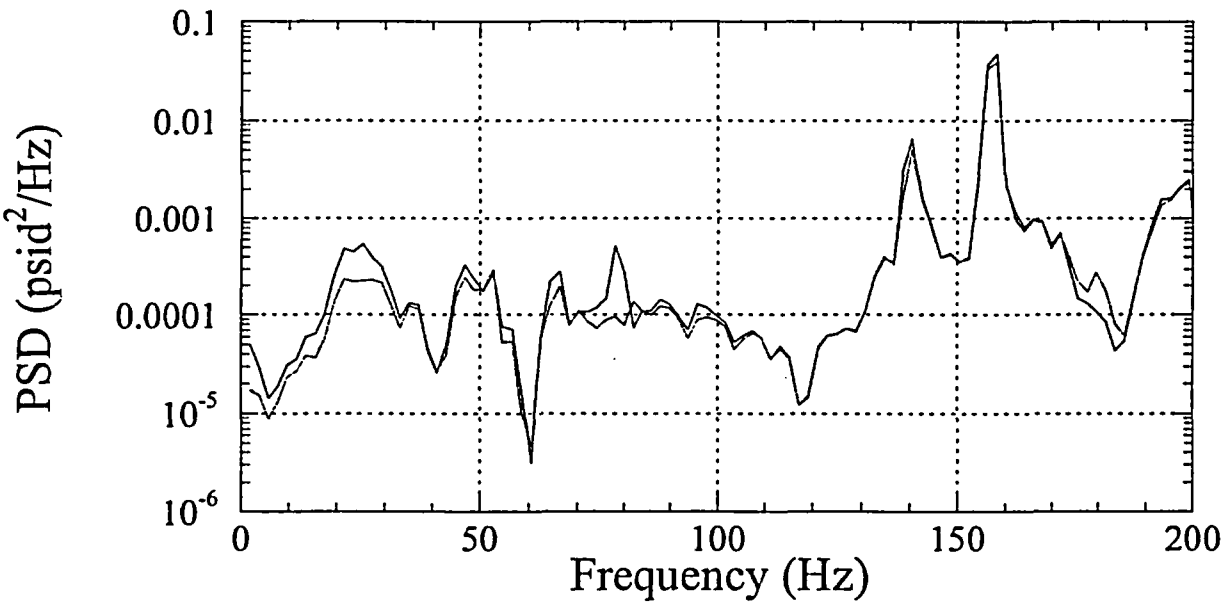

Figure 4. PSD comparison between TC15a (black curve) and TC15a_3 (blue curve) for pressure sensor number P3.

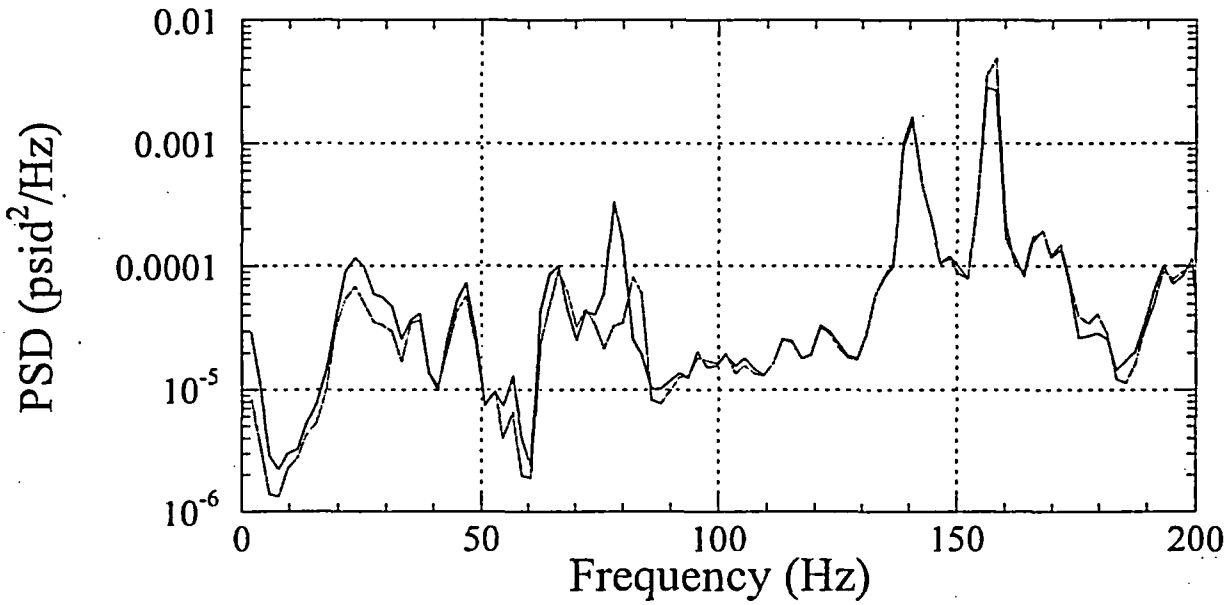

Figure 5. PSD comparison between TC15a (black curve) and TC15a_3 (blue curve) for pressure sensor number P4.

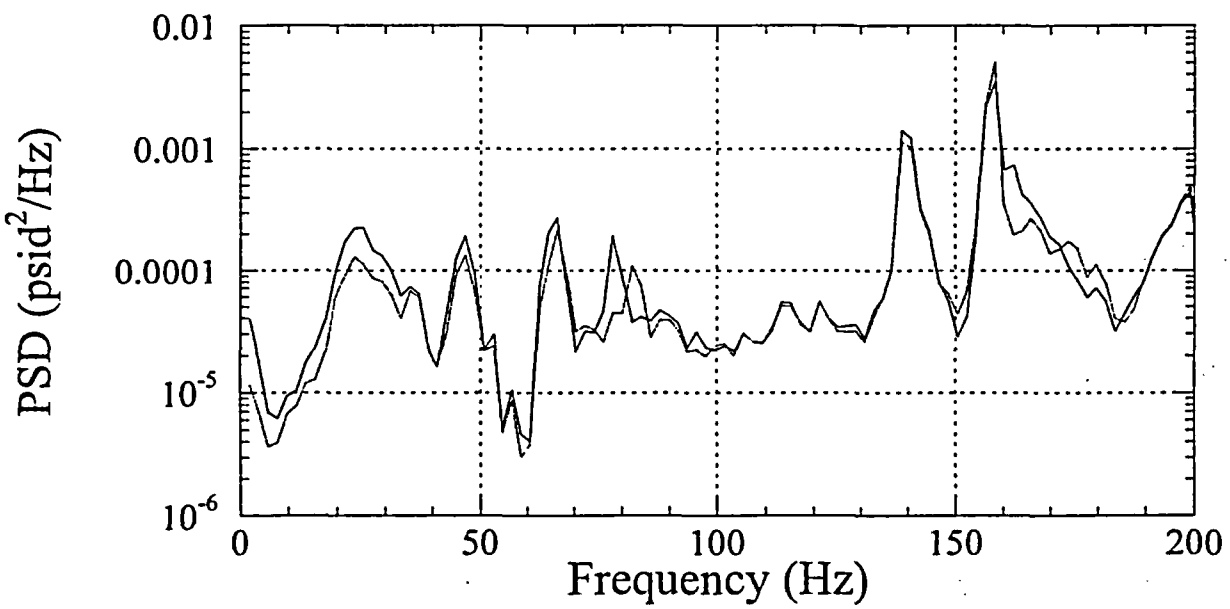

Figure 6. PSD comparison between TC15a (black curve) and TC15a_3 (blue curve) for pressure sensor number P5.

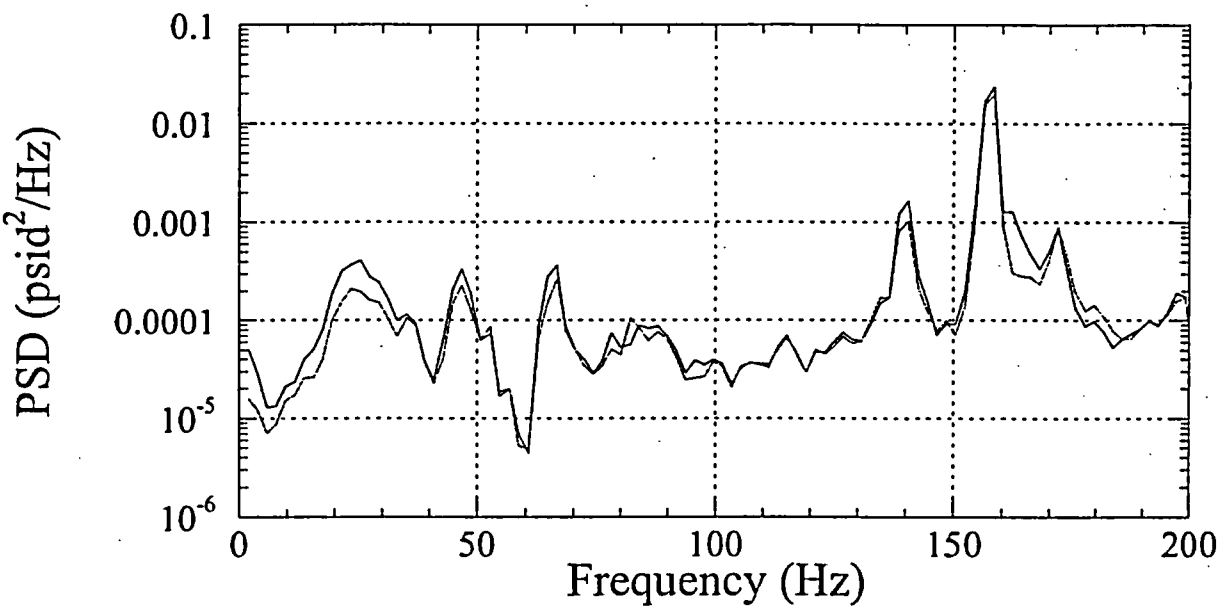

Figure 7. PSD comparison between TC15a (black curve) and TC15a_3 (blue curve) for pressure sensor number P6.

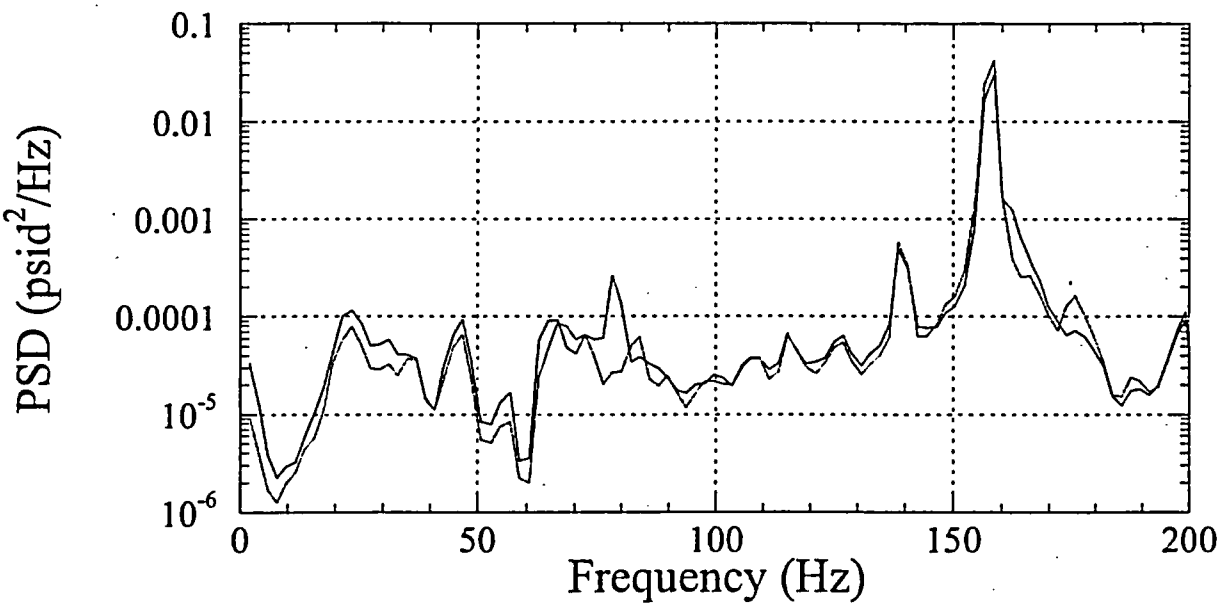

Figure 8. PSD comparison between TC15a (black curve) and TC15a_3 (blue curve) for pressure sensor number P7.

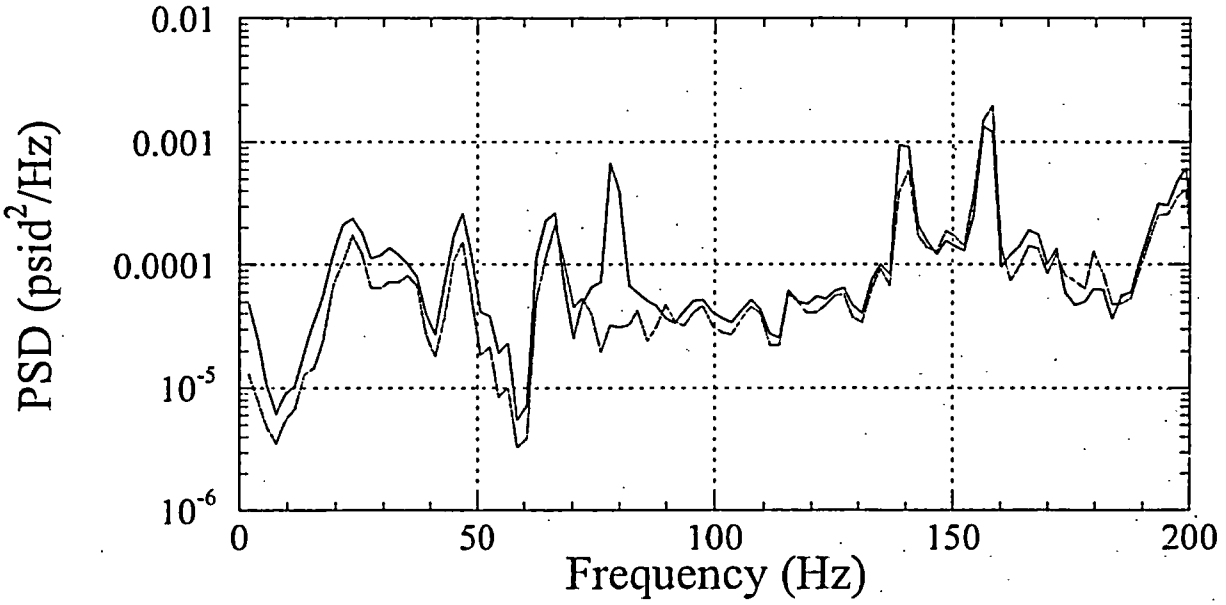

Figure 9. PSD comparison between TC15a (black curve) and TC15a_3 (blue curve) for pressure sensor number P8.

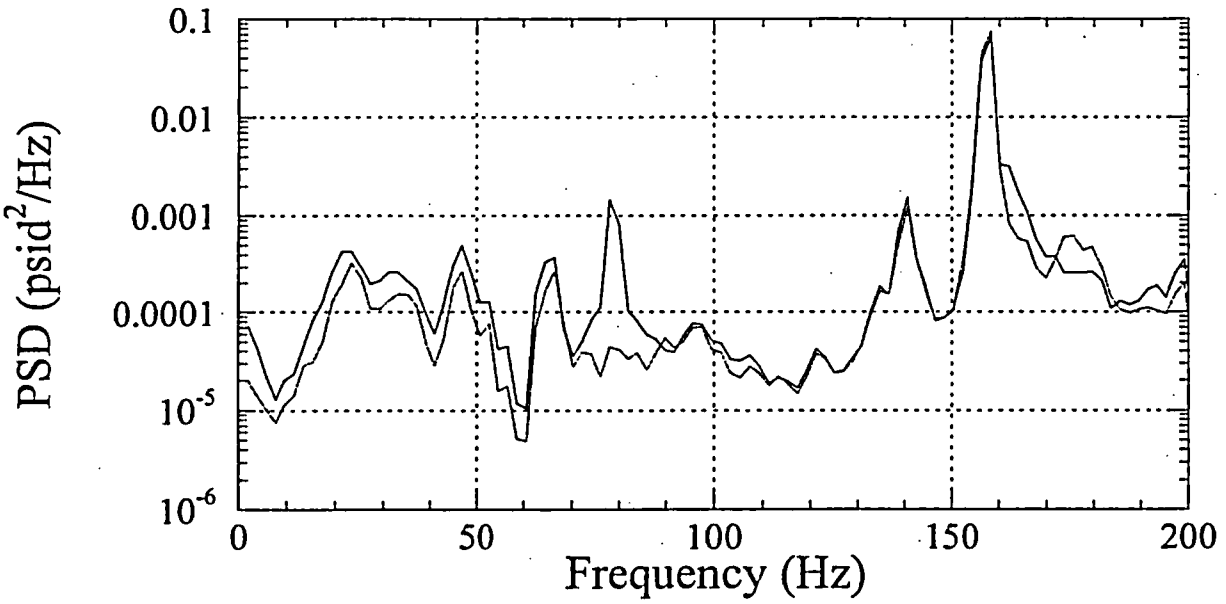

Figure 10. PSD comparison between TC15a (black curve) and TC15a_3 (blue curve) for pressure sensor number P9.

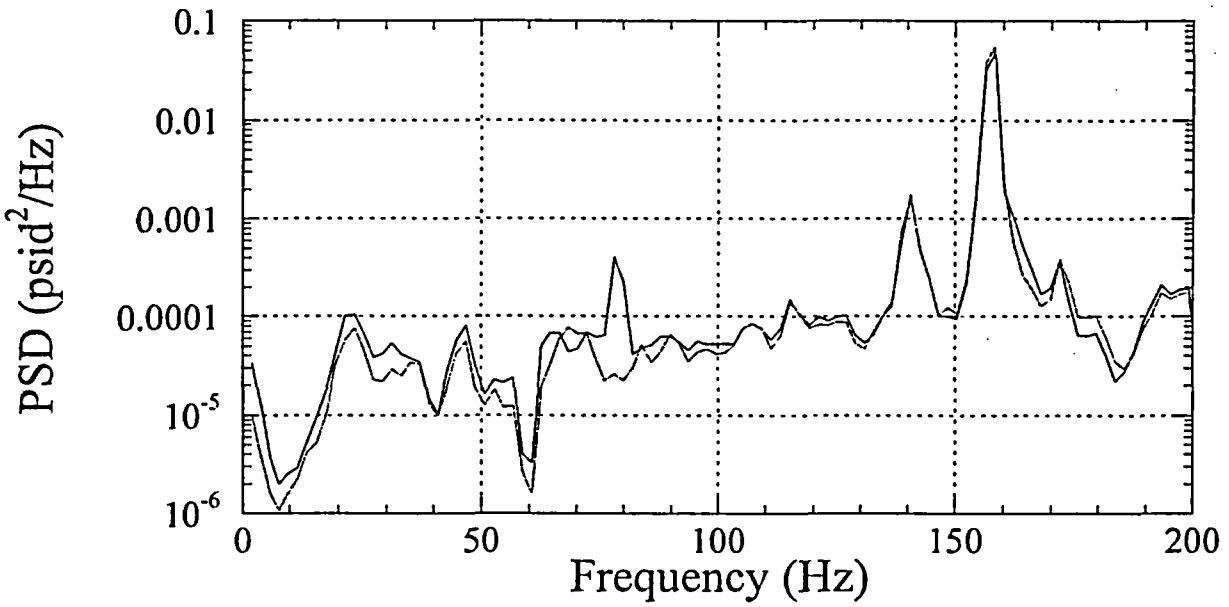

Figure 11. PSD comparison between TC15a (black curve) and TC15a_3 (blue curve) for pressure sensor number P10.

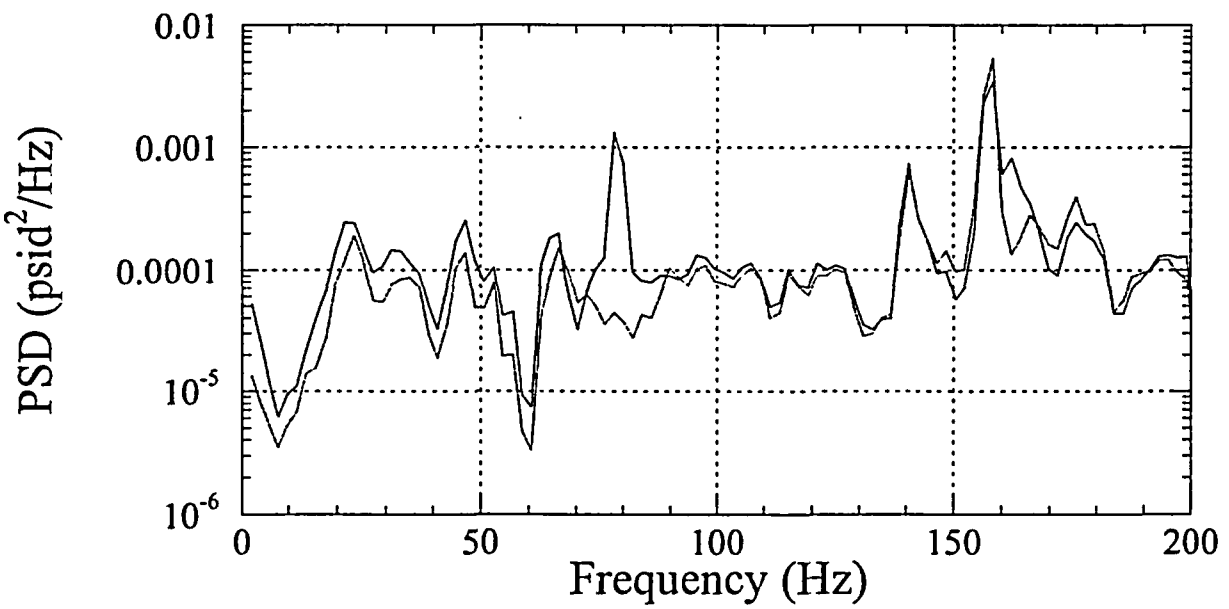

Figure 12. PSD comparison between TC15a (black curve) and TC15a_3 (blue curve) for pressure sensor number P11.

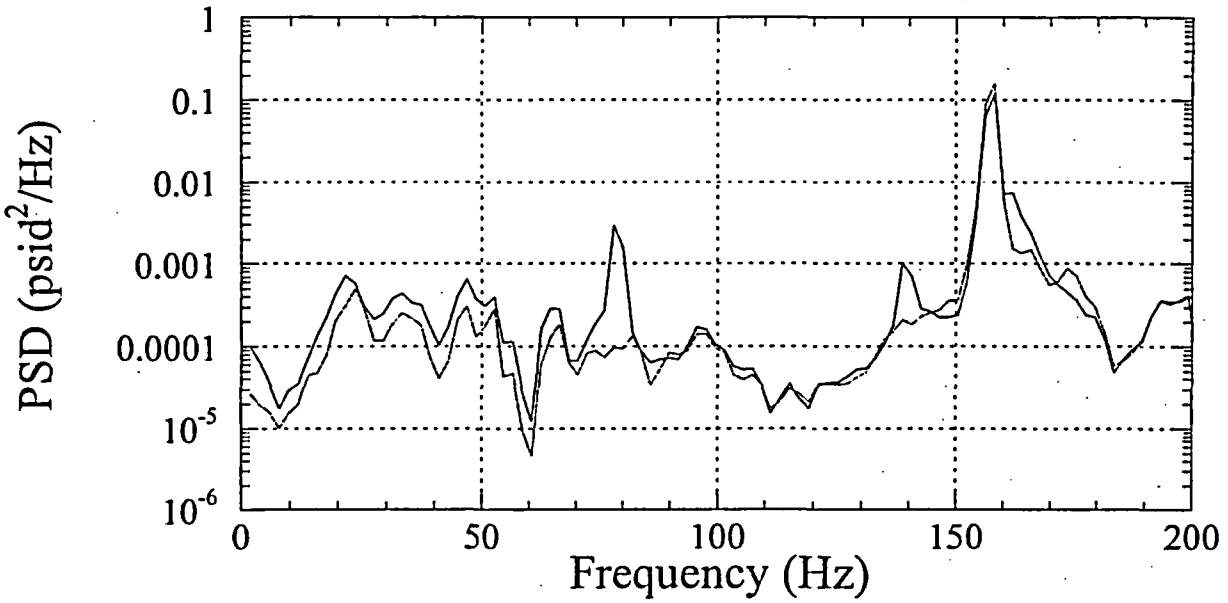

Figure 13. PSD comparison between TC15a (black curve) and TC15a_3 (blue curve) for pressure sensor number P12.

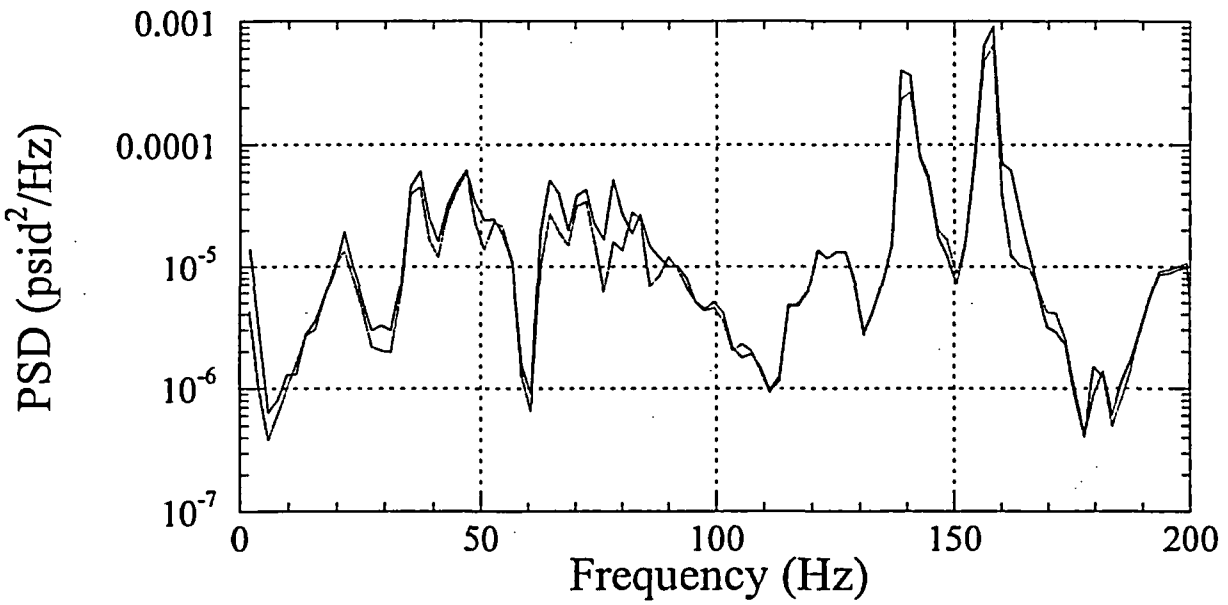

Figure 14. PSD comparison between TC15a (black curve) and TC15a_3 (blue curve) for pressure sensor number P13.

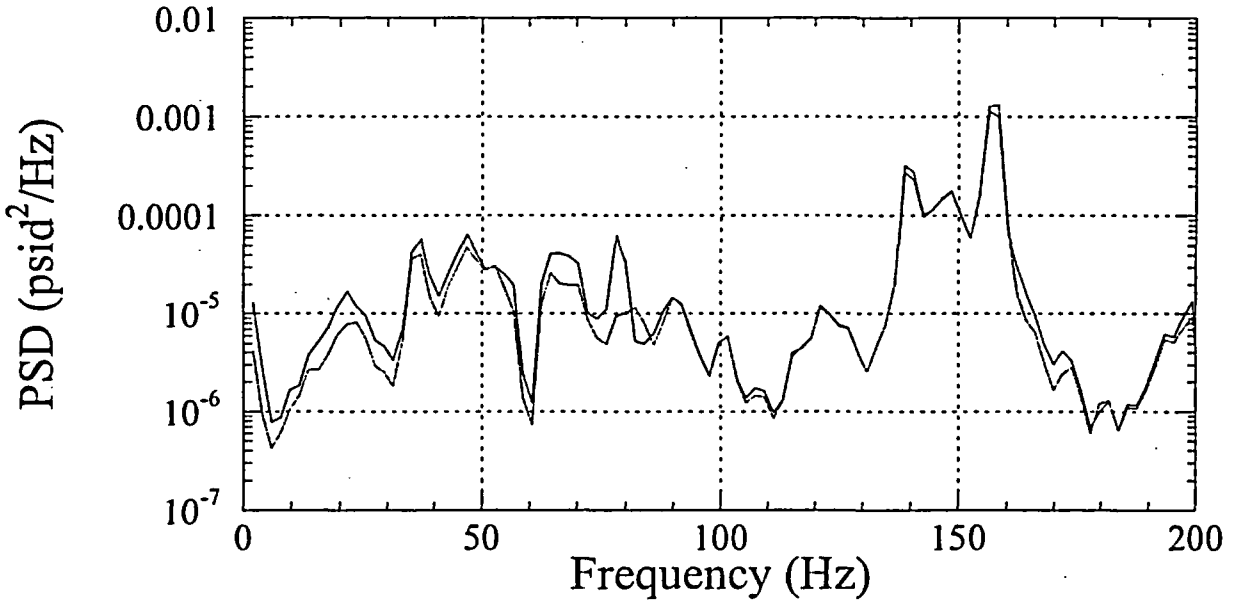

Figure 15. PSD comparison between TC15a (black curve) and TC15a_3 (blue curve) for pressure sensor number P14.

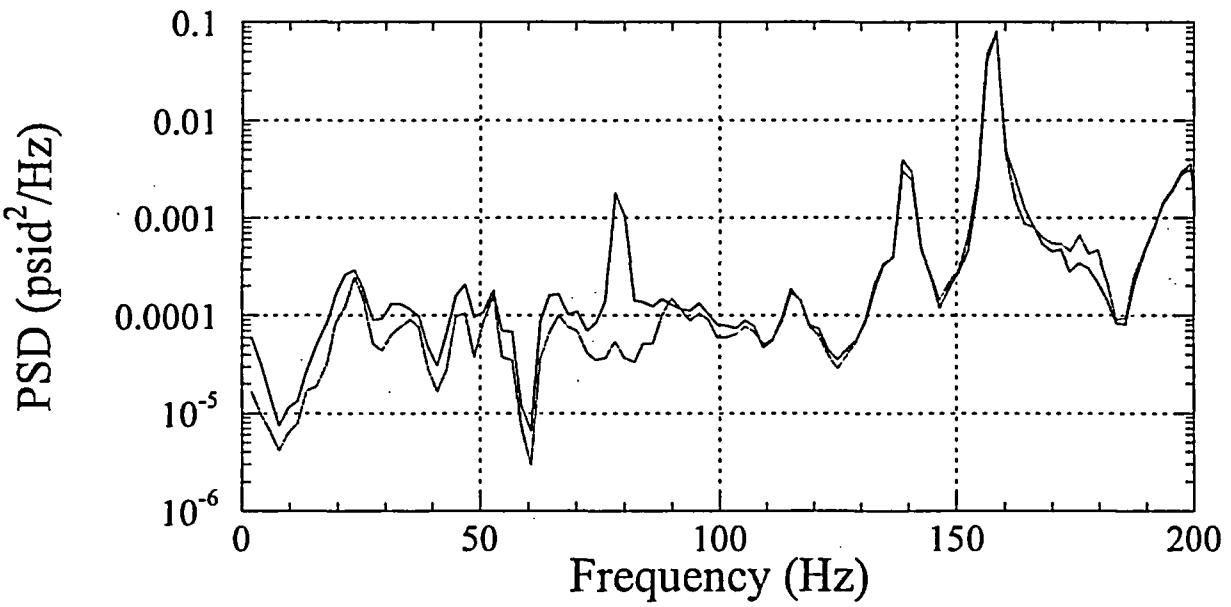

Figure 16. PSD comparison between TC15a (black curve) and TC15a_3 (blue curve) for pressure sensor number P15.

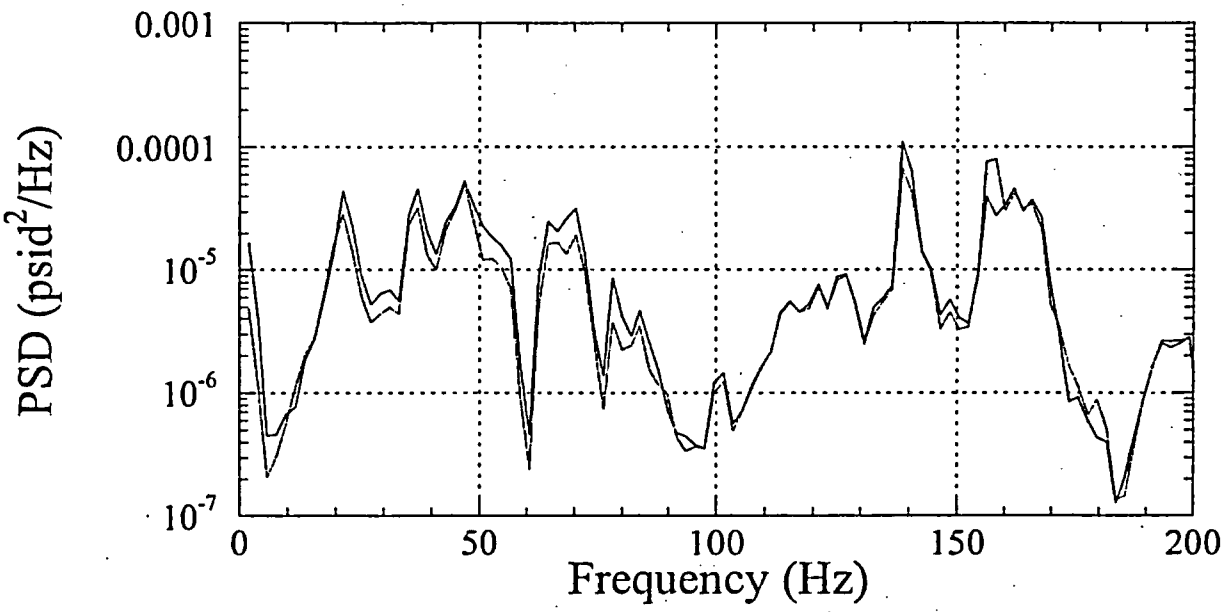

Figure 17. PSD comparison between TC15a (black curve) and TC15a_3 (blue curve) for pressure sensor number P16.

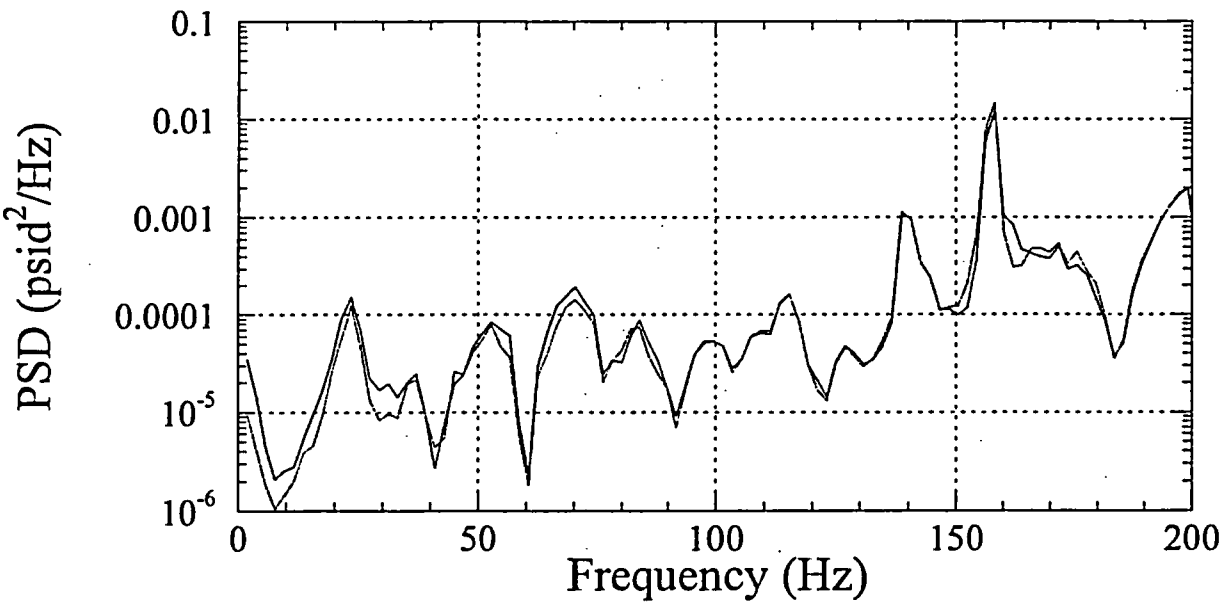

Figure 18. PSD comparison between TC15a (black curve) and TC15a_3 (blue curve) for pressure sensor number P17.

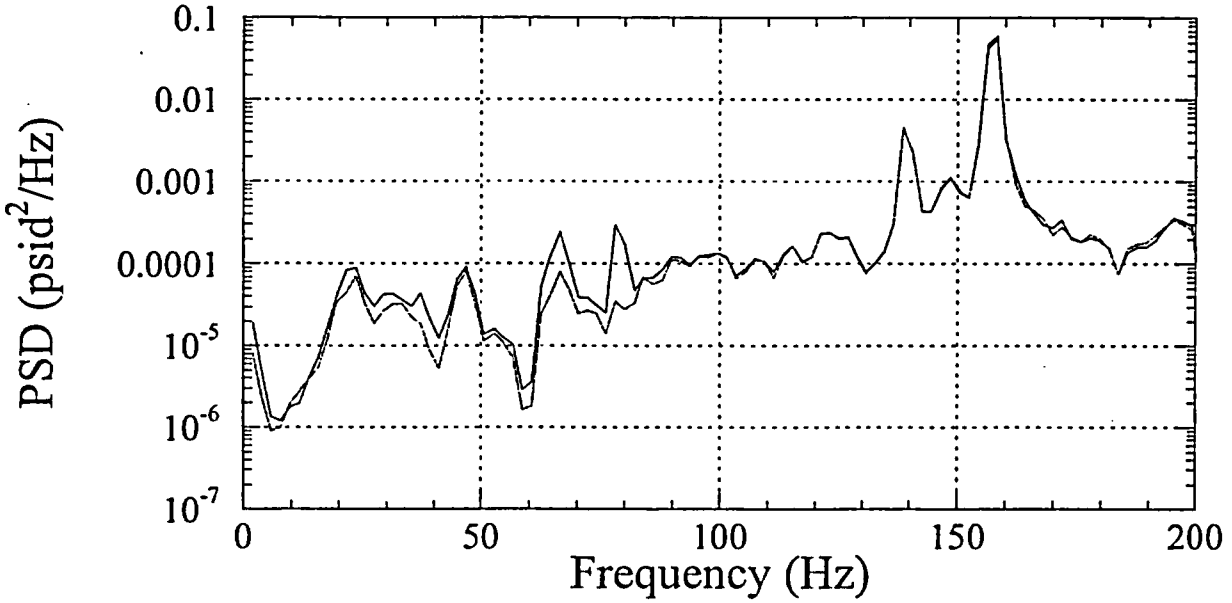

Figure 19. PSD comparison between TC15a (black curve) and TC15a_3 (blue curve) for pressure sensor number P18.

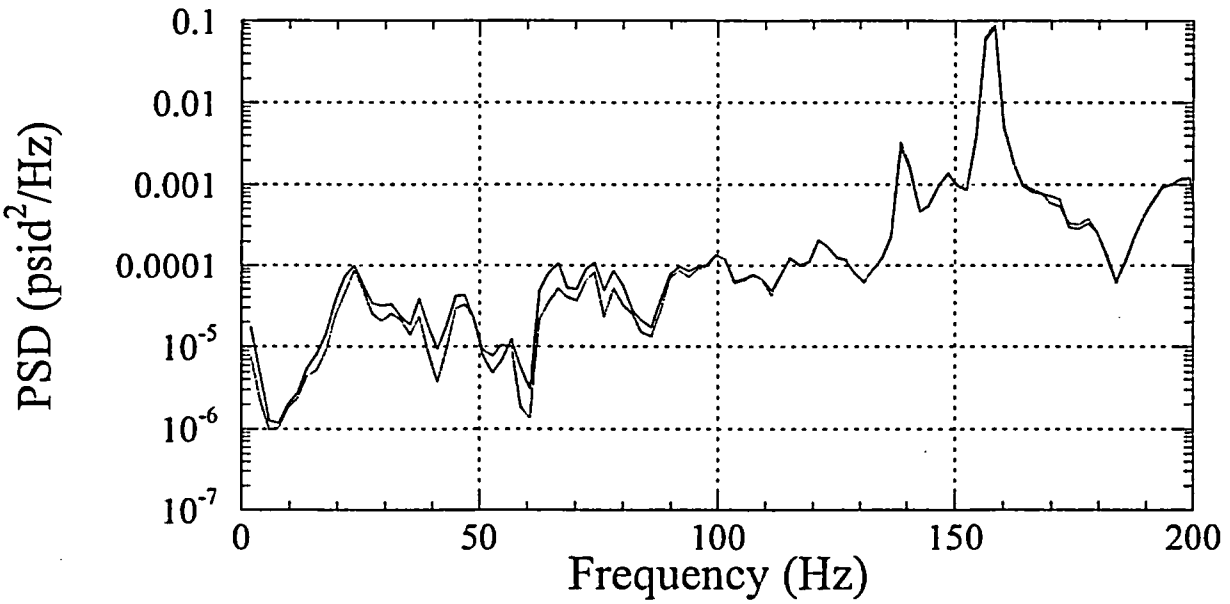

Figure 20. PSD comparison between TC15a (black curve) and TC15a_3 (blue curve) for pressure sensor number P19.

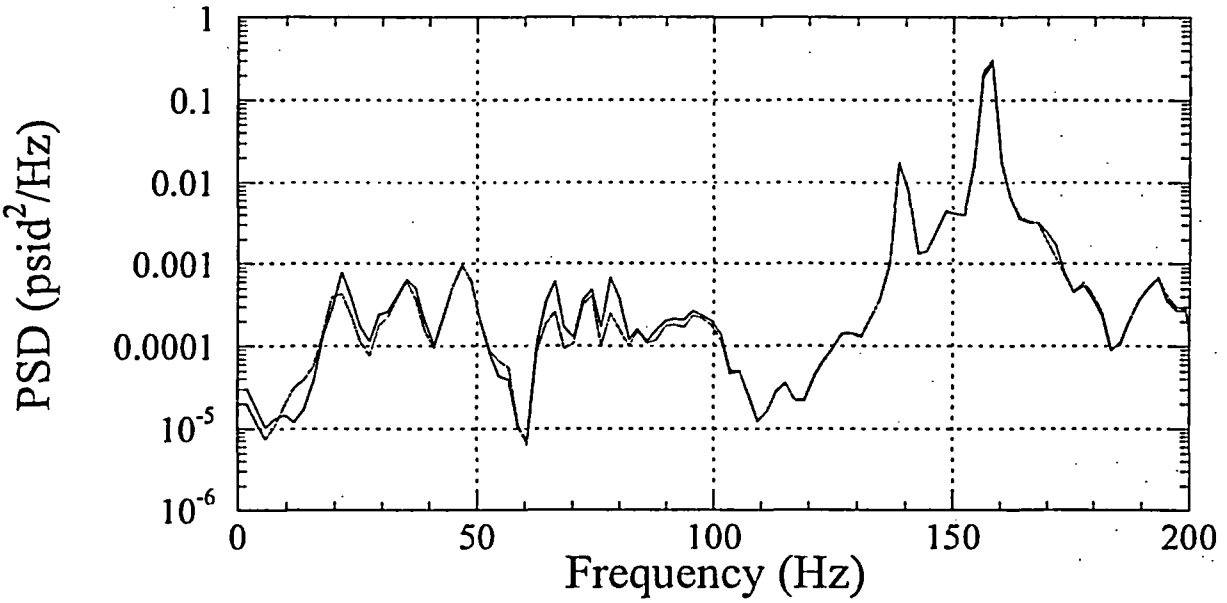

Figure 21. PSD comparison between TC15a (black curve) and TC15a_3 (blue curve) for pressure sensor number P20.

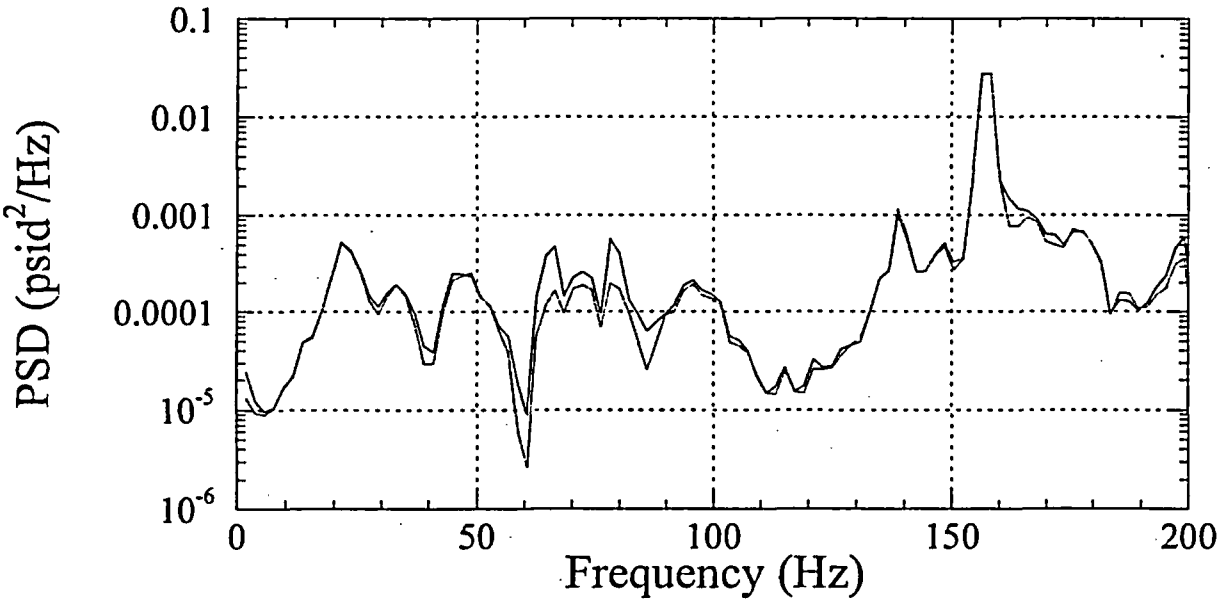

Figure 22. PSD comparison between TC15a (black curve) and TC15a_3 (blue curve) for pressure sensor number P21.

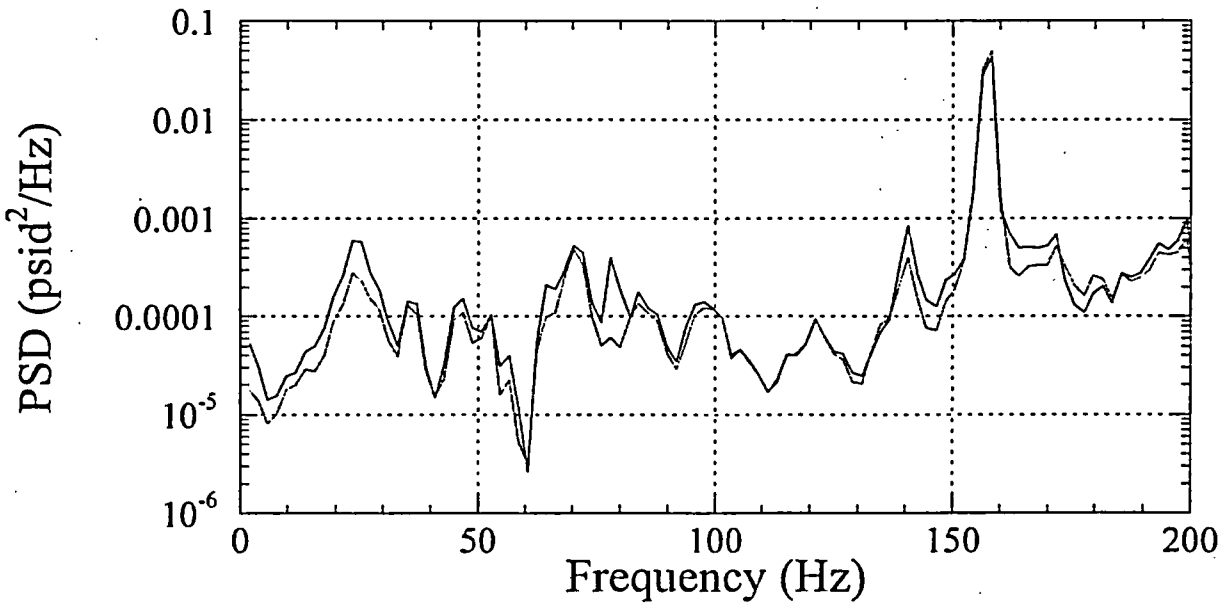

Figure 23. PSD comparison between TC15a (black curve) and TC15a_3 (blue curve) for pressure sensor number P22.

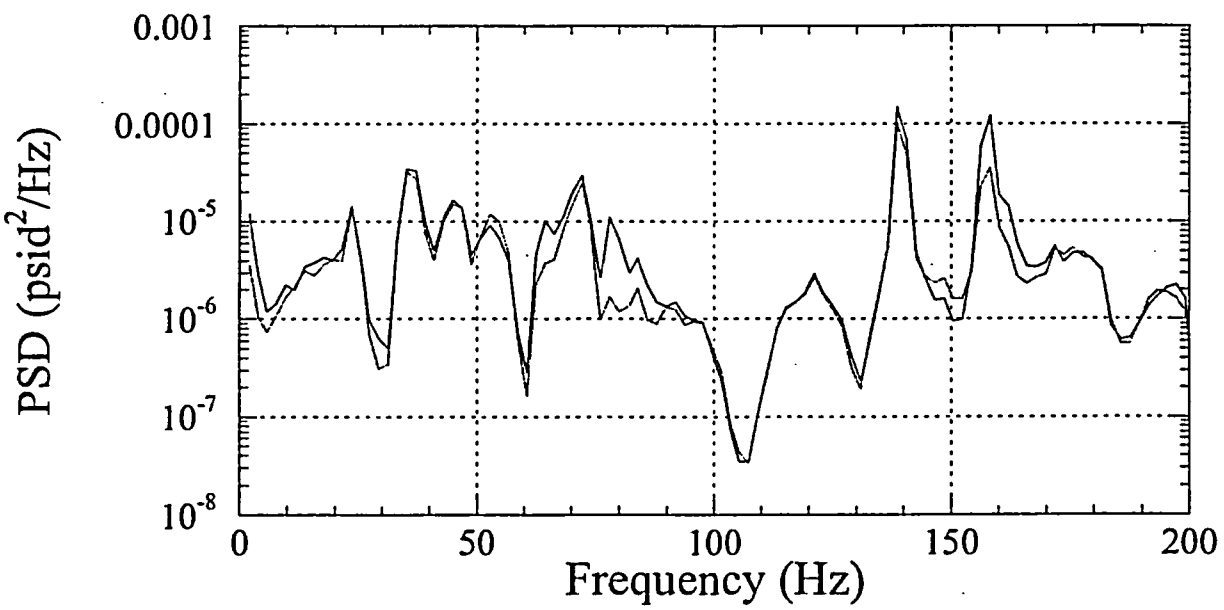

Figure 24. PSD comparison between TC15a (black curve) and TC15a_3 (blue curve) for pressure sensor number P23.

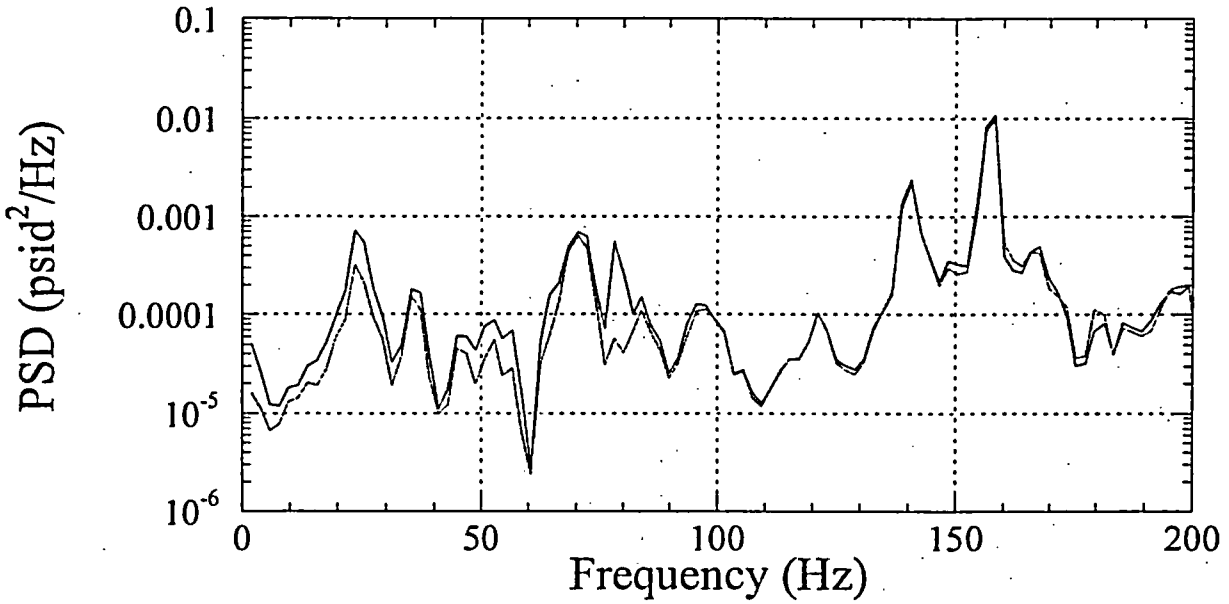

Figure 25. PSD comparison between TC15a (black curve) and TC15a_3 (blue curve) for pressure sensor number P24.

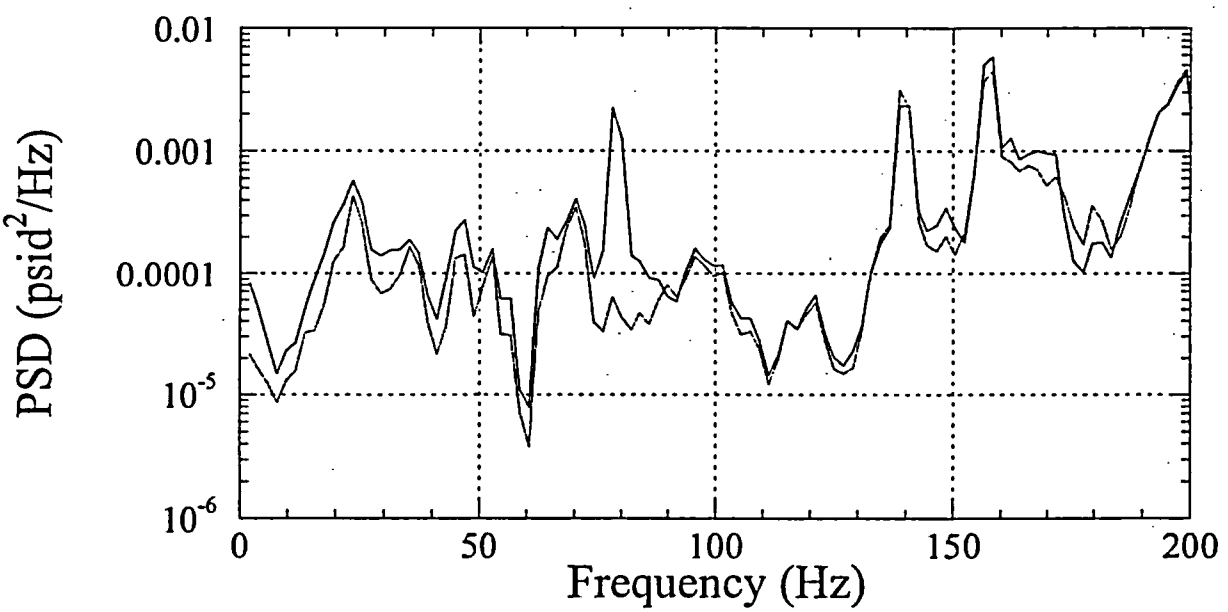

Figure 26. PSD comparison between TC15a (black curve) and TC15a_3 (blue curve) for pressure sensor number P25.

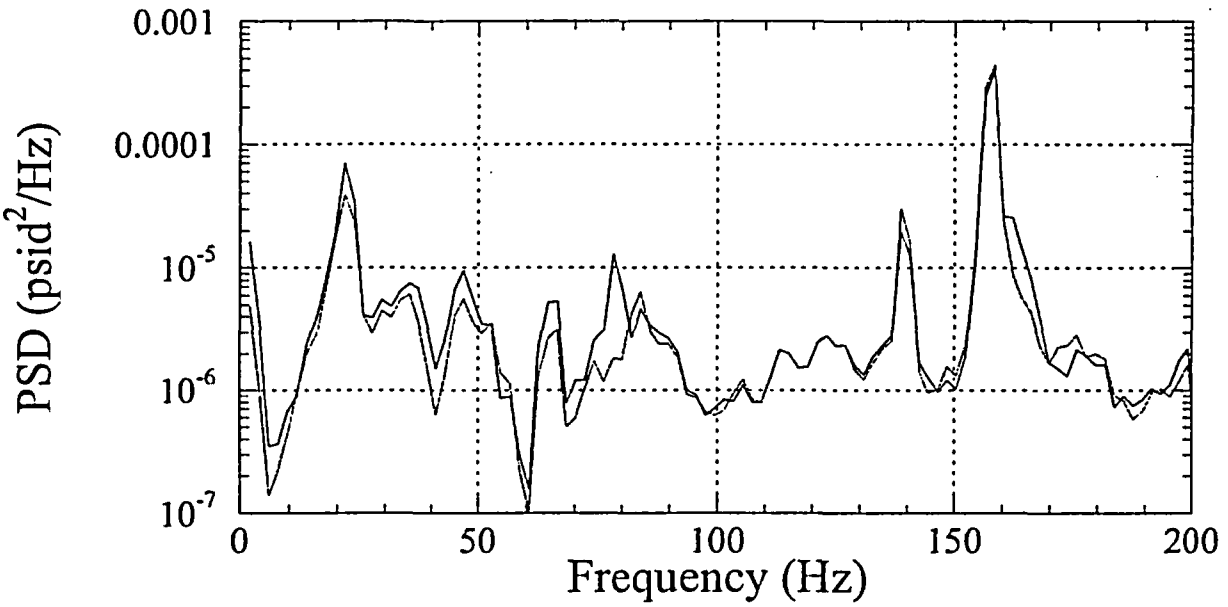

Figure 27. PSD comparison between TC15a (black curve) and TC15a_3 (blue curve) for pressure sensor number P26.

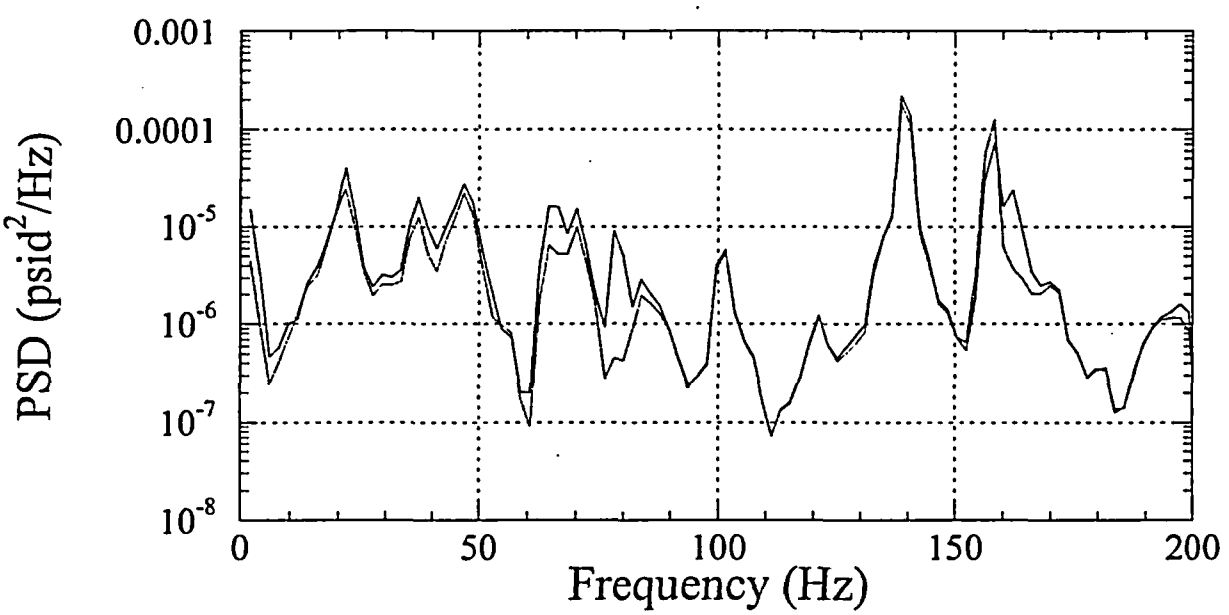

Figure 28. PSD comparison between TC15a (black curve) and TC15a_3 (blue curve) for pressure sensor number P27.

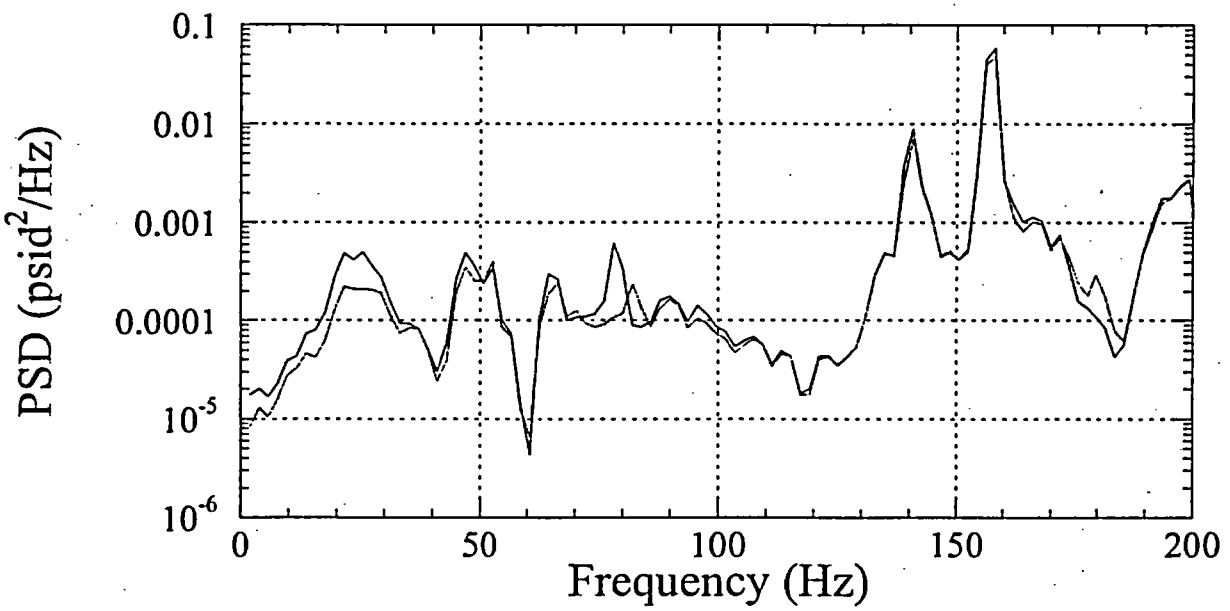

Figure 29. PSD comparison between TC15a (black curve) and TC15a_3 (blue curve) for the difference between pressure sensor number P3 and pressure sensor number P13.

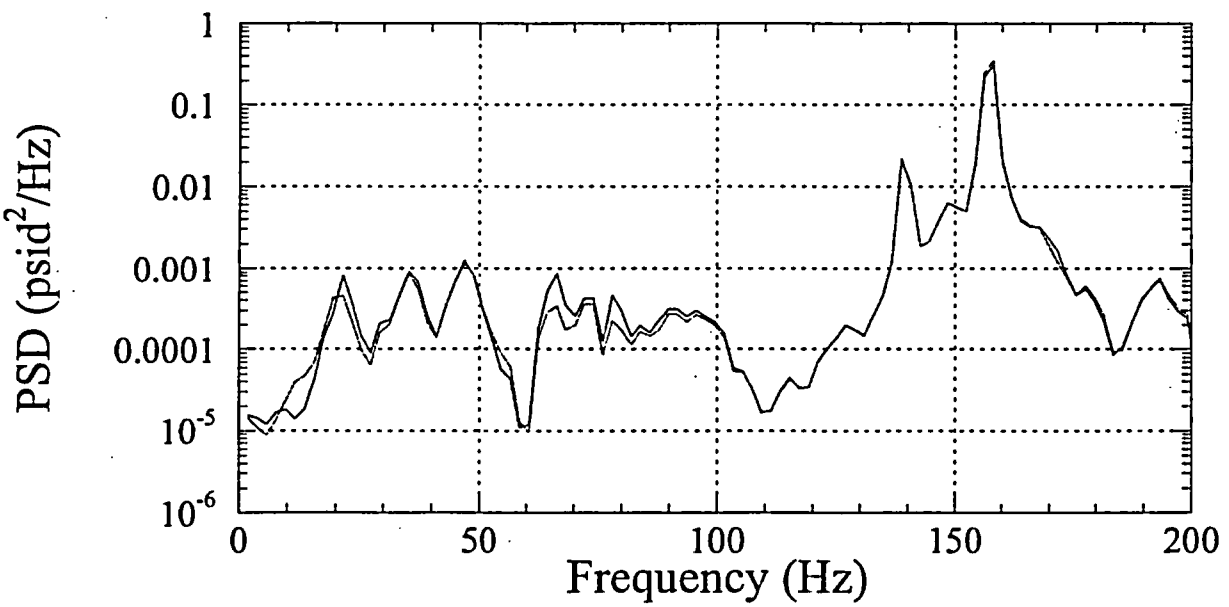

Figure 30. PSD comparison between TC15a (black curve) and TC15a_3 (blue curve) for the difference between pressure sensor number P20 and pressure sensor number P14.

ENCLOSURE 2

Attachment 9

GE Report GE-NE-0000-0041-9435, "Quad Cities 1 & 2 Steam Dryer Replacement – 4% Structural Damping for Steam Dryer Skirt FIV Analysis," dated June 16, 2005

GE NUCLEAR ENERGY
Structural Analysis and Hardware Design
6705 Vallecitos Road, Sunol, CA 94586-9525

June 16, 2005
dkh0513
Report No. GE-NE-0000-0041-9435

cc: M. R. Schrag
M. K. Kaul
C. E. Hinds
R. W. Wu

TO: GE Nuclear Energy DRF No.: eDRF-0000-0039-4747

FROM: D. K. Henrie

SUBJECT: **Quad Cities 1 & 2 Steam Dryer Replacement - 4% Structural Damping for Steam Dryer Skirt FIV Analysis.**

REFERENCES:

(1) GE Nuclear Energy Letter Report GE-NE-0000-0039-4749, from D. K. Henrie to J. Klapproth, "Exelon Steam Dryer Replacement Program – 2% structural Damping for Seismic and Non-Seismic (FIV) Dynamic Analysis", March 18, 2005. (dkh0503)

(2) GE Nuclear Energy Calculation No. eDRF Section 0000-0034-1855, "Damping Value for Steam Dryer Structural Dynamic Analysis", Richard Wu, November 5, 2004.

(3) GE Nuclear Energy Generic Design Specification No. 386HA596, Rev. 0, "Dynamic Load Methods & Criteria – NSSS Equipment, Piping, RPV & Internals", Issued July 2, 1986. **(GE Proprietary)**

(4) US Atomic Energy Commission Regulatory Guide 1.61, "Damping Values for Seismic Design of Nuclear Power Plants", October 1973.

(5) Quad Cities UFSAR

(6) GE Nuclear Energy Letter Report GE-NE-0000-0039-4768, from D. K. Henrie to DRF No./Section: eDRF-0000-0039-4747/4768, "Quad Cities 1 & 2 Steam Dryer Replacement - 4% structural Damping for Vane Bank FIV Analysis", April 21, 2005. (dkh0507)

(7) GE Nuclear Energy Report GE-NE-0000-0039-5860-01-P, Rev. 1, "Test and Analysis Report - Quad Cities New Design Steam Dryer – Dryer #1 Experimental Modal Analysis and Correlation with Finite Element Results", May 2005.

(8) GE Nuclear Energy Report GE-NE-0000-0041-1656-01-P, "Test and Analysis Report - Quad Cities New Design Steam Dryer – Dryer #2 Experimental Modal Analysis and Correlation with Finite Element Results", May 2005.

1.0 PURPOSE

This letter report provides the recommendation and technical justification for the structural damping to be utilized in the ongoing structural design adequacy evaluation of the Quad Cities 1 & 2 replacement dryer skirt. The recommended damping is to be used for the FIV load case, direct integration, time history analyses conducted by GE Nuclear Energy for Quad Cities 1 & 2.

2.0 CONCLUSIONS

Based on the present evaluation, it is concluded that an equivalent, linear viscous damping value, corresponding to 4.0% of critical damping, can be conservatively used for the FIV structural design adequacy analyses required for the Quad Cities 1 & 2 replacement dryer skirts. The technical basis for this conclusion is provided below.

The details of the present evaluation, as well as evidence of verification, are documented in the GE Nuclear Energy Design Record File, DRF No. 0000-0039-4747, Section 0000-0041-9435.

3.0 DRYER SKIRT DAMPING BASED ON TECHNICAL LITERATURE

The technical justification for the structural damping used in the overall seismic (OBE and SSE) and dynamic (FIV) structural integrity design adequacy evaluation for the Quad Cities 1 and 2 replacement steam dryers is provided in References 1 through 3 and 6. The Quad Cities structural damping, licensing requirement for all primary structure components, except the RPV and internals, is given in Reference 5 and the RPV and internals requirement in Reference 3.

3.1 <u>US NRC Regulatory Guide 1.61 Damping.</u> Table 1 of Regulatory Guide 1.61, Reference 4, tabulates modal damping values acceptable to the US NRC for the analysis and design of nuclear power plant seismic Category I structures, systems and components. The damping values in Table 1 are given in terms of percent of critical damping and are acknowledged to be conservative. Referring to Subsection C.2 of the guide, "*Damping values higher than the ones delineated in Table 1 my be used in a dynamic seismic analysis if documented test data are provided to support higher values.*" Conversely, the following caveat is also given in Subsection C.3 of the guide: "*If the maximum combined stresses due to static, seismic, and other dynamic loading are significantly lower than the yield stress and ½ yield stress for SSE and ½ SSE, respectively, in any structure or component, damping values lower than those specified in Table 1 of this guide should be used for that structure or component to avoid underestimating the amplitude of vibrations or dynamic stresses.*"

In particular, the damping values contained in Table 1 of the guide are highly dependent on: (i) the material and structural characteristics of the structure or component, and (ii) the dynamic excitation level to which the structure or component is subjected (hence, the excitation level to which it responds). With regard to material and structural characteristics, the dryer skirt corresponds to a welded steel structure. With regard to excitation level (hence response level), damping values are provided in Table 1 for OBE and SSE levels of excitation.

Referring to Table 1 of the guide for a welded steel structure, the conservative value of damping for the OBE level of excitation is 2% of critical and that for the SSE level of excitation is 4%. From the current, ongoing FIV analysis for the Quad Cities 2 replacement dryer skirt, the maximum stress at multiple locations in the skirt corresponding to 2% damping is 14,590 psi and corresponding to 4% damping is 10,800 psi. At 545°F, the yield stress for SS304L is 15,940 psi. It then fellows that in the dryer skirt the maximum FIV stress, corresponding to 2% structural damping, is equal to 0.92 of yield and for 4% structural damping, the dryer skirt maximum stress is equal to 0.68 of the yield stress, a response that is more representative of SSE excitation.

Based on the foregoing discussion, it then follows from Table 1 of Regulatory Guide 1.61 that the structural damping level for a welded steel structure subjected to the SSE level of excitation (hence, the SSE level of response) is appropriate for the dryer skirt FIV analysis. Therefore, it is concluded that 4% structural damping is appropriate for the FIV design adequacy evaluation of the Quad Cities 1 & 2 replacement steam dryer skirt.

Two finally observations are now made. First, it is noted that the damping values given in Table 1 of the guide all correspond to the vibration of the dynamically excited structures and components in the air. The corresponding damping values if the structures are submerged in water will be significantly higher. Because at least two-thirds of the dryer skirt is submerged at low water level, 4% damping is even more conservative.

Second, it is also noted that per the caveat quoted above, the maximum combined stress to be compared to the yield stress is due to static, seismic, and other dynamic loadings (i.e., FIV loadings). The stresses cited above in terms of the yield stress for 2% and 4% structural damping correspond to only FIV loading which occurs during normal plant operation.

3.2 <u>Quad Cities/Dresden UFSAR Damping.</u> The damping values provided in Tables 3.7-1 of the Quad Cities and Dresden UFSARs correspond to design licensing basis values to be applied to all safety related structures, components and equipment in the plants except the RPV internals and the RPV stabilizer. The footnote in Table 3.7-1 in the Dresden UFSAR reiterates that the design licensing basis damping values for the RPV and internals and the RPV stabilizer are GE Nuclear Energy proprietary and "*are provided in GENE-771-84-1194, Revision 2*", prepared by GE Nuclear Energy for the Dresden shroud repairs.

3.3 <u>GE Nuclear Energy Methods & Criteria Document Damping.</u> The RPV internals damping values provided in the above referenced GENE report are based on the GE Nuclear Energy Methods and Criteria document, Reference 3. The seismic damping values are contained in Table 5.8.1-1 and the nonseismic damping values in Table 5.8.2-1 of Reference 3. Similar to Regulatory Guide 1.61 damping, the design licensing basis damping values contained in Reference 3 are dependent on the material and structural characteristics of the structure or component being excited as well as on the level of the excitation (hence the level of the response). However, differing from Regulatory Guide 1.61, selected damping values contained in Reference 3 are also dependent on the direction, horizontal or vertical, in which the structure or component is excited.

Also, similar to the OBE level of excitation in Regulatory Guide 1.61, the seismic damping values in Table 5.8.1-1, designated as OBE, and the nonseismic damping values in Table5.8.2-1, designated as Normal or Upset, are to be used in the structure or component dynamic analysis in which the resulting maximum stresses are at, or not significantly below, the one-half yield stress. Again, similar to the SSE level of excitation in Regulatory Guide 1.61, the seismic damping values in Table 5.8.1-1, designated as SSE, and the nonseismic damping values in Table5.8.2-1, designated as Emergency or Faulted, are to be used in the structure or component dynamic analysis if the resulting maximum stresses are significantly above the one-half the yield stress and not significantly below the yield stress.

Referring to Table 5.8.2-1 of Reference 3, for a welded steel structure subjected to the Emergency or Faulted level of excitation (hence, level of response), the appropriate structural damping is 4% of critical. Therefore, it is concluded that 4% structural damping can be conservatively applied in the FIV structural design adequacy evaluation of the Quad Cities 1 & 2 and the Dresden 2 and 3 replacement steam dryer skirts. The result is the same as that for Regulatory Guide 1.61

4.0 DRYER SKIRT DAMPING BASED ON HAMMER TEST DATA

The results of the hammer tests, just completed for the Exelon replacement steam dryers 1 and 2, are summarized in References 7 and 8, respectively. The primary purpose of the hammer test is to identify the natural frequencies of the dryer assemblies. The vibration test data generated by the hammer test can also be utilized to determine representative, lower bound values of the structural damping inherent to the steam dryer assemblies. The (i) Logarithmic Decrement, (ii) Half Power Bandwidth (or equivalent), and (iii) Modal Curve Fitting (Individual FRFs), and (iv) Modal Curve Fitting (Whole Component) methods were all applied in References 7 and 8 to the hammer test data to generate approximate, lower bound structural damping values for the steam dryer hoods and skirts.

4.1 <u>Conservatism Inherent to Damping Values Based on Hammer Tests.</u> Typically, the hammer test is performed using a 2 lb to 3 lb soft tipped (load cell) hammer that is used to gently tap (impact) the dryer assembly. There is no metal-to-metal contact. The impact test should not cause local damage to the dryer surfaces, e.g., no dents or scratches. Furthermore, care is taken not to damage the installed sensors and the sensor leads.

From this description, it is clear that during the hammer test the excitation level, deformation, strain, stress, displacement, velocity, strain rate, etc., are all essentially zero. However as discussed in Subsections 3.1 and 3.3 above, the damping magnitude inherent to a structure or component is highly correlated to its excitation (hence response) level. Typically, the greater the excitation level the greater the structural damping magnitude; however, the correlation between the two is nonlinear.

Based on the foregoing discussion, it is concluded that the damping coefficients generated, based on hammer test vibration data, will correspond to very conservative, lower bound values when compared to the actual damping characteristics inherent to the replacement steam dryer assembly during normal plant operation.

4.2 <u>Dryer Skirt FIV Response Characteristic Frequencies.</u> The maximum strain (stress) in the dryer skirt, due to the FIV loading associated with the Quad Cities 2 post startup main steam line data taken at 2885 MWt, occurs at Node 66818 of the steam dryer assembly Finite Element Model (FEM). The frequency content of the corresponding strain (stress) time history, that is calculated at Node 66818 in the associated GE 1% structural damping, direct integration, time history analysis of the dryer FEM, is obtained from the FFT of that time history. The dominant characteristic frequency associated with the dryer skirt maximum strain (stress), defined in the corresponding strain time history FFT plot, is in the range 25Hz to 35Hz.

4.3 <u>Dryer Skirt Damping from Hammer Tests.</u> Referring to Table 1 of Reference 7 for Dryer #1 and Table 1a of Reference 8 for Dryer #2, it is observed that the dryer skirt hammer test calculated damping values vary dramatically depending on: (i) the frequency at which the damping is calculated is calculated, and (ii) which of the four methods mentioned above are applied in the damping calculation.

The damping in terms of percent critical damping in Dryer #1, Reference 7, ranged from 0.2% to 7.7% on the 90° skirt panel, with the higher frequencies generally showing lower damping. The 270° skirt panel showed a similar trend, with a damping range of 0.4% to 13%. In general, the skirt damping values generated based on strain gage hammer test data were slightly higher than the corresponding damping values generated based on accelerometer hammer test data.

For Dryer #2, Reference 8, the damping in terms of percent critical damping for the individual FRFs ranged from 0.2% to 3.7% on the 90° skirt panel, with the higher frequencies generally showing lower damping. The 270° skirt panel showed a similar trend, with a damping range of 0.5% to 5.6%. In general, the skirt damping values generated based on strain gage hammer test data were slightly higher than the corresponding damping values generated based on accelerometer hammer test data.

The procedure consisting of the four steps defined below is applied to the hammer test damping values contained in Table 1 of Reference 7 and Table 1a of Reference 8 to obtain an appropriate damping value which can be conservatively applied in the Quad Cities 1 & 2 FIV structural design adequacy evaluation of the replacement steam dryer skirt.

<u>Step 1:</u> Consistent with the conservatism inherent to damping values that are calculated based on hammer test data (discussed in Subsection 4.1 above), when a range of damping values is calculated at a given frequency by any one of the four methods noted at the beginning of Section 3.0, the maximum damping value in the range is taken as the damping value calculated by that method for that frequency.

<u>Step 2:</u> Whenever more than one of the four methods are applied to calculate dryer skirt damping value at a given frequency, the damping value at that frequency is taken as the average of the damping values calculated by the methods applied.

<u>Step 3:</u> Whenever damping values are calculated at multiple frequencies which fall in the frequency range of the dominant characteristic frequency of the dryer maximum strain (stress), the damping value for the entire frequency range can be taken as the average of the damping values calculated for each individual frequency in the range.

<u>Step 4:</u> The dryer skirt damping can be taken as the damping obtained by applying Step 1 through Step 3 for the frequency range which is equal to the dominant characteristic frequency range of the dryer skirt maximum strain (stress) as discussed in Subsection 4.2 above.

The dryer skirt structural damping, based on hammer test data, is now approximated for Dryer #1 and Dryer # 2 by applying Steps 1 through 4 above to the hammer test data contained in Table 1 of Reference 7 and Table 1a of Reference 8, respectively. The resulting damping values are tabulated in Table 1 below.

TABLE 1

Dryer Skirt Structural Damping
(% of Critical)

	Dryer #1	Dryer #2
90° Skirt Panel	4.76%	2.53%
270° Skirt Panel	5.71%	1.50%

4.4 Discussion Dryer Skirt Damping Results from Hammer Tests. Because the vertical plane that contains the dryer assembly horizontal 0° - 180° axis corresponds to a structural plane of symmetry, it is expected that the damping values on the 90° Skirt Panels and the 270° Skirt Panels would be the same. Also, because the structural characteristic of Dryer #1 and Dryer #2 are essentially identical it was also expected that damping values for the two dryers would be the same.

The apparent differences can be partly explained by comparing Table 1 from Reference 7 with Table 1a from Reference 8. In comparing the two tables, it is observed that: (i) the damping values were not generally calculated at the same frequencies for the two dryers, (ii) the damping values were generally not calculated using the same methodology for the two dryers, and (iii) for the same dryer, the damping values were not generally calculated at the same frequencies for the 90° and the 270° skirt panels even though the same methodology was applied. This does not fully explain the differences because there are several cases for which the dissimilar damping values were calculated at the same time point using the same methodology for the two dryers. Probably there are also some differences in the test setup or how the tests were performed between the two dryers or between the two dryer skirt planes for the same dryer.

The Dryer #1, hammer based, damping values given in Table 1 above for the 90° skirt panel and the 180° skirt panel are sufficient to justify 4% structural damping for the Quad Cities 2 dryer skirt structural design adequacy evaluation for the FIV load case. Based on the foregoing discussion, the justification can also be applied to the Quad Cities 1dryer skirt.

5.0 SUMMARY OF EXELON REPLACEMENT DRYER ASSEMBLY DAMPING

From the foregoing discussion it is recommended that 4% structural damping be conservatively applied for the FIV structural integrity evaluation of the dryer assembly skirt.

The FIV structural integrity of: (i) the steam dryer RPV vessel lugs, and (ii) the dryer upper assembly (excluding the vane banks, Reference 6) will still be based on 2% structural damping for the dryer assembly, Reference 1. Also, the FIV structural integrity evaluation of all other steam dryer assembly components will be based on 1% structural damping in the steam dryer assembly, Reference 2.

Based on the present evaluation, it is concluded that an equivalent linear viscous modal damping value of 4.0% of critical damping can be conservatively applied for direct integration time history analyses of the replacement steam dryer skirt for Quad Cities 1 & 2 for the FIV dynamic load case. The technical basis for this recommendation is presented above.

If there are any questions, or if I can be of additional help, please call me at (925) 862-4350 or on my cell phone at (408) 204-6244.

D.K. Henrie, Technical Leader
Structural Analysis & Hardware Design
Seismic & Dynamic Analysis

Verified by: _____
M. K. Kaul, Principal Engineer
Structural Analysis & Hardware Design
Seismic & Dynamic Analysis

ENCLOSURE 2

Attachment 11

GE Report GENE-0000-0043-5391-01, "Quad Cities Unit 1 Replacement Steam Dryer Stress and Fatigue Analysis at EPU Power Level of 2957 MWt Based on Measured EPU Conditions," Revision 1, Non-Proprietary, dated August 2005

GE Nuclear Energy

General Electric Company
6705 Vallecitos Road, Sunol CA 94586

GE Non-Proprietary Version

GENE-0000-0043-5391-01
DRF 0000-0043-5391
Revision: 1
Class I
August 2005

Engineering Report

Quad Cities Unit 1 Replacement Steam Dryer Stress and Fatigue Analysis at EPU Power Level of 2957 MWt Based on Measured EPU Conditions

Principal Contributors:

L. Wellstein
D. Pappone
A. Pinsker
K. Afjeh
I. Shekhtman
D. Slack

Principal Verifier:
J. Waal

Approval: _____
M. Schrag
Structural Mechanics and Materials Manager

PROPRIETARY INFORMATION NOTICE

Please Read Carefully

Non-Proprietary Notice

This is a non-proprietary version of the document GENE-0000-0043-5391-01-P, Rev. 1, which has the proprietary information removed. Portions of the document that have been removed are indicated by an open and closed bracket as shown here [[ ]].

IMPORTANT NOTICE REGARDING CONTENTS OF THIS REPORT

Please Read Carefully

The only undertakings of the General Electric Company (GENE) with respect to the information in this document are contained in the contract between EXELON and GENE, and nothing contained in this document shall be construed as changing the contract. The use of this information by anyone other than EXELON or for any purpose other than that for which it is intended, is not authorized; and with respect to any unauthorized use, GENE makes no representation or warranty, express or implied, and assumes no liability as to the completeness, accuracy, or usefulness of the information contained in this document, or that its use may not infringe upon privately owned rights.

TABLE OF CONTENTS

Section	Page
ACRONYMS AND ABBREVIATIONS	vi
1. EXECUTIVE SUMMARY	1
2. INTRODUCTION AND BACKGROUND	2
2.1 Dryer Design Bases and Historical Development	2
2.2 Quad Cities and Dresden EPU Dryer Experience	4
2.3 Motivation for Additional FIV and Structural Analysis	5
3. Dynamic Analysis Approach	6
3.1 Dynamic Loading Pressure Time Histories	6
3.2 Stress Recovery and Evaluation Methodology	6
4. Material Properties	7
5. Design Criteria	7
5.1 Fatigue Criteria	7
5.2 ASME Code Criteria for Load Combinations	8
6. Fatigue Analysis	8
6.1 Full Dryer Shell Finite Element Model	9
6.1.1 Model Modification for QC1 Evaluation	9
6.2 Dynamic Loads	11
6.2.1 Basis for QC1D and QC1B Loads	11
6.3 Frequency Content of Loads	13
6.4 Modal Analysis	13
6.5 Structural Response to Loads	13
6.6 Stress Results from Time History Analyses	14
6.7 Weld Factors	17
6.8 Disposition of High Stress Locations	19
6.9 Fatigue Analysis Results	20
7. ASME Code Load Combinations	22
8. Conclusions	30
9. References	31

List of Tables

Table 4-1 Properties of SS304L and SS316L 7
Table 5-1 ASME Code Stress Limits 8
Table 6-1 Shell Element Model Stress Intensity Summary for Time History Cases 16
Table 6-2 Maximum Stress Intensity with Weld Factors 18
Table 6-3 Components with High Stress Intensity and Disposition 19
Table 6-4 Fatigue Analysis Results Summary 21
Table 7-1 ASME Load Combinations 24
Table 7-2 ASME Code Combinations: Stress Summary Levels A and B 26
Table 7-2 (cont'd) ASME Code Combinations: Stress Summary Level D. 28
Table 7-3 ASME Code Margins 30

List of Figures

Figure 3-1 Maximum Applied Pressure (QC1D Loads) 34
Figure 3-2 Maximum Applied Pressure (QC1B Loads) 35
Figure 6-1 Replacement Dryer Shell Finite Element Model 36
Figure 6-1A Dryer Skirt Water Elements for Superelement Generation 37
Figure 6-1B FEA Model, Modified Components for Mounting Block 38
Figure 6-1C FEA Model Changes at Trough Attachment to Outer Hood 39
Figure 6-1D FEA Model, Closure Plate with Stiffener 40
Figure 6-2 Dryer Finite Element Model Boundary Conditions 41
Figure 6-3 Finite Element Model without Super Elements 42
Figure 6-4 Load Frequency Content – Hood & Vane Cap (QC1D Loads) 43
Figure 6-4A Load Frequency Content - Skirt (QC1D Loads) 44
Figure 6-5 Skirt Frequency: [[ ]] 45
Figure 6-6 Skirt Frequency: [[ ]] 46
Figure 6-7 Skirt Frequency: [[ ]] 47
Figure 6-8 Skirt Frequency: [[ ]] 48
Figure 6-9 Skirt Frequency: [[ ]] 49
Figure 6-10 Skirt Frequency: [[ ]] 50
Figure 6-11 Skirt Frequency: [[ ]] 51

Figure 6-12 Outer Hood Frequency: [[ ]] 52
Figure 6-13 Frequency Response QC1D –10%: Hoods & Vane Cap 53
Figure 6-14 Frequency Response QC1D –10%: Skirt 54
Figure 6-15 Frequency Response QC1D Nominal: Hoods & Vane Cap 55
Figure 6-16 Frequency Response QC1D Nominal: Skirt 56
Figure 6-17 Frequency Response QC1D +10%: Hoods & Vane Cap 57
Figure 6-18 Frequency Response QC1D +10%: Skirt ....**Error! Bookmark not defined.**
Figure 6-19 Time History Stress Intensity Results: Vane Cap Flat Portion 59
Figure 6-20 Time History Stress Intensity Results: Outer Hood 60
Figure 6-21 Time History Stress Intensity Results: Tie Bars 61
Figure 6-22 Time History Stress Intensity Results: Frames 62
Figure 6-23 Time History Stress Intensity Results: Troughs 63
Figure 6-24 Time History Stress Intensity Results: Gussets 64
Figure 6-25 Time History Stress Intensity Results: Vane Cap Curved Part 65
Figure 6-26 Time History Stress Intensity Results: Inner Hoods 66
Figure 6-27 Time History Stress Intensity Results: Closure Plates 67
Figure 6-28 Time History Stress Intensity Results: T-Section Webs 68
Figure 6-29 Time History Stress Intensity Results: T-Section Flanges 69
Figure 6-30 Time History Stress Intensity Results: Vane Bank Outer End Plates 70
Figure 6-31 Time History Stress Intensity Results: [[ ]] 71
Figure 6-32 Time History Stress Intensity Results: Cross Beams 72
Figure 6-33 Time History Stress Intensity Results: Support Ring 73
Figure 6-34 Time History Stress Intensity Results: Trough Ledge 74
Figure 6-35 Time History Stress Intensity Results: Trough Brace Gusset 75
Figure 6-36 Time History Stress Intensity Results: Inner Trough Brace 76
Figure 6-37 Time History Stress Intensity Results: Vertical Support Plates 77
Figure 6-38 Time History Stress Intensity Results: Center Support Gussets 78
Figure 6-39 Time History Stress Intensity Results: Center Plate 79
Figure 6-40 Time History Stress Intensity Results: Trough End Stiffeners 80
Figure 6-41 Time History Stress Intensity Results: Gusset Shoe at Cross Beams 81
Figure 6-42 Time History Stress Intensity Results: Frame to Cross Beam Gussets 82

Figure 6-43 Time History Stress Intensity Results: Lifting Lug Guide 83
Figure 6-44 Weld Factors to Use with Finite Element Results 84

ACRONYMS AND ABBREVIATIONS

Item	Short Form	Description
1	ACM	Acoustic Circuit Model used by CDI to predict pressure loads on the dryer based on measurements taken from main steam line strain gages.
2	ASME	American Society of Mechanical Engineers
3	BWR	Boiling Water Reactor
4	EPU	Extended Power Uprate
5	FEA	Finite Element Analysis
6	FEM	Finite Element Model
7	FFT	Fast Fourier Transform
8	FIV	Flow Induced Vibration
9	GE	General Electric
10	GENE	General Electric Nuclear Energy
11	Hz	Hertz
12	IGSCC	Intergranular Stress Corrosion Cracking
13	Mlbm/hr	Millions pounds mass per hour
14	CDI	Continuum Dynamics, Inc.
15	MSL	Main Steam Line
16	MW	Megawatt Thermal
17	NA	Not Applicable
18	NRC	Nuclear Regulatory Commission
19	OBE	Operational Basis Earthquake
20	OLTP	Original Licensed Thermal Power
21	Pb	Primary Bending Stress
22	Pm	Primary Membrane Stress
23	psi	Pounds per square inch
24	Ref.	Reference
25	RMS	Root-Mean-Squared
26	RPV	Reactor Pressure Vessel
27	SCF	Stress Concentration Factor
28	SRSS	Square Root Sum of Squares
29	SRV	Safety Relief Valve

1. EXECUTIVE SUMMARY

In 2002 Quad Cities Unit 2 first developed fatigue cracks in the cover plate portion of the steam dryer after the plant had been operating at extended power uprate (EPU). The result of the root cause evaluation showed the primary factor for this event was high cycle loadings on the dryer. Additional fatigue cracking was observed in 2003 and 2004 in the cover plate and outer hood portions of the repaired Quad Cities and Dresden steam dryers. A replacement dryer was designed to withstand these flow induced vibration loads. The design loads for the replacement dryer were based on time history analyses using acoustic circuit loads from both in-plant steam line data and scale model test (SMT) data at less than EPU conditions. The results of the analyses performed using the design loads are in Reference 17, which established that the replacement dryer components are not vulnerable to fatigue at EPU conditions.

As part of the replacement dryer program, the replacement dryer and main steam lines in Unit 2 were instrumented for the purpose of measuring the pressure loads acting on the dryer and for benchmarking the load prediction and measurement methodologies. In addition, the main steam lines in Unit 1 were instrumented for the purpose of calculating the pressure loads acting on the Unit 1 dryer. This report summarizes the structural analysis performed to demonstrate the adequacy of the replacement steam dryer design using Continuum Dynamics Inc. (CDI) predicted loads based on main steam line strain gage measurements obtained during the Unit 1 startup with the replacement dryer.

Finite element analyses were performed using a full three-dimensional model of the Exelon replacement dryer comprised of shell elements to determine the most highly stressed locations associated with EPU. The analyses consisted of time history dynamic analyses, frequency calculations, and stress and fatigue analyses. The acoustic circuit model by CDI, which was driven by strain gauge measurements on the main steam lines, was used to develop the dryer pressure loads for the time history analyses. In addition, ASME Code based load combinations were also analyzed using the finite element model. Where necessary, the locations of high stress identified in the time history analyses were further evaluated using solid finite element models to more accurately predict the stresses at these locations.

This report summarizes the dynamic, stress and fatigue analyses that demonstrate the Exelon replacement steam dryer is structurally adequate for EPU conditions based on plant measurements taken at Quad Cities Unit 1 during EPU operation of the replacement dryer. The replacement dryer satisfies both the fatigue limit and the

ASME Code limits for normal, upset and faulted events at EPU conditions (Reference 1).

2. INTRODUCTION AND BACKGROUND

2.1 Dryer Design Bases and Historical Development

The function of the steam dryer is to remove any remaining liquid in the steam exiting from the array of axial flow steam separators. GE BWR steam dryers use commercially available modules of dryer vanes that are enclosed in a GE designed housing to make up the steam dryer assembly. The modules or subassemblies of dryer vanes, called dryer units, are arranged in parallel rows called banks. Four to six banks are used depending on the vessel size. Dryer banks are attached to an upper support ring, which is supported by four to six steam dryer support brackets that are welded attachments to the RPV. The steam dryer assembly does not physically connect to the shroud head and steam separator assembly and it has no direct connection with the core support or shroud. A cylindrical skirt attaches to the upper support ring and projects downward forming a water seal around the array of steam separators. Normal operating water level is approximately mid-height on the dryer skirt. During refueling the steam dryer rests on the floor of the equipment pool on the lower support ring that is located at the bottom edge of the skirt. Dryers are installed and removed from the RPV using the reactor building crane. A steam separator and dryer strongback, which attaches to four steam dryer lifting rod eyes, is used for lifting the dryer. Guide rods in the RPV are used to aid dryer installation and removal. BWR steam dryers typically have guide channels or upper and lower guides that interface with the guide rods.

Wet steam flows upward from the steam separators into an inlet plenum, horizontally through the dryer vane banks, vertically in an outlet plenum and into the RPV dome. Steam then exits the reactor pressure vessel (RPV) through steam outlet nozzles. Moisture (liquid) is separated from the steam by the vane surface and the hooks attached to the vanes. The captured moisture flows downward under the force of gravity to a collection trough that carries the liquid flow to drain pipes and vertical drain channels. The liquid flows by gravity through the vertical drain channels to the lower end of the skirt where the flow exits below normal water level. The outlet of the drain channels is below the water surface in order to prevent reentrainment of the captured liquid.

GE BWR steam dryer technology evolved over many years and several product lines. In earlier BWR/2 and BWR/3 dryers, the active height of the dryer vanes was set at 48 inches. In BWR/4 and later steam dryer designs the active vane height was

increased to 72 inches. Perforated plates were included on the inlet and outlet sides of the vane banks of the 72-inch height units in order to distribute the steam flow uniformly through the bank. The addition of perforated plates resulted in a more uniform velocity over the height of the vanes. The performance for BWR/4 and dryer designs was established by testing in steam. The replacement dryer designed for Quad Cities and Dresden incorporates the performance features of the latest steam dryer designs along with structural design enhancements to better withstand the pressure loading that can result in fatigue crack initiation.

Most of the steam dryer is located in the steam space, with the lower half of the skirt extending below normal water level. These environments are highly oxidizing. All of the BWR/2-6 steam dryers are welded assemblies constructed from Type 304 stainless steel. The Type 304 stainless steel used in BWR/2-6 steam dryers was generally purchased with a maximum carbon content specification of 0.08% (typical ASTM standard). Therefore, the weld heat affected zone material is likely to be sensitized during the fabrication process making the steam dryer susceptible to intergranular stress corrosion cracking (IGSCC). Temporary welded attachments may have also been made to the dryer material that could result in unexpected weld sensitized material. Steam dryer parts such as support rings and drain channels were frequently cold formed, also increasing IGSCC susceptibility. Many dryer assembly welds included crevice areas at the weld root, which were not sealed from the reactor environment. Cold formed 304 stainless steel dryer parts were generally not solution annealed after forming and welding. Because of the environment and material conditions, most steam dryers have exhibited IGSCC cracking. The replacement dryer design specified materials and fabrication processes that will reduce the susceptibility of the dryer to IGSCC cracking compared to the original dryer.

Average steam flow velocities through the dryer vanes at OLTP conditions are relatively modest (2 to 4 feet per second). However, the outer hoods near the steam outlet nozzles are continuously exposed to steam flows in excess of 100 feet per second. These steam velocities have the potential for exciting acoustic resonances in the steam dome and steam lines, provided appropriate conditions exist, resulting in fluctuating pressure loads that act on the dryer.

The dryer is a Class I Seismic but non-safety related component and performs no safety functions. The steam dryer assembly is classified as an "internal structure" per ASME Boiler and Pressure Vessel Code, Section III, Subsection NG. Therefore the steam dryer needs only to be analyzed for those faulted load combinations for which loss of structural integrity of the steam dryer could interfere with the required performance of safety class equipment (i.e., generation of loose parts that may

interfere with closure of the MSIVs) or affect the core support structure integrity (shroud, top guide, core support and shroud support).

2.2 Quad Cities and Dresden EPU Dryer Experience

Exelon has experienced dryer cracking and failures at each of the Quad Cities and Dresden units following implementation of EPU. The first dryer failure, loss of the lower horizontal cover plate at Quad Cities Unit 2, occurred in June 2002 after about three months of EPU operation. The root cause of this failure was determined to be high cycle fatigue due to a high frequency fluctuating pressure load. The second dryer failure, also at Quad Cities Unit 2, occurred in May 2003 after a little more than a year of total EPU operation. This failure consisted of severe through-wall cracking in the outer hood, along with cracking of vertical and diagonal internal braces and tie bars. The root cause of this failure was determined to be high cycle fatigue due to fluctuating pressure loads [[

]]. The internal gussets for the diagonal braces created a local stress concentration where the fatigue cracking had initiated. Hood cracking was observed at all four outer hood gusset locations. In October 2003, the dryer at Dresden Unit 2 was inspected following a full two year cycle at EPU conditions. Incipient cracking was observed in the outer hoods at all four diagonal brace gusset locations. In November 2003, Quad Cities Unit 1 experienced a hood failure similar to the one that occurred in May 2003 at Quad Cities Unit 2, again after about a year of EPU operation. Following this failure, Dresden Unit 3, which had been operating at EPU for a little more than one year, was shut down and the dryer inspected. Dresden Unit 3 exhibited the same incipient cracking at the outer hood gusset locations as was observed in Dresden Unit 2. In all of these cases, the root cause was determined to be high cycle fatigue due to the fluctuating pressure loads at EPU conditions.

Cracking has also been observed in some of the repairs and modifications that were made to the dryers following these failures. This type of cracking has also been observed to varying degrees in the dryers in all four units. During the March 2004 refueling outage, inspection of the repairs in the Quad Cities Unit 2 dryer showed cracking in the hood plate at the tips of the external gussets on the outer hoods. In November 2004, cracking was observed at one end of the weld between the lower horizontal cover plate and support ring in the Dresden Unit 3 dryer. The lower horizontal cover plate had been replaced in response to the initial 2002 Quad Cities failure as part of the EPU modifications for the dryer. In November 2004, an inspection of the Dresden Unit 2 dryer revealed cracking in the same lower horizontal cover plate weld, this time near the base of one of the external gussets. Recently, a

crack was found in this same weld at Quad Cities Unit 1 during a March 2005 inspection, again at the base of one of the external gussets. This cracking experience highlighted the importance of local stress concentrations in determining the fatigue life of the structure. In addition, several of the dryers are beginning to experience fatigue cracking in the perforated plate inserts installed in each dryer as part of the EPU implementation modifications. Tie bar repairs have also experienced cracking. This experience demonstrates the uncertainty in the useful life of the repairs and modifications performed on the original Quad Cities and Dresden steam dryers.

2.3 Motivation for Additional FIV and Structural Analysis

The experiences at Quad Cities and Dresden demonstrated the need to better understand the nature of the loading and the dynamic structural response of the steam dryers during normal operation. The expense involved with inspection and repair of the dryers for the extended life of the plants provide motivation for determining the loads acting on the dryers and quantifying the stresses in the dryers at EPU conditions. GE and Exelon have initiated development programs to determine the fluctuating pressure loads acting on the dryer in order to confirm the continued acceptability of operating the current dryers and for use in designing a replacement dryer that will be able to accommodate the loading during EPU operation without experiencing cracking.

Based on these needs, this evaluation was initiated to perform the comprehensive structural assessment for the replacement dryer design to assure that it could operate at EPU conditions. The loads affecting the steam dryer were determined and used as input to a three-dimensional finite element model of the Exelon replacement steam dryer. Loads considered in the assessment included steady state pressure, fluctuating, and transient loads, with the primary interest in the steady state fluctuating loads that affect the fatigue life of the dryer. Additionally, ASME-based design load combinations were evaluated for normal, upset and faulted service conditions. A detailed finite element analysis using the dryer model subjected to these design loads was also performed. The analytical results identified the peak stresses and their locations. The results of the analysis also included the analytically determined structural natural frequencies for the different key components and locations in the dryer. Hammer tests were performed on the assembled dryer both dry and in water with varying water elevations. Frequencies from the hammer tests compared well with the finite element model frequencies and showed that no changes were required in the model.

The replacement dryer design has incorporated several design features that reduce the likelihood of fatigue cracking (References 3 and 4). These features include moving

welds out of high stress locations, reducing the number of fillet welds and increasing the number of full penetration welds, and allowing more flexibility in the tie bar attachments to the dryer banks. This report summarizes the dynamic, stress and fatigue analyses performed based on the in-plant load measurements to demonstrate that this new dryer design is structurally adequate for EPU conditions.

3. Dynamic Analysis Approach

3.1 Dynamic Loading Pressure Time Histories

The primary dynamic loads of concern on the dryer are the fluctuating pressure loads during normal operation. The fluctuating pressure loads are responsible for the fatigue damage experienced by the original and repaired steam dryers at all four Dresden and Quad Cities plants. As part of the replacement dryer program, main steam lines in Unit 1 were instrumented for the purpose of better defining the pressure loads acting on the dryer. Pressure measurements from the steam lines (inferred from strain gauge measurements on the piping) were used in CDI's acoustic circuit model to estimate the pressures acting on the dryer (References 5 and 5A). These measurements were taken at a power level of 2887 MWt. This load definition is basically the same as the "in-plant" load case in Reference 17; however, the steamline strain gauge placement was improved to provide a more accurate determination of the pressure in the steamline and the acoustic circuit model was refined based on the pressures measured by sensors mounted directly on the steam dryer on Unit 2. Additional details on the CDI acoustic circuit model are provided in Reference 6D. The pressure predicted from the CDI acoustic circuit model were applied as time history forcing functions to the structural finite element shell model of the dryer (Figure 3-1). Two sets of loads (referred to as QC1D and QC1B) were used in this analysis and are discussed in detail in Section 6.2.1.

3.2 Stress Recovery and Evaluation Methodology

The entire shell finite element model was divided into components with every element assigned to a component. An ANSYS macro was written to sweep through each time step on every component to determine the time and location of the maximum stress intensity. [[

]]. ANSYS maximum stress intensity results from this macro are presented in Table 6-1. In most cases these stresses from the shell finite element model meet the GENE fatigue design criteria of 10800 psi (References 1 and 7). In some locations that do not meet this criteria, solid element finite element models from Reference 17 are used and combined with hand calculations to determine more

accurate stresses (Table 6-3) such as for the cross beams and support ring. Solid models (Reference 17) are used to more accurately determine the stress state using forces and moments extracted from the shell model. Solid modeling of the weld attachment to the support ring gave a better representation of the local weld geometry and flexibility and thus resulting in more accurate stresses.

At high stress locations away from the outer hood (i.e., inner hoods), an alternate criteria was used as described in Section 5.1. [[
]], justified in Reference 18.

4. Material Properties

The dryer assembly was manufactured from solution heat-treated Type 316L and 304L conforming to the requirements of the material and fabrication specifications (Reference 3). ASME material properties were used (Reference 8). The applicable properties are shown in Table 4-1.

Table 4-1 Properties of SS304L and SS316L

Material / property	Room temperature 70°F	Operating temperature 545°F
SS304L		
S_y, Yield strength, psi	25000	15940
S_u, Ultimate strength, psi	70000	57440
E, Elastic modulus, psi	28300000	25575000
SS316L		
S_y, Yield strength, psi	25000	15495
S_u, Ultimate strength, psi	70000	61600
E, Elastic modulus, psi	28300000	25575000

5. Design Criteria

5.1 Fatigue Criteria

The fatigue evaluation consists of calculating the alternating stress intensity from FIV loading at all locations in the steam dryer structure and comparing it with the allowable design fatigue threshold stress intensity. The recommended fatigue threshold stress intensities that were developed specifically for the replacement dryer are the following (Reference 7):

1) The acceptable conservative fatigue threshold value of 10,800 psi is to be used as the baseline criterion. It should be used at all critical locations that include the outer hood as the maximum acceptable value for the stress intensity amplitude.

2) The higher ASME Code Curve C value of 13,600 psi may be used in specific cases. However, its use must be technically justified.

The fatigue design criteria for the dryer is based on Figure I-9.2.2 of ASME Section III (Reference 9), which provides the fatigue threshold values for use in the evaluation of stainless steels. A key component of the fatigue alternating stress calculation at a location is the appropriate value of the stress concentration factor. The shell finite element model of the full dryer is not capable of predicting the full stress concentrations in the welds. Therefore, additional weld factors are applied to the maximum stress intensities obtained from the shell finite element time history analyses at all weld locations (Reference 10). The stress intensities with the applied weld factors are then compared to the fatigue criteria given above.

5.2 ASME Code Criteria for Load Combinations

Table 5-1 ASME Code Stress Limits

Service level	Stress category	Class 1 Components Stress limits (NB)	
			Stress Limit, KSI
Service levels A & B	P_m	S_m	14.4
	$P_m + P_b$	$1.5S_m$	21.6
Service level D	P_m	Min(.7S_u or 2.4 S_m)	34.56
	$P_m + P_b$	1.5(P_m Allowable)	51.84

Legend:

P_m: General primary membrane stress intensity
P_b: Primary bending stress intensity
S_m: ASME Code stress intensity limit
S_U: Ultimate strength

6. Fatigue Analysis

Time history analyses were performed using ANSYS Version 8.1 (Reference 11). The direct integration time history method was used for all of the cases described in this report. [[

]]

A Rayleigh damping of 2% was used in all of the time history analyses. This was justified based on Reference 19. Knowledge of the significant frequencies that contribute to the total response is used to define the appropriate alpha and beta Rayleigh damping coefficients for the time history direct integration finite element analyses. [[

]] This is justified based on Reference 18 and the hammer test results (Reference 12).

6.1 Full Dryer Shell Finite Element Model

The three-dimensional shell model of the replacement dryer is shown in Figures 6-1 through 6-3. The model incorporates super elements for the vane banks, submerged portion of the skirt and tie bar supports. [[

]] The details of the finite element model and associated super elements are contained in Reference 17. For this analysis, the finite element model has been modified from that used in References 17 and 17A as described below.

6.1.1 Model Modification for QC1 Evaluation

[[

]]

6.2 Dynamic Loads

The primary dynamic loads of concern are the fluctuating pressure loads during normal operation. These are the loads responsible for the fatigue damage experienced by all four of the Dresden and Quad Cities steam dryers. As described in Section 3.1, pressure measurements from the steam lines (inferred from strain gauge measurements) were used in CDI's acoustic circuit model to estimate the pressures acting on the dryer (References 5 and 5A). Two sets of loads were developed (QC1D & QC1B) as explained in Section 6.2.1. Figures 3-1 and 3-1A show the applied load at the time when the pressure is a maximum for each load set.

Note that the loads used in this analysis were based on measurements taken at a power level of 2887 MWt, which is below the EPU power level of 2957 MWt. Consequently, the resulting stress results have been conservatively increased by 10% to account for extension to EPU. [[

]]

6.2.1 Basis for QC1D and QC1B Loads

CDI has calculated the steam dryer loads for Quad Cities Unit 1 (QC1) based on the measured steam line strain gauge data (Test Condition TC15a) taken during plant start-up in June 2005. This loading was calculated using the same methodology used previously (Reference 6D). This loading is referred to as the QC1D loads and is one

of the load sets used as the basis for further confirmation of the design adequacy of the replacement steam dryer at full EPU conditions. The two time histories used in this analysis were generated and transmitted in References 5 and 5A (TC15a_2 for QC1D and TC15a for QC1B).

The evaluation of this QC1D loading (Reference 5) has shown that the loading on the dryer skirt is overly conservative (Reference 6D). The use of overly conservative, unrealistic loads can result in the development of fictitiously high stresses that exceed the ASME Code stress limits. The conservatism of the loads is confirmed by comparison of the FEA results with the as-measured strain gauge data from the gauges on the Unit 2 steam dryer skirt (Section 6.9 of Reference 17A). Thus such level of over conservatism is generally undesirable.

To address the overly conservative skirt loading in the QC1D loading, a second set of loading considered more realistic for the dryer skirt was developed by CDI for QC1. This loading is referred to as the QC1B loads (Reference 5A). This methodology and the evaluation are discussed in an Exelon Report (Reference 6A), where References 6B and 6C describe the differences between QC1D and QC1B. This provides a more reasonable yet still conservative loading (QC1B) that can be used for confirmatory analysis of the dryer skirt.

Thus, if the dryer skirt is shown to meet design requirements for either loading QC1B or QC1D, the design adequacy is considered confirmed. In general, the QC1D loads are used for dryer evaluation. For the dryer skirt, the QC1B loads are used to avoid the unnecessary taxing of the design from the overly conservative QC1D skirt loading.

Note that the dryer skirt response is primarily a function of the lower frequency skirt loading. As an example, Figure 6-16 shows the lateral displacement response spectrum for a selected skirt node (note the low frequency content). As can be seen by referring to Figures 6-15 and 6-16, in the low frequency regime the skirt modes are decoupled from the rest of the structure.

In conclusion, the QC1D loading is used to evaluate the steam dryer except for the skirt, as this load case will provide overly conservative results on the skirt. The QC1B load case is used to evaluate the skirt as it represents a more reasonable yet still conservative loading on the skirt. Using two separate load cases is acceptable because

the skirt is considered decoupled from the rest of the dryer based on its unique response as discussed above.

6.3 Frequency Content of Loads

The frequency content of the Quad Cities in-plant loads is shown in Figures 6-4 and 6-4A. [[

]]

6.4 Modal Analysis

Frequency calculations were performed with the dryer supported from the RPV dryer support brackets. The support was modeled by fixing all translational degrees of freedom at the dryer support bracket interface. The entire dryer was surveyed for the component natural frequencies. However, the focus of the assessment was on the outer dryer surfaces. These calculated component natural frequencies for the skirt are shown in Figures 6-5 through 6-11. [[

]]

6.5 Structural Response to Loads

Structural frequency responses for the dryer outer hood and dryer vane caps [[ ]] are shown in Figures 6-13, 6-15 and 6-17. The structural response of the skirt is shown in Figure 6-18 for the QC1B load case [[ ]].

[[

]]

6.6 Stress Results from Time History Analyses

Maximum stress intensity results from ANSYS for all components of the dryer are shown in Table 6-1 [[

]] The stresses are shown in Figures 6-19 through 6-43 for the 2887 MWt power level. [[

]]

More detailed analyses using solid models of the cross beam and support ring were used to show adequate fatigue margin for those components. These models are described in more detail in Reference 17. The stresses, from these QC1D loads, presented in Table 6-2 are lower than those reported in Reference 17. Therefore, the solid model results reported in Reference 17 bound the stresses for QC-1 at 2957 MWt. Solid model results from the design basis loads are shown again, for information, in Table 6-3 of this attachment. The skirt stresses shown in Figure 6-31

are for the 2887 MWt power level and the stress intensities listed in Tables 6-1 and 6-2 include the scaling to 2957 MWt power.

Note, the loads used in this analysis and resulting stress contour plots are based on measurements taken at a power level of 2887 MWt that is below EPU power level of 2957 MWt. Consequently, the resulting stress results have been conservatively increased by 10% to account for extension to EPU. [[

]]

Table 6-1 Shell Element Model Stress Intensity Summary for Time History Cases

[[

]]

6.7 Weld Factors

The calculation of fatigue alternating stress using the prescribed stress concentration factors in Subsection NG is straightforward when the nominal stress is calculated using the standard strength of material formulas. However, when a finite element analysis (FEA) approach is used, the available stress component information is very detailed and requires added guidance (Reference 10) for determining a fatigue alternating stress intensity to be used in conjunction with the ASME Code S-N design curve. The replacement steam dryer welds are analyzed using FEA. Reference 10 provides the basis for calculating the appropriate fatigue factors for use in the S-N evaluation to assess the adequacy of these welds based on the FEA results. Figure 6-44 summarizes the Reference 10 criteria. For the case of full penetration welds, the recommended SCF value is 1.4. In this case, the finite element stress is directly multiplied by the appropriate SCF to determine the fatigue alternating stress intensity. The recommended SCF is 1.8 for a fillet weld when the FEA maximum stress intensity is used. Various studies have shown that the calculated fatigue alternating stress using this alternate approach at a fillet weld correlates with that using a nominal stress and a SCF of 4.0 (Reference 14). An alternative approach involves extracting forces and moments from the shell finite element model near the weld and calculating a nominal stress. This nominal stress would then have a factor of 4.0 applied for a fillet weld. Figure 6-44 shows a chart [[

]]

Note that the above discussion of stress concentration effects (SCF's, fatigue factors, weld factors) only applies to the fatigue evaluation. SCF, "fatigue factor," and "weld factor" are used interchangeably. These terms do not refer to 'weld quality factors' from ASME Subsection NG for primary stress evaluation used in Section 7.0 of this report.

Table 6-2 Maximum Stress Intensity with Weld Factors

[[

]]

Table 6-3 Components with High Stress Intensity and Disposition

[[

]]

6.8 Disposition of High Stress Locations

The high stress components for QC1 Load Combinations requiring special disposition are summarized in Table 6-3. Details of the disposition are described as follows:

[[

]]. Therefore, the crossbeams and support ring are considered acceptable.

6.9 Fatigue Analysis Results

The fatigue analysis results are a compilation of shell finite element model, solid model, and stress ratioing of previous results (Table 6-3) for assessing the acceptability of the steam dryer against the fatigue design criteria. [[

]]. The maximum stresses directly from the ANSYS shell finite element analysis are summarized in Table 6-1. The stresses [[ ]] are summarized in Table 6-2. The components requiring additional evaluations are summarized in Table 6-3. The fatigue evaluation results including use of previous solid models (Reference 17), different damping values, and an alternate fatigue limit in areas away from the outer hood are summarized in Table 6-4. All components listed meet the fatigue design allowables.

Table 6-4 Fatigue Analysis Results Summary

[[

]]

7. ASME Code Load Combinations

The objective of this evaluation is to determine the effect on the ASME load combination calculations as a result of the new (post-installation of new dryer) FIV loads from the in-plant nominal and +/-10% frequency calculations for the EPU power condition, (QC1D). Also included in this evaluation is a review of stresses in the trough longitudinal weld areas [[ ]].

The inputs for this evaluation are the original ASME load combinations (References 17 and 17A), and the new FIV loads (stresses) as shown in Reference 22A. The new FIV stresses include a multiplication factor of 1.1 to address full EPU conditions.

The ASME load combination evaluations contained in Reference 23 and reported in Reference 17A, are utilized in this evaluation. Because the only loads that changed were the FIV loads contained in the spreadsheet, "QC1D_Stress_Comp.xls" (Reference 22)] modified from Reference 23, the existing load combinations were evaluated to demonstrate that the allowable stress criteria were still being met. [[ ]]. In all other cases, because the FIV loads determined from the pre-installation analysis (Reference 17)] or QC2A analysis (Reference 17A) are greater than the new loads, re-evaluation is not required.

[[

]]

Note, the dryer finite element model from References 17 and 17A was modified slightly for this analysis. [[

]]

Results from Table 7-2 show that all stresses for the ASME Load Combinations meet the specified allowable stress criteria [[

]] The ASME Code combination results are summarized in Table 7-3.

[[

]].

Table 7-1 ASME Load Combinations

Load Case	Service Condition	Load Combination	Notes
A	Normal	DW + DPn ± FIVn	
B1	Upset	DW + DPn + TSV1 ± FIVn	
B2	Upset	DW + DPn + TSV2	1
B3	Upset	DW + DPu ± FIVu	2
B4	Upset	DW + DPn ± OBE ± FIVn	
D1A	Faulted	DW + DPn + $[SSE^2 + AC1^2]^{1/2}$ ± FIVn	3
D1B	Faulted	DW + $[DPf1^2 + SSE^2]^{1/2}$	3, 4
D2A	Faulted	DW + DPn + AC2 ± FIVn	
D2B	Faulted	DW + DPf2	4

Notes:

1. In the Upset B2 combination, FIVn is not included because the reverse flow through the steam lines will disrupt the acoustic sources that dominate the FIVn load component.
2. The relief valve opening decompression wave load (acoustic) associated with an inadvertent or stuck-open relief valve (SORV) opening is bounded by the TSV acoustic load (Upset B1); therefore, the acoustic phase of the SORV load need not be explicitly evaluated or included in the Upset load combination B3.
3. Loads from independent dynamic events are combined by the square root sum of the squares method.
4. In the Faulted D1B and D2B combinations, FIVn is not included because the level swell in the annulus between the dryer and vessel wall will disrupt the acoustic sources that dominate the FIVn load component.

AC1 = Acoustic load due to Main Steam Line Break (MSLB) outside containment, at the Rated Power and Core Flow (Hi-Power) Condition.

AC2 = Acoustic load due to Main Steam Line Break (MSLB) outside containment, at the Low Power/High Core Flow (Interlock) Condition.

DW = Dead Weight

DPn = Differential Pressure Load During Normal Operation
DPu = Differential Pressure Load During Upset Operation
DPf1 = Differential Pressure Load in the Faulted condition, due to Main Steam Line Break Outside Containment at the Rated Power and Core Flow (Hi-Power) condition
DPf2 = Differential Pressure Load in the Faulted condition, due to Main Steam Line Break Outside Containment at the Low Power/High Core Flow (Interlock) condition
FIVn = Flow Induced Vibration Load (zero to peak amplitude of the response) during Normal Operation
FIVu = Flow Induced Vibration Load (zero to peak amplitude of the response) during Upset Operation
OBE = Operating Basis Earthquake
SSE = Safe Shutdown Earthquake
TSV1 = The Initial Acoustic Component of the Turbine Stop Valve (TSV) Closure Load (Inward load on the outermost hood closest to the nozzle corresponding to the TSV closure)
TSV2 = The Flow Impingement Component (following the Acoustic phase) of the TSV Closure Load; (Inward load on the outermost hood closest to the nozzle corresponding to the TSV closure)

Table 7-2 ASME Code Combinations: Stress Summary Levels A and B

[[

Table 7-2 (cont'd) ASME Code Combinations: Stress Summary Level D.

]]

Table 7-3 ASME Code Margins

[[

]]

8. Conclusions

The fatigue evaluation of the dryer was based on time history analyses from acoustic circuit model loads using in-plant steam line measurements. The loads were run for nominal and +/-10% frequency shifts. Results of all three fluctuating pressure cases show that the replacement dryer is structurally adequate from a fatigue standpoint at EPU conditions. All locations in the steam dryer are below the design fatigue allowable stress limit as defined in the GENE Design Criteria (Reference 1). All stresses from the ASME service level A (normal), B (upset), and D (faulted) loads are within the ASME Code allowable stress limits for primary stresses. Based on these results, the Quad Cities Unit 1 replacement dryer is structurally adequate for EPU (2957 MWt) conditions.

9. References

[1] "Steam Dryer Design Specification" (DS) 26A6266, Revision 3; "Design Specification Data Sheet" (DSDS) 26A6266AB, Revision 5.

[2] NA

[3] GENE Material Specification: 26A6273, Revision 4.

[4] GENE Fabrication Specification: 26A6274, Revision 6.

[5] Memo F411/0212 from Continuum Dynamics, Inc. to Alex Pinsker dated July 2, 2005, QC1 High Resolution Loads (TC15A_2 @ 2887 MWt), QC1-D Loads.

[5A] Memo F411/0207 from Continuum Dynamics, Inc. to Alex Pinsker dated June 22, 2005, QC1 Dryer Loads at TC15A (2887 MWt) and TC12, QC1-B Loads.

[6] QDC-05-029, Revision 1, "Quad Cities Startup Testing High Resolution Loads from Continuum Dynamics Inc. (CDI)", July, 2005. (QC1-D Loads)

[6A] Exelon Report AM-2005-004, Rev 0 "Acoustic Circuit Benchmark Quad Cities Unit 2 Instrumented Steam Path Final Model Revision 930 MWe Power Level", dated July 22, 2005.

[6B] Exelon Report AM-2005-007, Rev 0 "Assessment of Revised QC1 Minimum Error ACM Loads Using All MSL Strain Gages"..

[6C] C.D.I. Technical Note No. 05-34, Test Condition TC15a Load Comparison for Quad Cities Unit 1, July 2005.

[6D] CDI Report No. 05-10 "Benchmarking of Continuum Dynamics, Inc. Steam Dryer Load Methodology Against Quad Cities Unit 2 In-Plant Data" dated July 2005.

[7] "Fatigue Stress Threshold Criteria for use in the Exelon Replacement Steam Dryer", GENE 0000-0034-8374, October 2004.

[8] ASME Code, Section II, 1998 Edition with 2000 Addenda.

[9] American Society of Mechanical Engineers (ASME) Boiler and Pressure Vessel Code, Section III, 1998 Edition with 2000 Addenda.

[10] "Recommended Weld Quality and Stress Concentration Factors for use in the Structural Analysis of the Exelon Replacement Steam Dryer", GENE 0000-0034-6079, February 2005.

[11] ANSYS Release 8.1, ANSYS Incorporated, 2002.

[12] "Test and Analysis Report Quad Cities New Design Steam Dryer Dryer #1 Experimental Modal Analysis and Correlation with Finite Element Results," LMS- Engineering Innovation, April 22, 2005

[13] "QC1 Modified Model-Modification & Design Notes", DRF GE-NE-0000-0043-4004, Section, GENE 0000-0043-4008, July 2005.

[14] "Exelon Steam Dryer Dynamic Time History Analyses," GENE 0000-0039-3540, April 2005.

[15] "Exelon Steam Dryer Replacement Program – 2% Structural Damping for Seismic and Non-Seismic (FIV) Dynamic Analysis", Letter Report dkh0503, March 18, 2005.

[16] "Quad Cities 1 & 2 Steam Dryer Replacement- 4% Structural Damping for Vane Bank FIV Analysis," GENE 0000-0039-4768, April 21, 2005.

[17] "Quad Cities Units 1 and 2 Replacement Steam Dryer Analysis Stress, Dynamic, and Fatigue Analyses for EPU Conditions," DRF GE-NE-0000-0034-3781, Section GE-NE-0000-0039-4902, Revision 0, April 2005.

[17A] "Quad Cities Unit 2 Replacement Steam Dryer Stress and Fatigue Analysis Based on Measured EPU Conditions," DRF GE-NE-0000-0043-3105-01, Section GE-NE-0000-0043-3119, Revision 0, July 2005.

[18] "Exelon Steam Dryer Replacement – 4% Structural Damping for Dryer Skirt FIV Analysis," DRF GE-NE-0000-0039-4747, Section GE-NE-0000-0041-9435, Revision 0, June 2005.

[19] "Exelon Steam Dryer Replacement – 2% Structural Damping Seismic & FIV Loads," DRF GE-NE-0000-0039-4747, Section GE-NE-0000-0039-4749, Revision 1, June 2005.

[20] "Weld Inspection Calculations for Replacement Dryer," DRF GE-NE-0000-0039-4028, Section GE-NE-0000-0039-4057, Revision 0.

[21] "Trough Drain Pipe Weld Disposition," DRF GE-NE-0000-0039-4028, Section GE-NE-0000-0039-5878, Revision 0.

[22] "Evaluation of ASME Load Combinations with New (Post-Installation) FIV Loads & Trough/Pipe Weld Evaluation for EPU Power for QC1," DRF GE-NE-0000-0042-4796, Section GE-NE-0000-0043-6796, Revision 0.

[22A] QC1 Stress Comparison and Evaluation Table," DRF GE-NE-0000-0043-0470, Section GE-NE-0000-0043-6788, Revision 0.

[23] "Evaluation of New FIV Loads in ASME Load Combinations and Weld Inspection Calcs for QC2A," DRF GE-NE-0000-0042-0176, Section GE-NE-0000-0042-0606, Revision 0.

[24] "Two Second Interval NRC Explanation," DRF GE-NE-0000-0041-3989, Section GE-NE-0000-0042-2761, Revision 0.

[25] "Additional Justification of Power Law Scaling of Stresses in Quad Cities Unit 2 Steam Dryer to Final EPU Level of 2957 MWt", eDRF 0000-0041-9352, eDRF Section 0000-0043-2935.

[[

]]

Figure 3-1 Maximum Applied Pressure (QC1D Loads)

[[

]]

Figure 3-2 Maximum Applied Pressure (QC1B Loads)

[[

]]

Figure 6-1 Replacement Dryer Shell Finite Element Model

[[

]]

Figure 6-1A Dryer Skirt Water Elements for Superelement Generation

[[

]]

Figure 6-1B FEA Model, Modified Components for Mounting Block

[[

]]

Figure 6-1C FEA Model Changes at Trough Attachment to Outer Hood

[[

]]

Figure 6-1D FEA Model, Closure Plate with Stiffener

[[

]]

Figure 6-2 Dryer Finite Element Model Boundary Conditions

[[

]]

Figure 6-3 Finite Element Model without Super Elements

[[

]]

Figure 6-4 Load Frequency Content – Hood & Vane Cap (QC1D Loads)

[[

]]

Figure 6-4A Load Frequency Content - Skirt (QC1B Loads)

[[

]]

Figure 6-5 Skirt Frequency: [[ ]]

[[

]]

Figure 6-6 Skirt Frequency: [[ ]]

[[

]]

Figure 6-7 Skirt Frequency: [[ ]]

[[

]]

Figure 6-8 Skirt Frequency: [[ ]]

[[

]]

Figure 6-9 Skirt Frequency: [[ ]]

[[

]]

Figure 6-10 Skirt Frequency: [[ ]]

[[

]]

Figure 6-11 Skirt Frequency: [[ ]]

[[

]]

Figure 6-12 Outer Hood Frequency: [[ ]]

[[

]]

Figure 6-13 Frequency Response QC1D –10%: Hoods & Vane Cap

[[

]]

Figure 6-14 DELETED

[[

]]

Figure 6-15 Frequency Response QC1D Nominal: Hoods & Vane Cap

[[

]]

Figure 6-16 Frequency Response QC1D Nominal: Skirt

[[

]]

Figure 6-17 Frequency Response QC1D +10%: Hoods & Vane Cap

[[

]]

Figure 6-18 Frequency Response QC1B +10% Case [[ ]]: Skirt

[[

]]

Figure 6-19 Time History Stress Intensity Results: Vane Cap Flat Portion

[[

]]

Figure 6-20 Time History Stress Intensity Results: Outer Hood

[[

]]

Figure 6-21 Time History Stress Intensity Results: Tie Bars

[[

]]

Figure 6-22 Time History Stress Intensity Results: Frames

[[

]]

Figure 6-23 Time History Stress Intensity Results: Troughs

[[

]]

Figure 6-24 Time History Stress Intensity Results: Gussets

[[

]]

Figure 6-25 Time History Stress Intensity Results: Vane Cap Curved Part

[[

]]

Figure 6-26 Time History Stress Intensity Results: Inner Hoods

[[

]]

Figure 6-27 Time History Stress Intensity Results: Closure Plates

[[

]]

Figure 6-28 Time History Stress Intensity Results: T-Section Webs

[[

]]

Figure 6-29 Time History Stress Intensity Results: T-Section Flanges

[[

]]

Figure 6-30 Time History Stress Intensity Results: Vane Bank Outer End Plates

[[

]]

Figure 6-31 Time History Stress Intensity Results: [[ ]]

[[

]]

Figure 6-32 Time History Stress Intensity Results: Cross Beams

[[

]]

Figure 6-33 Time History Stress Intensity Results: Support Ring

[[

]]

Figure 6-34 Time History Stress Intensity Results: Trough Ledge

[[

]]

Figure 6-35 Time History Stress Intensity Results: Trough Brace Gusset

[[

]]

Figure 6-36 Time History Stress Intensity Results: Inner Trough Brace

[[

]]

Figure 6-37 Time History Stress Intensity Results: Vertical Support Plates

[[

]]

Figure 6-38 Time History Stress Intensity Results: Center Support Gussets

[[

]]

Figure 6-39 Time History Stress Intensity Results: Center Plate

[[

]]

Figure 6-40 Time History Stress Intensity Results: Trough End Stiffeners

[[

]]

Figure 6-41 Time History Stress Intensity Results: Gusset Shoe at Cross Beams

[[

]]

Figure 6-42 Time History Stress Intensity Results: Frame to Cross Beam Gussets

[[

]]

Figure 6-43 Time History Stress Intensity Results: Lifting Lug Guide

[[

]]

Figure 6-44 Weld Factors to Use with Finite Element Results

ENCLOSURE 2

Attachment 12

Structural Integrity Associates Letter KKF-05-037, "Comparison of Quad Cities Unit 1 and Quad Cities Unit 2 Main Steam Line Strain Gage Data," Revision 1, dated July 18, 2005

Structural Integrity Associates, Inc.

6855 S. Havana Street
Suite 350
Centennial, CO 80112-3868
Phone: 303-792-0077
Fax: 303-792-2158
www.structint.com
kfujikawa@structint.com

July 18, 2005
SIR-05-223 Revision 1
KKF-05-037

Mr. Robert Stachniak
Exelon Nuclear
4300 Winfield Road
Warrenville, IL 60555

Subject: Comparison of Quad Cities Unit 1 and Quad Cities Unit 2 Main Steam Line Strain Gage Data

Dear Rob:

This letter report contains a comparison of the Quad Cities Unit 1 (QC1) and Quad Cities Unit 2 (QC2) strain gage data obtained during the power ascensions that occurred during Spring 2005.

Background

Main steam line strain gage data was obtained during the June 2005 power ascension at QC1 [1]. This data was used as input to the acoustic line analysis that determines the forcing function on the steam dryer. Prior to the power ascension, strain gages were installed on each of the four main steam lines (MSLs) at two axial locations. At each axial location two strain gage pairs are formed with two gages 180° apart. The two gages are connected to a Wheatstone bridge in the ½ bridge configuration where the two strain gages will sum to provide higher sensitivity and provide cancellation of the Poisson effect due to pipe bending. Strain gage were also installed on the main steam lines at QC2 using the same ½ bridge configuration and locations as QC1. Figures 1a and 1b shows sketches of the strain gage locations for QC1 and QC2 MSL A, B, C, and D.

Objective

The objective of this letter report is to compare the strain gage measurements between the two units and determine the degree of similarity between the units structural response and pressure excitation. The data has been analyzed for frequency content (rms spectra), time history characteristics (rms, maximum, and minimum), and relationship between orthogonal planes (Cross Spectral Density). Figures 1a and 1b provide sketches of the four MSL for both units with the strain gage locations designated.

Combined Spectra for QC1 and QC2

Figures 2 through 9 provide the combined spectra (individual ½ or ¼ bridge with their average) for the 651' and 624' elevations on each MSL. The figures provide the QC1 and QC2 spectra for the unique location for purposes of visual observations. A review of the spectra at each location provides the following observations. In addition, Table 1 summarizes the observations.

1. The profiles of the spectra are similar in that the overall amplitudes across the spectrum are the same except for QC1 A, C and D 651 where each has relatively higher amplitudes at 78.6 and 157.7 Hz. For example, the frequency spectra for D624 (Figure 9) has a very similar shape and amplitudes for both QC1 and QC2; both units at this location have large amplitudes.

2. QC1 has typically a very broad unique peak at 157.7 Hz whereas QC2 has 3 to 5 narrower peaks in the range of 150 to 160 Hz (see Figure 2 for a comparison of QC1 to QC2).

3. The predominant frequencies occurred in most of the spectra for QC1 at 23, 78.6, 138.7 and 157.7 Hz and for QC2 at 23, 139.2, 150.9 and 154.8 Hz.

4. A review of Table 1 shows that QC1 has the highest amplitudes in the low frequency range (15 to 35 Hz) and in the higher frequency range (135 to 160 Hz) the high amplitudes are evenly split between QC1 and QC2. The most number of peaks in the 135 to 160 Hz range is always QC2.

RMS Values for QC1 and QC2

Table 2 provides the RMS, Max-Min and Average amplitudes for the time histories of individual strain gage bridges and the average of the orthogonal bridges for each unit. The RMS is the root-mean-square value of the filtered strain time history over a bandwidth of 2 to 200 Hz in units of $\mu\varepsilon_{rms}$. The Max-Min value is the Maximum positive value minus the Maximum negative value over a bandwidth of 2 to 200 Hz for the entire time history. The Max-Min value is conservatively referred to in this document, as peak-to-peak, whereas the term peak-to-peak typically refers to consecutive peaks and valleys in the time history. The Average value is the average of the In-plane (IP) and the Out-of-plane (OP) time histories. The RMS, max-min, and average are characteristics of the time history, not the frequency spectra.

Table 2 is graphically portrayed in Figure 10 as a bar chart. General observations of Table 2 (Figure 10):

1. Many of the locations have similar RMS responses except for QC1-A651IP, C651IP, C651OP and D624IP and QC2-A624IP, A624OP, and D624OP where there are larger differences. When averaged, the RMS values are much closer except for a large amplitude difference for A624avg.

2. In Table 2, the averages of all the RMS/Max-Min values, and the IP and OP values, separately, are provided for both QC1 and QC2 along with the averages of the average RMS and Max-Min (M-M). Other than the average of the average RMS and Max-Min, QC1 and QC2 are extremely close in all the statistical values. For the averaged RMSavg, QC2 is 18% greater than QC1.

3. For both the RMS_{avg} and $Max\text{-}Min_{avg}$ (M-Mavg) the OP is 30 to 40% greater for both units.

4. Figure 11 is a graph of the ratios of the RMS averages (Table 2) for the 651 to 624 elevations for each unit. The results show that the ratios are similar for each unit. This figure shows that the 624 response is higher than the 651 response, except for MSL C. For MSL C, the 651 response is almost twice as large as the 624 response for both units.

Half Bridge Phase Relationships

The cross spectral density (CSD) between the two orthogonal bridges for all locations was calculated for both units. If only a quarter bridge was available at a location, it was used in lieu of the half bridge. The cross spectral density is calculated from the power spectral density (PSD) for each orthogonal bridge; the two complex functions are multiplied and graphed as magnitude and phase versus frequency, where the magnitude is proportional to the strain squared.

The magnitude accentuates frequencies that are common to both bridges. The phase provides the relationship in time between the two bridges at each frequency; i.e., one bridge leads or lags the other by the phase. Figures 12 and 13 are typical CSD plots for QC1 and QC2, respectively. For each figure the top plot is the relative magnitude and the bottom is phase.

From similar figures for each elevation, the CSD magnitude and phase at predominate frequencies were tabulated in Table 3. A quick overview of the table indicates that the phase varies significantly for the same frequency at different locations. Figure 14 provides a comparison of the phase for 157.7 Hz (QC1) and 154.8 Hz (QC2) for each location. The plot shows the absolute phase since the polarity only indicates which bridge is leading or lagging, but in averaging the two bridges the effect is the same.

It is observed that at each location except A651 the phase is relatively close in amplitude in the 10 to 40° range. For example the effect on amplitude of averaging two sine waves with the same amplitude 45 degrees out of phase is approximately an 8% decrease in amplitude, for a 90 degree phase difference it is ~30%. The effect is proportional to the cosine of the phase-angle/2.

Figure 15 provides a graph of the CSD magnitude for the same frequencies discussed above. Note the CSD magnitude is plotted on a log scale. Except for A624 the QC1 magnitude is always greater and sometimes significantly greater for the 157.7 Hz than the QC2 154.8 Hz

response. The higher CSD magnitude indicates a stronger response over the entire time history between the two orthogonal amplitudes at the 157.7 Hz response.

The other frequencies in Table 3 did not provide enough information for comparison of the units or did not have a counterpart in each unit.

QC2 Quarter Bridge Strain Gage Data

The QC2 strain gages did not experience the same number of failures that occurred at QC1, thus, ¼ bridge data was recently obtained at QC2. On July 6, 2005, Exelon recorded the ½ bridge data for main steam lines B and C, and then reconfigured the half bridges on the same main steam lines into quarter bridges and recorded ¼ bridge data on July 7, 2005 [4]. An initial review of this data shows that all the strain gages are functioning.

For QC2 MSL C 651, the ¼ bridge data was combined for the IP (S31/33) and OP (S32/34) to create ½ bridge results. Figures 16 and 17 show the equivalent ½ bridge results based on the ¼ bridge data. A fair comparison of the combined ¼ bridge results to the actual ½ bridge data was not possible as there were no two datasets gathered sufficiently close in time and power level.

The effect of losing strain gages in QC1 and using ¼ bridges with the ½ bridge to produce averages appears by the close results between the units to be insignificant; this is confirmed by using the QC2 ¼ bridge data. A review of the QC2 ¼ bridge data confirms that the combination of a ¼ bridge and a ½ bridge (Figure 18) produces results that are almost identical to the averaged two equivalent ½ bridge results (Figure 19). Other combinations of ¼ bridge strain gages was also performed for QC2 MSL C 651 to investigate the effect of losing more than one strain gage at a location. Since QC1 MSL C 651 S31 had failed, the remaining combinations of two ¼ bridges that include IP and OP are S32/33 and S33/34. Thus, the QC2 MSL C 651 combination of S32/33 and S33/34 was generated and is shown in Figures 20 and 21, respectively. A review of the S32/33 combination shows that the results are similar to the equivalent two ½ bridge combination (Figure 18), whereas the S33/34 combination shows some evidence of missing frequency content (e.g., 154.8 Hz and 161 Hz).

The four functioning gages per elevation on QC2 MSL C allowed the computation of amplitudes based PSDs and phase angles based CSDs using S31 as a reference. The two frequencies (150.9 Hz and 154.8 Hz) were selected based on statements made earlier in this report (Page 2) and the resulting amplitude and phase values are listed in the table below.

	150.9 Hz		154.8 Hz	
Location	Amplitude	Phase	Amplitude	Phase
	$uSTR^2/Hz$	deg	$uSTR^2/Hz$	deg
S31 (reference)	0.104	0	0.017	0
S32	0.115	67	0.032	19
S33	0.233	69	0.059	-7
S34	0.105	84	0.033	177
S35	0.004	-154	0.025	44
S36	0.044	-42	0.008	127
S35A	0.051	144	0.008	-135
S36A	0.028	-48	0.015	5

The resulting pipe cross-sectional movement is graphically represented on Figures 23 and 24. The point number assignments used in these plots and their relation to the strain gages are shown on Figure 22. The upper elevation (651) shows more movement at these frequencies than the lower (621) elevation. This may be in part due to the fact that this location is closer to the vessel and may be exposed to more dynamic fluid behavior internally. At 150.9 Hz, El 651 appears to be in a breathing mode while El 621 is showing a small amount of ovaling. At 154.8 Hz, El 651 appears to be an ovaling mode while El 621 appears to be closer to a breathing mode at much lower amplitudes.

Discussion

The MSL piping for both units are for all intents and purposes identical except for some valve locations and the HPCI connection. The MSL pipe characteristics (pipe size, material, configuration in the plant and in relationship to the vessel) are the same, therefore the dynamic response will be similar. In other words the piping's dynamic response (transfer function) is identical. That is for similar excitation (internal dynamic pressure) the pipes will respond the same and provide the same vibration and acoustic measurements.

The strain measurements were designed to measure only hoop strain which can consist of zero mode, concentric expansion and contraction and breathing modes such as ovaling and clover leaf modes. The bending mode Poisson effect is canceled by the bridge configuration for two gages, but it appears from the data that it is not significant if a ¼ bridge is used, since all the major frequencies can be accounted for in both the ½ and ¼ bridges.

The zero mode and ovaling mode natural frequencies were calculated to be greater than 300 Hz, therefore responses below 300 Hz would be considered a 'forced vibration', a non-resonant vibration. The response of a structure to a forced vibration that is below the first mode of vibration would be in a mode shape similar to the first mode, assuming the first mode is the least stiff mode (path of least resistance).

For hoop strain, the least stiff mode would be the ovaling mode. Assuming a uniform load at each axial location the pipe's hoop strain would follow the pattern of an oval. In orthogonal planes the pipes should be 180 degrees out of phase. For non-uniform loading both circumferentially and axially, the shape may not be a pure oval and may change along the length of the pipe depending on the loading distribution.

The results of the CSD analysis did not show a uniform response at the frequencies of interest by the variation of the phase relationships, but did show similar responses at the same pipe/elevation combination. This would indicate that the loading of the pipes are similar for both units yet are non-uniform both axially and circumferentially.

The structural and loading similarities are also shown in the results from the statistical averaging of the RMS and max-min values for the individual bridges. The most telling result that shows this similarity is the RMS averages provided below in Table 2. In comparing QC1 to QC2 the difference in the values for each category are less than 8%. Since several of the QC1 results include the ¼ bridges, this implies that the effect of ¼ versus ½ bridge may be minimal. A more detailed study of the ¼ bridges available for QC1 and QC2 would provide additional insight into the results of using ¼ versus ½ bridge strains.

Also, included in the table are the relationship between the OP and IP bridges with OP showing a 30 to 40% increase in overall response than the IP and again consistent in both plants.

	Unit 1		Unit 2	
	RMS	Max-Min	RMS	Max-Min
Total rms	8.993	72.515	9.456	68.968
RMS Avg	0.562	4.532	0.591	4.310
RMS IP avg	0.493	3.748	0.498	3.617
RMS OP avg	0.631	5.316	0.684	5.004

The Max-Min values are not considered a statistical representative of a time history, since they are a single, maximum point picked from the positive and negative sides of the time history, yet, even these are consistent. The implication of both units having the RMS and max-min similarity is that the excitation forces for both units are similar with similar loading.

The primary difference in the strain data observed between the units is the actual frequency content of the signals. The area where this is most obvious is in the 150 to 160 Hz range where QC1 is observed to have a single strong response at 157.7 Hz and QC2 has several frequencies in this frequency range, particularly 150.9 and 154.8 Hz. The 154.8 Hz seems to have many of the same characteristics as the 157.7 Hz, particularly, the phase relationships for the pipe/elevation combination, but from the CSD magnitude it appears that the QC1 157.7 Hz response is much stronger than the corresponding 154.8 Hz of QC2.

Another difference between QC1 and QC2 is the strain response at 78.6 Hz observed in three locations in QC1 at elevation 651 for MSL A, C, and D. The pressure at this frequency may contribute to the vibration response of the steam dryer.

Conclusion

In conclusion, the strain measurements acquired at both QC1 and QC2 appear to be consistently similar implying a similarity in both the pressure excitation of the piping and the response to the loading. The consistency provides a measure of the quality of the data for both units. The strain response at Elevation 624 is larger than that of Elevation 651 for both units except for MSL C. This phenomenon is seen at both units. The consistencies between the main steam line strain data shows that even though there are some structural differences between the two units, both units appear to respond the same due to the pressure excitation of the piping.

The effect of losing strain gages in QC1 and using ¼ bridges with the ½ bridge to produce averages appears by the close results between the units to be insignificant. A review of the QC2 ¼ bridge data confirms that the combination of a ¼ bridge and a ½ bridge produces results that are almost identical to the averaged two equivalent ½ bridge results.

A further understanding of the structural response of the pipe and the pressure distribution in the pipe has been performed which shows that some local shell phenomena are occurring at each strain gage location.

If you have any questions, please do not hesitate to contact me at (303) 792-0077.

Prepared By:

Lawrence S. Dorfman
Associate

Reviewed By:

Karen K. Fujikawa, P.E.
Associate

Approved By:

Karen K. Fujikawa, P.E.
Associate

kkf

REFERENCES:

1. Exelon Document No. TIC-1252, Revision 0, "Quad Cities Unit 1 Power Ascension Test Procedure for the Reactor Vessel Steam Dryer Replacement," SI File No. EXLN-20Q-201.

2. Exelon TODI No. ODC-05-0225, "Main Steam Line Strain Gauge Failures During Quad Cities Unit 1 Startup Testing," SI File No. EXLN-20Q-201.
3. Structural Integrity Associates, Inc. Report SIR-05-208 Revision 2, "Quad Cities Unit 1 Main Steam Line Strain Gage Reductions," SI File No. EXLN-20Q-401.
4. E-mail, from Brian Strub (Exelon) to Karen Fujikawa (SI), dated 7/7/05, "Ibackup has QC2 Half Bridge and Quarter Data," SI File No. EXLN-20Q-204.

cc: EXLN-20Q-402
Chuck Alguire (Exelon)
Guy DeBoo (Exelon)
Roman Gesior (Exelon)
Keith Moser (Exelon)
Kevin Ramsden (Exelon)
Brian Strub (Exelon)
K. Rach (SI)
G. Szasz (SI)

Table 1. Observations of Combined Spectra

		Max Avg Amplitude		Most Peaks 135 - 165
Location	Profile	15 - 35 hz	135-160 Hz	Hz
A651	similar*	U1	U1	U2
A624	similar	U2	U2	U2
B651	similar	=	U2	U2
B624	similar	U1	U1	U2
C651	similar*	U1	U1	U2
C624	similar	U1	U1	U2
D651	similar*	U2	U2	U2
D624	similar	=	U2	U2

*** Similar other than QC1-78.6 and 157.7 Hz amplitude**

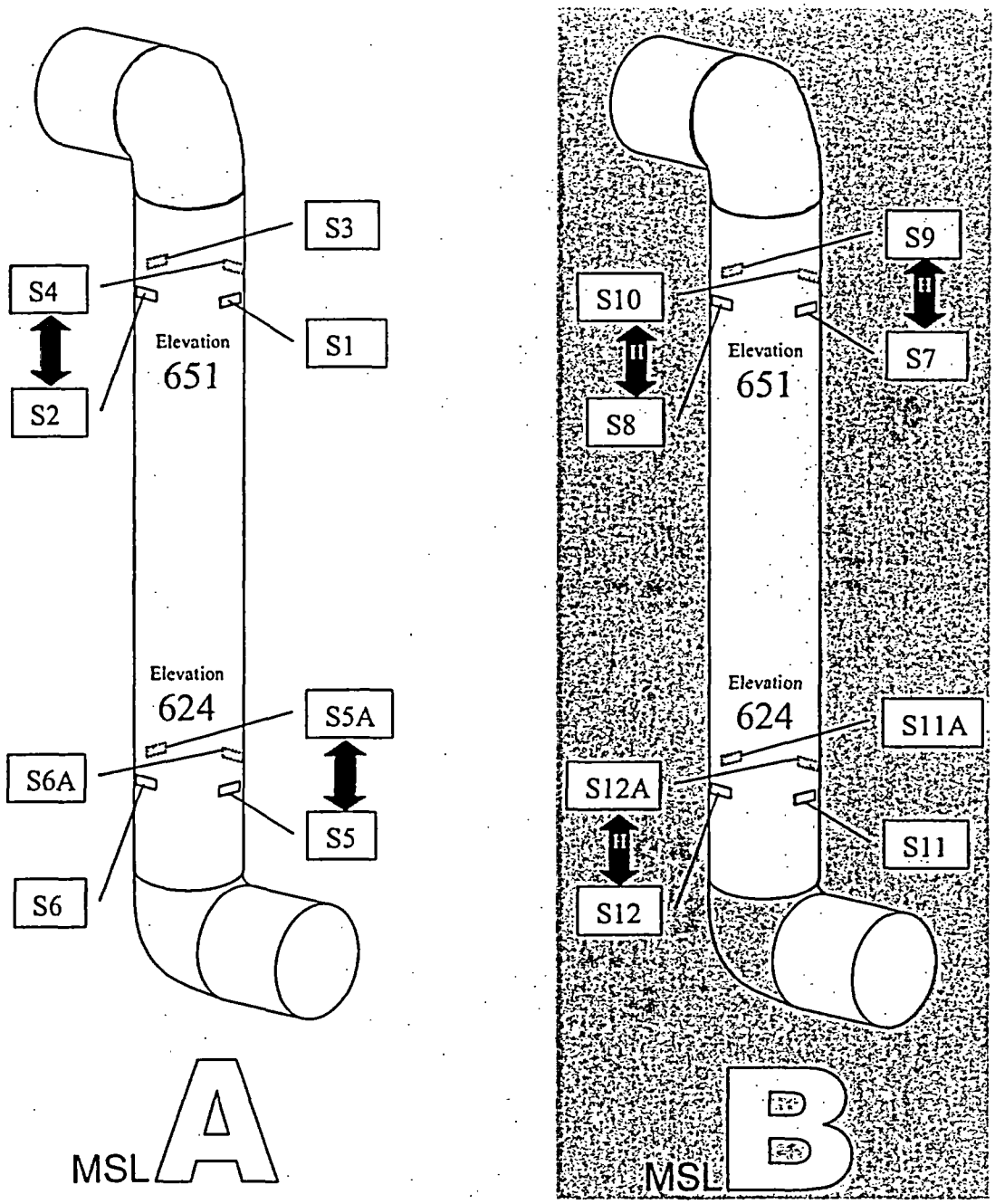

Figure 1a. Location of Strain Gages on QC1 and QC2 MSLs A and B

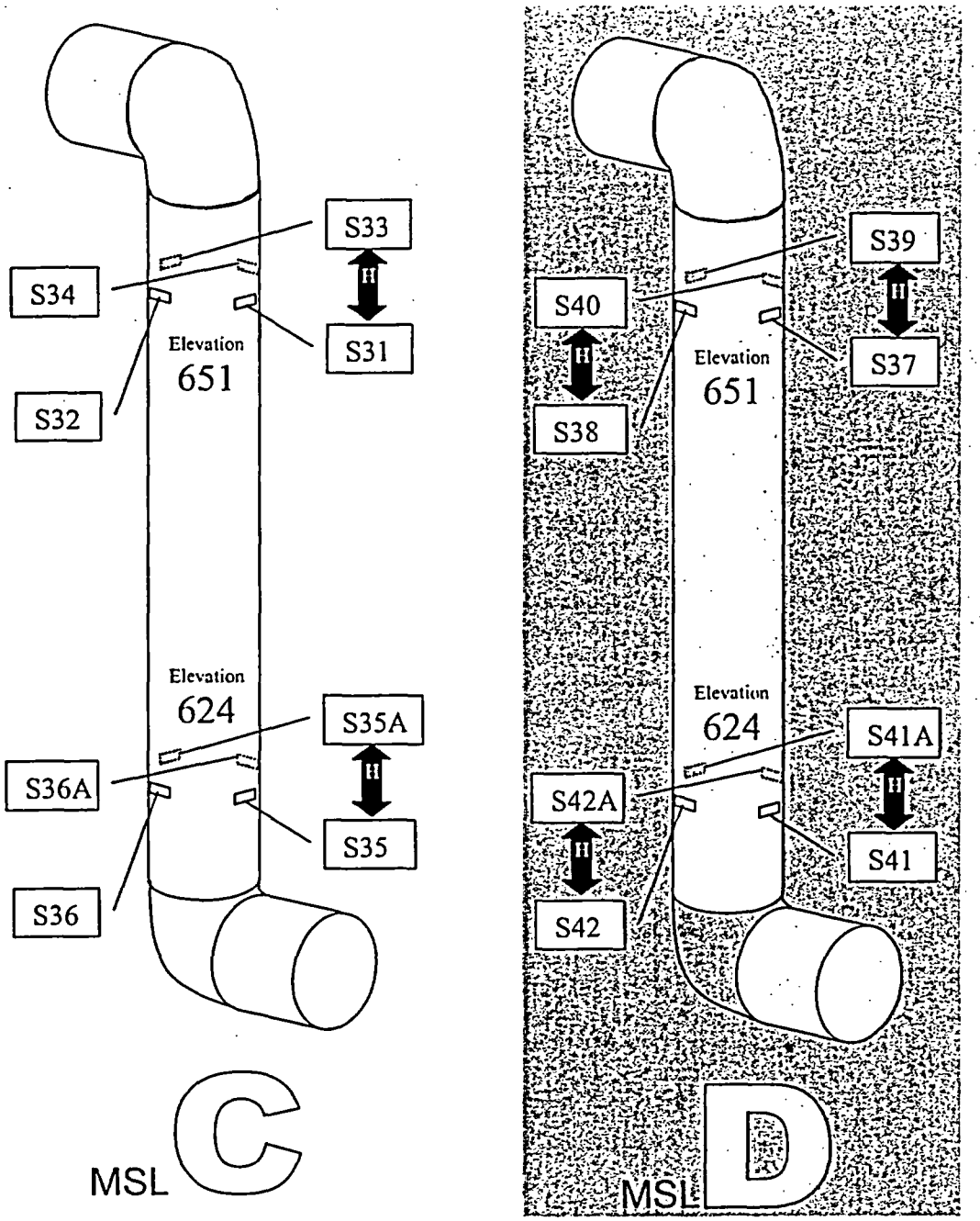

Figure 1b. Location of Strain Gages on QC1 and QC2 MSLs C and D

Table 2. QC1 and QC2 RMS and Max-Min Values

Unit 1					Unit 2				
Description	RMS	Max-Min	RMSavg	M-Mavg	Description	RMS	Max-Min	RMSavg	M-Mavg
S1 A651	0.678	4.483	--------	--------	S1/S3 A651	0.305	2.579	--------	--------
S2/S4 A651	0.459	4.275	0.490	3.660	S2/S4 A651	0.422	3.334	0.572	4.028
S5/S5A A624	0.303	2.530	--------	--------	S5/S5A A624	0.914	6.242	--------	--------
S6A A624	0.885	8.120	0.876	5.730	S6/S6A A624	1.223	8.946	1.151	6.278
S7/S9 B651	0.242	2.177	--------	--------	S7/S9 B651	0.323	2.624	--------	--------
S8/S10 B651	0.361	3.004	0.216	1.849	S8/S10 B651	0.416	3.529	0.333	2.529
S11 B624	0.314	2.911	--------	--------	S11/S11A B624	0.319	2.886	--------	--------
S12/S12A B624	0.353	3.138	0.340	5.450	S12/S12A B624	0.337	3.186	0.399	3.251
S33 C651	0.401	3.269	--------	--------	S31/S33 C651	0.250	2.245	--------	--------
S32/S34 C651	1.110	9.629	0.690	5.800	S32/S34 C651	0.593	4.462	0.593	4.462
S35/S35A C624	0.371	3.011	--------	--------	S35/S35A C624	0.272	2.236	--------	--------
S36A C624	0.444	3.774	0.330	1.270	S36/S36A C624	0.399	3.251	0.319	2.886
S37/S39 D651	0.256	2.381	--------	--------	S37/S39 D651	0.449	3.847	--------	--------
S38/S40 D651	0.397	3.524	0.237	2.166	S38/S40 D651	0.572	4.028	0.344	2.919
S41/S41A D624	1.382	9.221	--------	--------	S41/S41A D624	1.151	6.278	--------	--------
S42/S42A D624	1.036	7.066	0.325	2.529	S42/S42A D624	1.512	9.295	0.427	3.346
		Avg	0.438	3.557			Avg	0.517	3.712
Total rms	8.993	72.515			**Total**	9.456	68.968		
RMS Avg	0.562	4.532			**RMS Avg**	0.591	4.310		
RMS IP avg	0.493	3.748			**RMS IP avg**	0.498	3.617		
RMS OP avg	0.631	5.316			**RMS OP avg**	0.684	5.004		

Table 3a. QC1 Cross Spectral Density Magnitude and Phase

QC1	Frequency, Hz	157.70		141		139.20		78.6		22.95	
Rec 1		Amp	Deg	Amp	Deg	Amp	Deg	Amp	Deg	Amp	Deg
Ch	Description										
1	S1 A651										
2	S2/S4 A651	0.16	82							0.01	4
3	S5/S5A A624										
4	S6A A624	0.08	141							0.008	-0.53
5	S7/S9 B651										
6	S8/S10 B651	0.018	106	0.006	-100					0.004	6
7	S11 B624										
8	S12/S12A B624	0.03	-7	0.01	55					0.001	109
9	S33 C651										
10	S32/S34 C651	0.16	-61			0.04	112	0.01	-66	0.003	14
Rec 2											
Ch											
2	S35/S35A C624										
3	S36A C624	0.012	-122			0.08	-10	0.001	-150		
4	S37/S39 D651										
5	S38/S40 D651	0.03	-58					0.003	149	0.001	-20
6	S41/S41A D624										
7	S42/S42A D624	0.166	-171							0.04	158

Table 3b. QC2 Cross Spectral Density Magnitude and Phase

QC2	Frequency, Hz	154.80		150.9		139.20		78.6		22.95	
Rec 1		Amp	Deg	Amp	Deg	Amp	Deg	Amp	Deg	Amp	Deg
Ch	Description										
1	S1/S3 A651										
2	S2/S4 A651	0.09	-9	0.01	101						
3	S5/S5A A624										
4	S6/S6A A624	0.47	-105	1.1	-170					0.04	171
5	S7/S9 B651										
6	S8/S10 B651	0.01	155	0.06	51						
7	S11/S11A B624										
8	S12/S12A B624	0.013	25	0.02	169						
9	S31/S33 C651										
10	S32/S34 C651	0.028	80	0.01	-132	0.01	-92				
Rec 2											
Ch											
2	S35/S35A C624										
3	S36/S36A C624	0.001	96	0.002	20	0.001	3				
4	S37/S39 D651										
5	S38/S40 D651	0.002	-93	0.03	23						
6	S41/S41A D624										
7	S42/S42A D624	0.002	-161	0.03	-135	0.009	10				

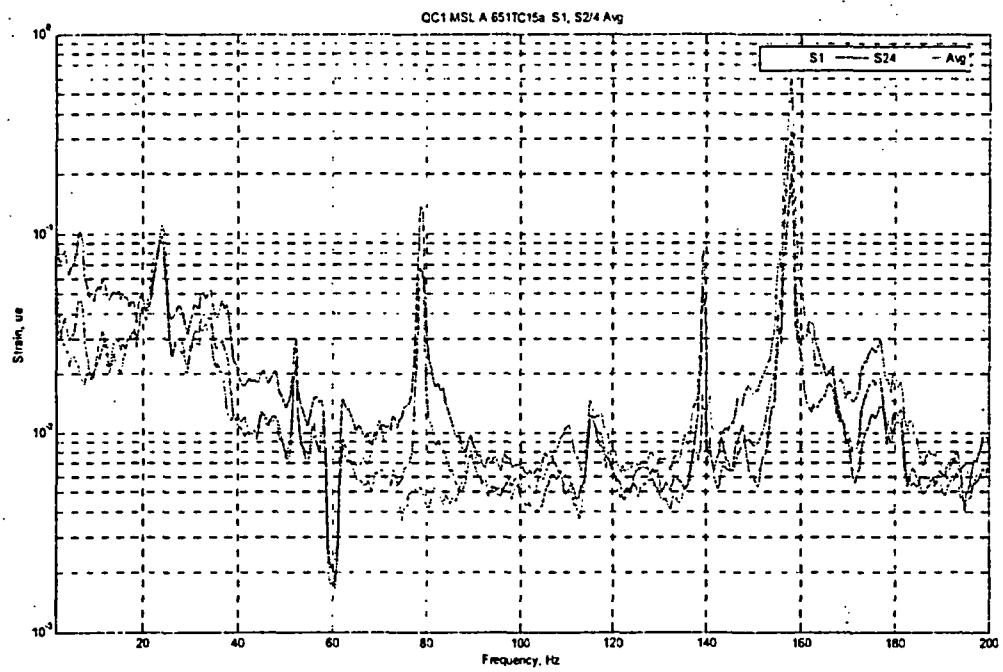

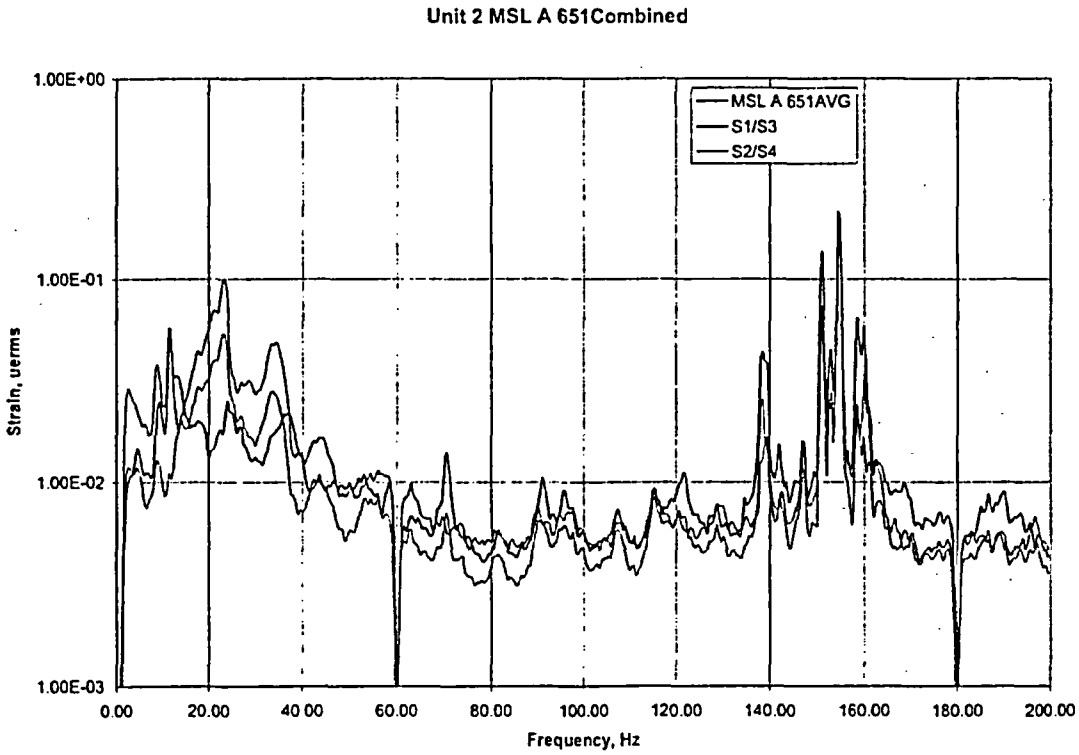

Figure 2. MSL A Elevation 651

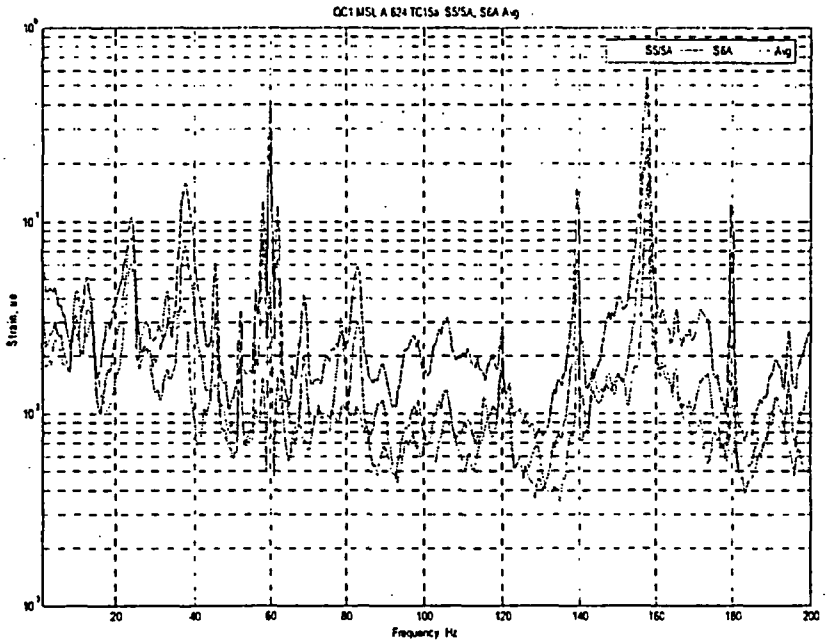

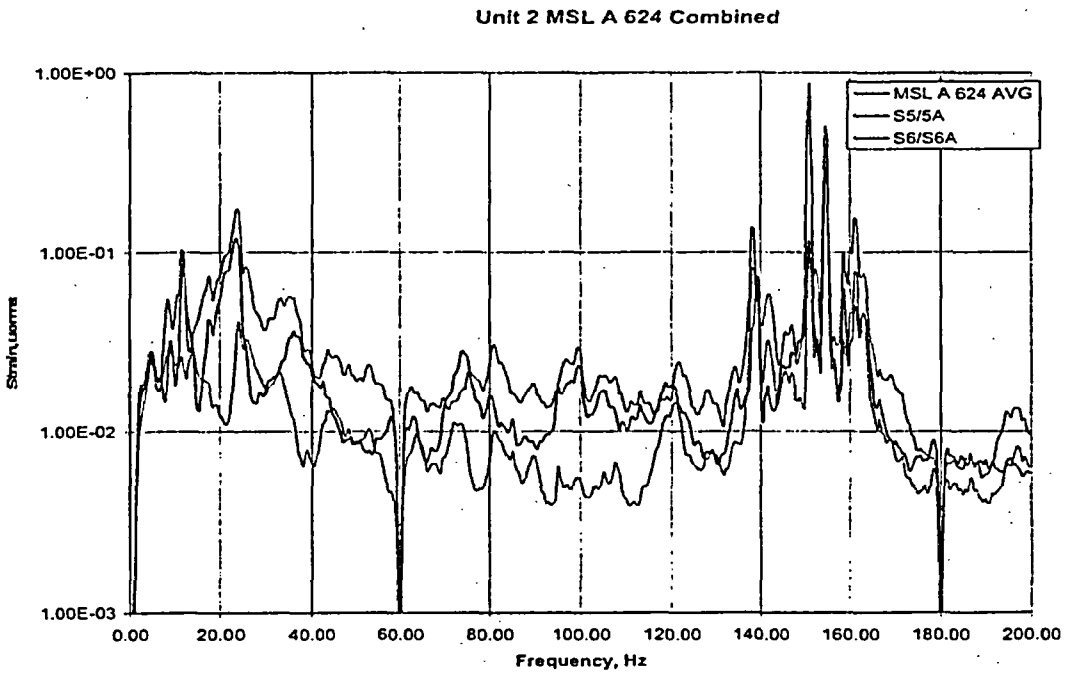

Figure 3. MSL A Elevation 624

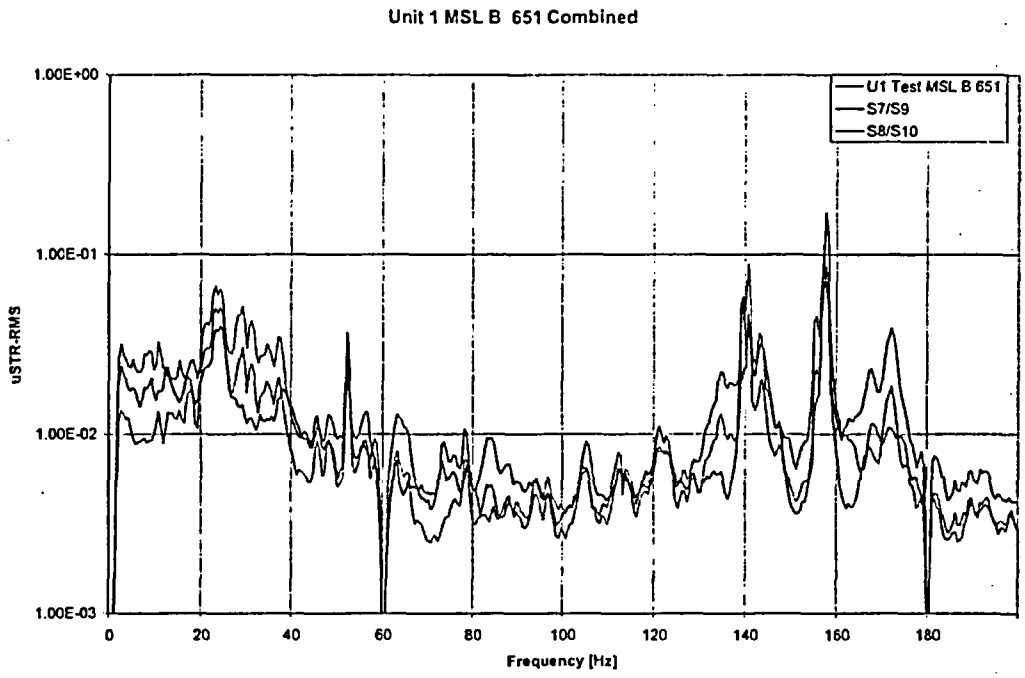

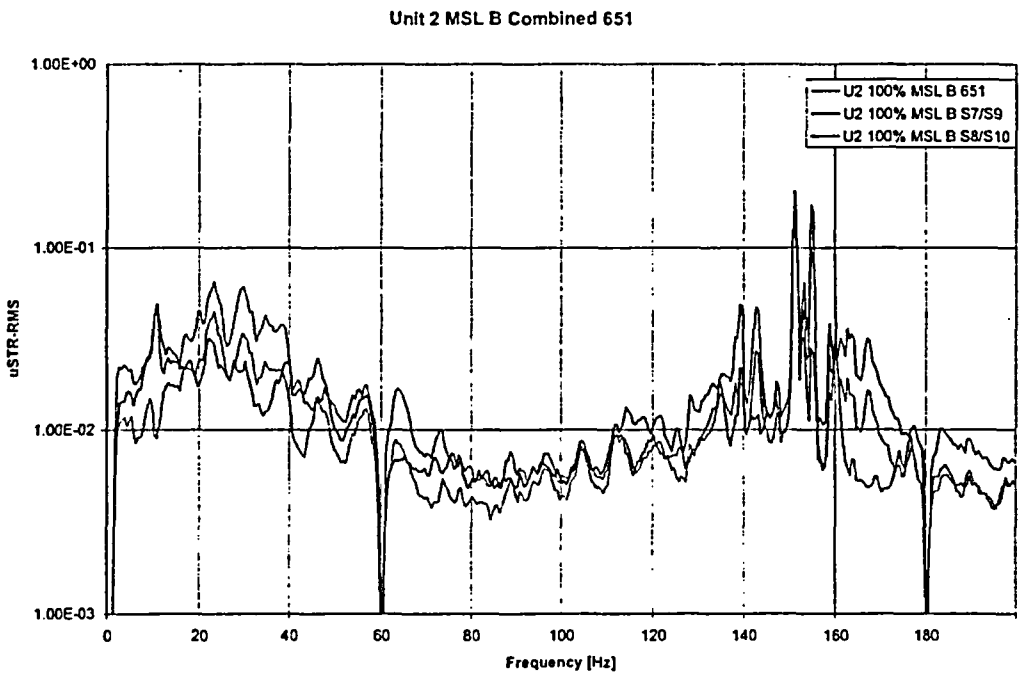

Figure 4. MSL B Elevation 651

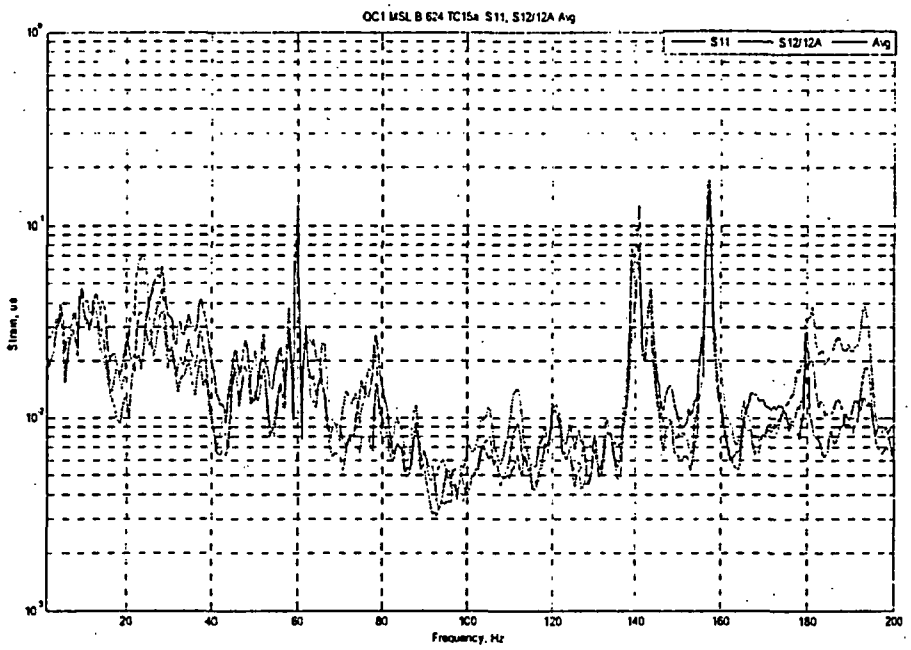

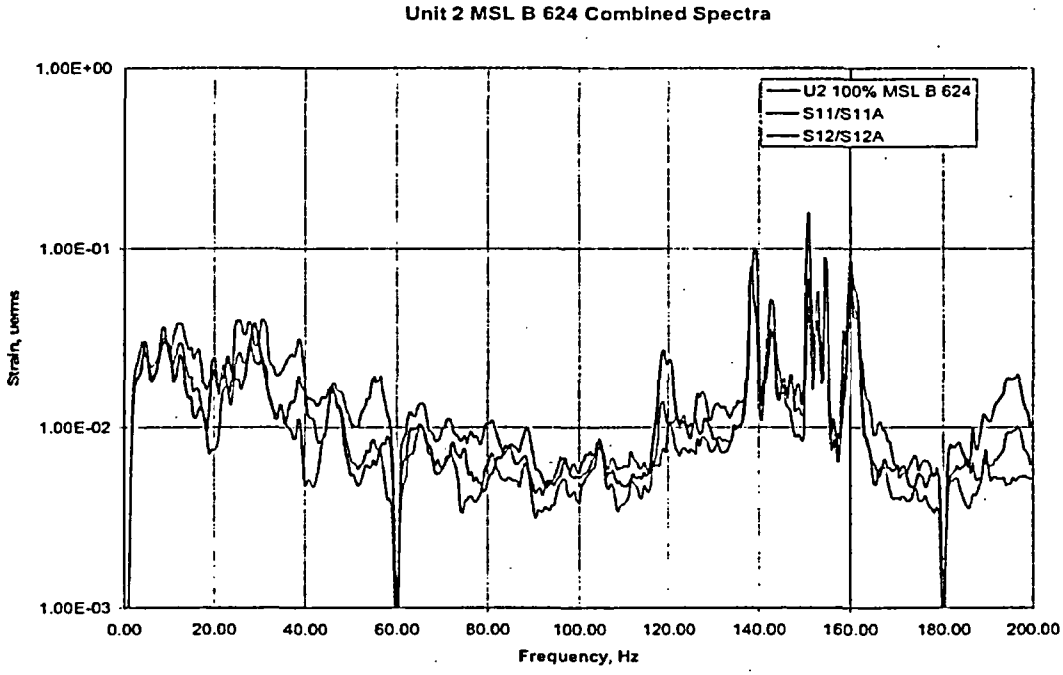

Figure 5. MSL B Elevation 624

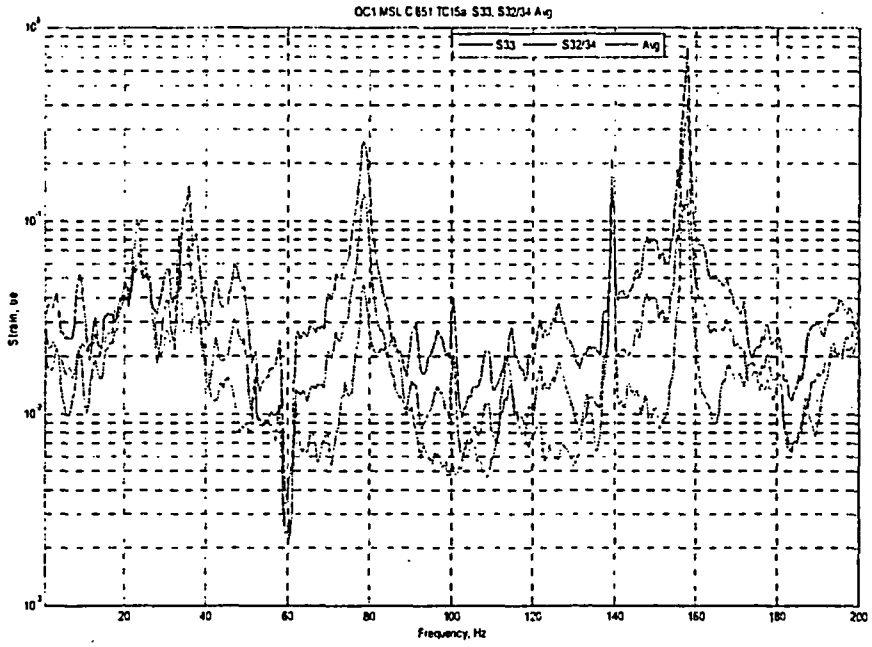

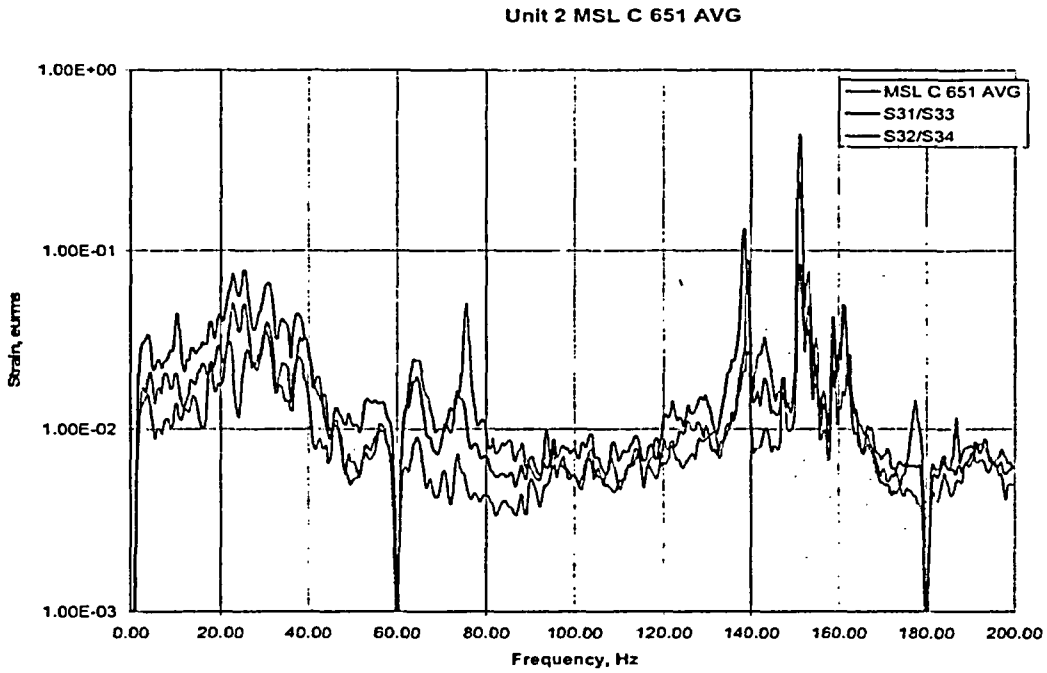

Figure 6. MSL C Elevation 651

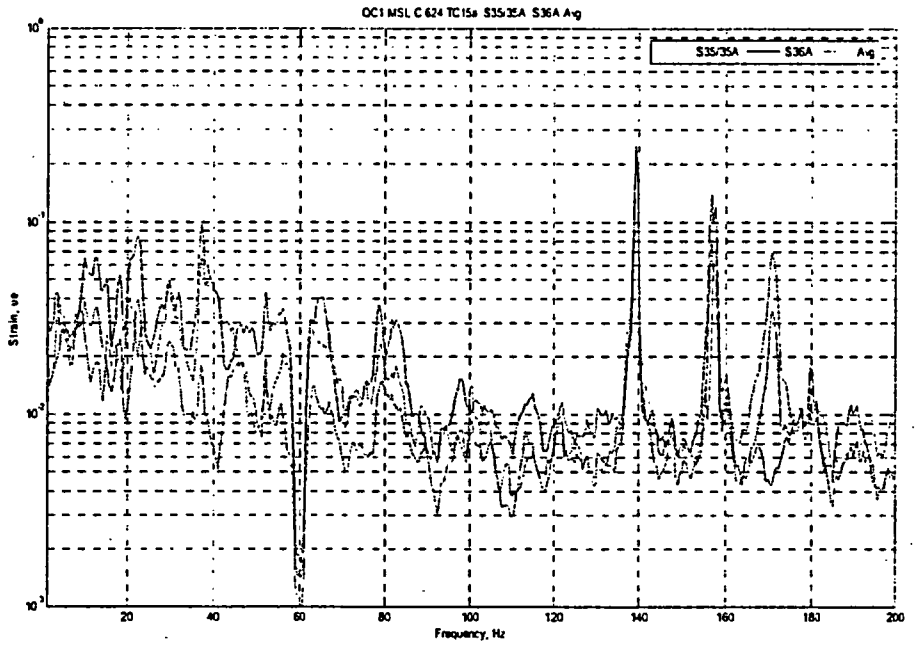

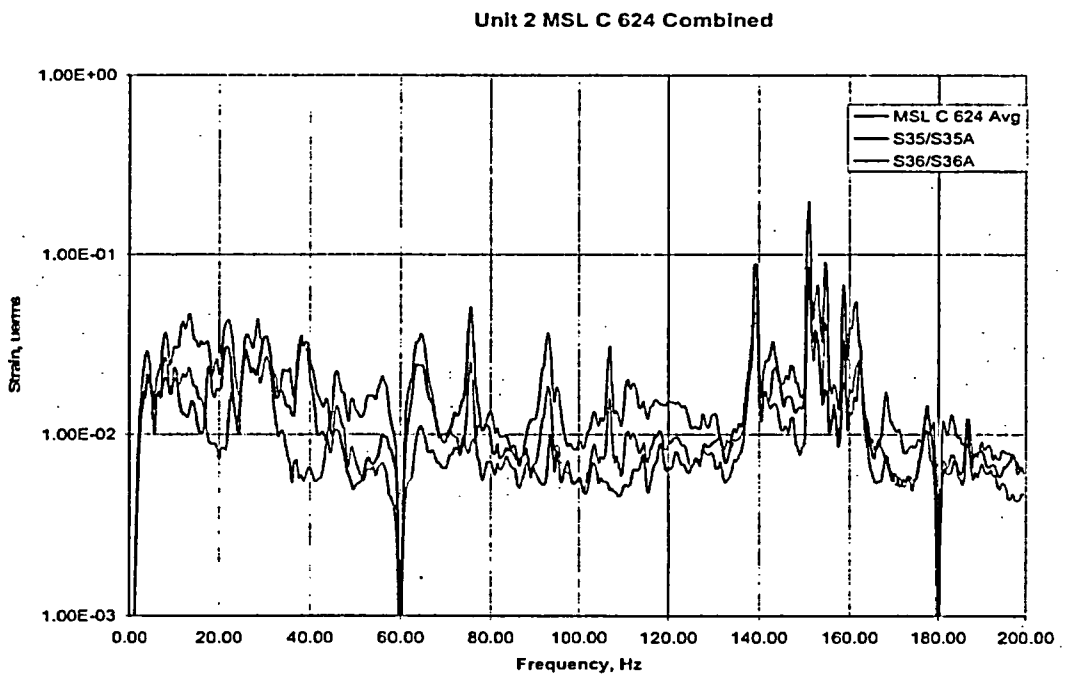

Figure 7. MSL C Elevation 624

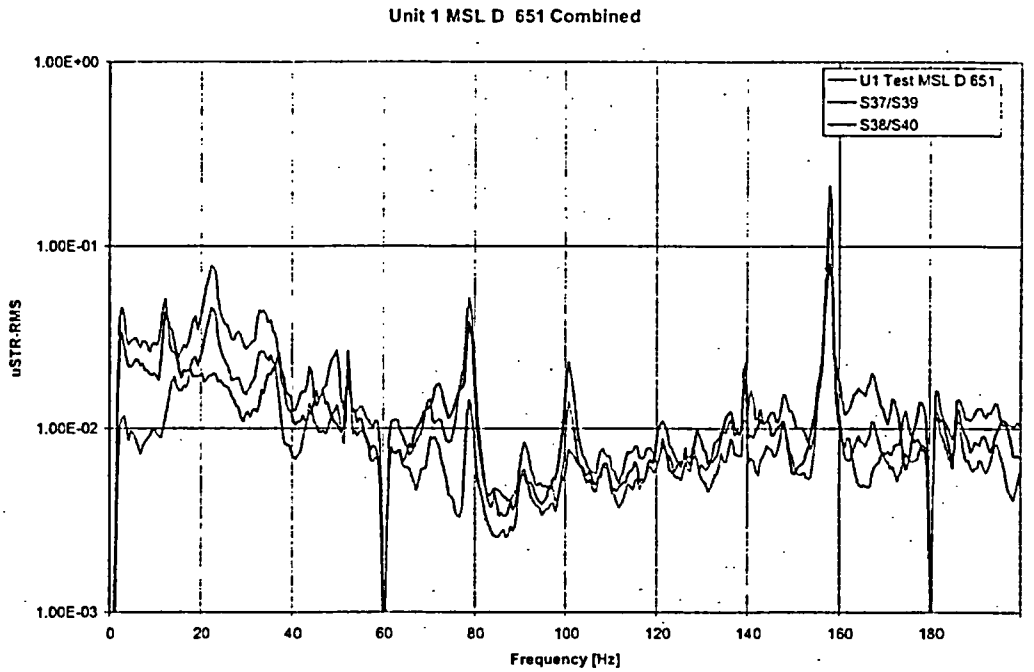

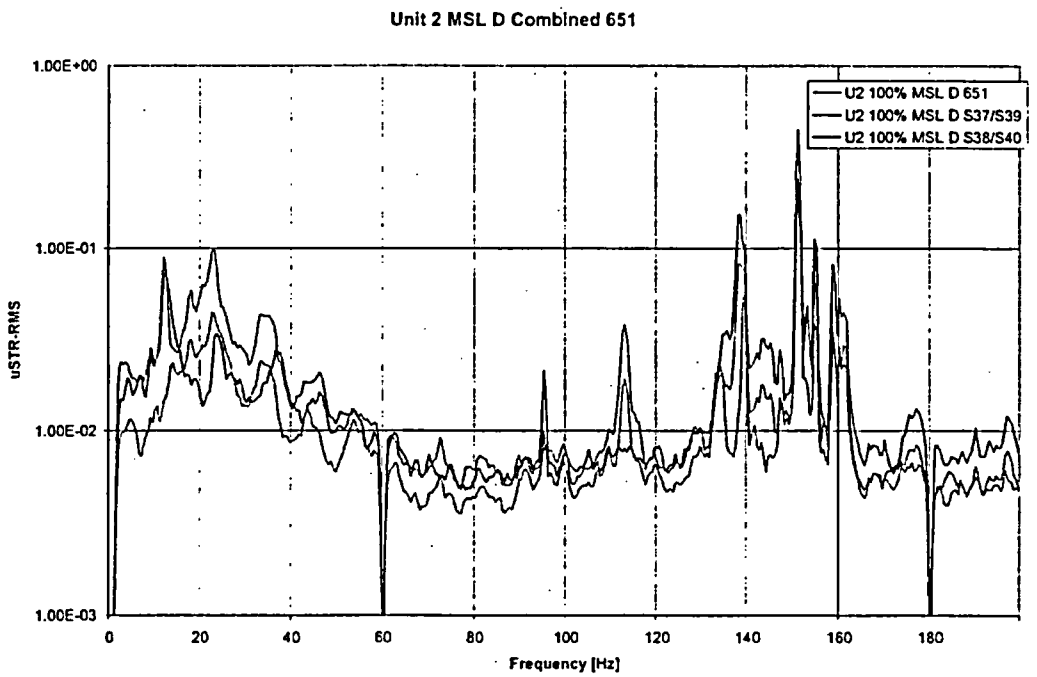

Figure 8. MSL D Elevation 651

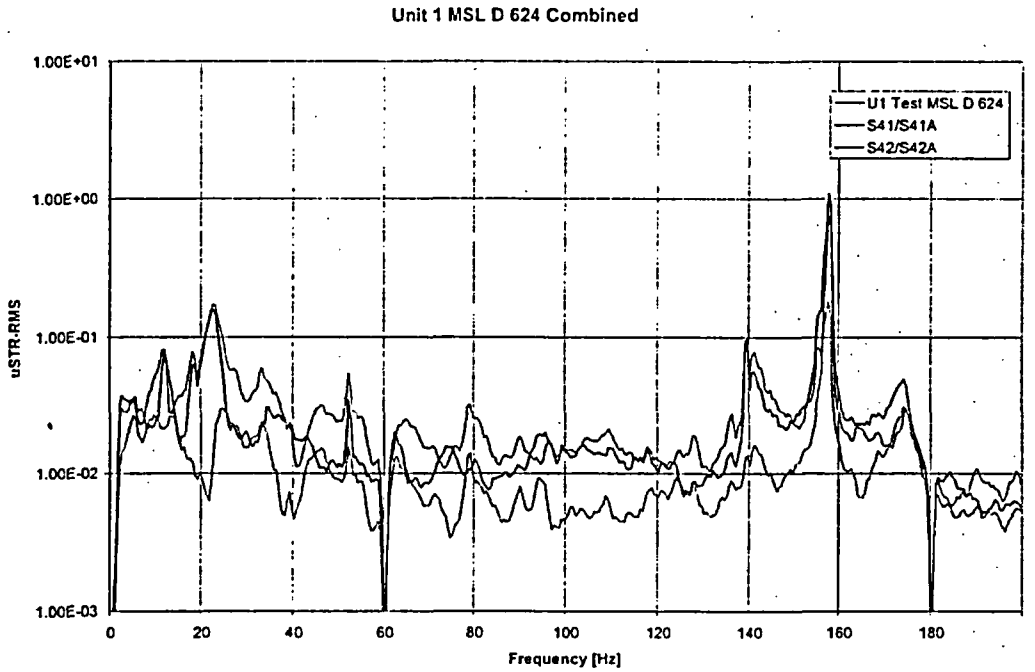

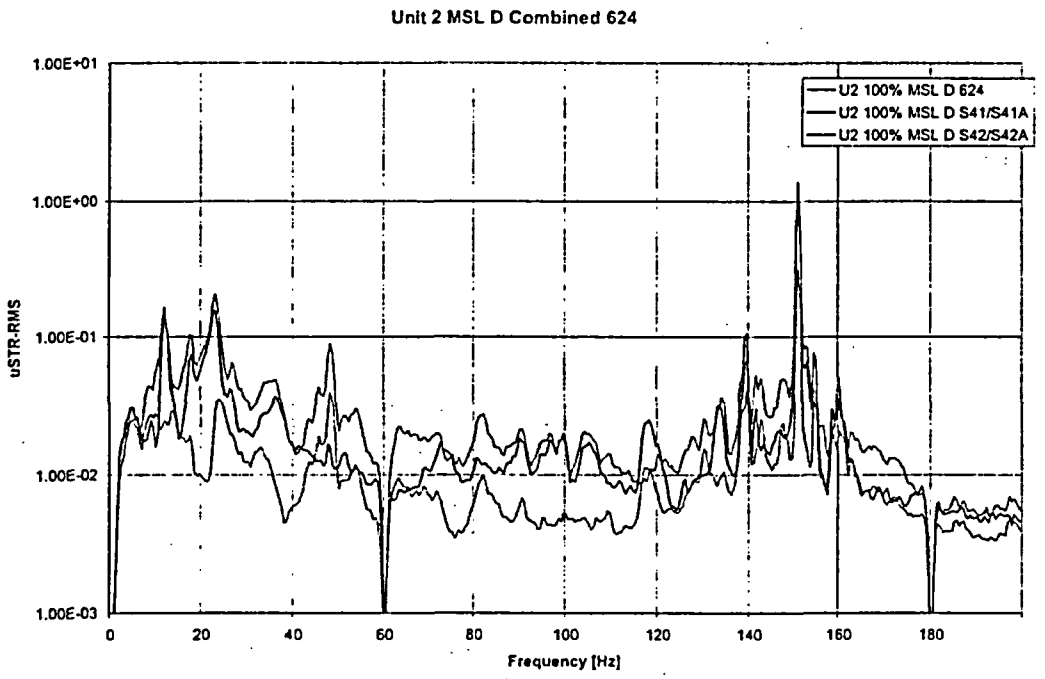

Figure 9. MSL D Elevation 624

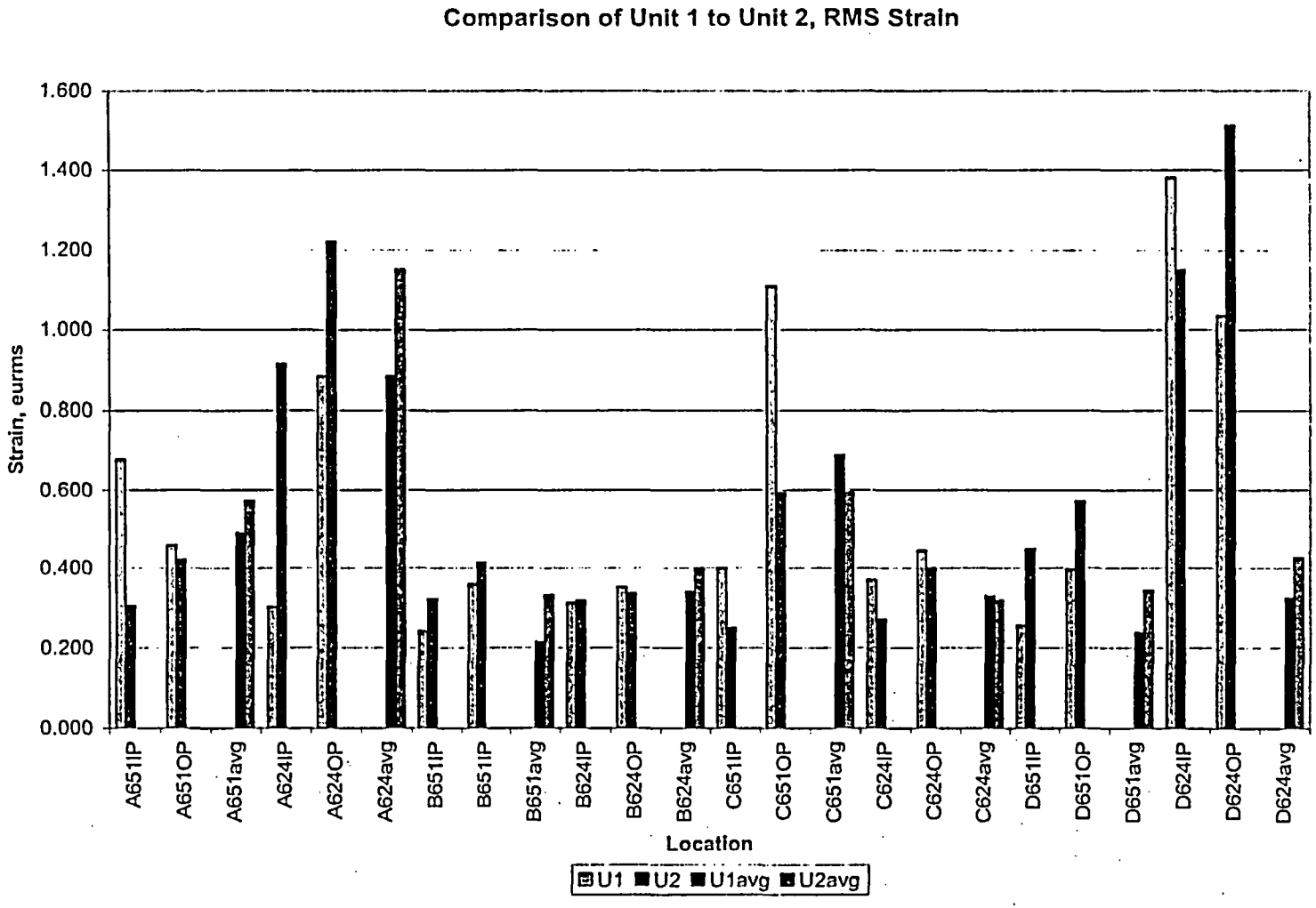

Figure 10. QC1 and QC2 RMS Strain

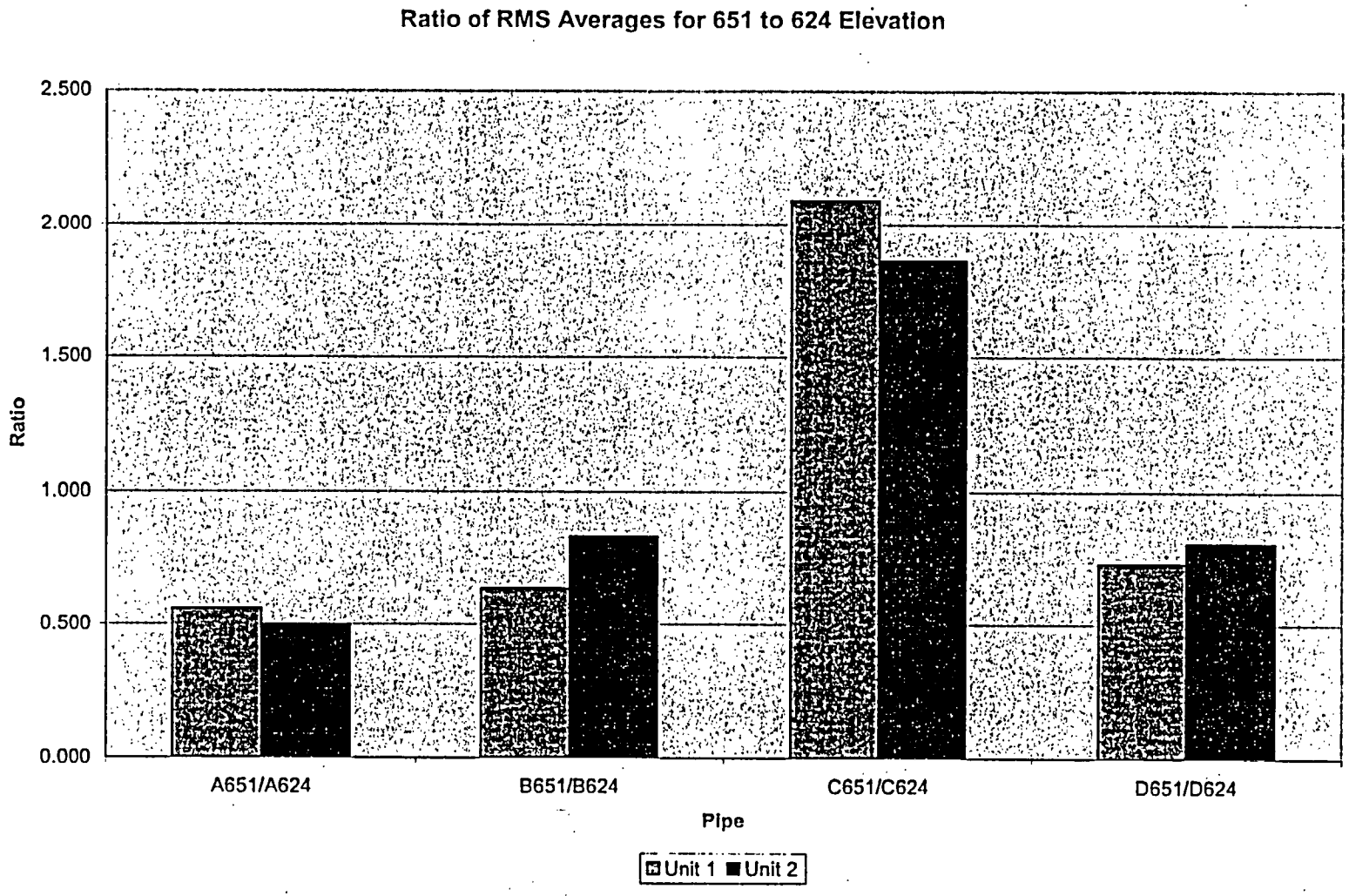

Figure 11. Ratio of RMS Averages for Elevations 651 to 624

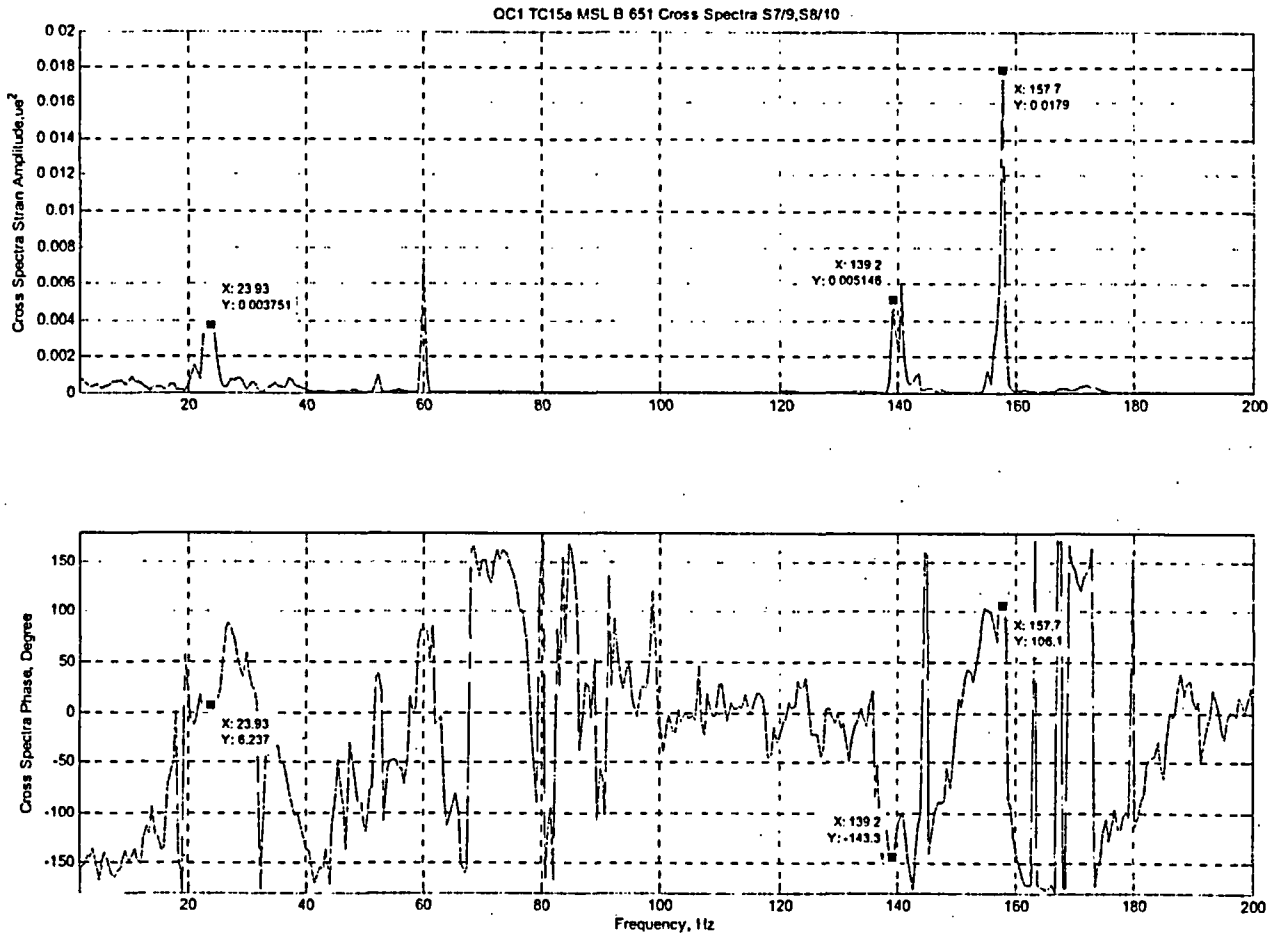

Figure 12. QC1 Cross Spectral Density – Example

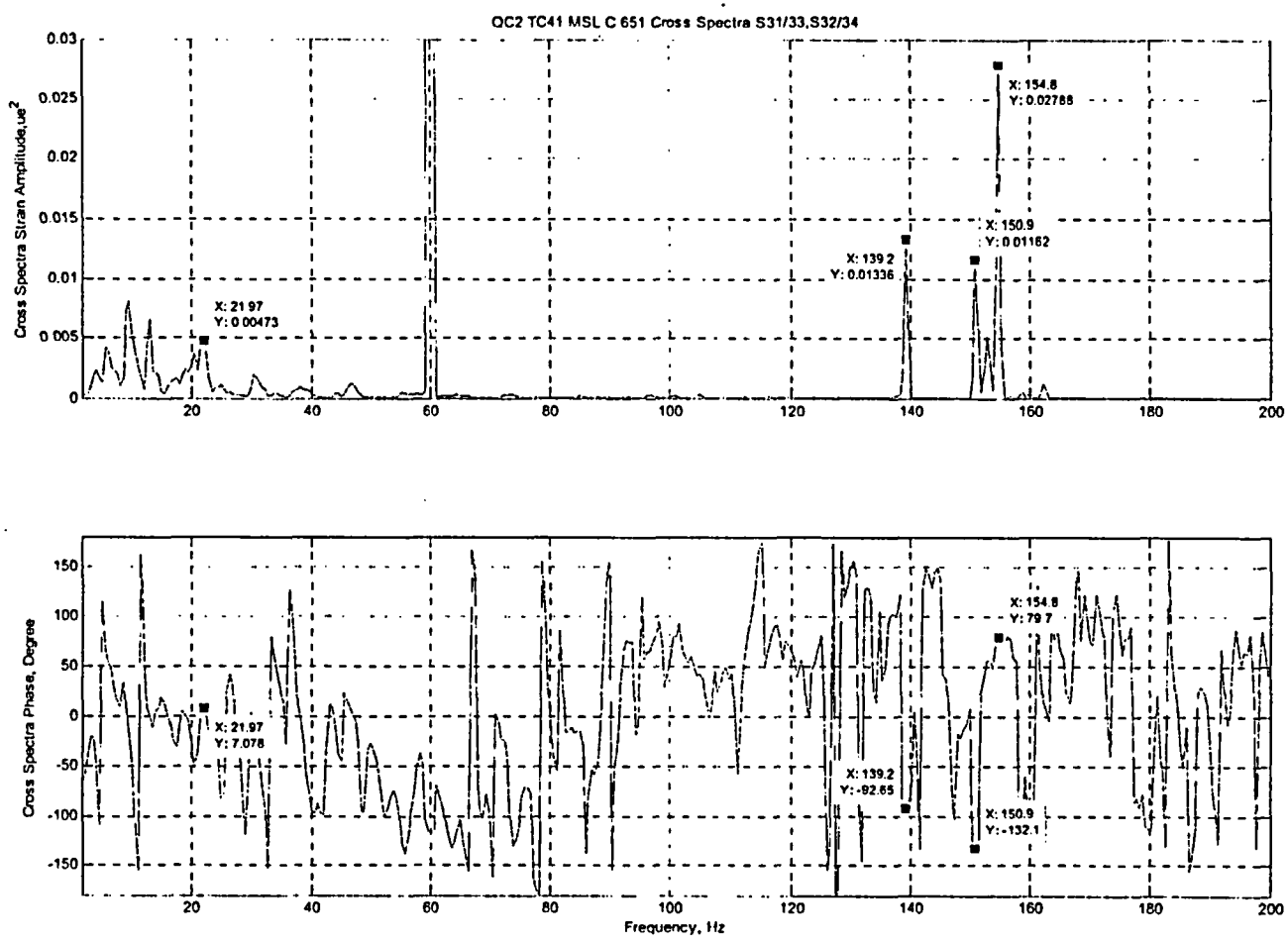

Figure 13. QC2 Cross Spectral Density – Example

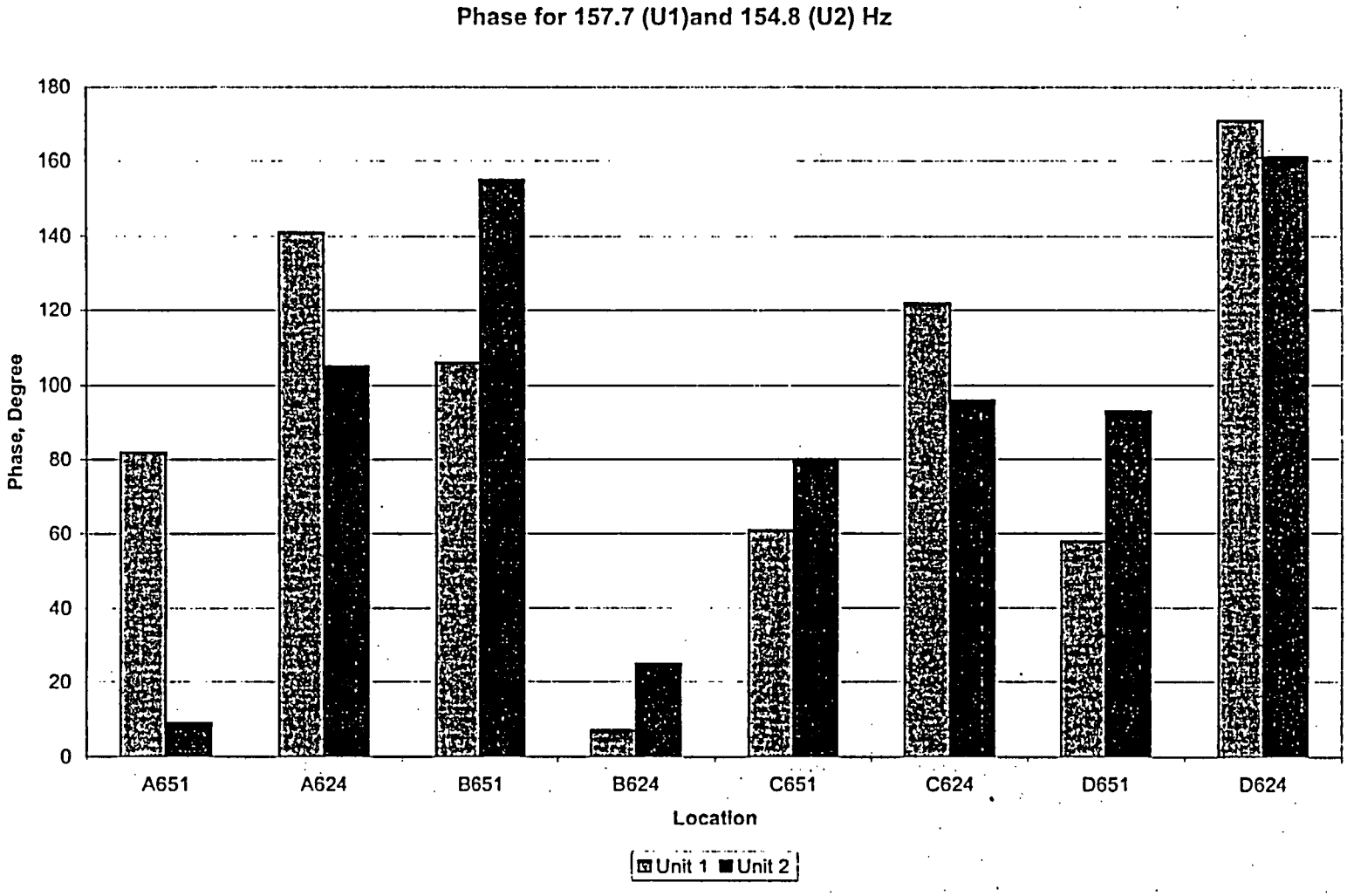

Figure 14. Phase for 157.7 Hz (QC1) and 154.8 Hz (QC2)

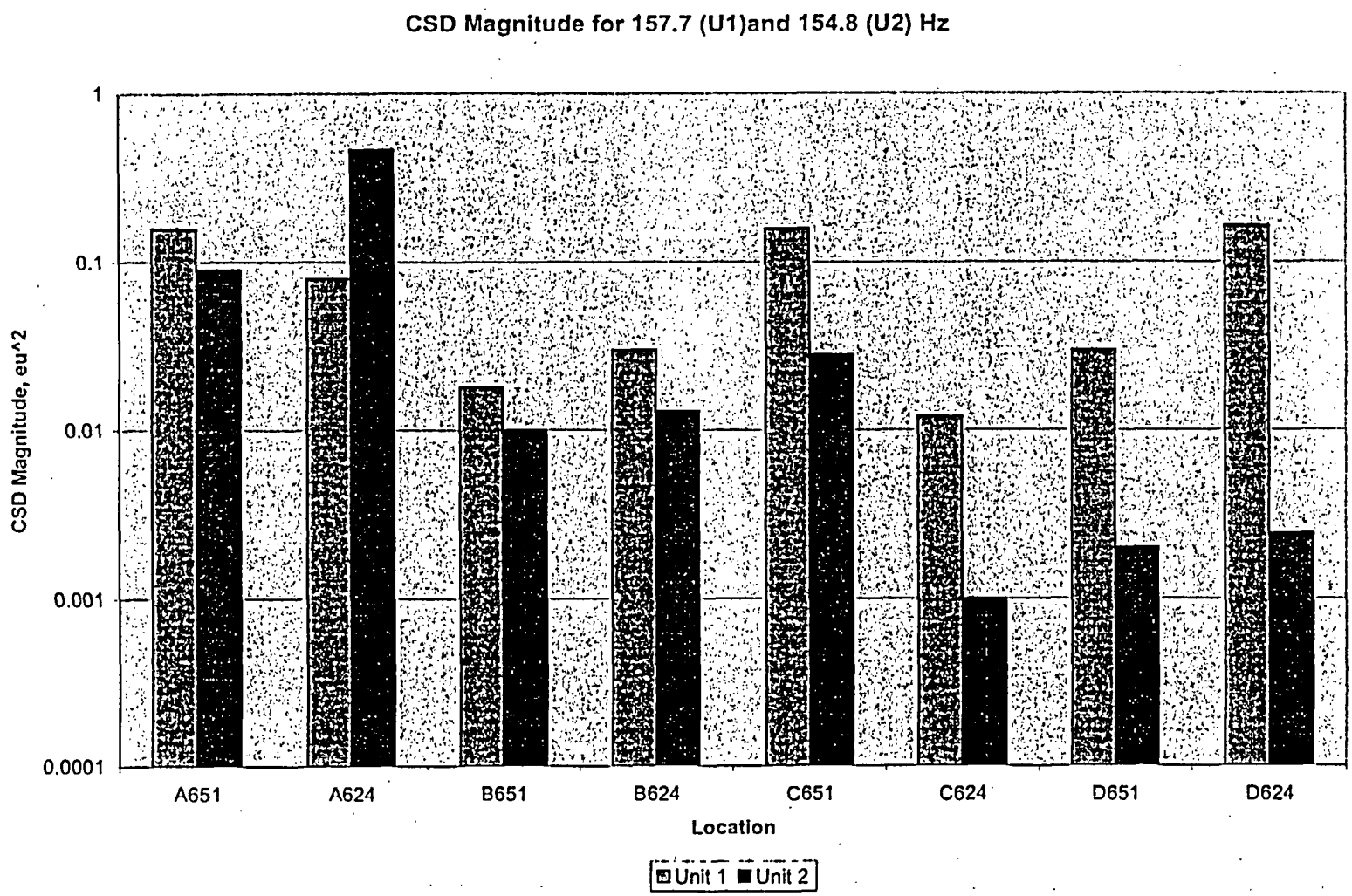

Figure 15. CSD Magnitude for 157.7 Hz (QC1) and 154.8 Hz (QC2)

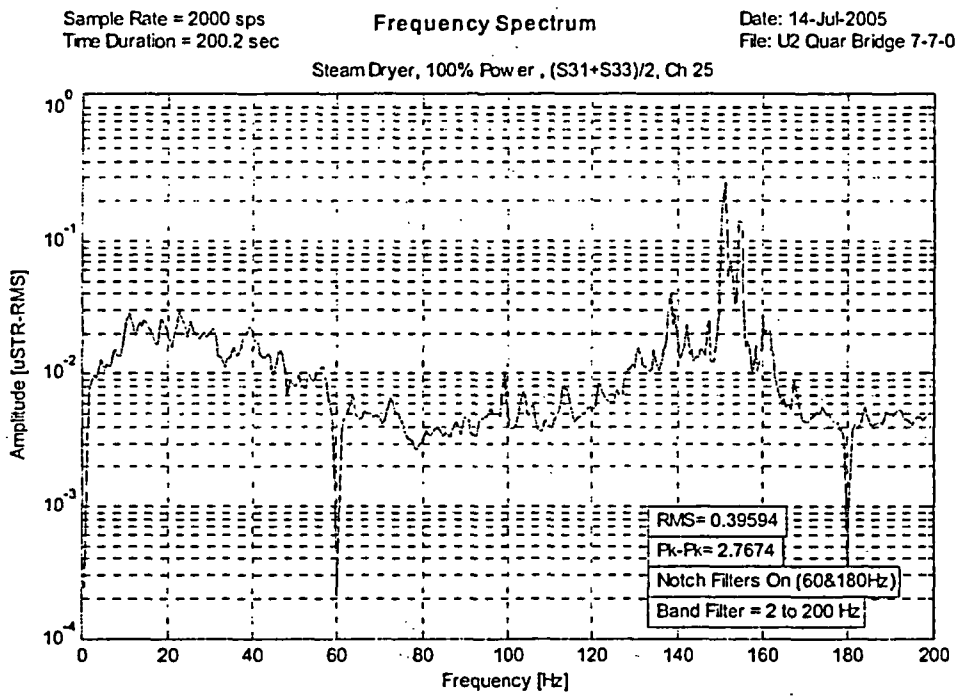

Figure 16. Quarter Bridge Data at S31 and S33 - Equivalent ½ Bridge Configuration

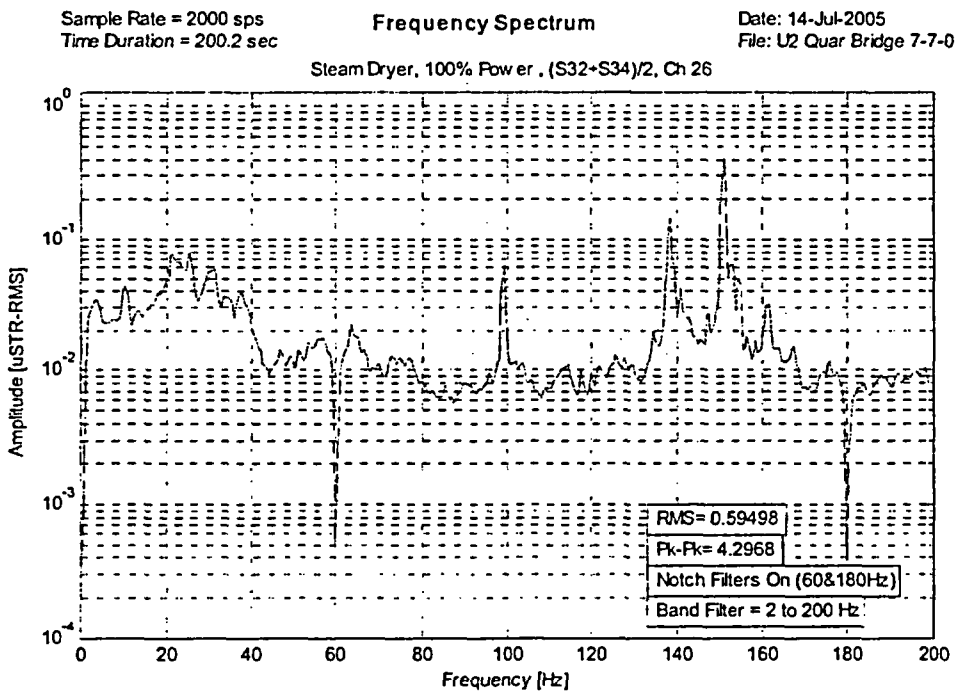

Figure 17. Quarter Bridge Data at S32 and S34 - Equivalent ½ Bridge Configuration

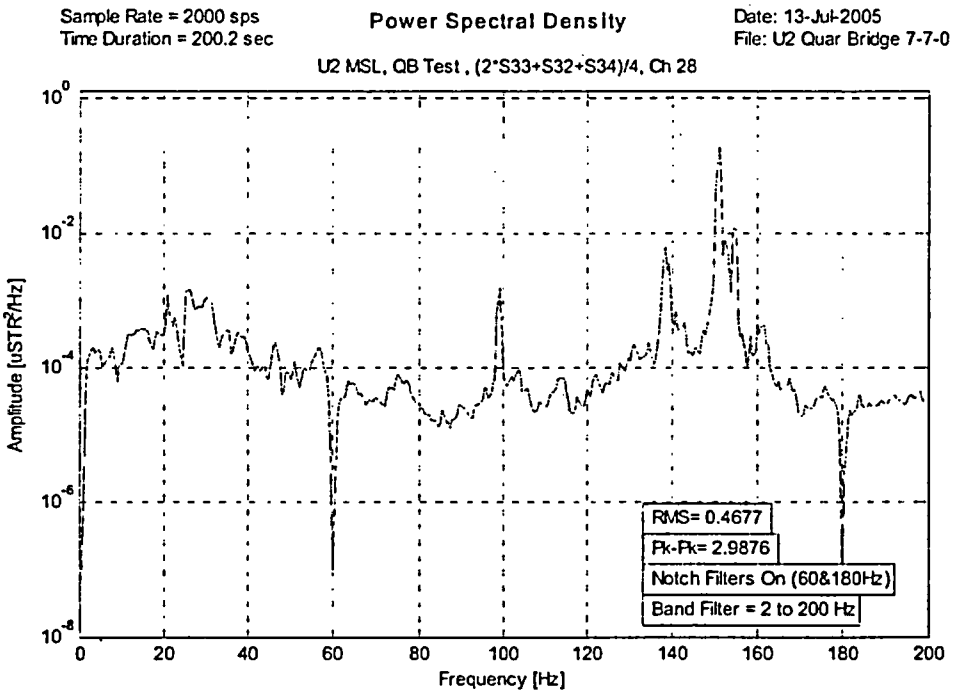

Figure 18. QC2 MSL C 651 – ¼ Bridge Plus ½ Bridge Combination

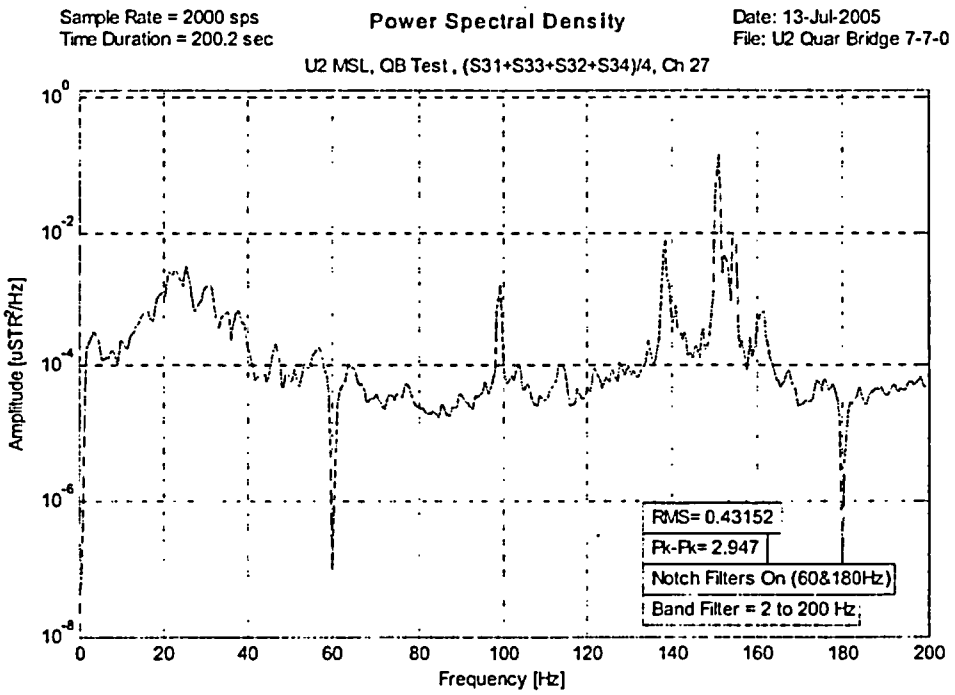

Figure 19. QC2 MSL C 651 – Two Equivalent ½ Bridge Combination

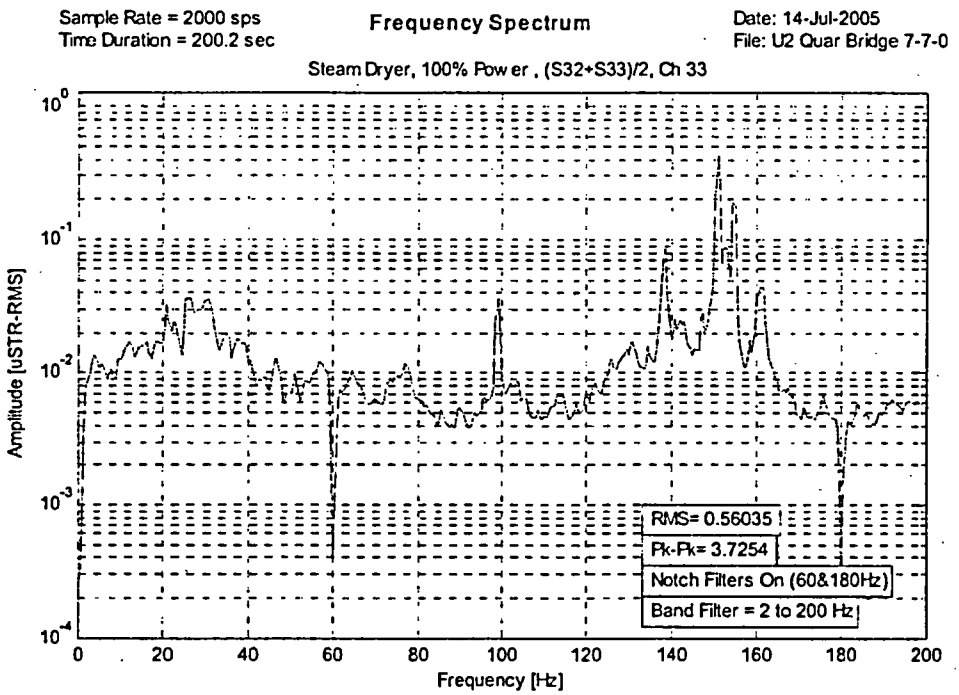

Figure 20. QC2 MSL C 651 – Combination of S32 and S33

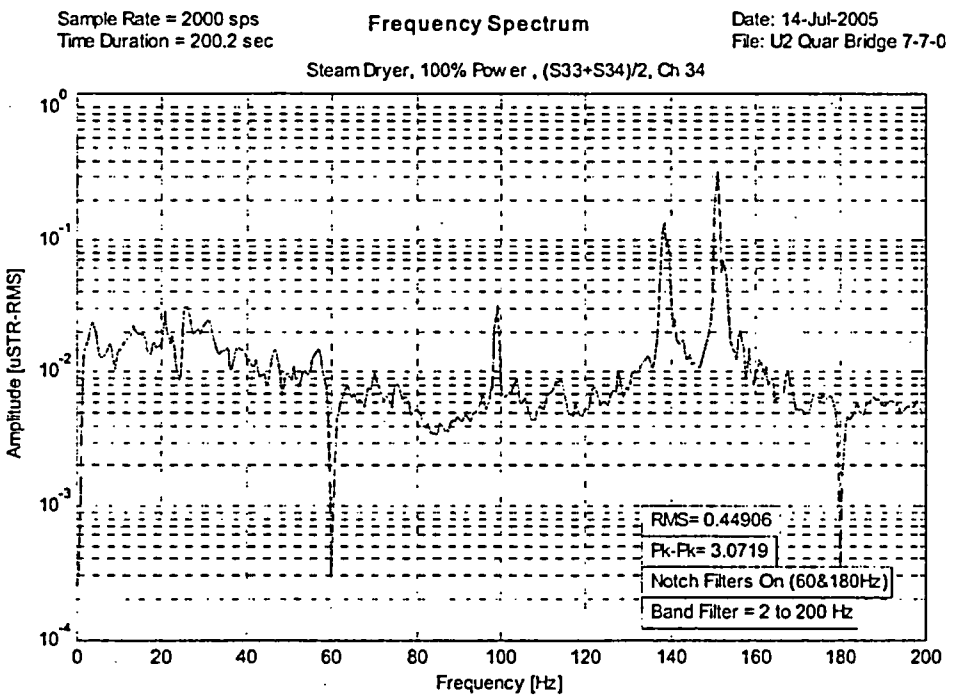

Figure 21. QC2 MSL C 651 – Combination of S33 and S34

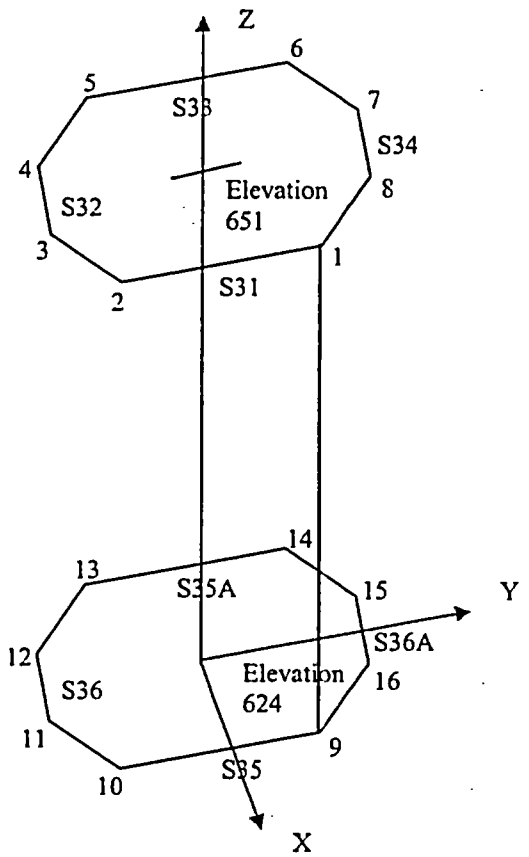

Figure 22. Association of Geometrical Points in 3D Space with Strain Gage Locations on MSL C

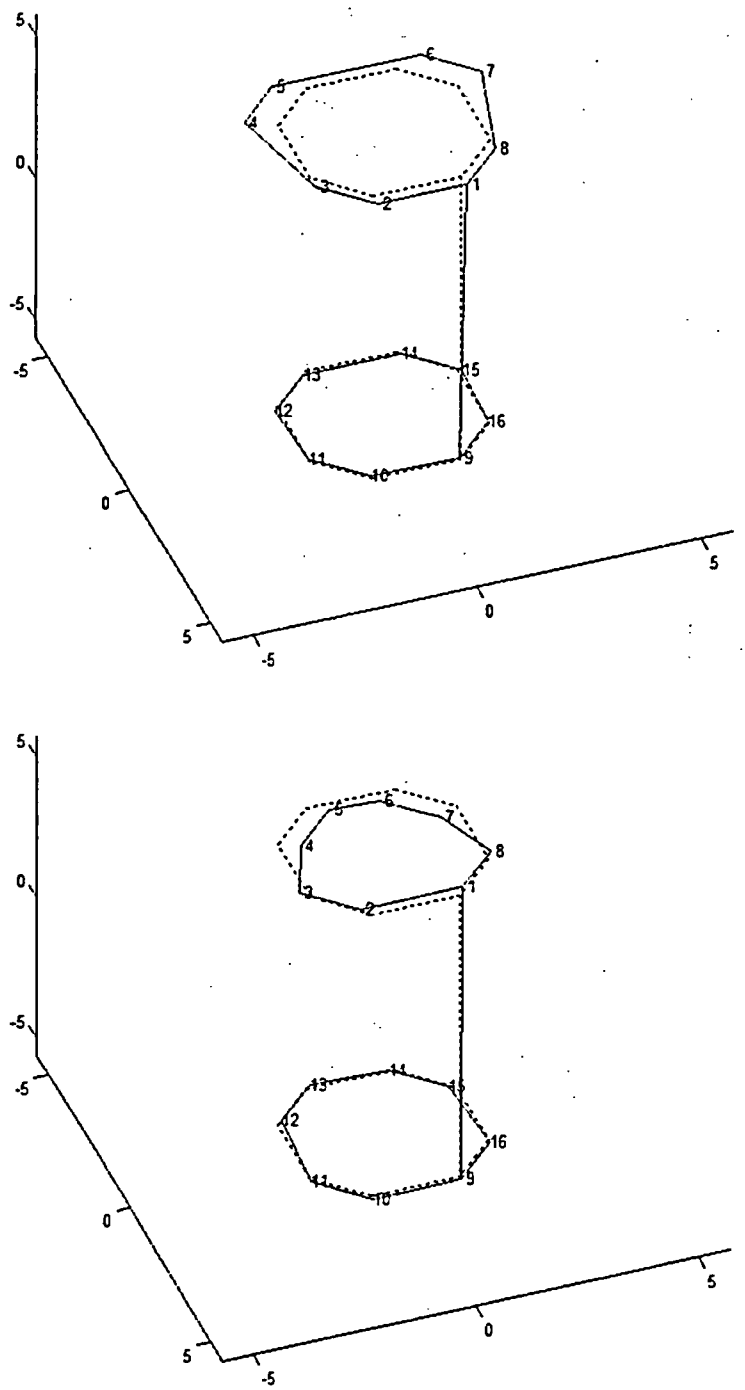

Figure 23. QC2 MSL C Cross-sectional Movements at 151 Hz

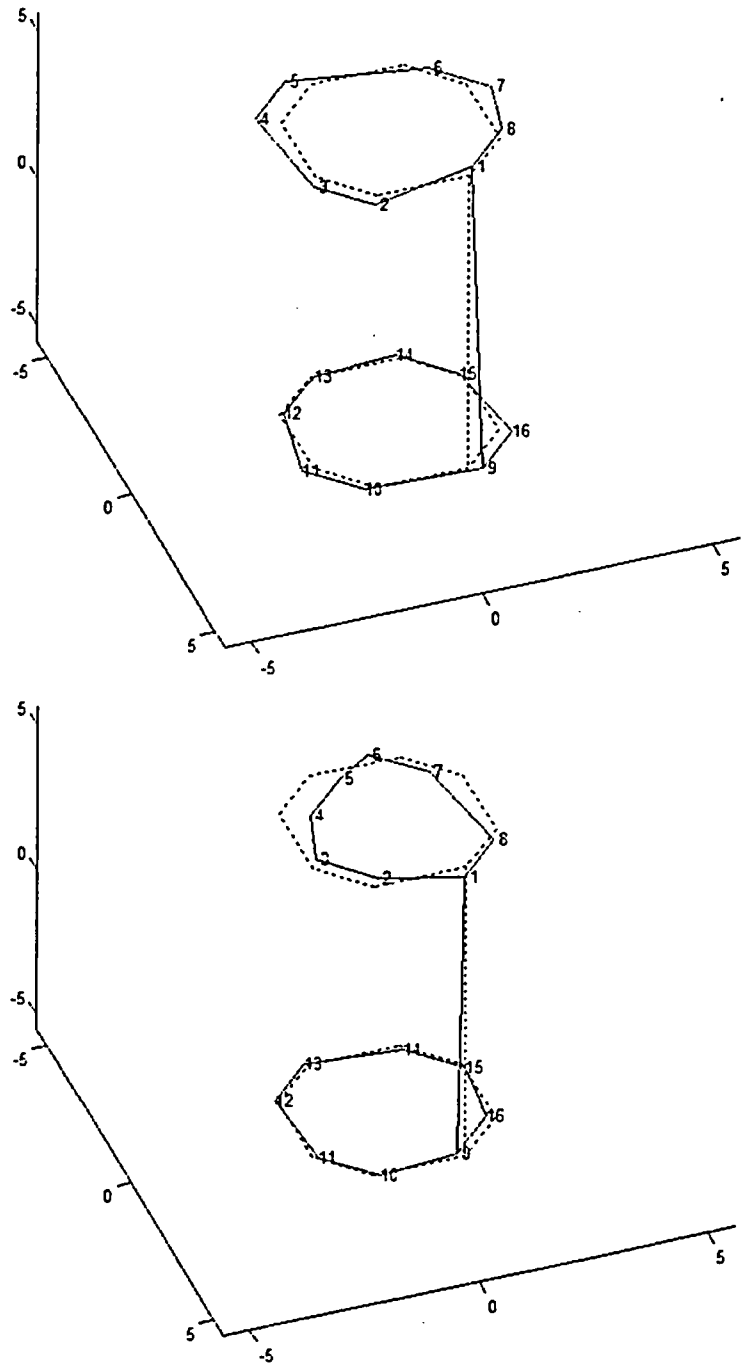

Figure 24. QC2 MSL C Cross-sectional Movements at 154.8 Hz